U.S. Department
of Commerce

Volume 106
Number 1
January 2008

Fishery Bulletin

U.S. Department of Commerce
Carlos M. Gutierrez
Secretary

National Oceanic and Atmospheric Administration
Vice Admiral
Conrad C. Lautenbacher Jr., USN (ret.)
Under Secretary for Oceans and Atmosphere

National Marine Fisheries Service
John Oliver
Acting Assistant Administrator for Fisheries

The *Fishery Bulletin* (ISSN 0090-0656) is published quarterly by the Scientific Publications Office, National Marine Fisheries Service, NOAA, 7600 Sand Point Way NE, BIN C15700, Seattle, WA 98115-0070. Periodicals postage is paid at Seattle, WA. POSTMASTER: Send address changes for subscriptions to Fishery Bulletin, Superintendent of Documents, Attn.: Chief, Mail List Branch, Mail Stop SSOM, Washington, DC 20402-9373.

Although the contents of this publication have not been copyrighted and may be reprinted entirely, reference to source is appreciated.

The Secretary of Commerce has determined that the publication of this periodical is necessary according to law for the transaction of public business of this Department. Use of funds for printing of this periodical has been approved by the Director of the Office of Management and Budget.

For sale by the Superintendent of Documents, U.S. Government Printing Office, Washington, DC 20402. Subscription price per year: $36.00 domestic and $50.40 foreign. Cost per single issue: $21.00 domestic and $29.40 foreign. **See back for order form.**

Fishery Bulletin

Scientific Editor
Adam Moles, Ph.D.

Associate Editor
Elizabeth Siddon

Ted Stevens Marine Research Institute
Auke Bay Laboratories
Alaska Fisheries Science Center
17109 Pt. Lena Loop Road
Juneau, Alaska 99801

Managing Editor
Sharyn Matriotti

National Marine Fisheries Service
Scientific Publications Office
7600 Sand Point Way NE, BIN C15700
Seattle, Washington 98115-0070

Editorial Committee

Jeffrey M. Leis	Australian Museum, Sydney, Australia
Thomas Shirley	Texas A&M University
David Somerton	National Marine Fisheries Service
Mark Terceiro	National Marine Fisheries Service

***Fishery Bulletin* web site: www.fishbull.noaa.gov**

The *Fishery Bulletin* carries original research reports and technical notes on investigations in fishery science, engineering, and economics. It began as the Bulletin of the United States Fish Commission in 1881; it became the Bulletin of the Bureau of Fisheries in 1904 and the *Fishery Bulletin* of the Fish and Wildlife Service in 1941. Separates were issued as documents through volume 46; the last document was No. 1103. Beginning with volume 47 in 1931 and continuing through volume 62 in 1963, each separate appeared as a numbered bulletin. A new system began in 1963 with volume 63 in which papers are bound together in a single issue of the bulletin. Beginning with volume 70, number 1, January 1972, the *Fishery Bulletin* became a periodical, issued quarterly. In this form, it is available by subscription from the Superintendent of Documents, U.S. Government Printing Office, Washington, DC 20402. It is also available free in limited numbers to libraries, research institutions, State and Federal agencies, and in exchange for other scientific publications.

U.S. Department
of Commerce
Seattle, Washington

Volume 106
Number 1
January 2008

Fishery Bulletin

Contents

Articles

1–11 **Rooper, Christopher N.**
An ecological analysis of rockfish (*Sebastes* spp.) assemblages in the North Pacific Ocean along broad-scale environmental gradients

12–23 **Brooks, Elizabeth N., Kyle W. Shertzer, Todd Gedamke, and Douglas S. Vaughan**
Stock assessment of protogynous fish: evaluating measures of spawning biomass used to estimate biological reference points

24–39 **Stevenson, Duane E., James W. Orr, Gerald R. Hoff, and John D. McEachran**
Emerging patterns of species richness, diversity, population density, and distribution in the skates (Rajidae) of Alaska

40–46 **Stiansen, Stian, Anders Fernö, Dag Furevik, Terje Jørgensen, and Svein Løkkeborg**
Efficiency and catch dynamics of collapsible square and conical crab pots used in the red king crab (*Paralithodes camtschaticus*) fishery

47–57 **Latour, Robert J., James Gartland, Christopher F. Bonzek, and RaeMarie A. Johnson**
The trophic dynamics of summer flounder (*Paralichthys dentatus*) in Chesapeake Bay

58–71 **Haddon, Malcolm, Craig Mundy, and David Tarbath**
Using an inverse-logistic model to describe growth increments of blacklip abalone (*Haliotis rubra*) in Tasmania

The National Marine Fisheries Service (NMFS) does not approve, recommend, or endorse any proprietary product or proprietary material mentioned in this publication. No reference shall be made to NMFS, or to this publication furnished by NMFS, in any advertising or sales promotion which would indicate or imply that NMFS approves, recommends, or endorses any proprietary product or proprietary material mentioned herein, or which has as its purpose an intent to cause directly or indirectly the advertised product to be used or purchased because of this NMFS publication.

72–81 **Byrd, Barbie L., Aleta A. Hohn, Fentress H. Munden, Gretchen N. Lovewell, and Rachel E. Lo Piccolo**
Effects of commercial fishing regulations on stranding rates of bottlenose dolphin (*Tursiops truncatus*)

82–92 **Schwenke, Kara. L., and Jeffrey A. Buckel**
Age, growth, and reproduction of dolphinfish (*Coryphaena hippurus*) caught off the coast of North Carolina

93–107 **Vasslides, James M., and Kenneth W. Able**
Importance of shoreface sand ridges as habitat for fishes off the northeast coast of the United States

108–109 **Guidelines for authors**

An ecological analysis of rockfish (*Sebastes* spp.) assemblages in the North Pacific Ocean along broad-scale environmental gradients

Christopher N. Rooper

Email address: Chris.Rooper@noaa.gov

Alaska Fisheries Science Center
National Marine Fisheries Service
7600 Sand Point Way NE
Seattle, Washington 98115

Abstract—Environmental variability affects the distributions of most marine fish species. In this analysis, assemblages of rockfish (*Sebastes* spp.) species were defined on the basis of similarities in their distributions along environmental gradients. Data from 14 bottom trawl surveys of the Gulf of Alaska and Aleutian Islands (n=6767) were used. Five distinct assemblages of rockfish were defined by geographical position, depth, and temperature. The 180-m and 275-m depth contours were major divisions between assemblages inhabiting the shelf, shelf break, and lower continental slope. Another noticeable division was between species centered in southeastern Alaska and those found in the northern Gulf of Alaska and Aleutian Islands. The use of environmental variables to define the species composition of assemblages is different from the use of traditional methods based on clustering and nonparametric statistics and as such, environmentally based analyses should result in predictable assemblages of species that are useful for ecosystem-based management.

Manuscript submitted 7 February 2007.
Manuscript accepted 1 August 2007.
Fish. Bull 106:1–11 (2008).

The views and opinions expressed or implied in this article are those of the author and do not necessarily reflect the position of the National Marine Fisheries Service, NOAA.

Ecosystem-based management of marine fish species requires all ecosystem components to be accounted for in the management framework (Livingston et al., 2005). This necessitates knowing the major environmental gradients along which important species are organized within marine systems. Rockfish (*Sebastes* spp.) comprise an important component of marine ecosystems; they are abundant, diverse, and a widely dispersed group found across a wide range of habitats on the Pacific coast of North America. Rockfish management is problematic because of the different habitat requirements of these species at different life history stages (Love et al., 1991; Rooper et al., 2007), their episodic recruitment (Ralston and Howard, 1995; Field and Ralston, 2005), and their susceptibility to overfishing (Parker et al., 2000). Knowledge of the environmental gradients upon which rockfish organize themselves should be useful in predicting where different species and age groups co-occur and, thus, the best strategies for managing rockfish as an important component of the marine ecosystem.

Analyses used to define fish assemblages typically are based on methods that cluster characteristics of the catch, such as the Bray-Curtis dissimilarity index (Weinberg, 1994; Williams and Ralston, 2002) and other measures of co-occurrence (Weinberg, 1994; Mueter and Norcross, 2002), or that classify stations into categories of similar catch (Methratta and Link, 2006; Zimmermann, 2006). These analyses do not explicitly take into account the distribution of species across environmental gradients, even though fish species are known to respond to characteristics such as water depth, temperature, salinity, and sediment type (Friedlander and Parrish, 1998; Rooper et al., 2005). According to ecological theory, species will inhabit a preferred niche of environmental conditions (Hutchinson, 1957). Application of this principle can be useful in predicting the biological basis for co-occurrence of rockfish species (Murawski and Finn, 1988), as well as for defining groups of species with similar habitat requirements. Additionally, the species comprising assemblages defined by ecological relationships may be expected to respond to environmental changes in a predictable fashion.

The objective of this study was to analyze the distribution of rockfish species across two large ecosystems: the Gulf of Alaska and the Aleutian Islands. Relationships based on niche theory were developed for rockfish life history stages, sexes, and species subgroups with depth, temperature, and geographical position in order to test for important overlaps and to infer common distributions among species. The co-occurrence of species in bottom trawl catches was compared to their environmental overlap to determine whether species with similar distributions were likely to be captured together. Finally, the major gradients along which rockfish species organize themselves were examined in relation to the varying life history stages of the species. These methods should allow for a more robust analysis of the assemblage of similar species, as well

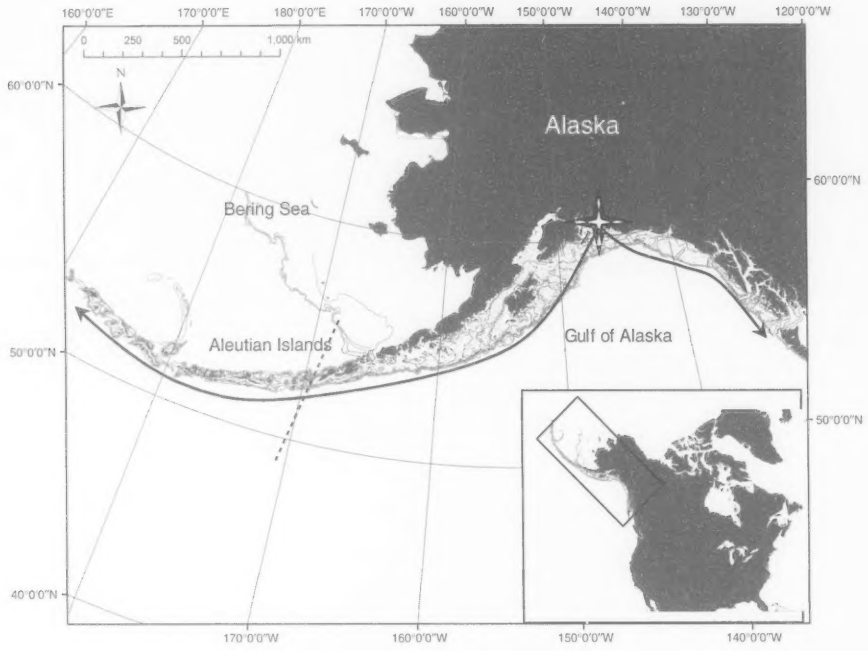

Figure 1

Map of Alaska showing the Gulf of Alaska and Aleutian Islands ecosystems (separated by a dashed line). The geographical position of each bottom trawl haul was calculated as the distance from Hinchinbrook Island (star). The distance of trawl hauls from Hinchinbrook Island along the southeastward arrow was coded as negative, and the distance along the westward arrow was coded as positive.

as documentation of the important differences among life-stage and species subgroups along environmental gradients.

Materials and methods

Study area

The data used for these analyses were collected during bottom trawl surveys of the Gulf of Alaska and Aleutian Islands ecosystems (Britt and Martin, 2001; Zenger, 2004). The Aleutian Islands are a chain of volcanic islands stretching from the Alaska Peninsula in southwest Alaska across the North Pacific Ocean and dividing the western Gulf of Alaska from the Bering Sea. The upper continental slope in the Aleutian Islands is narrow and steep. In the Gulf of Alaska, the continental shelf ranges in width from 20 km to greater than 200 km and the continental slope is steep and features periodic gullies and submarine canyons extending into the continental shelf. These two ecosystems encompass a large area of the Alaska continental shelf, from Dixon Entrance (133°W) in the southeastern Gulf of Alaska to Stalemate Bank (170°E) at the far western end of the Aleutian Islands (Fig. 1). The Gulf of Alaska bottom trawl survey is conducted from the Islands of Four Mountains (170°W) to Dixon Entrance. The Aleutian Islands bottom trawl survey is conducted along the island chain from 165°W to Stalemate Bank on the Bering Sea side and from the Islands of Four Mountains (170°W) to Stalemate Bank on the Gulf of Alaska side.

The Aleutian Islands and Gulf of Alaska ecosystems are connected by oceanic currents over the shelf. The Alaska Coastal Stream and Alaska Coastal Current flow westward (counter-clockwise) around the Gulf of Alaska from Dixon Entrance to the end of the Aleutian Island chain, whereas on the Bering Sea side of the Aleutian Islands the current flows eastward and provides extensive transport through passes in the chain from the Gulf of Alaska to the Bering Sea (Stabeno et al., 1999, 2002). The Islands of Four Mountains area is thought to be an area of change in both oceanographic properties (a higher influence of marine waters to the west) and biological properties (Ladd et al., 2005; Logerwell et al., 2005).

Trawl survey data

The National Marine Fisheries Service (NMFS) Alaska Fisheries Science Center (AFSC) has conducted standard bottom trawl surveys in the Gulf of Alaska and the

Aleutian Islands region since 1980 (Britt and Martin, 2001; Zenger, 2004). Surveys were conducted triennially between 1990 and 2000 and biennially thereafter (Table 1). For this analysis, the AFSC bottom trawl data from 1990 through 2005 were combined across years and survey areas in order to maximize the number of useful data points for each species. A Poly Nor'Eastern high-opening bottom trawl (with 24.2-m roller gear equipped with 36-cm rubber bobbins that are separated by 10-cm rubber disks) was used in these AFSC bottom trawl surveys. Trawl hauls were conducted at a speed of 5.6 km/h (3 knots) for 15 or 30 minutes. Bottom contact and net dimensions were recorded throughout each trawl haul by using net mensuration equipment. In a few cases, net width was not recorded (n=35); therefore the overall average net width (15.84 m, standard error [SE]=0.01) was used. For these analyses, records were used only if trawl performance was satisfactory and if the distance fished, geographical position, average depth, and bottom water temperature were recorded (n=6767). Trawl hauls were deemed satisfactory if the net opening was within a predetermined normal range, the roller gear maintained contact with the seafloor, and the net suffered little or no damage during the tow (Zenger, 2004).

All fish captured during a survey tow were sorted by species, counted, measured for total or fork length, and the total weight of each species in the catch was determined. For large catches, the total catch was weighed and subsampled for length data. Catch per unit of effort (CPUE, no of fish/ha) for each rockfish species was calculated by using the area swept computed from the net width for each tow multiplied by the distance towed recorded with geographical positioning systems. The rockfish catch data were transformed by using natural log (CPUE+1) before analyses, hereafter shortened to CPUE.

Table 1

Summary of the number of Alaska Fishery Science Center bottom trawl survey hauls used in the analysis of rockfish (*Sebastes* spp.) assemblages in the North Pacific Ocean. Data from trawl hauls with no temperature, depth, latitude, longitude, and inadequate gear performance were not used in the analyses. The Gulf of Alaska and Aleutian Islands bottom trawl surveys were the data source for each ecosystem, although in some years (i.e., 1998) a full survey of the ecosystem was not conducted.

Year	Ecosystem	Number of trawl hauls
1990	Gulf of Alaska	286
1991	Aleutian Islands	63
1993	Gulf of Alaska	727
1994	Aleutian Islands	389
1996	Gulf of Alaska	716
1997	Aleutian Islands	399
1998	Gulf of Alaska	5
1999	Gulf of Alaska	765
2000	Aleutian Islands	415
2001	Gulf of Alaska	550
2002	Aleutian Islands	417
2003	Gulf of Alaska	795
2004	Aleutian Islands	415
2005	Gulf of Alaska	825
Total		6767

Environmental variables

Three environmental variables were included in the analyses: depth, temperature, and geographic position along the Alaska coastline. Temperature measurements were collected throughout each trawl haul with a calibrated Branker bathythermograph, either a SeaBird-19 or SeaBird-39 microbathythermograph (Sea-Bird Electronics, Inc., Bellevue, WA) attached to the net. Depth was also recorded during each trawl haul either off the vessel echosounder or from the microbathythermograph attached to the net. The average bottom temperature and average depth from each trawl haul were used in the analyses. The final environmental variable included in the analyses was the relative position of each trawl haul along the Alaska coastline. Because the major axes of the Alaska coastline are from south to north in the southeastern Gulf of Alaska and from east to west in the remainder of the Gulf of Alaska and Aleutian Islands (Fig. 1), a reference point was chosen to standardize the spatial patterns in trawl hauls. The reference point was chosen in the central Gulf of Alaska at the eastern side of Hinchinbrook Island, (146.08°W, 60.37°N). The distance from this point to each trawl haul provided the change in spatial distribution (both by latitude and longitude) of rockfish species and the variable is hereafter referred to as the position of each trawl. Thus, a negative position indicates a trawl haul occurring in southeastern Alaska, and a positive position indicates a trawl haul occurring west of Hinchinbrook Island. Although geographical position is not actually an environmental variable, it was used as a proxy for longitudinal and latitudinal gradients that affect fish distribution and ranges.

Data analyses

In every bottom trawl haul, the CPUE of each rockfish species was divided into adult and juvenile stages by fish length (Table 2). The juvenile stage was broadly defined to include all subadult fish with lengths less than the size at 50% maturity from literature sources (Paraketsov, 1963; McDermott, 1994; NPFMC, 1998, 2005; Love et al., 2002; Pearson and Gunderson, 2003). The adult rockfish of each species were further divided into male and female CPUE components. Trawl hauls from which no length or sex data were collected were eliminated from the analyses for that species. Species for which catches occurred in fewer than 100 trawl hauls were also excluded from the analyses. For each trawl haul, these divisions resulted in three estimates of CPUE for each species: juveniles, adult females, and adult males.

Table 2

Species of rockfish captured in the Gulf of Alaska and Aleutian Islands trawl surveys across all years (1990–2005). The number captured in all years combined, the number of trawl hauls with catch, and the length distributions (FL, in mm) of juvenile and adult rockfish captured in the bottom trawl surveys are also provided. Dashed lines indicate either no catch in that category or insufficient length data were collected to distinguish juveniles and adults.

Species	Common name	No. captured	No. of trawl hauls with catch	Juvenile length distribution	Adult length distribution
Sebastes alutus	Pacific ocean perch	1,651,753	3059	40–250	250–620
Sebastes aleutianus	Rougheye rockfish	36,250	1894	50–439	439–820
Sebastes polyspinis	Northern rockfish	459,372	1547	50–361	361–500
Sebastolobus alascanus	Shortspine thornyhead	171,405	1515	40–215	215–770
Sebastes borealis	Shortraker rockfish	14,549	676	50–449	449–1030
Sebastes variabilis	Dusky rockfish	22,622	633	130–428	428–560
Sebastes babcocki	Redbanded rockfish	2985	509	110–420	420–630
Sebastes variegatus	Harlequin rockfish	28,834	462	60–230	230–420
Sebastes zacentrus	Sharpchin rockfish	63,343	442	Females 70–265, Males 70–240	Females 265–660, Males 240–660
Sebastes brevispinis	Silvergray rockfish	11,279	340	Females 150–415, Males 150–395	Females 415–720, Males 395–720
Sebastes helvomaculatus	Rosethorn rockfish	2447	158	100–215	215–360
Sebastes proriger	Redstripe rockfish	17,868	151	Females 100–290, Males 100–280	Females 290–480, Males 280–480
Sebastes ruberrimus	Yelloweye rockfish	287	125	Females 90–450, Males 90–540	Females 450–740, Males 540–740
Sebastes elongatus	Greenstriped rockfish	750	77	Females 100–220, Males 100–240	Females 220–380, Males 240–380
Sebastes ciliatus	Dark rockfish	1607	65	210–428	428–500
Sebastolobus altivelis	Longspine thornyhead	4463	46	60–190	190–340
Sebastes wilsoni	Pygmy rockfish	514	44	—	—
Sebastes crameri	Darkblotched rockfish	122	43	Females 120–390, Males 120–370	Females 390–500, Males 370–500
Sebastes melanops	Black rockfish	542	34	230–400	400–590
Sebastes maliger	Quillback rockfish	98	30	230–290	290–480
Sebastes reedi	Yellowmouth rockfish	690	20	Females 240–380, Males 240–370	Females 380–550, Males 370–550
Sebastes pinniger	Canary rockfish	182	20	Females 390–510, Males 390–430	Females 510–630, Males 430–630
Sebastes diploproa	Splitnose rockfish	55	20	90–270	270–270
Sebastes flavidus	Yellowtail rockfish	423	17	Females 330–405, Males 330–380	Females 405–580, Males 380–580
Sebastes entomelas	Widow rockfish	86	14	Females 350–365	Females 365–570, Males 345–570
Sebastes paucispinis	Bocaccio	9	8	—	690–720
Adelosebastes latens	Aleutian scorpionfish	6	3	—	—
Sebastes emphaeus	Puget Sound rockfish	11	2	—	170–180
Sebastes saxicola	Stripetail rockfish	9	2	—	100–270
Sebastolobus macrochir	Broadfin thornyhead	4	2	—	—
Sebastes miniatus	Vermilion rockfish	2	1	—	—
Sebastes nigrocinctus	Tiger rockfish	1	1	—	—

In order to determine the species composition of rockfish assemblages, the CPUE-weighted distribution of each of the species subgroups was computed for each environmental variable with the formulation given in May (1973) and Murawski and Finn (1988) (Fig. 2). A weighted mean value for each environmental variable

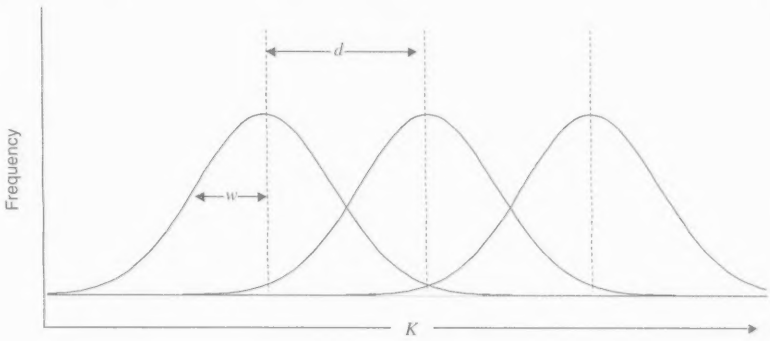

Figure 2

Theoretical distribution of three species along an environmental gradient (K). In this study, K was depth, temperature, or distance. The value w is the standard deviation of the resource utilization curve for a single species and d is distance between the weighted means for two species along a resource continuum. Reproduced from May (1973).

(depth, temperature, and position) was computed as

$$Mean = \frac{\sum(f_i x_i)}{\sum f_i},$$

where f_i = the CPUE of each rockfish species group in tow i; and
x_i = the value of the environmental variable at tow i.

The weighted standard deviation (SD) was then computed as

$$SD = \sqrt{\frac{\left(\sum\left(f_i x_i^2\right)\right) - \left(\left(\sum f_i\right) * mean^2\right)}{\left(\sum f_i\right) - 1}}.$$

These calculations yielded the niche dimensions for each species group defined along each of the three environmental gradients.

The overlap of each species group across each environmental gradient (A) can then be calculated as

$$A_{ij} = C_{ij} \exp\left[\frac{-d^2}{2\left(w_i^2 + w_j^2\right)}\right],$$

where the normalization constant (C_{ij}) is calculated by

$$C_{ij} = \sqrt{\frac{2w_i w_j}{\left(w_i^2 + w_j^2\right)}};$$

where d = the distance between means for a pair of species i and j;
w_i = the standard deviation (SD) for species i; and
w_j = the SD for species j (Murawski and Finn, 1988).

Overlap indices for each variable were calculated for each species and within each species, by the groupings of males, females, and juveniles. The overlaps between males and females were first examined and if the overlap index was greater than 0.9 across all three environmental gradients, these males and females were combined and the means and SDs for each environmental gradient were recalculated. The resulting groupings (adults and juveniles) were then compared and, again, where the indices exceeded 0.9, the catches for the entire species (all size and sex classes) were combined and the means and SDs for each environmental gradient were recalculated.

Finally, the overlap indices were compared to determine the amount of separation among both species and the remaining groupings by size and sex. The multinomial intersection in the overlap indices across the three environmental gradients was calculated by multiplying the individual overlap coefficients together. This was used as a measure of the relative similarity in environmental preferences computed for each pair of species subgroups and resulted in a matrix of overlap coefficients for all species-group pairs. The matrix was then clustered into assemblages with similar distributions across environmental gradients by using Primer Analysis software (PRIMER-E Ltd., Plymouth, UK). The combined overlap index was used as a measure of similarity and the average cluster linkage method was used to determine the species composition of rockfish

Table 3

The estimated mean weighted values and niche width (w) across each of the three resource gradients (position, depth, and temperature) for the species-subgroups examined in this analysis. Although the species were initially split into male, female, and juvenile components, they were recombined if overlaps within a species (i.e., between sexes or between juveniles and adults) were greater than 0.9 across all three environmental variables.

			Position (km)		Depth (m)		Temperature (°C)	
Species	Common name	Group	mean	w	mean	w	mean	w
Sebastes variabilis	Dusky rockfish	All	757	780	141.3	57.0	5.4	0.9
Sebastes variegatus	Harlequin rockfish	All	200	1124	159.8	50.3	5.6	0.7
Sebastes polyspinis	Northern rockfish	Adults	1265	818	134.1	54.4	5.0	0.9
		Juveniles	1819	1180	137.6	56.0	4.7	1.0
Sebastes alutus	Pacific ocean perch	Adults	1205	1176	211.8	75.9	4.7	0.9
		Juveniles	857	1231	164.2	47.9	5.1	0.9
Sebastes babcocki	Redbanded rockfish	All	−443	1532	232.5	78.5	5.4	0.6
Sebastes proriger	Redstriped rockfish	All	−676	1720	193.8	42.3	5.6	0.6
Sebastes helvomaculatus	Rosethorn rockfish	All	−779	1760	215.1	54.7	5.6	0.6
Sebastes aleutianus	Rougheye rockfish	Adults	1112	1043	315.7	164.6	4.4	1.0
		Juveniles	685	987	244.3	112.9	5.0	0.9
Sebastes zacentrus	Sharpchin rockfish	All	−430	1482	195.9	45.9	5.6	0.6
Sebastes borealis	Shortraker rockfish	All	1325	1124	354.4	194.5	4.2	1.1
Sebastolobus alascanus	Shortspine thornyhead	All	468	1160	318.4	192.9	4.7	0.9
Sebastes brevispinis	Silvergray rockfish	Adults	−713	1737	202.4	49.1	5.7	0.7
		Juveniles	−186	1319	153.0	54.2	6.0	1.0
Sebastes ruberrimus	Yelloweye rockfish	All	66	1101	143.8	45.8	5.7	0.7

assemblages that had similar distributions along the environmental gradients. The combined overlap indices for each species pair were also compared to the frequency of co-occurrence for the species pair in trawl hauls by using linear regression to determine if the distribution of species across environmental variables was directly linked to their co-occurrence in trawl hauls.

Results

There was little difference in the distributions of the examined rockfish species among sexes. For all species, the overlap indices exceeded 0.9 across all three environmental gradients between males and females and, thus, the CPUE data were combined across sexes. Some differences between adults and juveniles were observed in their distributions across all three environmental variables (Table 3). Juvenile Pacific ocean perch (POP) (*Sebastes alutus*) and silvergray rockfish (*S. brevispinis*) were distributed at shallower depths than were adults of the same species. There was also a distinct separation between juvenile and adult rougheye rockfish (*S. aleutianus*) along the temperature gradient; juveniles were found at slightly higher temperatures than were adults. Juvenile northern rockfish (*S. polyspinis*) were found farther west (approximately 600 km) along the Alaska Peninsula than were adults. In total, these preliminary analyses indicated that there were four species where juveniles and adults were found to be separate and nine species that did not have different distributions between either sexes or life stages for any of the three environmental gradients. As a result, 17 species subgroups were analyzed (Table 3).

The cluster analysis resulted in five assemblages of rockfish species subgroups (Fig. 3). There was a relatively shallow-water assemblage (Aleutian Islands-shelf) containing northern rockfish, juvenile POP, and dusky rockfish (*S. variabilis*). These species had mean weighted depths from 134 to 164 m and were widely distributed around the northern Gulf of Alaska and Aleutian Islands (mean weighted distances from 757 to 1819 km). A similar assemblage (central Gulf of Alaska-shelf) had mean weighted depths from 144 to 160 m and was distributed from 200 to −186 km. This assemblage contained three species subgroups: yelloweye rockfish (*S. ruberrimus*), harlequin rockfish (*S. variegatus*), and juvenile silvergray rockfish. The third assemblage (southeastern Alaska-break) consisted of a group of species found predominantly in southeastern Alaska (mean weighted distance −430 to −779) at depths centered around 208 m. These species included adult silvergray rockfish, redbanded rockfish (*S. babcocki*), rosethorn rockfish (*S. helvomaculatus*), sharpchin rockfish (*S. zacentrus*), and redstripe rockfish (*S. proriger*). The

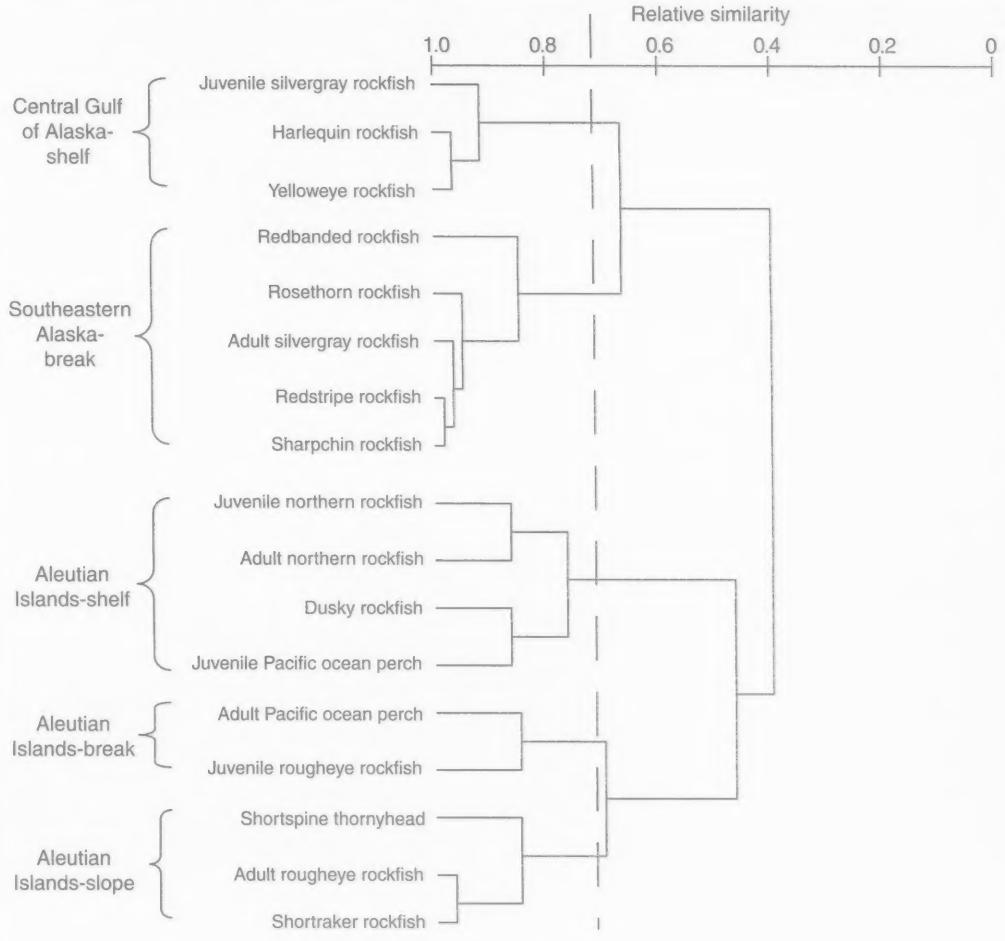

Figure 3

The results of cluster analysis of rockfish showing relative similarity amongst species-subgroups. The *x*-axis shows the relative similarity amongst species derived from the multinomial overlap indices among species-group pairs along the three environmental gradients (depth, position, and temperature). The dashed line (0.73) is where rockfish species assemblages were defined based on a similarity of 0.9 across the three environmental gradients.

fourth assemblage (Aleutian Islands-break) included juvenile rougheye rockfish and adult POP. These species were distributed at the shelf break at depths of 244 and 212 m, in the north Gulf of Alaska and Aleutian Islands (mean weighted distances 1205 and 685 km). A final assemblage (Aleutian Islands-slope) was composed of adult rougheye rockfish, shortraker rockfish (*S. borealis*), and shortspine thornyhead (*Sebastolobus alascanus*). These species were generally distributed in the north Gulf of Alaska and Aleutian Islands, at depths from 318 to 355 m. Bivariate plots of the three environmental variables indicate that the assemblages had very different distributions across the depth and position variables, and less distinct separation around the temperature variable (Fig. 4). There were clear lines of division along the depth variable between shelf and shelf break assemblages at 180 m, and between shelf break and slope assemblages at 275 m. There were also divisions along the position variable between southeastern Alaska species, central Gulf of Alaska species, and the Aleutian Island species at approximately Icy Strait (–350 km) and Seward, Alaska (250 km).

According to the trawl survey CPUE, the most abundant 10 species subgroups captured were adult POP, shortspine thornyhead, juvenile POP, juvenile northern rockfish, juvenile rougheye rockfish, adult northern

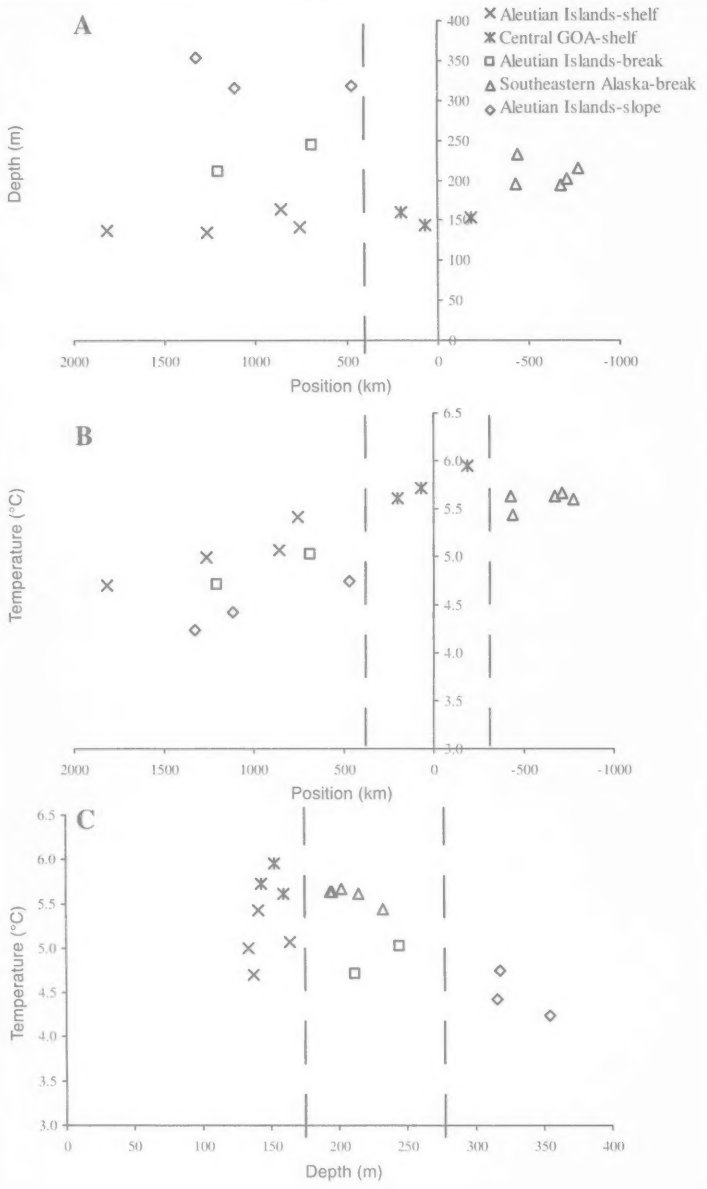

Figure 4

Plots of mean weighted (by catch per unit of effort) distributions of each rockfish species-group (n=17) along three environmental variables. Mean weighted distributions of rockfish species-groups are shown for (**A**) depth versus position, (**B**) temperature versus position, and (**C**) temperature versus depth. Position is the distance from Hinchinbrook Island, Alaska; positive values are west of this central point in the trawl surveys and negative values are southeastward. Dashed lines indicate break points in the mean-weighted environmental variables. Symbols indicate the assemblage membership (from Fig. 3) of each species-group as belonging to the Aleutian Islands-shelf, central Gulf of Alaska (GOA shelf), Aleutian Islands-break, southeastern Alaska-break, or Aleutian Islands-slope assemblage.

rockfish, adult rougheye rockfish, shortraker rockfish, sharpchin rockfish, and dusky rockfish. For these species the co-occurrence in trawl survey catches had a strong linear relationship to the amount of overlap in their distributions across environmental variables, and over 50% of the variance in co-occurrence was explained by species group overlap (Fig. 5). When all species subgroups were considered, the relationship was significant, but the overlap index explained only 32% of the variance in co-occurrence among pairs of species subgroups. This demonstrates that the co-occurrence of rockfish in the trawl survey data is positively correlated to their overlap in environmental preferences.

Discussion

The method used in this study provided resolution of the species composition of rockfish assemblages across large-scale environmental gradients that influence fish distribution (depth and geographical position). The results of these analyses were similar to findings on fish assemblages in other areas. Rockfish (and other species) on the west coast of North America distribute themselves by depth and latitude into distinct assemblages (Weinberg, 1994; Williams and Ralston, 2002; Tolimieri and Levin, 2006). In the Gulf of Alaska, an analysis conducted on 72 groundfish species (including rockfish species) with data from five NMFS trawl surveys revealed that the major gradients for variation in species diversity were depth and alongshore distance, whereas temperature and temporal gradients had only minor effects on species composition (Mueter and Norcross, 2002). As in the current study, Mueter and Norcross (2002) and Williams and Ralston (2002) found a peak in groundfish species richness near the shelf break (200 m), in the region of overlap between shallower species and those occurring at deeper depths.

The method of defining rockfish assemblages described here is very

different from more commonly used methods where trawl survey catches or stations with similar components are clustered together. More commonly used approaches define assemblages by comparing patterns of catch by species in trawl hauls (i.e., Weinberg, 1994; Williams and Ralston, 2002; Zimmermann, 2006). Although these methods are highly effective for determining patterns in catches, they typically are based on complex analyses such as nonmetric multidimensional scaling, principle components, and cluster analyses that can make interpretation difficult. Determining the scaling method to apply to catch data for abundant versus rare species, the patchy distribution of some species, and inherent differences in catchability (such as between small and large fish of the same species) are all problems that must be addressed with these methods. By first defining the relationship of a species to environmental variables, and then comparing the parameters of that relationship to parameters for other species or life history stages, this analysis method may avoid some of those potential pitfalls. For example, the absolute abundance or catchability should not matter in the identification of the correct assemblage membership for a species. If the proper distribution of a species along a depth gradient is known from the trawl data; the species will be placed within a group of species with similar depth distributions regardless of its total abundance.

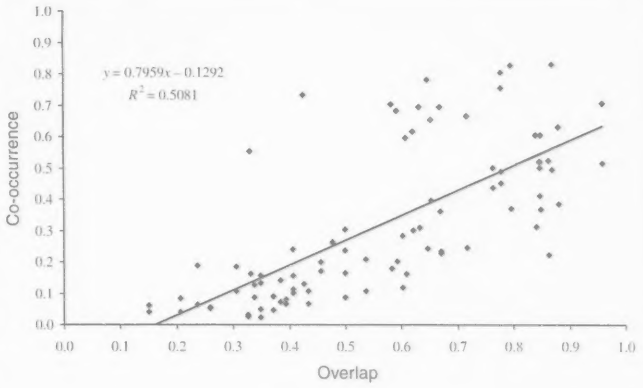

Figure 5

Frequency of co-occurrence of species in trawl hauls versus combined multinomial overlap index. Data are shown for the top 10 species-subgroups in terms of total catch per unit of effort for the Gulf of Alaska and Aleutian Island trawl surveys, and each dot represents a comparison of species-groups (n=90).

The issue of whether trawl survey data can be used to determine the underlying relationship of rockfish species to large-scale environmental gradients may have some limitations. Less sampling effort was directed at shallow inshore depths (0–50 m) than at greater depths; therefore shallow-water species were likely under-represented in the catches. Although this analysis included three environmental gradients, there are obviously more variables needed to fully describe the niche dimensions for any of the rockfish species. One important feature that was omitted from this analysis was the effect of small-scale habitat features on rockfish distribution. Variability in rockfish species assemblages on a small scale is often related to the local habitat, where higher habitat heterogeneity is correlated with higher diversity and abundance (Matthews, 1990; Stein et al., 1992; Yoklavich et al., 2000). The data used in this analysis was collected only on trawlable ground, and large tracts of untrawlable area were unsampled. Species composition and abundance can be starkly different between trawlable and untrawlable locations (Matthews and Richards, 1991). Even within trawlable areas, habitat characteristics such as presence of epibenthic invertebrates can be correlated with increased catches of some life history stages of rockfish, such as juveniles that seek out complex habitat features (Rooper and Boldt, 2005; Rooper et al., 2007). Larger-scale phenomena, such as patterns in prey productivity and the effects of local currents on rockfish distribution, were also absent from this analysis and can certainly affect the distribution of those species that prey on planktonic organisms. Geographical position was used as a proxy for these large-scale phenomena and other unknown variables influencing rockfish distributions. By pooling the data, I did not take into account interannual changes in geographical position due to climate events, such as El Nino or the Pacific decadal oscillation shifts. The effects of El Nino events are typically exhibited through changes in water temperature and there was only a weak response of the species to temperature gradients, and major climate shifts were not detected in Alaska during the years examined. Knowledge of the effects of climate shifts and local habitat features would further improve future assemblage analyses.

Because these analyses were based on rockfish relationships with environmental variables, they should result in predictable species assemblages useful for ecosystem-based management. For example, species that co-occur in trawl catches due to overlapping distributions with environmental variables would be likely to experience similar fishing mortalities. Additionally, based on these assemblage analyses, marine protected areas could be designed for specific depth and geographical areas that would protect portions of rockfish populations. A series of marine protected areas has been suggested for shortraker and rougheye rockfishes in the Gulf of Alaska as a first step towards spatial management (Soh et al., 2000). The spatial and depth separation of juveniles and adults in many of the species examined here could also provide information to implement spatially based management systems for

some species, where bycatch of smaller, immature members of a population would be protected from harvest.

Acknowledgments

This work would not have been possible without the assistance of numerous scientists and fishermen who have collected data on the trawl surveys of the Gulf of Alaska and Aleutian Islands. J. Boldt provided assistance in the use of the PRIMER software in the data analyses. The manuscript was improved with reviews by R. Reuter, D. Somerton, M. Wilkins, M. Zimmermann, and four anonymous reviewers.

Literature cited

Britt, L. L., and M. H. Martin.
2001. Data report: 1999 Gulf of Alaska bottom trawl survey. NOAA Tech. Memo. NMFS-AFSC-121, 249 p.

Field, J. C., and S. Ralston.
2005. Spatial variability in rockfish (*Sebastes* spp.) recruitment events in the California Current System. Can. J. Fish. Aquat. Sci. 62:2199–2210.

Friedlander, A. M., and J. D. Parrish.
1998. Habitat characteristics affecting fish assemblages on a Hawaiian coral reef. J. Exp. Mar. Biol. Ecol. 224:1–30.

Hutchinson, G. E.
1957. Concluding remarks. Cold Spring Harbor Symp. Quant. Biol. 22:415–427.

Ladd, C., G. L. Hunt Jr., C. Mordy, S. Salo, and P. Stabeno.
2005. Marine environment of the eastern and central Aleutian Islands. Fish. Oceanogr. 14:22–38.

Livingston, P. A., K. Aydin, J. Boldt, J. Ianelli, and J. Jurado-Molina.
2005. A framework for ecosystem impacts assessment using an indicator approach. ICES J. Mar. Sci. 62:592–597.

Logerwell, E. A., K. Aydin, S. Barbeaux, E. Brown, M. E. Conners, S. Lowe, J. W. Orr, I. Ortiz, R. Reuter, and P. Spencer.
2005. Geographic patterns in the demersal ichthyofauna of the Aleutian Islands. Fish. Oceanogr. 14:93–112.

Love, M. S., M. H. Carr, and L. J. Haldorson.
1991. The ecology of substrate-associated juveniles of the genus *Sebastes*. Environ. Biol. Fishes 30:225–243.

Love, M. S., M. Yoklavich, and L. Thorsteinson.
2002. The rockfishes of the northeast Pacific, 404 p. Univ. California Press, Berkeley, CA, and Los Angeles, CA.

Matthews, K. R.
1990. A comparative study of habitat use by young-of-the-year, subadult, and adult rockfishes on four habitat types in central Puget Sound. Fish. Bull. 88:223–239.

Matthews, K. R., and L. J. Richards.
1991. Rockfish (*Scorpaenidae*) assemblages of trawlable and untrawlable habitats off Vancouver Island, British Columbia. N. Am. J. Fish. Manag. 11:312–318.

May, R. M.
1973. Stability and complexity in model ecosystems, 265 p. Monographs in population biology—6. Princeton Univ. Press, Princeton, NJ.

McDermott, S. F.
1994. Reproductive biology of rougheye and shortraker rockfish, *Sebastes aleutianus* and *Sebastes borealis*. M. S. thesis, 76 p. Univ. Washington, Seattle, WA.

Methratta, E. T., and J. S. Link.
2006. Associations between surficial sediments and groundfish distributions in the Gulf of Maine-Georges Bank region. N. Am. J. Fish. Manag. 26:473–489.

Mueter, F. J., and B. L. Norcross.
2002. Spatial and temporal patterns in the demersal fish community on the shelf and upper slope regions of the Gulf of Alaska. Fish. Bull. 100:559–581.

Murawski, S. A., and J. T. Finn.
1988. Biological bases for mixed-species fisheries: species co-distribution in relation to environmental and biotic variables. Can. J. Fish. Aquat. Sci. 45:1720–1735.

NPFMC (North Pacific Fishery Management Council).
1998. Stock assessment and Fishery evaluation report for the groundfish resources of the Gulf of Alaska, 32 p. NPFMC, 605 W. 4th Ave, Suite 306, Anchorage, AK 99510.
2005. North Pacific groundfish stock assessment and fishery evaluation reports for 2006, 1188 p. NPFMC, 605 W. 4th Ave, Suite 306, Anchorage, AK 99510.

Paraketsov, I. A.
1963. On the biology of *Sebastodes alutus* of the Bering Sea. *In* Soviet fisheries investigations in the Northeastern Pacific, part I (P. A. Moiseev, ed.), p. 319–327. Available from United States Dep. Commer., Natl. Tech. Inf. Serv., Springfield, VA, as TT67-51203.

Parker, S. J., S. A. Berkeley, J. T. Golden, D. R. Gunderson, J. Heifetz, M. A. Hixon, R. Larson, B. M. Leaman, M. S. Love, J. A. Musick, V. M. O'Connell, S. Ralston, H. J. Weeks, and M. M. Yoklavich.
2000. Management of Pacific rockfish. Fisheries 25(3):22–30.

Pearson, K. E., and D. R. Gunderson.
2003. Reproductive biology and ecology of shortspine thornyhead rockfish, *Sebastolobus alascanus*, and longspine thornyhead rockfish, *S. altivelis*, from the northeastern Pacific Ocean. Environ. Biol. Fishes 67:117–136.

Ralston, S., and D. F. Howard.
1995. On the development of year-class strength and cohort variability in two northern California rockfishes. Fish. Bull. 93:710–720.

Rooper, C. N., and J. L. Boldt.
2005. Distribution of juvenile Pacific ocean perch *Sebastes alutus* in the Aleutian Islands in relation to benthic habitat. Alaska Fish. Res. Bull. 11:102–112.

Rooper, C. N., J. L. Boldt, and M. Zimmermann.
2007. An assessment of Pacific ocean perch (*Sebastes alutus*) habitat use in a deepwater nursery. Estuarine Coastal Shelf Sci. 75:371–380.

Rooper, C. N., M. Zimmermann, and P. Spencer.
2005. Distribution of flathead sole (*Hippoglossoides elassodon*) by habitat in the eastern Bering Sea. Mar. Ecol. Prog. Ser. 290:251–262.

Soh, S., D. R. Gunderson, and D. H. Ito.
2000. The potential role of marine reserves in the management of shortraker rockfish (*Sebastes borealis*) and rougheye rockfish (*S. aleutianus*) in the Gulf of Alaska. Fish. Bull. 99:168–179.

Stabeno, P. J., J. D. Schumacher, and K. Ohtani.
1999. The physical oceanography of the Bering Sea. *In* Dynamics of the Bering Sea (T. R. Loughlin, and

Ohtani, K., eds.), p. 1–59. Univ. Alaska Sea Grant College Program, AK-SG-99-03, Fairbanks, AK.

Stabeno, P. J., R. K. Reed, and J. M. Napp.
2002. Transport through Unimak Pass, Alaska. Deep-Sea Res. II 49:5919–5930.

Stein, D. L., B. N. Tissot, M. A. Hixon, and W. Barss.
1992. Fish-habitat associations on a deep reef at the edge of the Oregon continental shelf. Fish. Bull. 90:540–551.

Tolimieri, N., and P. S. Levin.
2006. Assemblage structure of eastern Pacific groundfishes on the U.S. continental slope in relation to physical and environmental variables. Trans. Am. Fish. Soc. 135:317–332.

Weinberg, K. L.
1994. Rockfish assemblages of the middle shelf and upper slope off Oregon and Washington. Fish. Bull. 92:620–632.

Williams, E. H., and S. Ralston.
2002. Distribution and co-occurrence of rockfishes (family: Sebastidae) over trawlable shelf and slope habitats of California and southern Oregon. Fish. Bull. 100:836–855.

Yoklavich, M. M., H. G. Greene, G. M. Cailliet, D. E. Sullivan, R. N. Lea, and M. S. Love.
2000. Habitat associations of deep-water rockfishes in a submarine canyon: an example of a natural refuge. Fish. Bull. 98:625–641.

Zenger, H. H., Jr.
2004. Data report: 2002 Aleutian Islands bottom trawl survey. NOAA Tech. Memo. NMFS-AFSC-143, 247 p.

Zimmermann, M.
2006. Benthic fish and invertebrate assemblages within the National Marine Fisheries Service U.S. west coast triennial bottom trawl survey. Cont. Shelf Res. 26:1005–1027.

Abstract—In stock assessments, recruitment is typically modeled as a function of females only. For protogynous stocks, however, disproportionate fishing on males increases the possibility of reduced fertilization rates. To incorporate the importance of males in protogynous stocks, assessment models have been used to predict recruitment not just from female spawning biomass (S^f), but also from that of males (S^m) or both sexes (S^b). We conducted a simulation study to evaluate the ability of these three measures to estimate biological reference points used in fishery management. Of the three, S^f provides best estimates if the potential for decreased fertilization is weak, whereas S^m is best only if the potential is very strong. In general, S^b estimates the true reference points most closely, which indicates that if the potential for decreased fertilization is moderate or unknown, S^b should be used in assessments of protogynous stocks. Moreover, for a broad range of scenarios, relative errors from S^f and S^b occur in opposite directions, indicating that estimates from these measures could be used to bound uncertainty.

Stock assessment of protogynous fish: evaluating measures of spawning biomass used to estimate biological reference points

Elizabeth N. Brooks (contact author)

Email addresss: Liz.Brooks@noaa.gov
National Marine Fisheries Service, NOAA
Southeast Fisheries Science Center
75 Virginia Beach Drive
Miami, Florida 33149

Present address: National Oceanic and Atmospheric Administration
National Marine Fisheries Service, Northeast Fisheries Science Center
166 Water Street
Woods Hole, Massachusetts 02543

Kyle W. Shertzer

National Marine Fisheries Service, NOAA
Southeast Fisheries Science Center
Center for Coastal Fisheries and Habitat Research
101 Pivers Island Road
Beaufort, North Carolina 28516

Todd Gedamke

Virginia Institute of Marine Science
College of William and Mary
P.O. Box 1346, Route 1208 Greate Road
Gloucester Point, Virginia 23063

Douglas S. Vaughan

National Marine Fisheries Service, NOAA
Southeast Fisheries Science Center
Center for Coastal Fisheries and Habitat Research
101 Pivers Island Road
Beaufort, North Carolina 28516

Manuscript submitted 25 April 2007.
Manuscript accepted 1 August 2007.
Fish. Bull 106:12–23 (2008).

The views and opinions expressed or implied in this article are those of the author and do not necessarily reflect the position of the National Marine Fisheries Service, NOAA.

Populations persistence requires that losses from mortality must at least be matched by gains from the production of new individuals (i.e., recruitment). The theory of stock reproduction relates recruitment to total egg production (Beverton and Holt, 1957). In practice, however, stock assessment often relates recruitment to the biomass of mature females rather than to total egg production. The two predictors are functionally similar if egg production of a mature female is highly correlated to body mass (Rothschild and Fogarty, 1989), as observed or assumed for many stocks.

With the use of either predictor—biomass of mature females or total egg production—the proportion of eggs fertilized is assumed to be constant. This assumption is believed to be valid for stocks with little fluctuation in sex ratio, as in most gonochoristic stocks (fish that remain the same sex throughout life). However, this assumption may be inappropriate for protogynous stocks (fish that begin life as female and later become male). Under natural mortality alone, sex ratios of protogynous stocks are expected to be skewed toward females (Allsop and West, 2004). The addition of fishing mortality could skew the ratio even further (Coleman et al., 1996; McGovern et al., 1998; Armsworth, 2001), particularly

if fishing preferentially removes males by targeting larger (older) individuals, for example through gear selectivity or management regulations. A disproportionate reduction of males could lower fertilization rates if not enough males are available to fertilize the eggs of mature females (i.e., the reduction could result in sperm limitation).

The possibility of reduced fertilization rates raises the question of whether protogynous stocks are more susceptible than gonochoristic stocks to overexploitation. Several studies have concluded that protogynous stocks are more susceptible, based on hypothesized patterns of reproduction, sexual transition, and fishing (Huntsman and Schaaf, 1994; Alonzo and Mangel, 2004, 2005). At least one study (Bannerot et al., 1987) indicates that, under some conditions, protogynous stocks are more resilient to exploitation. Either way, management of protogynous stocks merits the consideration of unconventional techniques (Shepherd and Idoine, 1993; Armsworth, 2001; Heppell et al., 2006).

In the United States, fishery management under the Magnuson-Stevens Fishery Conservation and Management Reauthorization Act of 2006 emphasizes the concept of maximum sustainable yield (MSY). Internationally, the use of MSY as a reference point for evaluating sustainable development is well established (FAO, 1999). Standard MSY-based biological reference points—the benchmarks used to gauge stock status—include fishing mortality rate at MSY (F_{MSY}), spawning biomass at MSY (S_{MSY}), and *MSY* itself. All depend fundamentally on the spawner-recruit relationship, which is typically a function of spawning biomass (S).

In conventional stock assessments, S is computed from females only (S^f), and fertilization rate is implicitly assumed to be constant. Some assessments of protogynous stocks have emphasized the importance of males, by computing S from spawning biomass of males alone (S^m) or from the sum of both sexes (S^b) (Punt et al., 1993; Vaughan et al., 1995). Early use of S^b was in per-recruit analyses (Vaughan et al., 1992; Punt et al., 1993; Vaughan et al., 1995), and later, in spawner-recruit relationships (Vaughan and Prager, 2001).

The measure of spawning biomass—S^f, S^m, or S^b—used in an assessment plays a key role in estimates of biological reference points, and thus in subsequent management advice. For example, in U.S. fishery management, a stock is considered to be overfished if the most recent estimate of S is sufficiently less than S_{MSY}. (The level associated with "sufficiently" varies by stock, but the criterion to determine that level often takes natural mortality into account.) Declaring a stock overfished triggers development of a rebuilding plan to increase the stock to S_{MSY}. In general, the choice of measure used to represent spawning biomass influences analyses on which management is based, including any estimate of stock status. Although various measures are used in assessments, the properties of reference points estimated from S^f, S^m, or S^b have not been examined comprehensively.

We use simulations to evaluate the performance of each measure of spawning biomass. To begin, we simulate a protogynous stock over an array of biological and fishery characteristics and calculate biological reference points for each case. Then we apply an assessment model to estimate those same reference points using each of the three S measures. The estimated reference points are compared to their simulated counterparts to quantify estimation error. These results are intended to help stock assessment biologists identify a robust measure of spawning biomass that is appropriate for the protogynous stock being modeled.

Materials and methods

Two deterministic models were constructed, both structured by age and sex, to describe a protogynous stock. The first, referred to as the simulation model, was considered a representation of the real world. It was used to compute true values of MSY-based biological reference points (BRPs), which determine stock status. The second, the assessment model, was used to estimate those same reference points. Both models included age-specific values of maturity, mortality, sex ratio, and size. They differed only in computation of recruitment: the simulation model derived recruits directly from fertilized eggs, and the assessment model derived recruits indirectly from the spawning biomass of males, females, or both. Thus, with the assessment model the common assumption is that fertilization rates are static. Because that assumption creates the only structural difference between the simulation and assessment models, the source of any estimation error of computed quantities (BRPs) could be isolated and the most robust measure of spawning biomass could be identified. In this sense, estimation error refers to error caused by model misspecification, rather than from fitting data. To quantify error systematically, BRPs were computed and estimated under many combinations of biological parameters and fishery conditions, as described below.

Simulation model

This study used an age-structured population model to compute the number of individuals at age (N_a),

$$N_a = \begin{cases} N_{a-1}e^{-(M+F_{a-1})} & 2 \le a < 50 \\ N_{a-1}e^{-(M+F_{a-1})}/(1-e^{-(M+F_a)}) & a = 50 \end{cases}, \qquad (1)$$

where N_1 represents the number of recruits (described below), and the maximum age (50) was treated as a plus group. The parameter M is natural mortality rate (constant across age), and F_a is fishing mortality rate at age, equal to the product of total fishing mortality rate (F) and selectivity at age (s_a). Selectivity was assumed to be knife-edge, that is, $s_a = 0$ for all ages younger than the first vulnerable age class (α_s) and $s_a = 1$ otherwise.

Length at age (l_a) was modeled with the von Bertalanffy equation (von Bertalanffy, 1938), $l_a=L_\infty(1-e^{-K(a-t_0)})$, in which L_∞ is the asymptotic length, K is the growth coefficient, and t_0 is the theoretical age at which length is zero ($t_0=0$ assumed arbitrarily). Length at age was converted to weight at age (w_a) by the allometric relationship

$$w_a = \upsilon_1 l_a^{\upsilon_2}, \tag{2}$$

where υ_1 and υ_2 are constants under the assumption of isometric growth. This relationship was also used to model fecundity at age (e_a, eggs per mature female),

$$e_a = \varepsilon_1 l_a^{\varepsilon_2}, \tag{3}$$

where ε_1 and ε_2 are constants. Fecundity often scales nearly linearly with weight, such that $\varepsilon_2 \approx \upsilon_2 \approx 3$.

Transition from female to male was modeled as a logistic function of age,

$$p_a = \frac{1}{1+e^{-\beta_p(a-\alpha_p)}} \tag{4}$$

with p_a the proportion male at age, β_p the slope of sexual transition, and α_p the age at 50:50 sex ratio. The same function was used to model female maturity at age (g_a), with parameter β_g = the slope, and α_g = the age at 50% maturity. All males were considered to be mature on the basis of low numbers of transitional fish observed in the field and the apparent ability to complete sex transition between spawning seasons (Collins et al., 1987).

Total egg production (E) was determined by the product of mature females and eggs per female, summed across ages,

$$E = \sum_a N_a(1-p_a)g_a e_a. \tag{5}$$

Because fertilization may become limited by sperm availability, fertilization rate (f) was modeled as a function of sex ratio,

$$f(x_F) = \frac{4\kappa x_F}{(1-\kappa)+(5\kappa-1)x_F}. \tag{6}$$

In Equation 6, x_F is the ratio of the proportion of males in the population (in numbers) under fishing rate F to the proportion males at the unfished level, a measure of male depletion ($x_F \in [0,1]$). The fertilization rate function f is a form of the Beverton-Holt recruitment model scaled to one for $x_F = 1$. It has similar shape to the fertilization function of Heppell et al. (2006) and has the following desirable properties. In the absence of males, f takes its minimum value of 0.0, and at the unfished sex ratio, f takes its maximum value, which is set arbitrarily to 1.0. In between these extrema, fertilization rate depends on the steepness parameter

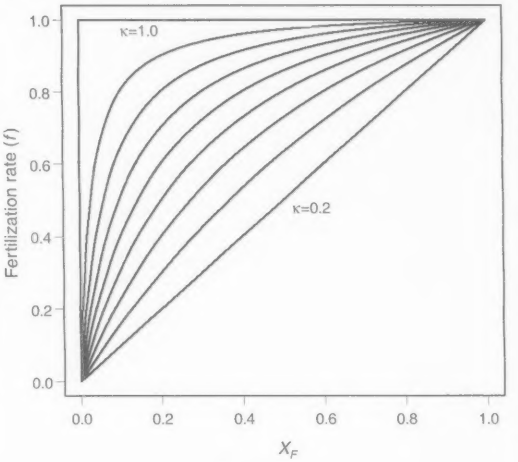

Figure 1

Fertilization rate (f) as a function of the ratio x_F, where x_F is defined as the proportion of males (in numbers) under fishing rate F to proportion of males (in numbers) at the unfished level. Fertilization rate is shown for all levels of steepness in fertilization considered in simulations (κ=0.2, 0.3, ...,1.0).

κ, which can range from 0.2 to 1.0 (Fig. 1). A high value of κ corresponds to a stock that can maintain its fertilization rate when males are scarce. In terms of life histories, one might expect group spawners to have higher κ than pair spawners. The number of fertilized eggs (ψ) under fishing rate F was computed as the product of fertilization rate and total egg production ($\psi=f(x_F)E$).

Recruitment was computed from fertilized eggs ($R(\psi)$) with the Beverton-Holt spawner-recruit model,

$$R(\psi) = \frac{4hR_0\psi}{R_0\varphi_0(1-h)+(5h-1)\psi}. \tag{7}$$

In this parameterization (Mace and Doonan, 1988), φ_0 is the unfished level of fertilized eggs per recruit, R_0 is unfished recruitment, and h is steepness (analogous to κ in the fertilization function).

Parameter values

Based on life-history theory and empirical study of protogynous fish, values of several parameters were related to natural mortality rate in order to avoid untenable parameter combinations and to maintain generality of results. Gardner et al. (2005) reported relationships between growth rate and natural mortality ($\bar{K}=0.64M$), age at 50% maturity and natural mortality ($\bar{\alpha}_g=0.96/M$), and size at 50:50 sex ratio and asymptotic length ($\bar{L}_{50}=0.77L_\infty$). The results from Gardner et al. (2005)

Table 1

Model parameters. Values in braces are levels used for the primary analysis, where the assessment model did not account for dynamics of fertilization.

Parameter	Value(s)	Description
M	{0.1, 0.2, 0.3}	Natural mortality rate
L_∞	1000	Asymptotic maximum length
K	0.64M	Growth coefficient (Gardner et al., 2005)
$\bar{\alpha}_g$	0.96/M	Mean age at 50% maturity (Gardner et al., 2005)
c_g	{0.75, 1.0, 1.25}	Age at 50% maturity relative to the mean
α_g	$\alpha_g=c_g\bar{\alpha}_g$	Age at 50% maturity
β_g	{0.2, 0.4, 0.8, 1.6}	Slope of logistic maturity function
α_p	2.3/M	Age at 50:50 sex ratio (Gardner et al., 2005)
β_p	{0.2, 0.4, 0.8, 1.6}	Slope of logistic sex-transition function
c_s	{0.75, 1.0, 1.25}	Age at selection relative to maturity
α_s	$\alpha_s=c_s\alpha_g$	Age at selection
υ_1	1×10^{-8}	Weight-at-age coefficient
υ_2	3.0	Weight-at-age exponent
ε_1	1.0	Fecundity-at-age coefficient
ε_2	3.0	Fecundity-at-age exponent
κ	{0.2, 0.3, ..., 1.0}	Steepness of fertilization function (f)
h	{0.4, 0.6, 0.8}	Steepness of spawner-recruit function
R_0	1×10^6	Unfished recruitment

were used to describe K and α_g, and to derive the age at 50:50 sex ratio by substituting $\bar{K}$ and $\bar{L}_{50}$ into the von Bertalanffy model and solving for a (α_p=2.3/M). Remaining parameters were set to values or ranges considered reasonable (Table 1). Note that results will be independent of ε_1, υ_1, and L_∞ because these parameters are merely scalars.

Biological reference points (BRPs)

This study focused on four BRPs: maximum sustainable yield (MSY) and the associated fishing mortality rate (F_{MSY}), spawning biomass (S_{MSY}), and spawning potential ratio (SPR_{MSY}), defined as fertilized eggs per recruit in relation to that at the unfished level. True values of BRPs were computed numerically from the simulation model by maximizing equilibrium yield computed over a range of F at intervals of 0.01. For each F, equilibrium yield (Y_F) was calculated from the Baranov catch equation (Baranov, 1918)

$$Y_F = \sum_a \frac{F_a}{Z_a} N_a w_a \left(1 - e^{-Z_a}\right). \quad (8)$$

The MSY was defined as maximum Y_F, F_{MSY} as the F resulting in MSY, and SPR_{MSY} as the corresponding spawning potential ratio (SPR). Unlike those three reference points, the value of S_{MSY} is specific to the measure of spawning biomass (f, m, and b) and was therefore computed as such,

$$\begin{aligned} S^f_{MSY} &= \sum_a \bar{N}_a (1-p_a) g_a w_a \\ S^m_{MSY} &= \sum_a \bar{N}_a p_a g_a w_a \\ S^b_{MSY} &= \sum_a \bar{N}_a g_a w_a \end{aligned} \quad (9)$$

where $\bar{N}_a$ = the equilibrium number at age at MSY. Although fertilized eggs, rather than spawning biomass, determined recruitment in the simulation model, values of $S^{f,m,b}_{MSY}$ were computed because of the key role that S_{MSY} plays in determining whether a stock is overfished. Equation 9 provided values in units comparable to estimates from the assessment model, where spawning biomass did determine recruitment.

Assessment model and estimation of biological reference points

The assessment model was structurally identical to the simulation model with the single exception that recruits were computed from a measure of spawning biomass (mature females, males, or both), rather than from fertilized eggs. This difference represents a simplifying assumption common to almost all assessment models. Its inclusion allowed examination of how that assumption affects estimates of BRPs and identification of a robust measure of spawning biomass.

In the assessment model, recruitment (R) was computed from spawning biomass (S=S^f, S^m, or S^b) by using the same functional form as Equation 7,

$$R(S)=\frac{4hR_0S}{R_0\phi_0(1-h)+(5h-1)S}, \quad (10)$$

where R_0 = unfished recruitment;
h = steepness; and
ϕ_0 = unfished spawning biomass per recruit.

Because fertilization rate is not considered in the assessment model, it is assumed that κ=1.0 always. Given the spawner-recruit relationship of Equation 10, we computed catch per F assuming equilibrium population structure. The estimate of MSY ($\hat{MSY}$) was taken to be maximum catch, and $\hat{F}_{MSY}$ was the F that produced that maximum. Also estimated were the associated spawning biomass ($\hat{S}_{MSY}$) and SPR ($\hat{SPR}_{MSY}$). These four estimates of BRPs were computed by using each measure of spawning biomass and compared to the true values from the simvulation model.

Scope of analyses

These analyses were designed to quantify systematically the magnitude and direction of error of estimated BRPs. Initially, only model misspecification was considered. This part of the study is described as the primary analysis, because it addresses the main goal of isolating error associated with predicting recruits from spawning biomass. Subsequently, additional sources of error were introduced into the assessment model, described as the secondary analysis. Primary and secondary analyses are detailed below.

Primary analysis—model misspecification

The assessment model was misspecified in the sense that it did not explicitly account for dynamics of fertilization. Otherwise, the simulation and assessment models were identical, both in structure and in parameter values. These values were assigned according to a factorial design that included seven factors at various levels (Table 1). The factors were natural mortality rate (M, 3 levels), steepness of spawner-recruit function (h, 3 levels), steepness of fertilization function (κ, 9 levels), slope of sex-transition function (β_p, 4 levels), age at 50% maturity in relation to its mean (c_g, 3 levels), slope of maturity function (β_g, 4 levels), and age at selection by the fishery in relation to maturity (c_s, 3 levels). Thus, the simulations covered a wide array of biological and fishery conditions, with n = 11,664 factor-level combinations. At each combination, BRPs were computed with the simulation model, and then estimated with the assessment model by using each of the three measures of spawning biomass (S^f, S^m, S^b).

Secondary analysis—additional misspecifications

Further analysis included additional sources of misspecification. One subset of this analysis examined misspecification of the parameter controlling age at 50:50 sex ratio (α_p). Estimates of this parameter used in an assessment model may be inaccurate because of sampling error or adaptations in response to fishing mortality (Goodyear, 1980; Harris and McGovern, 1997; Barot et al., 2004). Sex transition in the assessment model remained the same (α_p=2.3/M; Eq. 4) but was adjusted in the simulation model by a scalar multiple χ_p (α_p=2.3χ_p/M). In a second subset of this analysis we examined violation in the assessment assumption that fecundity scales linearly with weight. This was accomplished by redefining the fecundity exponent in the simulation model (ε_2=3; Eq. 3) by a scalar multiple χ_e (ε_2=3χ_e), without adjusting the assessment model. For the secondary analysis (Table 2), the remaining model parameter values were as in the primary analysis (Table 1), with the following three exceptions: the slope of maturation was set to a moderate value (β_g=0.8), age at 50% maturity was set to its mean (c_g=1), and age at selection was set to age at 50% maturity (c_s=1). As before, the intent was to characterize error of estimated BRPs and thereby identify robust measures of spawning biomass.

Table 2

Factors (model parameters) and levels (parameter values) of the secondary analysis, where an incorrect value of age at 50:50 sex ratio was assumed in the assessment model or where fecundity was assumed to scale linearly with weight.

Factor	Levels	Description
M	{0.1, 0.2, 0.3}	Natural mortality rate
κ	{0.2, 0.3, ..., 1.0}	Steepness of fertilization function (f)
h	{0.4, 0.6, 0.8}	Steepness of spawner-recruit function
β_p	{0.2, 0.4, 0.8, 1.6}	Slope of logistic sex-transition function
χ_p	{0.75, 1.0, 1.25}	Multiple of age at 50:50 sex ratio (α_p=2.3χ_p/M)
χ_f	{0. 75, 1.0, 1.25}	Multiple of fecundity-at-age exponent (ε_2=3χ_f)

Evaluation of assessment results

Assessment results were evaluated in terms of relative error, i.e., the relative difference between reference points known from the simulation model (Eqs. 8 and 9) and the corresponding estimates from the assessment model. At each combination of factor and level, relative error (RE) was computed as

$$\mathrm{RE}(\hat{BRP}^i)=\frac{\hat{BRP}^i-BRP}{BRP}$$
$$\mathrm{RE}(\hat{S}^i_{MSY})=\frac{\hat{S}^i_{MSY}-S^i_{MSY}}{S^i_{MSY}} \quad (11)$$

Table 3

Summary statistics of relative error (RE) in biological reference points (BRPs) estimated by each measure of spawning biomass. BRPs are maximum sustainable yield (*MSY*) and the corresponding fishing mortality rate (F_{MSY}), spawning biomass ($S^{f,m,b}_{MSY}$), and spawning potential ratio (SPR_{MSY}). Statistics are 25th quantile, 50th quantile (median), 75th quantile, distance covered by interquartile range (IQD), proportion of model runs with relative error greater than zero (RE>0), mean, and standard deviation (SD). Bold font designates for each BRP the median error closest to zero, mean error closest to zero, proportion of positive RE closest to 0.5, smallest IQD, and smallest SD.

BRP	Spawning biomass	25th quantile	50th quantile	75th quantile	IQD	RE>0	Mean	SD
MSY	female	0.02	0.09	0.25	0.23	0.99	0.19	0.25
	male	−0.34	−0.23	−0.14	0.20	0.05	−0.24	**0.14**
	both	−0.15	**−0.07**	0.01	**0.16**	**0.27**	**−0.05**	0.16
F_{MSY}	female	0.06	0.26	0.68	0.62	0.82	0.50	0.63
	male	−0.50	−0.37	−0.25	**0.25**	0.02	−0.36	**0.19**
	both	−0.22	**−0.10**	0.11	0.33	**0.3**	**−0.01**	0.33
S^f_{MSY}	female	−0.11	−0.05	−0.01	**0.10**	0.12	−0.07	**0.07**
S^m_{MSY}	male	0.15	0.33	0.66	0.51	0.94	0.54	1.05
S^b_{MSY}	both	−0.09	**0.01**	0.08	0.17	**0.54**	**0.01**	0.12
SPR_{MSY}	female	0.01	**0.06**	0.18	0.17	0.93	0.14	0.19
	male	−0.24	−0.13	−0.07	0.17	0.06	−0.16	0.13
	both	−0.14	−0.08	−0.03	**0.11**	**0.17**	**−0.08**	**0.11**

where $i \in \{f, m, b\}$ indicates female, male, or both, and *BRP* represents *MSY*, F_{MSY}, or SPR_{MSY}.

When interpreting relative error, one should be aware that RE has no upper bound but has a lower bound of −1 because the BRPs and estimates are always nonnegative. The distribution of relative errors was used to evaluate estimated reference points and thus to provide a general picture of which measure of spawning biomass is most robust.

Analysis of variance (ANOVA) of relative errors was conducted as a form of sensitivity analysis. Factors that explained a significant proportion of total variation represent biological or fishery parameters to which estimates were sensitive. Factors found to be important were then examined in greater detail.

Results

Primary analysis—model misspecification

Aggregated across model runs, variability in estimation error, as indicated by distance covered by interquartile ranges and standard deviations of relative errors, was similar among the three measures of spawning biomass (Table 3). Two exceptions occurred: variability was relatively large when $\hat{F}_{MSY}$ was computed from females only (S^f) and when $\hat{S}_{MSY}$ was computed from males only (S^m).

Estimates of BRPs were closest to the true values (from simulations) when the assessment model counted both males and females (S^b), as indicated by mean and median relative error near zero (Table 3). The assessment model based on females only tended to overestimate F_{MSY}, *MSY*, and SPR_{MSY}, and it tended to underestimate S^f_{MSY} slightly. The assessment model based on males only showed the opposite pattern; more than 90% of relative errors in $\hat{F}^m_{MSY}$, $\hat{MSY}^m$, and $\hat{SPR}^m_{MSY}$ were negative, and more than 90% in $\hat{S}^m_{MSY}$ were positive. Relative error in $\hat{S}^m_{MSY}$ could be quite large when fertilization rates were independent of male availability (κ=1). In those cases, males could be almost completely removed from the simulation model without detriment to the population's persistence, but not from the assessment model based on males only. Consequently, the computation of relative error of $\hat{S}^m_{MSY}$ (Eq. 11) included a denominator that approached zero, which magnified the relative error to values much greater than one. The interquartile range of relative error from S^f and from S^m did not include the value of zero for any reference point, where a relative error of zero would correspond to a perfect estimate (Table 3). These relative errors, with opposite signs, were mediated when both sexes (S^b) defined spawning biomass in the assessment model.

For all measures of spawning biomass, the steepness of the fertilization function (κ) explained more of the variation in estimated BRPs than any other model factor (Table 4). The slope of sex transition (β_p) and steepness of the spawner-recruit function (h) explained much of the remaining variation. The remaining factors explained very little. The residual or unexplained error (Table 4) is attributable to interaction terms, which were not included in the ANOVA.

Relative errors of estimated BRPs were further examined by levels of κ and β_p (Fig. 2, A and B). These two parameters were chosen for related reasons: because es-

Table 4

Sensitivity of relative errors in estimated biological reference points to each model factor in the primary analysis, where the assessment model did not account for dynamics of fertilization. For each reference point (F_{MSY}, $S^{f,m,b}_{MSY}$, *MSY*, and SPR_{MSY}), the measure of spawning biomass (female, male, or both) with the smallest total model error (total SS) demonstrated the least variability (values in italics). Table cells give the proportion of total SS explained by each factor. Values ≥0.1 are indicated by bold font and values ≤0.01, by dashes. The term "Residual" is variation explained by all possible interaction terms. Factors (model parameters) are defined in Table 1.

	F_{MSY}			S^f_{MSY}	S^m_{MSY}	S^b_{MSY}	*MSY*			SPR_{MSY}		
Factor	Female	Male	Both	Female	Male	Both	Female	Male	Both	Female	Male	Both
M	0.03	—	0.02	0.08	—	0.02	0.03	—	—	—	—	—
κ	**0.42**	**0.60**	**0.56**	**0.23**	**0.17**	**0.46**	**0.49**	**0.47**	**0.64**	**0.33**	**0.32**	**0.54**
h	—	0.05	0.07	0.07	0.02	0.05	0.09	**0.28**	0.08	**0.23**	**0.41**	0.06
β_p	**0.16**	0.02	0.08	**0.16**	0.04	**0.10**	**0.11**	0.03	0.02	0.08	—	—
β_g	—	—	—	—	—	—	—	—	—	—	—	—
c_g	0.03	0.03	—	—	0.02	—	—	—	—	—	—	0.02
c_s	0.05	0.09	—	—	0.03	—	—	0.04	—	—	0.02	0.02
Residual	0.31	0.22	0.27	0.45	0.72	0.36	0.27	0.15	0.23	0.34	0.23	0.36
Total SS	4624	*441*	1283	*57*	12,894	179	728	*240*	307	423	183	*144*

timates were sensitive to them (Table 4) and because of their influences on the dynamics of fertilization (Fig. 1). Examining relative error by steepness of fertilization revealed that the most appropriate measure of spawning biomass depended on the level of κ. If male depletion had little effect on fertilization success (κ in the range 0.8–1.0), the conventional measure, S^f, produced estimates with the least error. However, as fertilization became more limited by male depletion ($0.2<\kappa<0.8$), error in estimates from S^f became increasingly more variable and further from the true values. At intermediate values of κ (~0.4–0.7), S^b produced the best estimates. Only for the most limiting values of κ (0.2, 0.3) did S^m appear to be appropriate.

The influence of β_p on fertilization success was perhaps more subtle than that of κ. A shallower slope of sex transition (smaller β_p) provided a broader range of age classes where both males and females were present. This decreased the propensity for fishing-induced male depletion, thereby allowing sex ratio to remain in the range where fertilization rates were relatively high. Conversely, if sex transition occurred across only a few ages (large β_p), disproportionate fishing on males was more likely. The tendency for the depletion of males with a steeper slope of sex transition explains why the assessment model based on S^f performed progressively worse as β_p increased (Fig. 2, A and B). In general, our examination of relative error by slope of sex transition revealed that S^b provided the best estimates.

A consistent pattern in relative errors was that BRPs based on S^f had the opposite sign from those based on S^m, and in most cases ($\kappa>0.4$), from those based on S^b as well (Table 3, Fig. 2, A and B). Specifically, S_{MSY} tended to be underestimated by S^f and overestimated by S^b, and the other three reference points (*MSY*, F_{MSY}, and SPR_{MSY}) tended to show the reverse. This result indicates that, in most cases, estimates from S^f and from S^b could be used to bound uncertainty.

Secondary analysis—additional misspecifications

When the true age at 50:50 sex ratio (α_g) was younger than the age used in the assessment model, S^f provided the best estimates of BRPs; when the true age used in the simulation model was older than the age used in the assessment model, S^b provided the best estimates (Fig. 3). When it was assumed incorrectly with the assessment model that fecundity increased linearly with weight, whether too quickly or too slowly, S^b generally provided the best results (Fig. 3).

As was seen in the primary analysis, resilience of fertilization to male depletion (κ) explained the most variation in relative errors of estimated BRPs, followed closely by the parameter (χ_p) defining misspecification in the age at 50:50 sex ratio (Table 5). Steepness of the spawner-recruit function (h) and slope of sex transition (β_p) also explained some variation. Neither natural mortality (M) nor the parameter (χ_f) defining misspecification of the fecundity exponent explained much variation.

Discussion

We used simulations to investigate the performance of three measures of spawning biomass—females only (S^f), males only (S^m), and both sexes combined (S^b)— for their ability to estimate BRPs. Performance was quantified in terms of relative errors, which were computed across many sets of values of biological and fishery parameters. In the primary analysis, with misspecification in the spawner-recruit relationship only, an

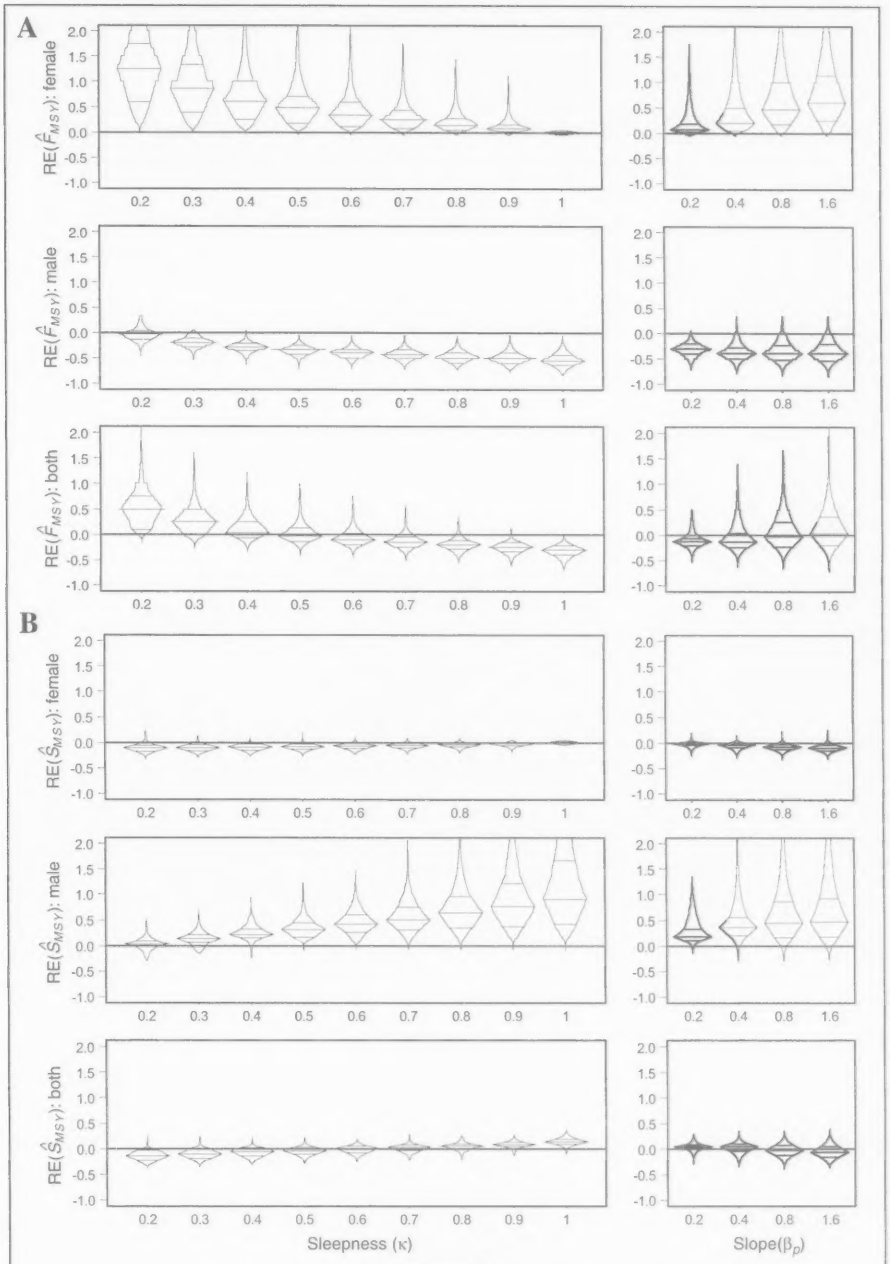

Figure 2

Box-percentile plots of relative error (RE) in estimates of biological reference points, shown across levels of steepness in fertilization (κ) and slope of sex transition (β_p). Rows correspond to the measure of spawning biomass (female, male, or both) used in the assessment model. (**A**) RE in $\hat{F}_{MSY}$, (**B**) RE in $\hat{S}_{MSY}$. Values of S_{MSY} were calculated separately for each measure of spawning biomass as in Equation 9. Width at each percentile is proportional to the percent of observations more extreme than that percentile. The 25th, 50th, and 75th percentiles are indicated by horizontal lines within each box-percentile plot. Distributions of RE in $\hat{MSY}$ and $\hat{SPR}_{MSY}$ were qualitatively similar to $\hat{F}_{MSY}$, but were less variable (typically ±0.5).

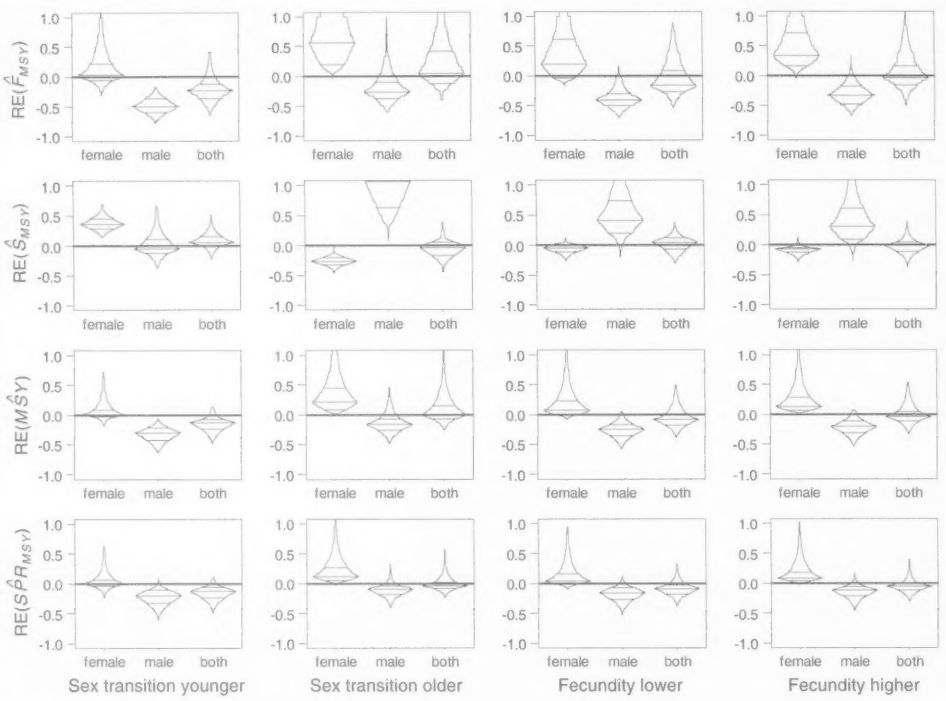

Figure 3

Box-percentile plots of relative error (RE) in estimates of biological reference points from each measure of spawning biomass (female, male, and both), computed in secondary analyses, where an incorrect value of age at 50:50 sex ratio was assumed in the assessment model or where fecundity was incorrectly assumed to scale linearly with weight. Values of S_{MSY} were calculated separately for each measure of spawning biomass as in Equation 9. The first column of panels corresponds to sex transition occurring at a younger age than that assumed in the assessment (χ_p=0.75), the second column to sex transition occurring at an older age than that assumed in the assessment (χ_p=1.25), the third column to fecundity at age being lower than that assumed in the assessment (χ_f=0.75), and the fourth column to fecundity at age being higher than that assumed in the assessment (χ_f=1.25). Width at each percentile is proportional to the percent of observations more extreme than that percentile. The 25th, 50th, and 75th percentiles are indicated by horizontal lines within each box-percentile plot.

assessment model using spawning biomass of both sexes generally provided the best results. When we incorporated additional misspecifications, the assessment model based on both sexes still performed best, with the exception of cases where the age of sex transition in the assessment model was biased towards an older age. Such bias could occur if sex change is adaptive (i.e., if fish alter the timing of sex transition). However, if the age of sex transition is derived from an exploited population, we would expect an estimate used in the assessment to already reflect any adaptation, and thus it seems more likely that any bias in the estimate would be towards a younger age.

Of all the parameters in the factorial design, resilience of fertilization to male depletion, quantified by κ, explains the most variation in relative error of estimates. When $\kappa \geq 0.8$, an assessment model based on females only provides the best estimates of BRPs. This result is logical, because for the largest values of κ, the proportion of males can be driven quite low before fertilization is limited, and therefore, the number of fertilized eggs will be exactly (κ=1) or approximately (κ=0.8 or 0.9) proportional to S^f (given that the exponents of weight at age and fecundity at age are equal). A value of κ=1 is a limiting case because it implies fertilization can occur even in the absence of males (x_F=0). When κ is in the range of about 0.4–0.7, an assessment model based on both sexes provides the best results. For these levels of κ, fertilization rates decline moderately with depletion of males—an effect that is captured by the use of S^b. Only at the most limiting values of κ (0.2, 0.3), where fertilization rates decline dramatically with depletion of males, did an assessment model based on males provide the best estimates.

Table 5

Sensitivity of relative errors in estimated biological reference points to each model factor in secondary analysis, where an incorrect value of age at 50:50 sex ratio was assumed in the assessment model or where fecundity was incorrectly assumed to scale linearly with weight. For each reference point (F_{MSY}, $S^{f,m,b}_{MSY}$, *MSY*, and SPR_{MSY}), the measure of spawning biomass (female, male, or both) with the smallest total model error (total SS) demonstrated the least variability (values in italics). Table cells give proportion of total SS explained by each factor. Values ≥0.1 are indicated by bold font and values ≤0.01, by dashes. The term "Residual" is variation explained by all possible interaction terms. Factors (model parameters) are defined in Table 2.

	F_{MSY}			S^f_{MSY}	S^m_{MSY}	S^b_{MSY}	*MSY*			SPR_{MSY}		
Factor	Female	Male	Both	Female	Male	Both	Female	Male	Both	Female	Male	Both
M	0.02	—	—	—	—	—	0.02	—	—	—	—	—
κ	**0.38**	**0.45**	**0.41**	—	**0.19**	**0.32**	**0.37**	**0.38**	**0.45**	**0.29**	**0.26**	**0.39**
h	—	0.05	0.07	0.02	0.02	**0.12**	0.06	**0.21**	0.05	**0.16**	**0.39**	0.08
β_p	**0.13**	0.02	0.05	—	0.05	0.05	0.08	0.03	0.02	0.05	—	—
χ_p	**0.20**	**0.24**	**0.22**	**0.89**	**0.34**	**0.14**	**0.16**	**0.17**	**0.20**	**0.13**	**0.12**	**0.18**
χ_e	—	—	—	—	—	0.02	—	—	—	—	—	—
Residual	0.25	0.22	0.24	0.08	0.39	0.35	0.30	0.20	0.27	0.34	0.22	0.33
Total SS	1044	*148*	419	*226*	2869	64	248	*78*	116	112	55	*48*

Sensitivity of results to κ may indicate that estimates of fertilization success, if obtainable, would be quite valuable. Although κ itself may be difficult to estimate directly, fertilization success could be assessed qualitatively if it shifts, for example from high to low, with a change in sex ratio. Such information would make it possible to infer a likely range for steepness of the fertilization function, and hence, to select the measure of spawning biomass most appropriate for that range.

In addition to influencing assessment error, κ influences the values of BRPs themselves, and lower κ results in higher S_{MSY} and lower F_{MSY} and *MSY*. Comparing the BRPs of these simulated protogynous stocks with those of gonochoristic equivalents, we found that, on average, protogynous stocks could support higher F_{MSY} and *MSY* when $\kappa \geq 0.5$. This finding resulted from the condition that if age structures are equivalent, protogynous stocks are not inherently more vulnerable to exploitation than gonochoristic stocks, at least over moderate ranges of fishing mortality (Bannerot et al., 1987). It indicates that protogynous stocks are not inherently more vulnerable to exploitation than gonochoristic stocks, at least over moderate ranges of fishing mortality. We caution, however, that higher F_{MSY} does not imply more resilience to all levels of F. If fertilization rate depends on sex ratio, some level of $F > F_{MSY}$ is still likely to be more detrimental to a protogynous stock, where that level would depend on characteristics of the stock in question. For example, if sex transition is rapid, and occurs across only a few ages, fishing could more readily deplete males, leading to fertilization failure and thus recruitment failure.

Reproductive behavior could also affect a stock's vulnerability to exploitation. Spawning aggregations can make a species easier to target but probably better able to adapt to changes in sex ratios. Pair spawners, on the other hand, may be less easy to target, but more susceptible to effects of male depletion.

Without any information on fertilization rates, a likely range of κ could be postulated from evolutionary considerations. We expect that nature would select against values of κ near its limits (0.2 and 1.0). At the lower bound of κ=0.2, any decline in the proportion of males would lead to a relatively steep reduction in fertilization success. Individual fitness could be increased by greater sperm production per male, thereby increasing fertilization success and driving κ above 0.2. However, greater sperm production would likely be associated with an energetic cost. Thus, a tradeoff should exist between energy allocated toward sperm production versus other functions, such as somatic maintenance, foraging, or reproductive behavior (Alonzo and Warner, 2000; Scaggiante et al., 2005). The tradeoff may be worth the cost, but only to the extent that an increase in fertilization success improves fitness. At the upper range of κ, the marginal gains in fertilization success are only realized if males are extremely depleted (i.e., as $x_F \rightarrow 0$ in Fig. 1). Furthermore, the value of κ=1.0 implies that a single male can fertilize the eggs of every female in the population, which is obviously not realistic. We therefore hypothesize that moderate values of κ should be most prevalent. Theoretical predictions, and several field experiments, indicate that fertilization is less than 100% and may decline as less sperm is released per spawning event (Petersen et al., 1992; Petersen and Warner, 2002).

Moderate values of κ correspond to the range where BRPs are best estimated from spawning biomass of both sexes, and we therefore recommend a default choice of S^b when the degree of sperm limitation is unknown. The direction and degree of relative error indicate that S^b would produce nearly perfect estimates of S_{MSY} and risk-averse estimates of F_{MSY}, and only a

small loss in potential *MSY* (negative relative error was slight).

Results of this study are insensitive to the assumption that fecundity is linearly related to body weight, most likely because there are few females remaining at ages where curves of fecundity at age and weight at age would diverge if $\varepsilon_2 \neq 3$. This finding provides support for using spawning biomass as a proxy for total egg production, which is reassuring given that this assumption is commonplace in assessments. However, it does not support the conventional proxy (S^f) unless fertilization rates are nearly constant over a wide range of sex ratios. Furthermore, this finding does not address whether total egg production itself represents reproductive potential adequately. As discussed by Murawski et al. (2001), total egg production does not include potentially important influences such as spawning experience or effects of maternal age and size on offspring quality.

For simplicity, the simulations considered only knife-edge selectivity. In some fisheries, selectivity is dome shaped, as a result of regulations (e.g., slot limits), gear type (e.g., traps), or migration patterns (e.g., if larger fish leave the fishing grounds). In protogynous fish, dome-shaped selectivity would reduce fishing pressure mainly on males. If enough fish can survive the ages of full exploitation, dome-shaped selectivity could allow the proportion of males to remain sufficiently high to avoid severe decline in fertilization success. This effect should maintain sex ratio in the range where S^f and S^b would perform comparatively well. Indeed, this expectation was confirmed by additional simulations where we repeated our primary analysis but with dome-shaped rather than knife-edge selectivity.

Although this simulation study focuses on protogynous fish, we expect the results to hold for any stock that experiences preferential fishing on males. This may occur in gonochoristic stocks, for example, if sexually dimorphic growth or spatial segregation renders males more vulnerable to fishing gear.

This investigation was deterministic by design, so that error from model misspecification could be isolated. A useful extension would be to include other sources of error—observation, process, or both. Data sets that incorporate these additional sources could be generated with the simulation model, and then fitted with the assessment model. This type of approach would make it possible to evaluate the effect of additional error sources on estimates of key population parameters (for example, unfished recruitment [R_0] or steepness [h] in the spawner-recruit relationship) and on management advice.

Although S^b performs best in general, no measure of spawning biomass is best in all cases. One consistent finding is that the relative errors of S^f and S^b tend to have opposite signs over the range of κ that we consider probable; therefore, the use of S^f and S^b in assessments should bound uncertainty in estimates of BRPs. This pattern of relative errors tending to have opposite signs occurred because S^f never accounts for reduction in fertilization success and S^b always does. As a result, S^f tends to overestimate the ability of a stock to support exploitation, and S^b tends to provide more conservative reference points.

This consistent pattern in the relative errors of S^f and S^b indicates that error in reference points could be reduced by creating a measure of spawning biomass that counts both sexes, but with a heavier weight on females (the measure S^b counted both sexes equally). Alternatively, error could be reduced by combining estimates through model averaging (e.g., Brodziak and Legault, 2005). Either way, estimates from S^f and S^b could be used to bound uncertainty in biological reference points for managing protogynous fish.

Acknowledgments

This work was supported by Marine Fisheries Initiative Program (MARFIN) grant 04MFIH10. The authors are grateful for comments from G. Fitzhugh, C. Porch, J. Powers, M. Prager, G. Scott, A. Stephens, and E. Williams.

Literature cited

Allsop, D. J., and S. A. West.
2004. Sex-ratio evolution in sex changing animals. Evolution 58:1019–1027.

Alonzo, S. H., and M. Mangel.
2004. The effects of size-selective fisheries on the stock dynamics of and sperm limitation in sex-changing fish. Fish. Bull. 102:1–13.
2005. Sex-change rules, stock dynamics, and the performance of spawning-per-recruit measures in protogynous stocks. Fish. Bull. 103:229–245.

Alonzo, S. H., and R. R. Warner.
2000. Allocation to mate guarding or increased sperm production in a Mediterranean wrasse. Am. Nat. 156:266–275.

Armsworth, P. R.
2001. Effects of fishing on a protogynous hermaphrodite. Can. J. Fish. Aquat. Sci. 58:568–578.

Bannerot, S., W. W. Fox, Jr., and J. E. Powers.
1987. Reproductive strategies and the management of snappers and groupers in the Gulf of Mexico and the Caribbean. *In* Tropical snappers and groupers: biology and fisheries management (J. J. Polovina, and S. Ralston, eds.), p. 561–603. Westview Press, Boulder, CO.

Baranov, F. I.
1918. On the question of the biological basis of fisheries. Nauchn. Issled. Ikhtiologicheskii Inst. Izv. 1:81–128. [Translated from Russian by W. E. Ricker.]

Barot, S., M. Heino, L. O'Brien, and U. Dieckmann.
2004. Long-term trend in the maturation reaction norm of two cod stocks. Ecol. Appl. 14:1257–1271.

Beverton, R. J. H., and S. J. Holt.
1957. On the dynamics of exploited fish populations, 533 p. Facsimile reprint (1993). Chapman and Hall, London.

Brodziak, J., and C. M. Legault.
2005. Model averaging to estimate rebuilding targets for

overfished stocks. Can. J. Fish. Aquat. Sci. 62:544–562.

Coleman, F. C., C. C. Koenig, and L. A. Collins.
1996. Reproductive styles of shallow-water groupers (Pisces: Serranidae) in the eastern Gulf of Mexico and the consequences of fishing spawning aggregations. Environ. Biol. Fish. 47:129–141.

Collins, M. R., C. W. Waltz, W. A. Roumillat, and D. L. Stubbs.
1987. Contribution to the life history and reproductive biology of gag, *Mycteroperca microlepis* (Serranidae) in the South Atlantic Bight. Fish. Bull. 85: 648–653.

FAO (Food and Agriculture Organization) Fishery Resources Division.
1999. Indicators for sustainable development of marine capture fisheries. FAO Technical Guidelines for Responsible Fisheries. No. 8, 68 p. FAO, Rome.

Gardner, A., D. J. Allsop, E. L. Charnov, and S. A. West.
2005. A dimensionless invariant for relative size at sex change in animals: explanation and implications. Am. Nat. 165:551–566.

Goodyear, C. P.
1980. Compensation in fish populations. *In* Biological monitoring of fish (C. H. Hocum, and J. R. Stauffer Jr, eds.), p. 253–280. Lexington Books, D. C. Heath and Co., Lexington, MA.

Harris, J. P., and J. C. McGovern.
1997. Changes in the life history of red porgy, *Pagrus pagrus*, from the southeastern United States, 1972–1994. Fish. Bull. 95:732–747.

Heppell, S. S., S. A. Heppell, F. C. Coleman, and C. C. Koenig.
2006. Models to compare management options for protogynous fish. Ecol. Appl. 16:238–249.

Huntsman, G. R., and W. E. Schaaf.
1994. Simulation of the impact of fishing on reproduction of a protogynous grouper, the graysby. N. Am. J. Fish. Manag. 14:41–52.

Mace, P. M., and I. J. Doonan.
1988. A generalized bioeconomic simulation model for fish population dynamics. New Zealand Fishery Assessment, Res. Doc. 88/4, 51 p.

McGovern, J. C., D. M. Wyanski, O. Pashuk, C. S. Manooch III, and G. R. Sedberry.
1998. Changes in the sex ratio and size at maturity of gag, *Mycteroperca microlepis*, from the Atlantic coast of the southeastern United States during 1976–1995. Fish. Bull. 96:797–807.

Murawski, S. A., P. J. Rago, and E. A. Trippel.
2001. Impacts of demographic variation in spawning characteristics on reference points for fishery management. ICES J. Mar. Sci. 58:1002–1014.

Petersen, C. W., and R. R. Warner.
2002. The ecological context of reproductive behavior. *In* Coral reef fishes: dynamics and diversity in a complex ecosystem (P. F. Sale, ed.), p. 103–118. Academic Press, San Diego, CA.

Petersen, C. W., R. R. Warner, S. Cohen, H. C. Hess, and A. T. Sewell.
1992. Variable pelagic fertilization success: Implications for mate choice and spatial patterns of mating. Ecology 73:391–401.

Punt, A. E., P. A. Garratt, and A. Govender.
1993. On an approach for applying per-recruit methods to a protogynous hermaphrodite, with an illustration for the slinger *Chrisoblephus puniceus* (Pisces: Sparidae). S. Afr. J. Mar. Sci. 13:109–119.

Rothschild, B. J., and M. J. Fogarty.
1989. Spawning-stock biomass: A source of error in recruitment/stock relationships and management advice. J. Cons. Int. Explor. Mer 45:131–135.

Scaggiante, M., M. B. Rasotto, C. Romualdi, and A. Pilastro.
2005. Territorial male gobies respond aggressively to sneakers but do not adjust their sperm expenditure. Behav. Ecol. 16: 1001–1007.

Shepherd, G. R., and J. S. Idoine.
1993. Length-based analyses of yield and spawning biomass per recruit for black sea bass *Centropristis striata*, a protogynous hermaphrodite. Fish. Bull. 91:328–337.

Vaughan, D. S., M. R. Collins, and D. J. Schmidt.
1995. Population characteristics of the black sea bass *Centropristis striata* from the Southeastern. U.S. Bull. Mar. Sci. 56:250–267.

Vaughan, D. S., G. R. Huntsman, C. S. Manooch III, F. C. Rohde, and G. F. Ulrich.
1992. Population characteristics of the red porgy *Pagrus pagrus* off the Carolinas. Bull. Mar. Sci. 50:1–20.

Vaughan, D. S., and M. H. Prager.
2001. Severe decline in abundance of the red porgy (*Pagrus pagrus*) population off the southeastern United States. Fish. Bull. 100:351–375.

von Bertalanffy, L.
1938. A quantitative theory of organic growth. Hum. Biol. 10:181–213.

Emerging patterns of species richness, diversity, population density, and distribution in the skates (Rajidae) of Alaska

Duane E. Stevenson (contact author)[1]
James W. Orr[1]
Gerald R. Hoff[1]
John D. McEachran[2]

E-mail address for D. E. Stevenson: duane.stevenson@noaa.gov

[1] National Oceanic and Atmospheric Administration
National Marine Fisheries Service, Alaska Fisheries Science Center
Resource Assessment and Conservation Engineering Division
7600 Sand Point Way NE
Seattle, Washington 98115

[2] Department of Wildlife and Fisheries Sciences
Texas A&M University
College Station, Texas 77843

Abstract—Six years of bottom-trawl survey data, including over 6000 trawls covering over 200 km^2 of bottom area throughout Alaska's subarctic marine waters, were analyzed for patterns in species richness, diversity, density, and distribution of skates. The Bering Sea continental shelf and slope, Aleutian Islands, and Gulf of Alaska regions were stratified by geographic subregion and depth. Species richness and relative density of skates increased with depth to the shelf break in all regions. The Bering Sea shelf was dominated by the Alaska skate (*Bathyraja parmifera*), but species richness and diversity were low. On the Bering Sea slope, richness and diversity were higher in the shallow stratum, and relative density appeared higher in subregions dominated by canyons. In the Aleutian Islands and Gulf of Alaska, species richness and relative density were generally highest in the deepest depth strata. The data and distribution maps presented here are based on species-level data collected throughout the marine waters of Alaska, and this article represents the most comprehensive summary of the skate fauna of the region published to date.

Manuscript submitted 16 May 2007.
Manuscipt accepted 1 August 2007.
Fish. Bull. 106:24–39 (2008).

The views and opinions expressed or implied in this article are those of the author and do not necessarily reflect the position of the National Marine Fisheries Service, NOAA.

Patterns of species richness, diversity, density, and distribution for the species of skates inhabiting the North Pacific Ocean and Bering Sea are still largely unknown. Earlier studies have been limited because of problems with identification of skates in the field and, to some degree, in the laboratory. Summarizing trawl survey data for commonly encountered species, Allen and Smith (1988) reported serious problems in the fisheries and survey data reported for even the most common skates throughout Alaska and the eastern North Pacific Ocean because of widespread problems with field identification of skates. Similarly, in the only previously published analyses of skate abundance and distribution data for Alaska, Teshima and Wilderbuer (1990) and Raschi et al. (1994) treated their data in the aggregate at the family level because of difficulty with identification of species. In contrast, Japanese and Russian authors have published several studies including general species-level information on the skate fauna of the western North Pacific Ocean and Sea of Okhotsk (Dudnik and Dolganov, 1992; Nakaya and Shirai, 1992; Dolganov, 1999, 2001).

Skates present difficulties for identification because they are a morphologically conservative group of fishes, and although they represent a large proportion of the diversity of elasmobranchs worldwide, external morphological differences among species (or even genera) are often subtle. Moreover, the extent of morphological variation in many species is poorly known despite earlier taxonomic work (Ishiyama and Ishihara, 1977; Ishihara and Ishiyama, 1985, 1986), and although molecular methods have shown promise for species identification in the laboratory (Tinti et al., 2003; Bremer et al., 2005; Spies et al., 2006), skates are often difficult to identify in the field. In Alaska waters, namely the eastern Bering Sea, Aleutian Islands, and Gulf of Alaska, this has been particularly true as Allen and Smith (1988), Teshima and Wilderbuer (1990), and Raschi et al. (1994) have noted. More recently, Mecklenburg et al. (2002) stated that the poorly understood taxonomic relationships of the skates in this region complicate the determination of species distributions. These challenges are compounded by the fact that skates are generally large fishes and are, thus, difficult to collect, preserve, and curate. Therefore, they are poorly represented in museum collections and difficult to study in the laboratory.

Because of identification difficulties and a relative lack of commercial im-

portance, species-specific data on skate populations are often not available, and catch statistics are commonly recorded only at the aggregate (genus or family) level. This lack of data is a concern in that skates may be particularly vulnerable to fishing pressure, even if they are only encountered as bycatch, because of their large size, relatively long life expectancy, and low fecundity, and are considered highly vulnerable to extinction or extirpation due to overfishing or habitat disturbances (Casey and Myers, 1998; Stevens et al., 2000; Dulvy and Reynolds, 2002). Moreover, apparent stability or increases in aggregate skate catches may mask declines in some components of those species aggregates, particularly among larger species (Dulvy et al., 2000). Therefore, species-level management, which can only be achieved through accurate identification, reporting, and monitoring, is essential for maintaining viable skate populations (Stevens et al., 2000).

Although skate populations in the eastern North Pacific Ocean and Bering Sea have been inadequately studied and inaccurately represented because of questionable field identifications, recent research efforts are improving the resolution and consistency with which skates can be identified by field survey personnel. The taxonomic works of Ishihara and Ishiyama (1985, 1986), Dolganov (1985), and Stevenson et al. (2004) have helped to clarify the taxonomy of North Pacific skates. In addition, range extensions of species previously unknown from Alaskan waters (Stevenson and Orr, 2005), the ongoing development of a comprehensive field guide to the skates of the region (Stevenson et al., 2007), and the establishment of a voucher collection process that allows for laboratory verification or reidentification of significant specimens, have greatly improved field identifications on Alaska Fisheries Science Center (AFSC) resource assessment surveys.

Because of advances in the knowledge of the skates of the North Pacific Ocean and Bering Sea, species-level skate identifications made by AFSC personnel beginning with the 1999 survey year are reliable and consistent. The purpose of this article is to describe species richness, diversity, relative density, and distribution of skates throughout Alaskan waters, based on data from six years of groundfish bottom-trawl surveys in the Bering Sea, Aleutian Islands, and Gulf of Alaska from 1999 through 2004.

Materials and methods

Specimens were collected aboard a variety of commercial fishing vessels chartered by the AFSC Resource Assessment and Conservation Engineering (RACE) Division from May through August in the eastern Bering Sea, Aleutian Islands, and Gulf of Alaska, between 1999 and 2004 (Fig. 1). Survey gear and methods differed substantially among the four resource assessment surveys (Bering Sea shelf, Bering Sea slope, Aleutian Islands, and Gulf of Alaska), and bottom habitat types differ among regions, resulting in differences in the catchability of skates. The effects of these differences on estimates of skate species richness, diversity, density, and distribution remain largely unknown; therefore the eastern Bering Sea shelf, Bering Sea slope, Aleutian Islands, and Gulf of Alaska were treated separately in this study.

The eastern Bering Sea shelf survey has been conducted annually in approximately its present form since 1982, and data from survey hauls during the years 1999–2004 were used in this study. This survey covered the eastern Bering Sea shelf from the Alaska Peninsula north beyond St. Matthew Island to approximately 62°40′N, from 20 m to 200 m depth, and was conducted with an 83-112 Eastern otter trawl. Hauls were made at previously established survey stations on a 20×20 nautical mile grid, and bottom time for each haul was approximately 30 minutes. For the purposes of this study, the region was divided into three subregions of approximately equal survey effort, each including three depth ranges (<50 m, 51–100 m, and 101–200 m). Subregion 1 comprised the southeastern part of the eastern Bering Sea shelf, extending from the Alaska Peninsula to the southeastern rim of Pribilof Canyon; subregion 2 comprised the central part of the eastern Bering Sea shelf, from the northwestern boundary of subregion 1 to the southeastern rim of Zhemchug Canyon; and subregion 3 comprised the northernmost portion of the survey area, bounded on the northwest by the U.S.-Russian border, with the northernmost hauls at approximately 62°40′N (Fig. 2A). For more information on the design and methods of this survey, see Stauffer (2004) and Lauth and Acuna (2007).

The eastern Bering Sea slope survey was conducted in 2000, 2002, and 2004. It covered the eastern Bering Sea upper continental slope (200 m to >1200 m depth) from just north of Unalaska Island north to the U.S.-Russian border, and was conducted with a Poly Nor'eastern bottom trawl equipped with mud-sweep roller gear on the footrope. Haul locations were chosen according to a stratified random sampling design, with the region divided into six subregions and five depth strata, and bottom time for each haul was approximately 30 minutes. For the purposes of this study the same six sub-regions were used. Subregions 1 and 6 consisted of a broad, low-angle slope, and form the southeastern and northwestern edges of the survey area; subregions 2 and 4 consisted of Pribilof and Zhemchug Canyons, respectively; and subregions 3 and 5 were intercanyon faces characterized by a steep-angle slope (Fig. 2A). For this study, depth strata were combined into two depth ranges, representing the upper slope (200–600 m) and the lower slope (>600 m). For more information on the design and methods of this survey, see Hoff and Britt (2005).

The Aleutian Islands survey was conducted in 2000, 2002, and 2004. These surveys covered the continental shelf and upper slope (to 500 m) of the entire Aleutian Archipelago from Unimak Pass (165°W) to Stalemate Bank (170°30′E), and were conducted with a Poly Nor'eastern bottom trawl equipped with rubber bobbin

Figure 1

Map of the area covered in bottom-trawl surveys conducted by the Resource Assessment and Conservation Engineering Division of the Alaska Fisheries Science Center between 1999 and 2004. Surveys of the Bering Sea extended from the Alaska Peninsula to the U.S.-Russian border northwest of St. Matthew Island, surveys of the Aleutian Islands extended from Unimak Pass west to Stalemate Bank, and surveys of the Gulf of Alaska extended from Unimak Pass east to the U.S.-Canada border at Dixon Entrance. Black lines (west and east) denote U.S.-Russian and U.S.-Canadian border. Depth contour = 200 m.

roller gear on the footrope. The southern part of the eastern Archipelago from the Islands of Four Mountains to Unimak Pass has been assessed as part of the Gulf of Alaska survey but because zoogeographically it is part of the Aleutian Islands and because survey methods are the same (Britt and Martin, 2000), it was included in our regional study of the Aleutian Islands. Haul locations were chosen on the basis of a stratified random sampling design, and the region was divided into 45 area-depth strata, and bottom time for each haul was approximately 15 minutes. For the purposes of this study the region was divided into four subregions, numbered from west to east, bounded by the major deep-water passes and gaps bisecting the archipelago. Subregion 1 comprised Stalemate Bank and the Near Islands, extending to approximately 174°30′E; subregion 2 extended east to Amchitka Pass, at the 180° line; subregion 3 extended from Amchitka Pass to Amukta Pass (approximately 171°30′W); and subregion 4 extended from Amukta Pass to Unimak Pass (Fig. 2B). For this study, depth strata were combined into three depth ranges (<100 m, 101–200 m, and >200 m). For more information on the design and methodology of this survey, see Zenger (2004).

The Gulf of Alaska survey was conducted in 1999, 2001, and 2003. It covered the continental shelf and upper slope (to 500 m in 2001, 700 m in 2003, and 1000 m in 1999) of the Gulf of Alaska from the southern part of the eastern Aleutian Islands beginning at the Islands of Four Mountains (included for this study in the Aleutian Islands region) to the U.S.-Canada border at Dixon Entrance, except in 2001 when the survey ended to the east at Hinchinbrook Entrance. Survey design, methods, and gear were the same as those of the Aleutian Islands survey (see Britt and Martin, 2000). For the purposes of the present study the region was divided into five subregions, numbered from west to east, corresponding approximately with National Marine Fisheries Service (NMFS) management areas. Subregion 1 extended from the tip of the Alaska Peninsula west to 159°W; subregion 2 extended from 159°W to the west side of Kodiak Island; subregion 3 extended from the west side of Kodiak Island to Hinchinbrook Entrance (147°W); subregion 4 extended from Hinchinbrook Entrance to Cross Sound at the northern tip of the Alexander Archipelago; and subregion 5 included the Alexander Archipelago, extending to the U.S.-Canada border (Fig. 2C). As in the Aleutian Islands region,

depth strata were combined into three depth ranges (<100 m, 101–200 m, and >200 m).

In all surveys, skate specimens were either examined and discarded at sea or fixed onboard in 10% seawater-buffered formalin or frozen for later study. Many of the specimens were photographed at sea, and the majority of fixed specimens were transferred to 70% ethanol and archived at the University of Washington (UW) fish collection. In compiling a list of skates for Alaska, we followed the comprehensive guide of Mecklenburg et al. (2002), with the following updates. We included *Bathyraja mariposa* (butterfly skate), described in Stevenson et al. (2004), and *Amblyraja badia* (roughshoulder skate), recently documented in the Bering Sea (Stevenson and Orr, 2005).

Species richness was defined as the number of skate species encountered and identified in each haul. Mean species richness values were calculated for each depth-and-subregion stratum as a simple average of the number of skate species encountered in all hauls performed in that stratum, including zero values for hauls in which no skates were encountered. Because mean species richness figures were heavily influenced by zero values in some regions, and because simple species richness gives no indication of evenness, we also calculated a single Shannon's diversity index (H′) for each depth-and-subregion stratum. This index was calculated as

$$H' = \sum_{i=1}^{S} \left[(n_i / n) \ln(n_i / n) \right],$$

where n_i = the number of individuals belonging to the ith of S species in the depth-and-subregion stratum; and

n = the total number of individuals captured in the depth-and-sub-region stratum (Ludwig and Reynolds, 1988).

Bottom area swept was calculated for each haul by multiplying the distance fished by the mean net spread. Density was calculated as the number of individuals per km^2 of bottom area swept. Means are presented ± standard error (SE). Because the distributions of both species richness and density values were heavily skewed, and had a large proportion of zero values, tests for significant differences among means were not performed. Species distributions represent a summary of all recorded encounters of each species during standard survey operations in successful survey hauls.

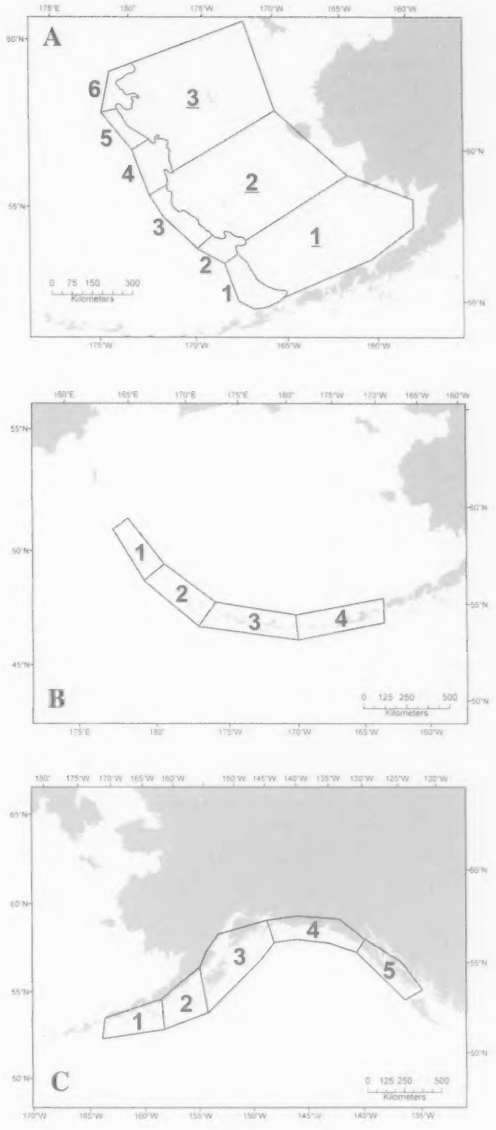

Figure 2

Boundaries of sampled subregions covered in bottom-trawl surveys from 1999 through 2004 in (**A**) the eastern Bering Sea shelf (underlined numbers) and slope (numbers not underlined), (**B**) the Aleutian Islands, and (**C**) the Gulf of Alaska.

Results

The total amount of effort represented in this data set consisted of 6096 successful bottom trawls covering over 201 km^2 of bottom area (Table 1). The Bering Sea shelf accounts for significantly more trawling effort than any of the other regions, because of differences in survey frequency (annual [Bering Sea shelf] vs. biennial [other regions]) and standard tow duration (30 minutes [Bering Sea shelf and slope] vs. 15 minutes [Aleutian Islands and Gulf of Alaska]). Thirteen of the 14 described species of skates known from Alaskan waters (all but *Bathyraja violacea*) were encountered in bottom-trawl surveys from 1999 through 2004. Survey trawls collected 0–7 species per haul (mean=0.93 ±0.01), and at least one species of skate was collected in 62.8% of hauls. The number of

Table 1

Total number of hauls (n) and bottom area swept (km^2) by subregion and depth range for bottom-trawl surveys conducted in the eastern Bering Sea (shelf and slope), Aleutian Islands, and Gulf of Alaska from 1999 through 2004 (see text for subregion boundaries).

	Subregion											
	1		2		3		4		5		6		Total	
Depth range (m)	n	km^2	n	km^2	n	km^2	n	km^2	n	km^2	n	km^2	n	km^2
Bering Sea shelf														
<50	182	7.68	245	10.90	18	0.81							445	19.39
51–100	386	17.86	361	17.18	302	15.03							1049	50.07
101–200	141	7.33	147	7.11	328	16.51							616	30.95
Total	709	32.87	753	35.19	648	32.35							2110	100.40
Bering Sea slope														
201–600	112	4.38	31	1.09	32	1.10	32	1.08	15	0.55	53	1.94	275	10.14
601+	57	2.30	32	1.12	33	1.23	30	1.12	23	0.87	33	1.15	208	7.78
Total	169	6.68	63	2.21	65	2.33	62	2.20	38	1.42	86	3.09	483	17.92
Aleutian Islands														
<100	34	0.78	83	1.83	67	1.54	171	3.90					355	8.05
101–200	103	2.37	154	3.37	164	3.73	103	2.37					524	11.84
201+	70	1.63	134	3.05	170	3.99	156	3.72					530	12.38
Total	207	4.78	371	8.25	401	9.26	430	9.99					1409	32.27
Gulf of Alaska														
<100	247	5.74	174	4.02	280	6.60	50	1.19	15	0.33			766	17.87
101–200	121	2.87	188	4.52	365	8.90	104	2.51	58	1.33			836	20.12
201+	30	0.72	128	3.17	138	3.64	119	3.68	77	1.79			492	13.00
Total	398	9.33	490	11.71	783	19.14	273	7.38	150	3.45			2094	50.99

individual skates captured in a single haul ranged from 0 to 833, yielding aggregate density (all species combined) estimates for individual survey hauls ranging from 0 to 22,005 individuals per km^2 (mean=160.55 ±5.39). For individual species, maximum density figures ranged over several orders of magnitude, from 26.42 individuals/km^2 for the rare and deepwater *B. abyssicola* to over 19,759 individuals/km^2 for an extraordinarily large haul of *B. parmifera* on the northern Bering Sea slope.

Bering Sea shelf

The Bering Sea shelf received as much trawling effort as the other three regions combined and skates were common, but skate species richness and diversity were low. Approximately half of the effort was expended in the 51–100 m depth range, and the other half of the effort was almost equally distributed between the other two depth strata (Table 1). The southern, central, and northern subregions were sampled approximately evenly, and the depth distribution of the effort was similar in subregions 1 and 2. However, the depth distribution of the effort was significantly different in subregion 3, where the deepest depth stratum (100–200 m) was most heavily sampled, and very little sampling was conducted in the shallow stratum. Skates were encountered throughout the entire geographic and bathymetric range of the survey area in over 87% (1830 of 2110) of the hauls conducted in this region. Skate species richness was highest in subregion 3 and lowest in subregion 1 (1.21 vs. 0.94), increasing with depth in all three subregions (Table 2). In all three subregions, species richness was highest in the deepest strata, and the lowest species richness was encountered in the shallow stratum of subregion 1. For all subregions combined, species richness increased significantly ($P<0.0001$) with depth (Fig. 3). Diversity indices were near zero in all three subregions in the shallow and middle depth strata, but were slightly higher in the deepest depth zone (Table 3).

Skates were often encountered at moderate to high densities on the Bering Sea shelf. Aggregate skate density on the eastern Bering Sea shelf ranged from 0 to 5103 individuals/km^2, and an overall mean of 229.49 ±5.97. The largest mean density values were encountered in the middle depth stratum (51–100 m) of subregion 2 and the shallow and deep strata of subregion 3, although the variability associated with the mean in the shallow stratum of subregion 3 was extremely high. The smallest mean density was encountered in the shallow stratum of subregion 1 (Table 4). Overall mean density for the entire region was considerably lower in the shallow depth stratum than in either of the two

Table 2

Mean skate species richness (no. of species/haul, with standard error in parentheses) by subregion and depth range for bottom-trawl surveys conducted in the eastern Bering Sea (shelf and slope), Aleutian Islands, and Gulf of Alaska from 1999 through 2004.

	Subregion						
Depth range (m)	1	2	3	4	5	6	Total
Bering Sea shelf							
<50	0.51 (0.04)	0.79 (0.03)	0.72 (0.11)				0.67 (0.02)
51–100	0.93 (0.03)	1.06 (0.02)	0.96 (0.02)				0.98 (0.01)
101–200	1.52 (0.06)	1.58 (0.06)	1.47 (0.04)				1.51 (0.03)
Total	0.94 (0.03)	1.07 (0.02)	1.21 (0.02)				1.07 (0.01)
Bering Sea slope							
201–600	2.43 (0.11)	3.16 (0.32)	2.22 (0.22)	3.59 (0.18)	2.87 (0.40)	3.81 (0.16)	2.91 (0.08)
601+	1.91 (0.16)	3.19 (0.24)	2.94 (0.18)	2.63 (0.28)	1.52 (0.20)	2.27 (0.24)	2.39 (0.09)
Total	2.25 (0.09)	3.17 (0.20)	2.58 (0.15)	3.13 (0.17)	2.05 (0.22)	3.22 (0.16)	2.69 (0.06)
Aleutian Islands							
<100	0.59 (0.10)	0.52 (0.06)	0.51 (0.08)	0.38 (0.04)			0.46 (0.03)
101–200	0.89 (0.11)	0.59 (0.07)	0.77 (0.06)	0.50 (0.07)			0.69 (0.04)
201+	0.69 (0.12)	0.93 (0.08)	1.04 (0.07)	0.90 (0.07)			0.92 (0.04)
Total	0.77 (0.07)	0.70 (0.04)	0.84 (0.04)	0.60 (0.04)			0.72 (0.02)
Gulf of Alaska							
<100	0.25 (0.03)	0.39 (0.04)	0.39 (0.04)	0.44 (0.09)	0.27 (0.12)		0.34 (0.02)
101–200	0.27 (0.05)	0.70 (0.06)	0.74 (0.04)	0.46 (0.06)	0.26 (0.07)		0.60 (0.03)
201+	0.30 (0.10)	1.02 (0.10)	0.65 (0.07)	0.47 (0.07)	0.40 (0.08)		0.64 (0.04)
Total	0.26 (0.02)	0.67 (0.04)	0.60 (0.03)	0.46 (0.04)	0.33 (0.05)		0.51 (0.02)

Table 3

Shannon's diversity index (H′) by subregion and depth range for bottom-trawl surveys conducted in the eastern Bering Sea (shelf and slope), Aleutian Islands, and Gulf of Alaska from 1999 through 2004.

	Subregion						
Depth range (m)	1	2	3	4	5	6	Total
Bering Sea shelf							
<50	0.02	0.01	0.00				0.01
51–100	0.15	0.06	0.03				0.09
101–200	0.57	0.62	0.34				0.46
Total	0.28	0.20	0.25				0.24
Bering Sea slope							
201–600	1.48	1.44	1.33	1.42	1.67	1.70	1.71
601+	1.47	1.33	1.30	1.07	1.10	0.99	1.46
Total	1.65	1.42	1.57	1.38	1.85	1.85	1.82
Aleutian Islands							
<100	0.72	0.46	0.70	1.65			1.27
101–200	0.80	1.20	1.04	1.52			1.13
201+	1.31	1.22	0.97	0.93			1.10
Total	0.94	1.32	1.18	1.33			1.33
Gulf of Alaska							
<100	1.01	0.87	0.93	0.52	0.17		0.91
101–200	1.43	1.53	1.32	0.90	0.90		1.42
201+	0.79	1.51	1.35	0.68	1.56		1.44
Total	1.33	1.64	1.46	1.00	1.44		1.53

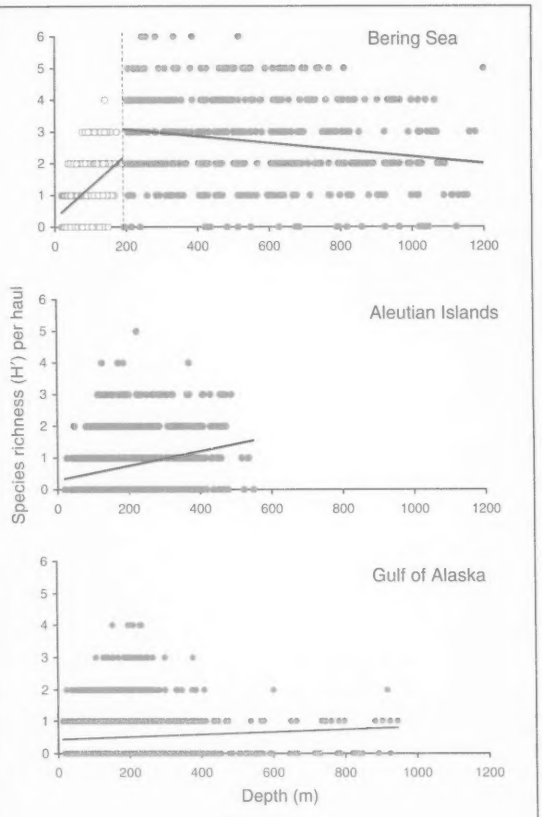

Figure 3

Relationship between skate species richness (H') per haul and depth for bottom-trawl survey hauls completed in the Bering Sea, Aleutian Islands, and Gulf of Alaska from 1999 through 2004. Solid lines represent linear regressions of species richness values, dashed line in upper panel divides Bering Sea shelf records (open circles) from Bering Sea slope records (closed circles).

deeper strata, yielding a significant trend ($P<0.0001$) of increasing density with increasing depth for combined subregions (Fig. 4). Subregions 2 and 3 exhibited a higher overall mean density than subregion 1. *Bathyraja parmifera* (Alaska skate) was by far the most common species in this region, appearing in over 86% of hauls and with a mean density an order of magnitude larger than the next most common species, *B. interrupta* (Bering skate) (Table 5). A total of seven skate species were encountered in this region, two of which (*B. maculata* and *R. rhina*) were encountered in only one or two hauls over the entire six-year period.

Bering Sea slope

The Bering Sea slope received comparatively little trawling effort, but skates were common and species richness and diversity were high. Slightly more effort was expended on the upper slope (201–600 m depth) than on the lower slope (>601 m). Subregion 1, in the southern part of the eastern Bering Sea, received the most effort and the remaining five subregions were sampled approximately evenly (Table 1). Skates were encountered throughout the entire geographic and bathymetric range of the survey region, occurring in 95% (460 of 483) of hauls conducted. Species richness was approximately 50% higher in subregions 2, 4, and 6 (canyons and northern gentle slope habitats) than in subregions 1, 3, and 5 (intercanyons and southern gentle slope habitats). In four of the six subregions, mean species richness was higher on the upper slope than on the lower slope (Table 2), and the overall trend was for richness to decrease significantly ($P<0.0001$) with increasing depth (Fig. 3). Mean species richness was highest on the upper slope in subregion 6 and lowest on the lower slope in subregion 5. Diversity indices for the three southern subregions were similar on the upper and lower slope, whereas in the three northern subregions the diversity index was notably higher on the upper slope (Table 3).

Skates were encountered at high densities on the Bering Sea slope. Aggregate skate density ranged from 0 to 22,005 individuals/km^2, and had an overall mean of 545.81 ±53.48. These figures are heavily influenced by one particularly large haul of *B. parmifera* during the 2002 survey. With this haul removed, the density range and overall mean became 0 to 5350 individuals/km^2 and 501.29 ±29.69 individuals, respectively. The largest mean density was encountered on the upper slope in the northernmost subregion (subregion 6), although this mean was also influenced by the large haul of *B. parmifera*. With the aberrant haul removed from the data set, the largest mean was that of the lower slope in subregion 2 (Table 4). The smallest mean density was encountered on the lower slope in subregion 5. Subregions 2, 4, and 6 exhibited considerably higher overall mean density values than those of subregions 1, 3, and 5—a pattern similar to that of species richness in this region. Overall mean density was similar for the two depth ranges, but slightly higher on the lower slope and increasing nonsignificantly ($P=0.128$) with increasing depth (Fig. 4). Although *B. parmifera* exhibited the highest maximum density, *B. aleutica* produced the highest mean density value in this region, followed by *B. lindbergi* and *B. interrupta* (Table 5). A total of ten skate species were encountered in this region, although two of these (*A. badia* and *B. abyssicola*) were encountered in only two hauls.

Aleutian Islands

The Aleutian Islands received moderate trawling effort, and skates were inconsistently encountered. Trawling effort in this region was distributed approximately evenly between the two deeper depth strata, whereas the shallow stratum received slightly less effort (Table 1). The easternmost subregion (subregion 4) was most heavily sampled, but effort progressively decreased in the more western subregions. Skates were encountered

Table 4

Mean aggregate density (no. of individuals/km^2, with standard error in parentheses) of all skates combined by subregion and depth range for bottom-trawl surveys conducted in the eastern Bering Sea (shelf and slope), Aleutian Islands, and Gulf of Alaska from 1999 through 2004. * = calculations for this area of the Bering Sea slope did not include the particularly large catch of *B. parmifera* on 29 June 2002 (see text for details).

Depth range (m)	Subregion 1	2	3	4	5	6	Total
Bering Sea shelf							
<50	86.20 (10.09)	191.85 (14.24)	340.92 (119.05)				154.67 (10.46)
51–100	220.24 (16.53)	330.91 (15.70)	175.03 (9.74)				245.31 (8.83)
101–200	216.34 (38.33)	215.94 (14.67)	292.13 (11.16)				256.60 (11.24)
Total	185.06 (12.25)	263.22 (9.58)	238.91 (8.27)				229.49 (5.97)
Bering Sea slope							
201–600	311.32 (43.28)	492.60 (83.61)	328.23 (64.99)	670.47 (121.44)	277.00 (57.20)	797.53 (134.44)*	466.14 (38.02)*
601+	255.91 (48.04)	1046.67 (171.08)	467.24 (80.55)	735.72 (145.61)	105.51 (18.05)	784.85 (111.65)	547.59 (47.09)
Total	292.63 (32.92)	774.03 (101.66)	398.81 (52.25)	702.04 (93.61)	173.20 (28.21)	792.61 (92.51)*	501.29 (29.69)*
Aleutian Islands							
<100	135.65 (77.68)	44.54 (7.89)	55.32 (15.28)	21.51 (2.80)			44.21 (8.38)
101–200	279.19 (55.00)	50.33 (7.95)	110.12 (29.89)	45.39 (8.73)			113.06 (15.03)
201+	69.72 (30.45)	99.90 (14.49)	219.66 (32.47)	151.07 (22.86)			149.39 (13.72)
Total	184.78 (32.47)	66.94 (6.55)	147.4 (18.83)	74.24 (9.06)			109.38 (7.96)
Gulf of Alaska							
<100	12.21 (1.68)	35.60 (6.11)	31.92 (4.10)	67.41 (26.64)	76.97 (65.26)		29.60 (3.04)
101–200	12.52 (2.36)	43.31 (4.96)	48.66 (3.61)	30.45 (5.15)	13.96 (4.43)		37.56 (2.14)
201+	18.08 (7.61)	66.67 (7.29)	50.14 (8.04)	41.87 (7.17)	22.25 (4.84)		46.10 (3.59)
Total	12.75 (1.38)	46.67 (3.5)	42.94 (2.66)	42.16 (6.13)	24.52 (7.16)		36.65 (1.64)

Table 5

Mean and maximum density (no. of individuals/km^2) by species for skates collected in bottom-trawl survey hauls performed in the eastern Bering Sea (shelf and slope), Aleutian Islands, and Gulf of Alaska from 1999 through 2004. * = not collected in this region, n = total number of hauls performed within each region.

Species	Bering Sea shelf (n=2110) Mean	Max	Bering Sea slope (n=483) Mean	Max	Aleutian Islands (n=1409) Mean	Max	Gulf of Alaska (n=2094) Mean	Max	All regions (n=6096) Mean	Max
Bathyraja parmifera	217.09	5103.83	55.00	19759.77	18.36	1012.26	1.64	201.97	84.30	19759.77
B. aleutica	0.99	575.15	214.16	3981.10	8.52	639.17	5.07	207.53	21.02	3981.10
B. maculata	0.01	19.47	43.07	2350.51	52.37	4414.28	0.12	88.94	15.56	4414.28
B. interrupta	10.95	565.55	60.59	1057.54	1.01	340.40	5.60	238.45	10.75	1057.54
B. taranetzi	0.13	41.67	31.48	1117.97	27.31	1781.36	0.02	40.11	8.86	1781.36
B. lindbergi	*	*	78.02	1953.68	0.09	46.22	0.04	82.24	6.22	1953.68
B. minispinosa	*	*	36.26	1094.62	0.11	66.08	0.02	36.02	2.90	1094.62
B. trachura	*	*	26.79	468.10	0.08	83.66	0.69	502.86	2.38	502.86
B. mariposa	*	*	*	*	0.34	103.78	*	*	0.08	103.78
B. abyssicola	*	*	0.10	26.42	*	*	*	*	0.01	26.42
Raja rhina	0.01	44.67	*	*	0.10	50.81	13.83	592.97	4.78	592.97
R. binoculata	0.25	197.37	*	*	1.08	178.52	9.61	986.51	3.64	986.51
Amblyraja badia	*	*	0.25	80.00	*	*	*	*	0.02	80.00
All skates	229.43	5103.83	545.81	22,005.20	109.38	4609.02	36.65	986.51	160.52	22,005.20

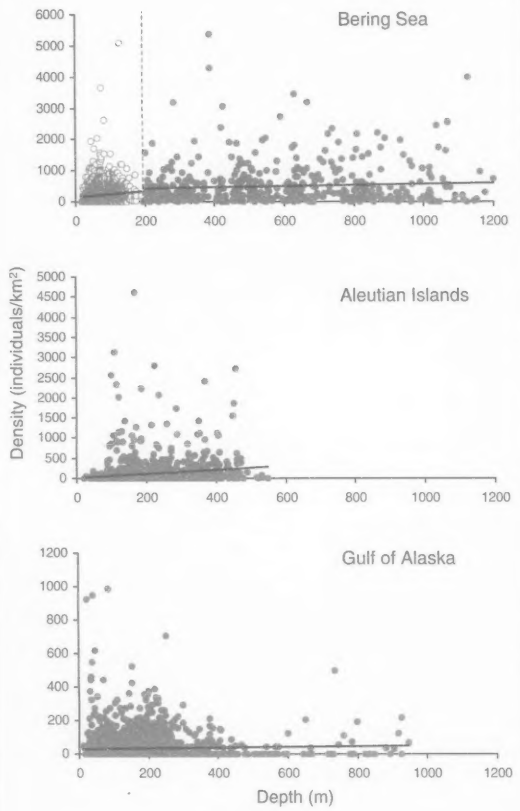

Figure 4

Relationship between overall skate density (no. of individuals/km^2) and depth for bottom-trawl survey hauls completed in the Bering Sea, Aleutian Islands, and Gulf of Alaska from 1999 through 2004. Solid lines represent linear regressions of estimated skate density values, dashed line in upper panel divides Bering Sea shelf records (open circles) from Bering Sea slope records (closed circles).

throughout the survey area, but in only 51% (718 of 1409) of the hauls conducted in this region. Species richness was similar among the four subregions of the Aleutian Islands (Table 2) and increased with depth in all but subregion 1, the westernmost subregion. For all subregions combined, species richness increased significantly (P<0.0001) with increasing depth (Fig. 3). Maximum species richness was encountered in the deepest strata of subregions 2, 3, and 4 and the intermediate depth of subregion 1, whereas the minimum species richness was encountered in the shallow stratum of subregion 4. More species of skates were encountered in the Aleutian Islands (11) than in any of the other regions (vs. 10 in the Gulf of Alaska, 9 on the Bering Sea slope, and 7 on the Bering Sea shelf). Diversity indices were lowest in the shallow strata in all but subregion 4, where the shallow stratum exhibited the highest diversity and the deepest stratum exhibited the lowest (Table 3).

Skate population densities were variable in the Aleutian Islands. Aggregate skate density ranged from 0 to 4609 individuals/km^2, and had an overall mean of 109.38 ±7.96. The spatial pattern of mean density was similar to that of mean species richness and diversity, increasing with depth in all but one subregion (Table 4), although in this case it was the easternmost subregion (subregion 1) that contrasted with the other subregions. The minimum mean density was encountered in the shallow stratum of subregion 4. The maximum mean density was encountered in the middle depth stratum of subregion 1 and in the deep stratum of subregion 3, and mean density was not as uniform as mean species richness across the four subregions. Subregions 1 and 3 yielded overall mean density values considerably higher than those of subregions 2 and 4. For all subregions combined, density increased significantly (P<0.0001) with increasing depth (Fig. 4). The three most common skate species in the Aleutian Islands were *B. maculata*, *B. taranetzi*, and *B. parmifera* (Table 5). *Bathyraja aleutica* was also moderately common.

Gulf of Alaska

The Gulf of Alaska received moderate trawling effort, which was concentrated in the western and central subregions, and skates were comparatively rare in this region. Effort was similar for the shallow and middle depth strata, but the deep stratum was not as heavily sampled (Table 1), and central subregion 3 received the most effort whereas southeastern subregion 5 received by far the least. Although skates were encountered throughout the survey area, they occurred in less than 40% (828 of 2094) of the hauls conducted in the region. Mean species richness was generally higher in the central Gulf of Alaska (subregions 2, 3, and 4) than in either the western (subregion 1) or southeastern subregions (subregion 5) (Table 2). Although the overall trend in this region was for species richness to be higher at deeper depth strata, and the relationship between richness and depth for all subregions combined was significant (P=0.0047) (Fig. 3), this pattern was clearly evident only in subregion 2. Maximum species richness was encountered in the deep stratum of subregion 2, whereas the minimum species richness was encountered across all strata of subregion 1 and the two shallow strata of subregion 5. Diversity indices were not as clearly related to subregion, and only subregion 5 showed a strong trend toward increasing diversity with increasing depth (Table 3).

Skate densities were generally low in the Gulf of Alaska. Aggregate skate density ranged from 0 to 986 individuals/km^2, and had an overall mean of 36.65 ±1.64. The highest mean density was encountered in the shallow depth stratum of subregion 5, but the variability associated with this mean was extremely high. The lowest mean density was encountered in the shallow stratum of subregion 1 (Table 4). Overall mean density generally increased with depth (Fig. 4), although the

Table 6

Depth range (m) for skate species encountered in bottom-trawl survey hauls performed in the eastern Bering Sea (shelf and slope), Aleutian Islands, and Gulf of Alaska from 1999 through 2004. * = not collected in this region.

Species	Bering Sea shelf	Bering Sea slope	Aleutian Islands	Gulf of Alaska	Overall
Bathyraja parmifera	19–190	202–392	47–283	62–375	19–392
B. aleutica	77–173	202–1200	47–535	29–882	29–1200
B. maculata	174	206–1200	91–488	185–208	91–1200
B. interrupta	53–190	202–1017	64–369	37–566	37–1017
B. taranetzi	77–153	202–1063	82–488	64	64–1054
B. lindbergi	*	342–1200	342–458	917	342–1200
B. minispinosa	*	206–1200	223–368	666	206–1200
B. trachura	*	221–1200	369–407	345–946	221–1200
B. mariposa	*	*	95–457	*	95–457
B. abyssicola	*	951–1400	*	*	951–1400
Raja rhina	70–139	*	87–133	24–601	24–601
R. binoculata	37–135	*	26–192	16–376	16–376
Amblyraja badia	*	1508–1556	*	*	1508–1556

relationship was not significant (P=0.117). Subregions 4 and 5 seemed to contradict this trend, with considerably higher mean density values in the shallow stratum, but the standard errors of these means indicated that catches in these subregions were highly variable. Like species richness, mean density was higher in the central subregions and lower in the western and southeastern subregions. The two Alaskan species of the genus *Raja* (*R. binoculata* and *R. rhina*) were the most common skates in this region (Table 5). The only two species of *Bathyraja* that were relatively common in the Gulf of Alaska were *B. interrupta* and *B. aleutica*. A total of ten skate species were encountered in this region, but four of these were recorded in five or fewer hauls.

Species distributions

Of the 14 species of skates currently known from Alaska, 13 were encountered on the surveys included in this study, and 5 of these species were found in all four regions. Two species (*B. abyssicola* and *Amblyraja badia*) were encountered only on the Bering Sea slope, and one (*B. mariposa*) was encountered only in the Aleutian Islands. *Bathyraja violacea*, although known from Alaskan waters, was not encountered in these surveys.

Some species of the genus *Bathyraja* were commonly and widely encountered in all survey regions (Table 6). *Bathyraja parmifera*, the most common species of skate in Alaskan waters, was found throughout all the survey regions (Fig. 5A). *Bathyraja aleutica* (Fig. 5B) and *B. interrupta* (Fig. 5C) were also widespread, both geographically and bathymetrically. Although much more rarely encountered than the aforementioned species, *B. trachura* (Fig. 5D) was also found throughout all survey regions in deep hauls.

Other species were common in some survey regions, but rarely (if ever) encountered in others. *Bathyraja maculata* (Fig. 6A) and *B. taranetzi* (Fig. 6B) were commonly encountered on the Bering Sea slope and in the Aleutian Islands at broad depth ranges (Table 6), but *B. maculata* was recorded only a few times in the Gulf of Alaska, and *B. taranetzi* was not recorded east of Unimak Pass. *Bathyraja lindbergi* (Fig. 6C) and *B. minispinosa* (Fig. 6D) were common only on the Bering Sea slope, but rarely encountered elsewhere. *Raja binoculata* (Fig. 7A) and *R. rhina* (Fig. 7B) were common only in the Gulf of Alaska, although *R. binoculata* was also encountered several times in the Bering Sea and eastern Aleutian Islands.

Three skate species were encountered in only a few hauls throughout the 1999–2004 survey period (Fig. 8). *Bathyraja abyssicola* and *A. badia* were encountered only in a few deep hauls on the Bering Sea slope at depths greater than 950 m, and *Bathyraja mariposa* was encountered only in the central Aleutian Islands.

Discussion

Recent NMFS bottom-trawl surveys provide a wealth of reliable species-specific data on the geographic and bathymetric distributions of the skates of Alaska, as well as insight into relative population densities and regional species assemblages. Although most of the skate species of Alaska have relatively widespread distributions, each geographic and bathymetric region of Alaska has its own characteristic skate fauna and demographic characteristics.

The eastern Bering Sea shelf supports large populations of fishes and invertebrates and serves as an important commercial fishing area. Among skates, *B. parmifera* is by far the most common species, accounting for over 90% of the skate catch of this region. Therefore, even though skates are encountered in the

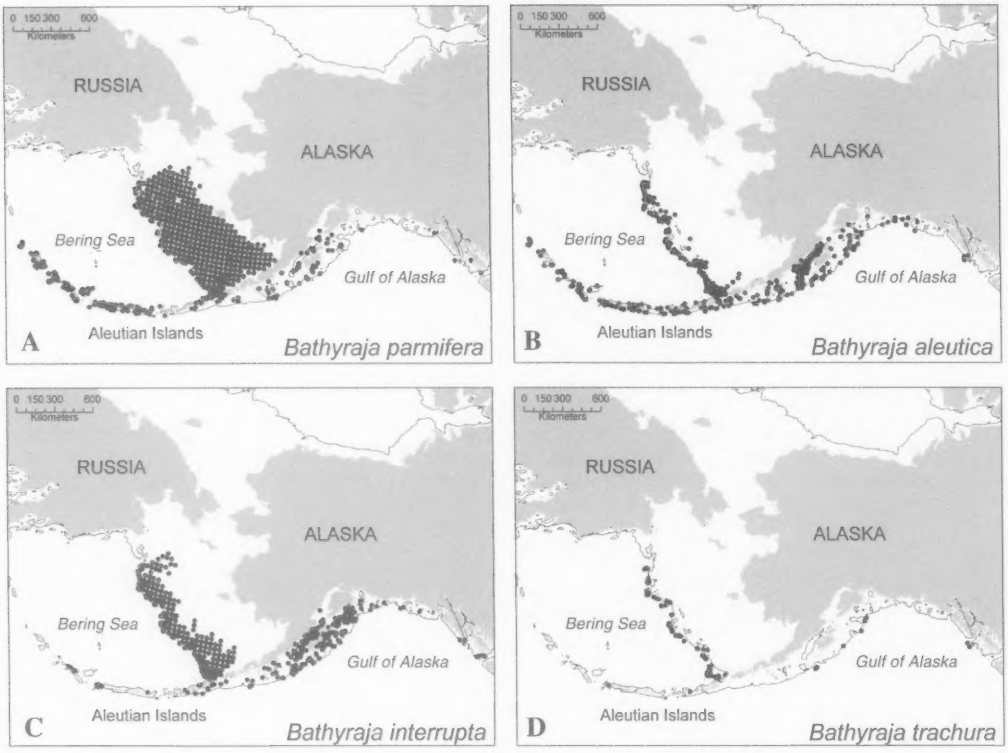

Figure 5

Distribution of (**A**) *Bathyraja parmifera* (Alaska skate), (**B**) *B. aleutica* (Aleutian skate), (**C**) *B. interrupta* (Bering skate), and (**D**) *B. trachura* (roughtail skate) based on data from bottom-trawl surveys conducted in the eastern Bering Sea, Aleutian Islands, and Gulf of Alaska from 1999 through 2004. Black circles indicate the presence of the species in one or more survey hauls. Depth contour = 200 m.

large majority of the hauls, and overall skate numbers have been increasing over the past 20 years (Hoff, 2006), the mean species richness and skate diversity are quite low in this region. In the deeper waters near the shelf-slope break, the skate fauna is more diverse, and *B. aleutica* and *B. interrupta*, two of the most geographically and bathymetrically widespread species in Alaska, are encountered with greater frequency. In addition to widespread distributions in Alaskan waters, both of these species are also found farther south along the North American west coast and have been collected at depths of 20 to over 1000 m. *Bathyraja taranetzi* and *B. maculata* also begin to appear near the shelf break in the eastern Bering Sea, although they are much more common on the continental slope. The presence of these species near the shelf break accounts for the high mean species richness values in the deep depth strata in this region. In the southeastern corner of the Bering Sea shelf, near the eastern Aleutian Islands, the two Alaskan species of *Raja* are occasionally encountered, and their effect on the mean species richness values in subregion 1 are offset by the fact that this area includes the extensive shallow waters of Bristol Bay, where skates are less frequently encountered.

There were no clear bathymetric or geographic trends in skate population density on the eastern Bering Sea shelf. Although overall mean density generally increased with increasing depth, the middle and deep depth strata yielded similar overall means. The low overall mean density values for both the shallow depth stratum and the southern subregion (subregion 1) appeared to be heavily influenced by the relatively low skate densities in the shallow waters of Bristol Bay. The mean density for the shallow stratum of subregion 3 was probably not meaningful because of the relatively low sample size and high variability in density data for this stratum.

The continental slope of the eastern Bering Sea is a region of high skate species richness and diversity, and skates are encountered in nearly every haul. Several species, including *B. aleutica*, *B. interrupta*, *B. taranetzi*, and *B. maculata*, are encountered from the shelf break down to well over 1000 m depth. Another group of species, characterized by a dark ventral surface—*B. lindbergi*, *B. minispinosa*, and *B. trachura*—begin to

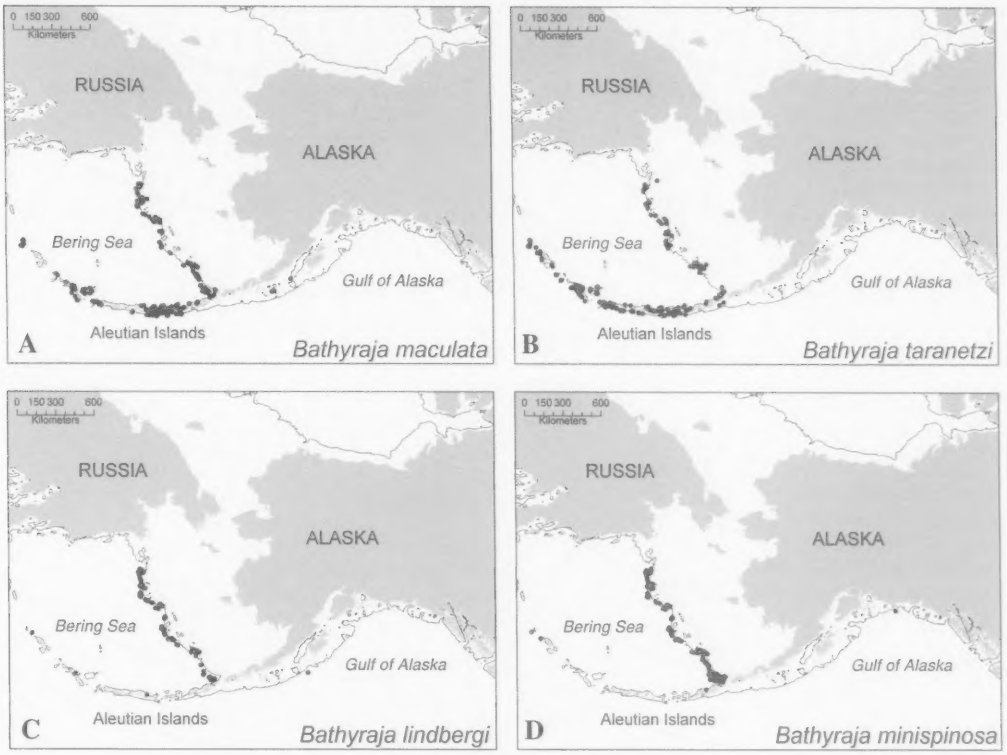

Figure 6

Distribution of (**A**) *Bathyraja maculata* (whiteblotched skate), (**B**) *B. taranetzi* (mud skate), (**C**) *B. lindbergi* (Commander skate), and (**D**) *B. minispinosa* (whitebrow skate) based on data from bottom-trawl surveys conducted in the eastern Bering Sea, Aleutian Islands, and Gulf of Alaska from 1999 through 2004. Black circles indicate the presence of the species in one or more survey hauls. Depth contour = 200 m.

appear at depths of 300–400 m and are more common in deeper waters. Thus, there is a degree of assemblage separation; one suite of species is found on the lower slope and another suite is found on the upper slope but overall species richness remains relatively consistent throughout the depth range of the survey. A similar skate fauna has been reported from the northern Kuril Islands and southern Kamchatka (Orlov, 2005; Orlov et al., 2007), although trends in species richness in that region are unclear. Two additional species, *A. badia* and *B. abyssicola*, have been only rarely encountered in the deep waters of the eastern Bering Sea slope, although these species are widely distributed and have been recorded from both sides of the North Pacific Ocean (Zorzi and Anderson, 1990; Stevenson and Orr, 2005). Species richness and density both show a clear geographic pattern in this region; subregions 2, 4, and 6 exhibit higher species richness and density than the other three subregions, although this effect is less pronounced in the diversity indices. These areas of high species richness and density are generally associated with canyon features on the Bering Sea slope; this association may indicate that skates aggregate near these features. Alternatively, it may simply indicate that the skates in these areas cluster in the same habitats that are most suitable for bottom trawling.

In the eastern Bering Sea, skate density increased with depth from shallow areas to the shelf break, and remained relatively uniform on the upper continental slope. A similar density pattern has also been observed along the Oregon coast (Pearcy et al., 1982) and in northwestern Australia (Williams et al., 2001). In the subregion encompassing Pribilof Canyon the pattern was slightly different; skate density was highest at greater depths on the lower slope, in the same general deeper depth range (700+ m) as noted by Gordon and Duncan (1985) and Merrett et al. (1991) in the northeast Atlantic. Although several distributional studies published for the western Pacific region have included basic distribution, depth range, and relative abundance information for some of the same species of skates reported here (Dudnik and Dolganov, 1992; Nakaya and Shirai, 1992; Dolganov, 1998, 1999; Orlov, 1998, 2003; Orlov et al., 2007), none of these studies have provided

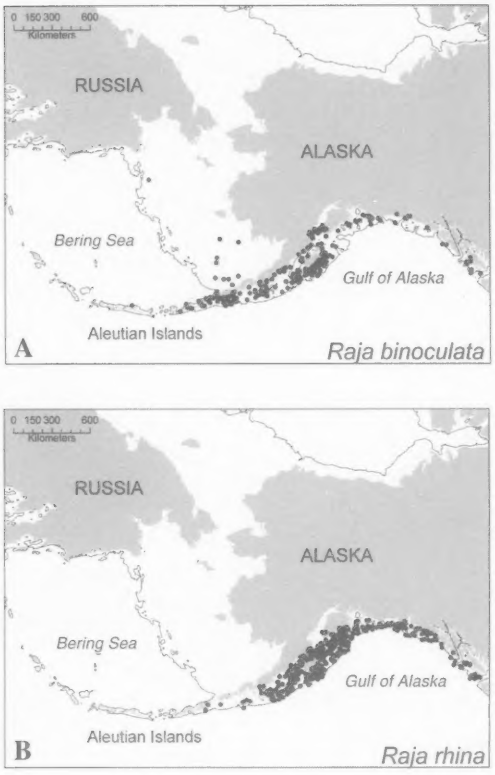

Figure 7

Distribution of (**A**) *Raja binoculata* (big skate) and (**B**) *R. rhina* (longnose skate) based on data from bottom-trawl surveys conducted in the eastern Bering Sea, Aleutian Islands, and Gulf of Alaska from 1999 through 2004. Black circles indicate the presence of the species in one or more survey hauls. Depth contour = 200 m.

Figure 8

Distribution of *Amblyraja badia* (roughshoulder skate: squares), *Bathyraja abyssicola* (deepsea skate: triangles), and *B. mariposa* (butterfly skate: circles) based on data from bottom-trawl surveys conducted in the eastern Bering Sea, Aleutian Islands, and Gulf of Alaska from 1999 through 2004. Black circles indicate the presence of the species in one or more survey hauls. Depth contour = 200 m.

data on overall skate density in enough detail for direct comparison with the present work. Similarly, limited sampling effort on the continental slope of the Aleutian Islands and Gulf of Alaska have precluded us from demonstrating a similar pattern in other regions of the eastern North Pacific.

More species of skates have been recorded from the Aleutian Islands than from any other survey region, and yet the mean species richness figures are relatively low for this region. This finding is a result of the low encounter rate, because skates were present in only about half of the survey hauls completed in the Aleutian Islands. In areas where skates were encountered in the Aleutian Islands, Shannon's diversity indices were relatively high, which may indicate that many species have similar habitat preferences. The most commonly encountered species of skates in the Aleutian Islands were *B. maculata*, *B. taranetzi*, and *B. parmifera*. *Bathyraja aleutica* was also relatively common throughout the archipelago. Although the Aleutians Islands survey did not explore depths greater than 500 m, some of the species commonly found on the Bering Sea slope, such as *B. lindbergi*, *B. minispinosa*, and *B. trachura*, have occasionally been collected in the archipelago, and therefore the skate fauna on the continental slope of the Aleutian Islands is probably similar to that of the eastern Bering Sea slope. The fact that these species were only encountered in the deepest hauls in the Aleutian Islands survey explains why mean species richness increases with increasing depth in this region.

The skate fauna of the Aleutians also displayed some regional variation. *Bathyraja interrupta* was relatively common in the eastern Aleutians but only rarely encountered in the central and western Aleutians, and *Raja binoculata* was not collected west of Unalaska Island. *Bathyraja mariposa* appeared to be endemic to the central Aleutian Islands. In the western Aleutians *B. parmifera* is apparently replaced by a similar undescribed species (Stevenson et al., 2007), treated here as *B. parmifera*, and the western Pacific species *B. violacea* is known from one specimen collected by a groundfish fisheries observer near Buldir Island in the western Aleutians. According to Orlov (2005) and Orlov et al. (2007), *B. maculata*, *B. aleutica*, and *B. violacea* are the most abundant skate species farther west in the northern Kuril Islands and along the southern Kamchatka Peninsula. At least two of the skate species found in the Aleutian Islands, *B. parmifera* and *B. taranetzi*, exhibit very different coloration in the Aleutian Islands than in other regions where they are known. In the eastern Bering Sea, both of these species are a relatively uniform brown, often with dark brown or black blotches and occasionally pale yellow markings.

However, specimens of both species collected from the Aleutian Islands are much more colorful, usually with vivid yellow or olive-green markings on the disc. Additional investigation of these regional differences may lead to the recognition of more undescribed species. The deepwater species *A. badia* and *B. abyssicola* have not been encountered in the Aleutian Islands in recent trawl surveys, although this may be due to the lack of deep trawling effort in the region because both species are known to inhabit the North Pacific and the eastern Bering Sea (see Stevenson and Orr, 2005), and *B. abyssicola* has been recorded from the Aleutian Islands (Zorzi and Anderson, 1990).

Unlike the eastern Bering Sea and Aleutian Islands, the skate fauna of the Gulf of Alaska is dominated by the two Alaskan species of the genus *Raja*. Moreover, the encounter rate of skates in the Gulf of Alaska is even lower than that of the Aleutians. These two factors combine to produce very low mean species richness values. The depth distributions of the two species of *Raja* appear to be somewhat complementary, in that *R. binoculata* generally inhabits shallower waters than *R. rhina*, but neither species is found frequently below 400 m. Like these two species of *Raja*, *Bathyraja interrupta* and *B. aleutica* are both found throughout the Gulf of Alaska, and the ranges of both species extend well south of the Alaska border. *Bathyraja parmifera* is also found throughout the Gulf of Alaska, but is rare west of Kodiak (i.e., in subregions 3, 4, and 5). Like species richness values for the Aleutian Islands, species richness values are low in the Gulf of Alaska, but Shannon's diversity indices are not particularly low. Some of the species common in the slope waters of the Bering Sea and Aleutian Islands, such as *B. lindbergi* (2005 survey data) and *B. minispinosa* (Love et al., 2005), have recently been recorded in the Gulf of Alaska, as well. *Bathyraja trachura*, a species relatively abundant off the U.S. west coast from Washington to California (Lauth, 2000) as well as on the eastern Bering Sea slope, is also probably common throughout the deeper waters of the Gulf of Alaska, and it seems probable that the deepwater species *B. abyssicola* and *A. badia* (both known from around the Pacific Rim; Zorzi and Anderson, 1990; Stevenson and Orr, 2005) would be found in the Gulf of Alaska if additional deep sampling efforts were initiated.

Interpretations of these data should be viewed within the context of the sampling limitations. Groundfish assessment surveys conducted in Alaska have been primarily restricted to the shelf and the shallowest portion of the continental slope. Although recent surveys on the eastern Bering Sea slope have improved our understanding of the distribution of skates and other deeper dwelling fishes, the lack of deeper samples from the Gulf of Alaska and Aleutian Islands is problematic because without these samples we are unable to make meaningful comparisons among regions. Another limitation of this data set concerns the gear used for AFSC bottom-trawl surveys. All surveys included in this study were performed with otter trawls. However, the sea floor substrate and topographic features differ markedly among the regions surveyed. Because of differences in the suitability of the sea bottom for trawling, many areas within Alaskan waters (particularly in the Aleutians and Gulf of Alaska) have been considered "untrawlable," and therefore remain unsampled. Moreover, the relatively rough trawling conditions typically encountered in some regions necessitate the use of different types of trawl gear. The effects that these differences may have on the catchability of skates, and how these catchability differences may affect comparisons among surveys, are unknown (Kotwicki and Weinberg, 2005). Finally, information on any seasonal changes that may affect skate distributions (Dolganov, 1998, 1999) in Alaska is very limited. Virtually all NMFS groundfish assessment surveys in Alaska have been conducted during summer months, and we know little about the distributions of these species during the rest of the year.

This study represents a major advance in our knowledge of the species richness, diversity, population density, and distribution of the skate fauna of Alaska. It provides a reference strategy for the reliable assessment and monitoring of skate diversity and abundance with data from resource assessment surveys. It also provides an example of how advances in taxonomy and field identification tools can enable more detailed and robust assessments of species diversity than were previously possible. These considerations are particularly critical for the skates of this region because of their high species diversity and their vulnerability to fishing pressure and habitat disturbance. We hope this study will serve for comparison with similar studies of other regions or other groups of fishes, as well as provide a baseline for monitoring future changes in the skate fauna of Alaska.

Acknowledgments

We thank the scientific staffs of the Alaska Fisheries Science Center groundfish bottom-trawl surveys conducted from 1999 through 2004, as well as the crews of the FV *Aldebaran*, FV *Arcturus*, FV *Dominator*, FV *Gladiator*, FV *Morning Star*, FV *Northwest Explorer*, FV *Sea Storm*, and FV *Vesteraalen*. We also thank T. Pietsch and K. Maslenikov (Univ. of Washington Fish Collection) for curation of specimens and access to collections. North Pacific groundfish observer R. Morse collected the only specimen of *B. violacea*. M. Martin, R. Lauth, and S. Kotwicki provided critical reviews of earlier drafts of this manuscript.

Literature cited

Allen, M. J., and G. B. Smith.
1988. Atlas and zoogeography of common fishes in the Bering Sea and northeastern Pacific. U.S. Dep. Commer., NOAA Tech. Rep. NMFS 66, 151 p.

Bremer, J. R. A., M. G. Frisk, T. J. Miller, J. Turner, J. Vinas, and K. Kwil.
2005. Genetic identification of cryptic juveniles of little skate and winter skate. J. Fish. Biol. 66:1177–1182.

Britt, L. L., and M. H. Martin.
2000. Data report: 1999 Gulf of Alaska bottom trawl survey. U.S. Dep. Commer., NOAA Tech. Memo. NMFS-AFSC-121, 249 p.

Casey, J. M., and R. A. Myers.
1998. Near extinction of a large, widely distributed fish. Science 281:690–691.

Dolganov, V. N.
1985. New species of skates of the family Rajidae from the northwestern Pacific Ocean. Vopr. Ikhtiol. 25:415–425.
1998. Distribution and migration of skates of the family Rajidae in Far East Seas of Russia. Izv. Tikhookean. Nauchno-Issled. Inst. Rybn. Khoz. Okeanogr. 124:433–437.
1999. Geographical and bathymetric distribution of the skates of the Rajidae family in the Far Eastern Seas of Russia and adjacent waters. J. Ichthyol. 39:340–344.
2001. Origin and distribution of skates of the suborder Rajoidei of the Far East Seas of Russia. J. Ichthyol. 41:355–361.

Dudnik, Y. I., and V. N. Dolganov.
1992. Distribution and abundance of fish on the continental slopes of the Sea of Okhotsk and of the Kuril Islands during the summer of 1989. J. Ichthyol. 32:58–76.

Dulvy, N. K., J. D. Metcalfe, J. Glanville, M. G. Pawson, and J. D. Reynolds.
2000. Fishery stability, local extinctions, and shifts in community structure in skates. Conserv. Biol. 14: 283–293.

Dulvy, N. K., and J. D. Reynolds.
2002. Predicting extinction vulnerability in skates. Conserv. Biol. 16:440–450.

Gordon, J. D. M., and J. A. R. Duncan.
1985. The ecology of the deepsea benthic and benthopelagic fish on the slopes of the Rockall Trough, northeastern Atlantic. Prog. Oceanogr. 15:37–69.

Hoff, G. R.
2006. Biodiversity as an index of regime shift in the eastern Bering Sea. Fish. Bull. 104:226–237.

Hoff, G. R., and L. L. Britt.
2005. Results of the 2004 eastern Bering Sea upper continental slope survey of groundfish and invertebrate resources. NOAA Tech. Memo. NMFS-AFSC-156, 276 p.

Ishihara, H., and R. Ishiyama.
1985. Two new North Pacific skates (Rajidae) and a revised key to *Bathyraja* in the area. Jpn. J. Ichthyol. 32:143–179.
1986. Systematics and distribution of the skates of the North Pacific (Chondrichthyes, Rajoidei). *In* Indo-Pacific fish biology: proceedings of the second international conference on Indo-Pacific fishes (T. Uyeno, R. Aria, T. Taniuchi, and K. Matsuura, eds.), p. 269–280. Ichthyol. Soc. of Japan, Tokyo, Japan.

Ishiyama, R., and H. Ishihara.
1977. Five new species of skates in the genus *Bathyraja* from the western North Pacific, with reference to their interspecific relationships. Jpn. J. Ichthyol. 24:71–90.

Kotwicki, S., and K. L. Weinberg.
2005. Estimating capture probability of a survey bottom trawl for Bering Sea skates (*Bathyraja* spp.) and other fish. Alaska Fish. Res. Bull. 11:135–145.

Lauth, R. R.
2000. The 2000 Pacific west coast upper continental slope trawl survey of groundfish resources off Washington, Oregon, and California: estimates of distribution, abundance, and length composition. U.S. Dep. Commer., NOAA Tech. Memo. NMFS-AFSC-120, 284 p.

Lauth, R., and E. Acuna.
2007. Results of the 2006 eastern Bering Sea continental shelf bottom trawl survey of groundfish and invertebrate resources. U.S. Dep. Commer., NOAA Tech. Memo. NMFS-AFSC-176, 175 p.

Love, M. S., C. W. Mecklenburg, T. A. Mecklenburg, and L. K. Thorsteinson.
2005. Resource inventory of marine and estuarine fishes of the west coast and Alaska: a checklist of North Pacific and Arctic Ocean species from Baja California to the Alaska-Yukon border, 276 p. U.S. Geological Survey, Seattle, WA.

Ludwig, J. A., and J. F. Reynolds.
1988. Statistical ecology: a primer on methods and computing, 337 p. John Wiley and Sons, New York, NY.

Mecklenburg, C. W., T. A. Mecklenburg, and L. K. Thorsteinson.
2002. The fishes of Alaska, 1037 p. Am. Fish. Soc., Bethesda, MD.

Merrett, N. R., J. D. M. Gordon, M. Stehmann, and R. L. Haedrich.
1991. Deep demersal fish assemblage structure in the Porcupine Sea Bight (eastern North Atlantic): slope sampling by three different trawls compared. J. Mar. Biol. Assoc. UK 71:329–358.

Nakaya, K., and S. Shirai.
1992. Fauna and zoogeography of deep-benthic chondrichthyan fishes around the Japanese Archipelago. Jpn. J. Ichthyol. 39:37–48.

Orlov, A.
1998. The diets and feeding habits of some deep-water benthic skates (*Bathyraja* spp., Rajidae) in the Pacific waters off the northern Kuril Islands and southeastern Kamchatka. Alaska Fish. Res. Bull. 5:1–17.
2003. Diets, feeding habits, and trophic relations of six deep-benthic skates (Rajidae) in the western Bering Sea. Aqua J. Ichthyol. Aquat. Biol. 7:45–60.
2005. Bottom trawl-caught fishes and some features of their vertical distribution in the Pacific waters off the north Kuril Islands and south-east Kamchatka, 1993–1999. Aqua J. Ichthyol. Aquat. Biol. 9:139–160.

Orlov, A., A. Tokranov, and R. Fatykhov.
2007. Common deep-benthic skates (Rajidae) of the northwestern Pacific: basic ecological and biological features. Cybium 2007:1–17

Pearcy, W. G., D. L. Stein, and R. S. Carney.
1982. The deep-sea benthic fish fauna of the Northeastern Pacific Ocean on Cascadia and Tufts Abyssal Plains and adjoining continental slopes. Biol. Ocean. 1:375–428.

Raschi, W., D. V. Preziosi, and G. E. Walters.
1994. Recent trends in skate (family Rajidae) stocks from the eastern Bering Sea and Aleutian Islands. *In* Systematics and evolution of Indo-Pacific fishes: proceedings of the fourth Indo-Pacific fish conference (H. L. Pratt, Jr., S. H. Gruber, and T. Taniuchi, eds.), p. 187–199. Faculty of Fisheries, Kasetart University, Bangkok, Thailand.

Spies, I. B., S. Gaichas, D. E. Stevenson, J. W. Orr, and M. F. Canino.
2006. DNA-based identification of Alaska skates (*Amblyraja*, *Bathyraja*, and *Raja*: Rajidae) using cytochrome c oxidase subunit I (coI) variation. J. Fish. Biol. 69:283–292.

Stauffer, G.
2004. NOAA protocols for groundfish bottom trawl surveys of the nation's fishery resources. U.S. Dep. Commer., NOAA Tech. Memo. NMFS-F/SPO-65, 205 p.

Stevens, J. D., R. Bonfil, N. K. Dulvy, and P. A. Walker.
2000. The effects of fishing on sharks, rays, and chimaeras (chondrichthyans), and the implications for marine ecosystems. ICES J. Mar. Sci. 57:476–494.

Stevenson, D. E., and J. W. Orr.
2005. Records of two deepwater skate species from the eastern Bering Sea. Northwest. Natur. 86:71–81.

Stevenson, D. E., J. W. Orr, G. R. Hoff, and J. D. McEachran.
2004. *Bathyraja mariposa*: a new species of skate (Rajidae: Arhynchobatinae) from the Aleutian Islands. Copeia 2004:305–314.

Stevenson, D. E., J. W. Orr, G. R. Hoff, and J. D. McEachran.
2007. Field guide to sharks, skates, and ratfish of Alaska, 77 p. Alaska Sea Grant, Fairbanks, AK.

Teshima, K., and T. K. Wilderbuer.
1990. Distribution and abundance of skates in the eastern Bering Sea, Aleutian Islands region, and the Gulf of Alaska. *In* Elasmobranchs as living resources: advances in the biology, ecology, systematics, and the status of fisheries (H. L. Pratt Jr., S. H. Gruber, and T. Taniuchi, eds.), p. 257–267. U.S. Dep. Commer., NOAA Tech. Rep. NMFS 90.

Tinti, F., N. Ungaro, P. Pasolini, M. DePanfilis, F. Garoia, I. Guraniero, B. Sabelli, G. Marano, and C. Piccinetti.
2003. Development of molecular and morphological markers to improve species-specific monitoring and systematics of Northeast Atlantic and Mediterranean skates (Rajiformes). J. Exp. Mar. Biol. Ecol. 288:149–165.

Williams, A., J. A. Koslow, and P. R. Last.
2001. Diversity, density and community structure of the demersal fish fauna of the continental slope off western Australia (20–35°S). Mar. Ecol. Prog. Ser. 212:247–263.

Zenger, H. H.
2004. Data report: 2002 Aleutian Islands bottom trawl survey. U.S. Dep. Commer., NOAA Tech. Memo. NMFS-AFSC-143, 247 p.

Zorzi, G. D., and M. E. Anderson.
1990. Summary of records of the deep-water skates, *Raja* (*Amblyraja*) *badia* Garman, 1899 and *Bathyraja abyssicola* (Gilbert, 1896), in the eastern North Pacific. *In* Elasmobranchs as living resources: advances in the biology, ecology, systematics, and the status of fisheries (H. L. Pratt Jr., S. H. Gruber, and T. Taniuchi, eds.), p. 389–390. U.S. Dep. Commer., NOAA Tech. Rep. NMFS 90.

Efficiency and catch dynamics of collapsible square and conical crab pots used in the red king crab (*Paralithodes camtschaticus*) fishery

Stian Stiansen[1,2]
Anders Fernö[1,2,*]
Dag Furevik[1,*]
Terje Jørgensen (contact author)[1*]
Svein Løkkeborg[1,*]

Email address for T. Jørgensen: terjej@imr.no

[1] Institute of Marine Research
PO Box 1870 Nordnes
NO-5817 Bergen, Norway

[2] Department of Biology
University of Bergen
NO-5020 Bergen, Norway

Abstract—We compared the capture efficiency and catch dynamics of collapsible square and conical pots used in resource assessment and harvesting of red king crabs (*Paralithodes camtschaticus* [Tilesius, 1815]) in the Barents Sea. After two days of soaking, square pots caught three times as many crabs as conical pots, and their catches consisted of a higher proportion of male crabs and male crabs larger than 160 mm carapace length compared to the catches in the conical pots. Catches in the square pots did not increase as soak times were increased beyond two days, which indicates equilibrium between the rate of entries into and the rate of exits from the pots. Catches in conical pots, however, increased with increasing soak times up to eight days, the longest soak time examined in this study. These findings demonstrate the higher efficiency of square pots and the importance of understanding catch dynamics when making population assessments based on catch-per-unit-of-effort data. The favorable catch characteristics and handling properties of the collapsible square pot may make this pot design suitable for other crab fisheries, as well.

Manuscript submitted: 16 January 2007.
Manuscript accepted 3 August 2007.
Fish. Bull. 106:40–46 (2008).

The views and opinions expressed or implied in this article are those of the author and do not necessarily reflect the position of the National Marine Fisheries Service, NOAA.

The introduction of red king crab (*Paralithodes camtschaticus* [Tilesius, 1815]) (RKC) in the Barents Sea in the 1960s led to a commercial pot fishery in this area. In Norwegian waters, surveys conducted with conical pots in order to estimate population abundance on the basis of catch-per-unit-of-effort (CPUE) data began in 1993. In 2002, the first licenses for commercial fishing of RKC were issued. To harvest this new resource, an efficient, selective, and habitat-friendly fishing gear is required. Only small coastal fishing vessels (<15 m) are licensed in the Norwegian RKC fishery and these vessels are too small to effectively operate large rigid pots. Initially, conical pots were used because they have been used in the Russian and Japanese fishery for king crabs (Ivanov, 2002). Preliminary studies with a modified square, collapsible cod pot showed higher catches, and according to the fishermen, the square pot had better handling properties than the conical pot. The industry therefore requested adoption of this modified square pot design in the RKC fishery.

The introduction of new fishing gear in the commercial fishery, and subsequently in population assessments, requires a knowledge of its catching properties in order to ensure sustainable harvesting practices and to interpret changes in CPUE data (Hilborn and Walters, 1992; Nizyaev and Bukin, 2002). Thus, before the collapsible square pot was adopted, fishing trials had to be carried out to compare the catching efficiency and selection characteristics of the square pot with those of the conical pot.

Fishing with pots without escape-preventing devices (e.g., triggers or soft-eyed entrances) is a dynamic process, in which the ratio of crabs entering the pot to those escaping the pot usually decreases as soak time increases (Zhou and Shirley, 1997a; Watanabe and Yamasaki, 1999). Our fishing trials were therefore carried out with soak time as an explanatory variable.

The objectives of the experiment were to compare the two different pot designs with regard to 1) catch efficiency, 2) size distribution and sex ratio of the catch, and 3) the degree to which these characteristics (catch efficiency, size distribution, and sex ratio) are affected by soak time. Such

* signifies equal authorship.

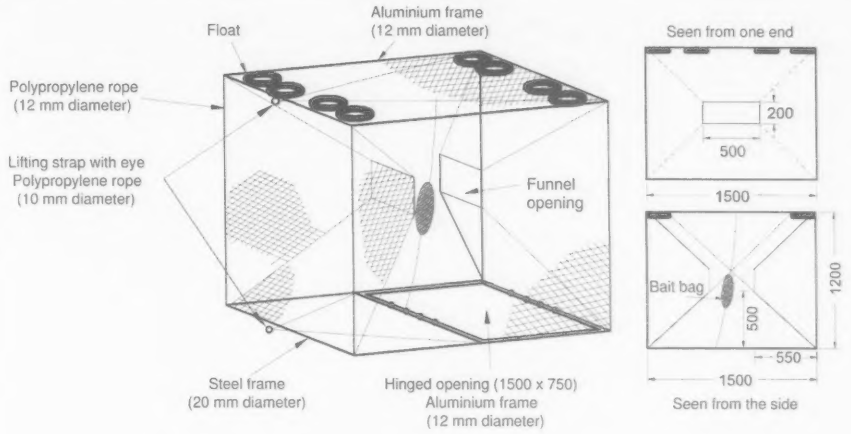

Figure 1

Drawing of the square pot design used to capture red king crab (*Paralithodes camtschaticus*). The frame is lined with 3-mm braided polyethylene netting with a mesh size of 100 mm. The 20-cm long bait bag is made of polyamide netting and has a mesh size of 22 mm. The pot weighs 37 kg out of water. All pot dimensions are in mm.

information is crucial for both improved population estimates and resource-friendly harvesting practices.

Materials and methods

The square pot (Fig. 1) had two funnel-shaped entrances with outer openings of 150×120 cm. The entrance area thus made up half of the pot's horizontal circumference. The netting used to line the frames had a mesh size of 100 mm. The 20-cm long bait bag was made of small-mesh netting (22 mm mesh size) and was placed in the center of the pot between the entrance openings. The weight of the pot out of water was 37 kg. The funnel of the conical pot (Fig. 2) was made of hard plastic, had an outer diameter of 45 cm, and was located at the top of the pot. The mesh size of the netting liner was 150 mm. A bait bag similar to that used in the square pots was located at the center of the pot, 10 cm below the inner funnel opening. The weight of the pot out of water was 17 kg.

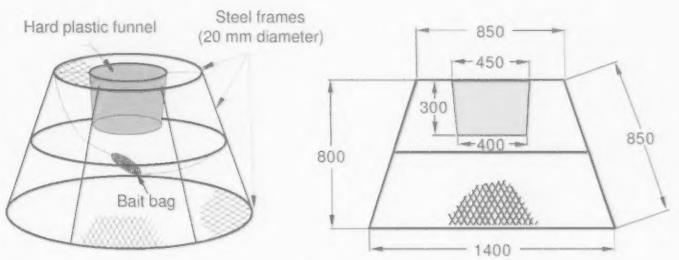

Figure 2

Drawing of the conical pot design used to capture red king crab (*Paralithodes camtschaticus*). The frames are made of 20-mm steel bars and lined with 4-mm polyethylene diamond netting with a mesh size of 150 mm. The 20-cm long bait bag is made of polyamide netting with mesh size of 22 mm. The pot weighs 17 kg in air. All pot dimensions are in mm.

The fishing trials were carried out between 19 October and 6 November 1998 in the Varangerfjord (close to the Russo-Norwegian border) (Fig. 3), which is the area with the highest density of RKC in Norwegian waters. Four commercial coastal fishing vessels of 10–12 m length were chartered for the experiment. The pots were set at depths of 50–250 m on silty and muddy bottom substrates.

Each vessel fished with 24 pots, arranged in six strings—each string consisting of two square and two conical pots (Fig. 4). The two types of pots were attached alternately to a 12-mm diameter rope at intervals of about 30 m, a between-pot distance commonly used by commercial fishermen. Each pot was baited with about 1 kg of chopped (~2 cm pieces), thawed Atlantic herring (*Clupes harengus*).

The analyses were based on the 112 string settings where there was catch in at least one of the four pots.

Four different categories of soak times were analyzed. The strings that were given a nominal two days of soak time (as is commonly used in commercial fishing) were physically in the water for 36 to 57 h (N = 61 string settings; mean=46.7 ±0.5 SE, standard error). The strings that were given three days of soak time were left out for 68 to 78 h (N= 30 string settings; mean=71.6 ±0.5 SE). Strings that were soaked for 90 to 120 h were classified as soaking for four to five days (N=8 string settings; mean=107.4 ±3.6 SE). A soak time of seven to eight days was ascribed to strings that were left to fish for 167 to 192 h (N=13 string settings; mean=176 ±3.0 SE).

During pot hauling, the sex of the crabs was identified and the carapace length (CL) was measured to the nearest millimeter with a caliper gauge (Zhou and Shirley, 1997b). The difference in mesh size between the square (100-mm mesh) and conical pots (150-mm mesh) may have contributed to differences in catchability of the smallest crabs. All crabs below 91 mm CL (a total of 54 crabs in the square pots and 16 in the conical pots) were therefore excluded from the length analysis because crabs with a CL of up to 90 mm are capable of escaping through a 152-mm mesh (Zhou and Shirley, 1997c).

The pooled catch of crabs from the two pots of the same type within a string was used as a single observation in the statistical analyses to prevent inflation of tests by the use of pseudoreplicates (here: individual pots of the same type in the same string) and to minimize the effects of current (Sinoda and Kobayasi, 1969; Vienneau et al., 1993), and differences in depth, bottom conditions, and patchy distribution of the crabs (Wallace et al., 1949; Zhou and Shirley, 1998).

The catch and length observations were not normally distributed. Non-parametric statistics were therefore employed in the analyses. Paired comparisons (Wilcoxon test) of catch of RKC in square and conical pots in each string were carried out for each soak time. The Kruskal-Wallace one-way analysis of variance of ranks (Zar, 1999) was used to test for whether catch rates varied with soak time within each type of pot. The size composition of male and female crabs in the square and conical pots was com-

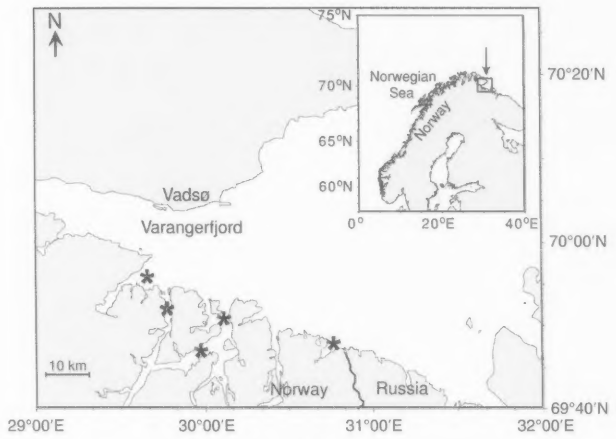

Figure 3

Map of the study area where the square and concical pots were used to capture red king crab (*Paralithodes camtschaticus*). Sampling locations are marked with asterisks.

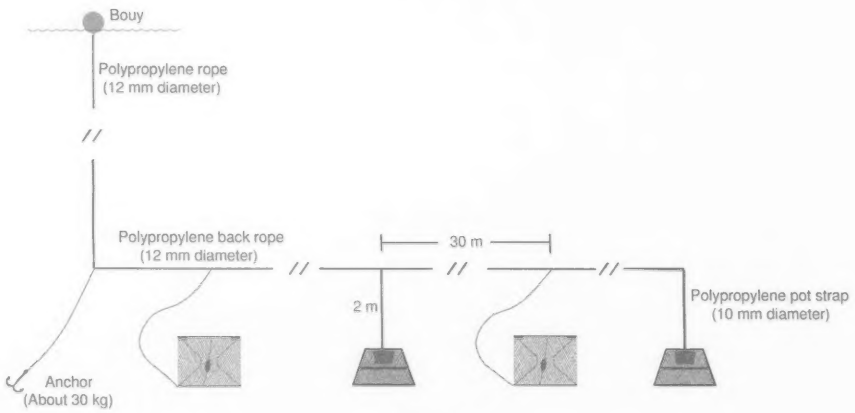

Figure 4

Drawing of the rigging formation used to capture red king crab (*Paralithodes camtschaticus*) in square and conical crab pots. Square and conical pots were arranged alternately along the string.

Table 1

Catch data from the comparative fishing experiment with square and conical red king crab (*Paralithodes camtschaticus*) pots. Total catch and catch by sex of red king crab (*Paralithodes camtschaticus*) at different soak times is shown. Within-string catches of red king crab for square and conical pots were compared by using a Wilcoxon paired comparisons test. n_p is number of pot settings for each type of pot, and N is the number of strings with nonzero catch. SE = standard error.

		Number of crabs caught							
		Square pots			Conical pots			Paired comparisons	
Soak time (days)	n_p	Median	Mean	SE	Median	Mean	SE	N	P value
Males									
2	122	12.0	14.9	0.86	2.0	3.5	0.37	61	<0.001
3	60	14.0	13.9	1.04	5.0	6.2	0.66	30	<0.001
4–5	16	10.0	10.9	1.26	5.0	6.0	0.90	8	<0.05
7–8	26	13.0	14.0	1.68	9.0	9.7	1.43	13	>0.05
Females									
2	122	15.0	16.1	1.02	5.0	6.2	0.53	61	<0.001
3	60	18.0	17.4	136	12.0	11.5	1.08	30	<0.001
4–5	16	20.5	19.6	3.57	11.0	10.6	1.10	8	>0.05
7–8	26	20.0	21.2	1.56	18.0	17.8	1.69	13	>0.1
Total catch									
2	122	29.0	31.0	1.66	7.5	9.7	0.79	61	<0.001
3	60	32.0	31.3	1.81	15.5	17.6	1.43	30	<0.001
4–5	16	29.0	30.5	3.90	15.5	16.6	1.33	8	<0.05
7–8	26	34.0	35.2	2.83	26.5	27.5	2.54	13	<0.05

pared by means of the Mann-Whitney U-test for each soak time.

A Wilcoxon test was used to test for differences between the pot types in the proportion of male crabs and males that were larger than 160 mm CL (the smallest commercial size in the Norwegian RKC fishery). In order to reduce the effect of small sample size (Zar, 1999), proportions equal to zero were replaced by $1/4n$ (where n is the denominator in the calculation of the original proportion) and proportions equal to one were replaced by $1–(1/4n)$. Only observed data on strings with catches in both types of pots were included in these analyses. All statistical tests were performed with Statistica, vers. 8.0 (StatSoft Inc., Tulsa, OK).

Results

The square pots caught significantly more crabs than the conical pots at all soak times (Table 1). At the shortest soak times, the catch ratio of square to conical pots exceeded 3:1, whereas the mean ratio (square:conical) for the two longest soak times was close to 3:2. Except for the longest soak time, the square pots caught more of both male and female crabs (Table 1, Fig. 5). Total catches and the catches of both male and female crabs in the conical pots increased with increasing soak time ($P<0.001$), but catches in the square pots did not increase beyond two days of soak time.

The percentage of male crabs in the catch was higher in the square than in the conical pots after the two, three, and four to five days of soak time (Table 2). The difference was greatest for the shortest soak times because the proportion of female crabs in the square pots increased with increasing soak time ($P<0.05$). No significant changes were found in the percentage of female crabs taken in conical pots over time.

The overall percentages of male crabs larger than 160 mm were 60% (SE=3) and 50% (SE=3) in the square and conical pots, respectively. At all soak times, the proportion of male crabs larger than 160 mm was significantly higher in the square pots ($P<0.001$, Fig. 5). The median length of males was larger in the square pots for all but the longest soak time tested (Table 3). There were no differences between the types of pots with respect to the size of female crabs caught.

Discussion

The square pots caught up to three times more red king crab than the conical pots, but the difference decreased with increasing soak time. Provided that the two types of pots attracted equal numbers of crabs (identical bait was used), the differences in catches must be due to different rates of entry versus exit. Because escape rates from the conical pot have been shown to be low (Godøy et al., 2003), the low catch rate for the conical pot was

presumably due to low entry rates. RKC and other species of crabs have been shown to restrict their horizontal search movement to the area suffused by the odor plume from the bait (Miller, 1980; Zhou and Shirley, 1997c; Archdale et al., 2003). However, the differences in the probability of crabs finding their way into the two pots is not explained by the size of the horizontal entrance sector (area available for entry) because the less efficient conical pots had an entrance sector of 360°, whereas only half of the perimeter of square pots led to a funnel opening. Vertical search behavior of chemically stimulated RKC has also been observed to be limited to the extent of the odor plume (Stiansen, 2004). In the square pot, the bait and funnel were at the same vertical height, whereas the entrance of the conical pot was located above the plume. Crabs were seldom observed to search for the source of the odor outside the odor plume (Miller, 1978; Vienneau, 1993; Stiansen, 2004), which they have to do to locate the entrance of conical pots.

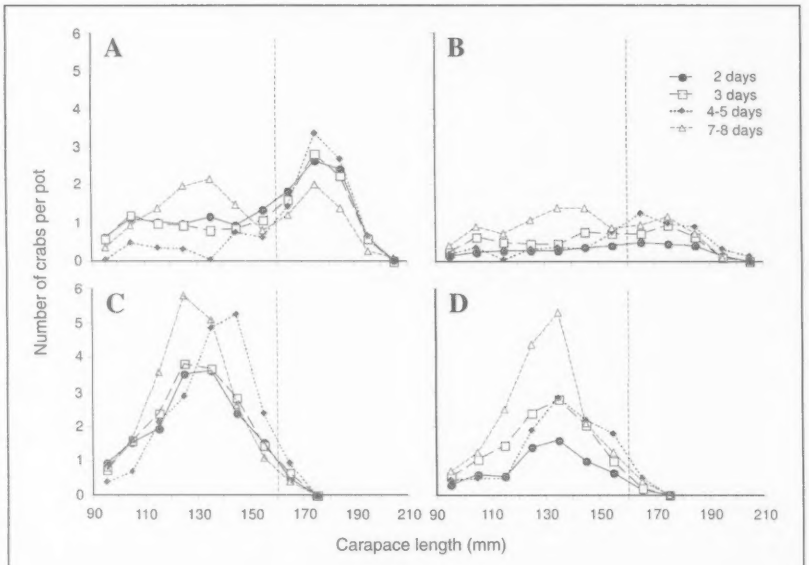

Figure 5

Size distribution of red king crabs (*Paralithodes camtschaticus*) caught in the comparative fishing experiment. The four panels give the size distribution of (**A**) male crabs in square pots; (**B**) male crabs in conical square pots, (**C**) female crabs in square pots, and (**D**) female crabs in conical pots. The *x*-axis is divided by size intervals of 10-mm carapace length. Note that the minimum commercial landing size of male crabs is 160 mm, marked with a vertical dashed line.

Although the catches in the conical pots continued to increase beyond two days of soak time, the catch appeared to stabilize in the square pots, indicating that the two pot types were at different phases of the catch cycle even after two days of soak time. An approximately linear increase in catches with time in the conical pots indicates that the ratio of entries to exits was relatively constant throughout the period of observation. The vertical plastic funnel used in the conical pots effectively prevents crabs from escaping (Miller,

Table 2

Catch data from the comparative fishing experiment with square and conical red king crab (*Paralithodes camtschaticus*) pots. Median and mean percentages of female red king crabs in catches taken by square and conical pots at different soak times are shown. Calculations were made on a string basis, i.e., the pooled catch from the two pots of the same type within a string was used as a single observation. The hypothesis of no difference in percentage of females in square and conical pots was tested by a Wilcoxon paired comparisons test. Only string settings with catch in both types of pots were used in the test. N is the number of strings with nonzero catches, SE is the standard error, and N_b is number of strings with catch in both types of pot.

	Percentages of female crabs caught								Statistical test	
	Square pots				Conical pots				Paired comparisons	
Soak time (days)	N	Median	Mean	SE	N	Median	Mean	SE	N_b	P value
2	57	53.4	51.0	2.17	52	66.7	63.8	2.46	51	<0.001
3	29	56.5	52.0	4.21	27	71.0	66.4	3.76	26	<0.005
4–5	8	65.9	58.2	8.31	8	69.8	63.3	6.82	8	<0.05
7–8	13	62.9	62.2	2.82	13	65.3	67.0	4.30	13	>0.5

Table 3

Catch data from square and conical pots used to capture red king crab (*Paralithodes camtschaticus*). Median and mean carapace length of male and female red king crabs caught by the two types of pot at different soak times are shown. The length distributions were compared by means of a nonparametric Mann-Whitney *U* test for each soak time. *n* is the number of crabs caught, SE is the standard error.

	Carapace length of crabs caught (mm)								
	Square pots				Conical pots				
Soak time (days)	*n*	Median	Mean	SE	*n*	Median	Mean	SE	*U* test *P* value
Males									
2	1797	161	154	0.69	412	154	150	1.38	<0.01
3	823	164	154	1.04	369	151	148	1.44	<0.001
4–5	232	174	168	1.46	95	166	159	2.37	<0.01
7–8	364	142	146	1.42	250	142	143	1.65	>0.2
Females									
2	1954	131	130	0.39	755	132	131	0.60	>0.1
3	1030	130	130	0.53	683	131	130	0.63	>0.7
4–5	312	139	137	0.85	170	137	136	1.22	>0.6
7–8	548	129	128	0.62	463	131	130	0.67	>0.05

1990; Cyr and Sainte-Marie, 1995), and it is not until catches are large, and crabs (by climbing on top of each other) can reach to the funnel top, that the entry and exit rates reach equilibrium (Zhou and Shirley, 1997a). The linear increase in catches, the relative low catches, and the stable sex ratio (60% females) until seven to eight days of soak time indicated that the exit rate was low for the conical pots.

Unlike the catch in the conical pots, the amount of catch taken by the square pots did not increase after two days of soak time as was also observed by Zhou and Kruse (2000) who used a different square-pot design. The initially high rate of entry into pots may lead to the bait being eaten within a short time and to the result that few additional crabs are attracted into the pot. In addition, the likelihood of escape should be higher for square pots that have two horizontally orientated funnels, which are placed lower and made of netting that enable crabs to climb up the funnel and escape (Zhou and Shirley, 1997c).

The square pots caught a higher proportion of male crabs and male crabs larger than 160 mm CL than did the conical pots. If the largest crabs take longer to escape than small crabs, large crabs will accumulate in the square pots over the course of time. Sexual dimorphism, where the two sexes have different probabilities of leaving the square pot, would result in more males in the catch. Although large crabs accumulated in the square pots over time, the proportion of female crabs increased from 50% to 60% with longer soak time. This increase may also be explained by sex-dependent escape probability. Generally, total body length and height (critical dimensions in entering and escaping) are greater for females than for males of the same carapace length (Zhou and Shirley, 1997b), and the differences increase with increasing carapace length. Thus, at a carapace length of 100 mm, Wallace et al. (1949) found female crabs to be 6 mm longer and 11 mm taller than male crabs with the same carapace length. Moreover, in the autumn (the season of this study) most female crabs larger than 100 mm CL were carrying external eggs, which would further increase body length and height. Motivational differences related to sex and condition may also have influenced the ability of RKC to climb into and out of pots (Zhou and Shirley, 1997c).

The catch characteristics and design (collapsible) of the square pots make them highly suitable for commercial fishing. This pot design may also prove to be efficient and practical in other regions, e.g., in the Alaskan king crab and Tanner crab (*Chionoecetes bairdi*) fisheries. The size selection of the square pots resulted in them taking five times as many large male crabs (>160 mm CL, approximately 3.5 kg) as the conical pots after two days of soak time. The selectivity and catch efficiency of the square pots also resulted in a 50% reduction in the catch of females and males smaller than 137 mm CL (minimum legal landing size). Even though discard mortality should be minimal with correct on-deck handling, there is nevertheless the likelihood that some crabs are injured, e.g., spines, rostrum, and limbs can be damaged during handling (Zhou and Shirley, 1995). RKC without all legs intact are of no commercial value and have to be discarded. This problem would be mitigated with the use of square pots. A further advantage of the square pot over the conical pot is that the higher escapement rate afforded by the square pot reduces crab mortality at sea when pots that are lost at sea continue to fish (ghost fish); the pots used in the

Norwegian fishery do not at present contain a degradable escapement panel. Such panels are mandatory in some regions, such as Alaska.

Catch rates, sex ratio, and size distribution were clearly different for square and conical pots. CPUE data from the square pots will provide much higher estimates of the exploitable part of the population (i.e., large male crabs) than data from conical pots. Large differences were also observed in the catch dynamics; the square pot reached equilibrium at much shorter soak times than did the conical pot. Gear saturation may lead to underestimation of population abundance at high densities of crabs. In an area with high crab density, no effects of increasing soak time beyond two days were found (Zhou and Kruse, 2000), and smaller pots underestimated population density to a higher extent than did the larger pots (Nizyaev and Bukin, 2002). The relationship between pot design, catch dynamics, and selectivity observed in the present study demonstrates the importance of adjusting for and standardizing the duration of soak time when CPUE data from pots are used in population assessments. Most importantly, when using effective pots like the square pot tested in this study, soak time needs to be short in order to prevent underestimation of population size and biased sex and size distributions.

Acknowledgments

The authors are grateful for the invaluable comments and advice from the referees and the editorial staff. We also thank B. K. H. Ulvestad and A.-B. S. Tysseland for preparing the figures.

Literature cited

Archdale, M. V., K. Anraku, T. Yamamoto, and N. Higashitani.
2003. Behavior of the Japanese rock crab 'Ishigani' *Charybdis japonica* (A. Milne Edwards) towards two collapsible baited pots: evaluation of capture effectiveness. Fish. Sci. 69:785–791.

Cyr, C., and B. Sainte-Marie.
1995. Catch of Japanese crab traps in relation to bait quantity and shielding. Fish. Res. 24:129–139.

Godøy, H., D. M. Furevik, and S. Stiansen.
2003. Unaccounted mortality of red king crab (*Paralithodes camtschaticus*) in deliberately lost pots off Northern Norway. Fish. Res. 64:171–177.

Hilborn, R., and C. J. Walters.
1992. Quantitative fisheries stock assessment, 570 p. Chapman and Hall, Inc., New York, NY.

Ivanov, B. G.
2002. Red king crab (*Paralithodes camtschaticus*) in the eastern Okhotsk Sea: problems and stock management and research. *In* Crabs in cold water regions: biology, management, and economics (A. J. Paul, E. G. Dawe, R. Elner, G. S. Jamieson, G. H. Kruse, R. S. Otto, B. Sainte-Marie, T. C. Shirley, and D. Woodby, eds.), p. 651–680. Univ. Alaska Sea Grant College Program, AK-SG-02-01, Fairbanks, AK.

Miller, R. J.
1978. Entry of *Cancer productus* to baited traps. J. Cons. Int. Explor. Mer 38(2):220–225.
1980. Design criteria for crab traps. J. Cons. Int. Explor. Mer 39:140–147.
1990. Effectiveness of crab and lobster traps. Can. J. Fish. Aquat. Sci. 47:1228–1251.

Nizyaev, S. A., and S. D Bukin.
2002. Methodological problems associated with assessing crab resources based on trap catch data. *In* Crabs in cold water regions: biology, management, and economics (A. J. Paul, E. G. Dawe, R. Elner, G. S. Jamieson, G. H. Kruse, R. S. Otto, B. Sainte-Marie, T. C. Shirley, and D. Woodby, eds.), p. 521–536. Univ. Alaska Sea Grant College Program, AK-SG-02-01, Fairbanks, AK.

Sinoda, M., and T. Kobayasi.
1969. Studies on the fishery of Zuwai crab in the Japan Sea—VI. Efficiency of the Toyama Kago (a kind of crab trap) in capturing the Beni-zuwai crab. Bull. Jpn. Soc. Sci. Fish. 25(10):948–956.

Stiansen, S.
2004. Catch differences between two types of king crab pots—behavior studies in the near field and comparative fishing trials. Cand. scient. thesis, 85 p. Univ. Bergen, Norway. [In Norwegian.]

Vienneau, R., A. Paulin, and M. Moriyasu.
1993. Evaluation of catch mechanism of conventional conical snow crab (*Chinoecetes opilio*) traps by underwater video camera observations. Can. Tech. Rep. Fish. Aqua. Sci. 1903:1–22 p.

Wallace, M. M., C. J. Pertuit, and A. H. Nvatum.
1949. Contributions to the biology of the king crab *Paralithodes camtschtica* (Tilesius). U.S. Fish and Wildlife Service. Fish. Leafl. 340:1–49.

Watanabe, T., and S. Yamasaki.
1999. Catch variation and the soak time of gear in the pot fishery for the red queen crab *Chinoecetes japonicus*. Nippon Suisan Gakkaishi 65(4):642–649. [In Japanese]

Zar, J. H.
1999. Biostatistical analysis, 4th ed., 931 p. Prentice-Hall, Upper Saddle River, NJ.

Zhou, S., and G. H. Kruse.
2000. Capture efficiency and size selectivity of two types of pots for red king crabs in the Bering Sea. Alaska Fish. Res. Bull. 6(2):94–103.

Zhou, S., and T. C. Shirley.
1995. Effects of handling on feeding, activity and survival of red king crabs, *Paralithodes camtschaticus* (Tilesius, 1815). J. Shellf. Res. 14:173–177.
1997a. A model expressing the relationship between catch and soak time for trap fisheries. N. Am. J. Fish. Manag. 17:482–487.
1997b. Behavioural responses of red king crab to crab pots. Fish. Res. 30:177–189.
1997c. Performance of two red king crab pot designs. Can. J. Fish. Aquat. Sci. 54:1858–1864.
1998. A submersible study of red king crab and Tanner crab distribution by habitat and depth. J. Shellfish Res. 17:1477–1479.

The trophic dynamics of summer flounder (*Paralichthys dentatus*) in Chesapeake Bay

Robert J. Latour (contact author)
James Gartland
Christopher F. Bonzek
RaeMarie A. Johnson

Email address for R. J. Latour: latour@vims.edu

Department of Fisheries Science
Virginia Institute of Marine Science
College of William and Mary
Route 1208 Greate Road
Gloucester Point, Virginia 23062

Abstract—Data on the trophic dynamics of fishes are needed for management of ecosystems such as Chesapeake Bay. Summer flounder (*Paralichthys dentatus*) are an abundant seasonal resident of the bay and have the potential to impact foodweb dynamics. Analyses of diet data for late juvenile and adult summer flounder collected from 2002–2006 in Chesapeake Bay were conducted to characterize the role of this flatfish in this estuary and to contribute to our understanding of summer flounder trophic dynamics throughout its range. Despite the diversity of prey, nearly half of the diet comprised mysid shrimp (*Neomysis* spp.) and bay anchovy (*Anchoa mitchilli*). Ontogenetic differences in diet and an increase in diet diversity with increasing fish size were documented. Temporal (inter- and intra-annual) changes were also detected, as well as trends in diet reflecting peaks in abundance and diversity of prey. The preponderance of fishes in the diet of summer flounder indicates that this species is an important piscivorous predator in Chesapeake Bay.

Manuscript submitted: 8 May/2007.
Manuscript accepted: 28 September 2007.
Fish. Bull. 106:47–57 (2008).

The views and opinions expressed or implied in this article are those of the author and do not necessarily reflect the position of the National Marine Fisheries Service, NOAA.

Summer flounder (*Paralichthys dentatus*) are found along the eastern seaboard of North America from Nova Scotia to Florida, but are most abundant between Massachusetts and North Carolina (Ginsberg, 1952; Leim and Scott, 1966; Gutherz, 1967). This species supports both commercial and recreational fisheries throughout southern New England and the Mid-Atlantic Bight. The commercial fishery for summer flounder has historically accounted for about 60% of the annual landings and occurs mainly in the offshore waters of the continental shelf during late fall and winter. The majority of the recreational fishery, which on occasions has exceeded the commercial harvest, takes place in state waters (i.e., estuaries and the coastal waters out to 3 nautical miles) during summer and early fall. Both fisheries contribute millions of dollars to economies on local and regional scales (Terceiro, 2002).

The trophic dynamics of summer flounder have been fairly well studied (Poole, 1964; Smith and Daiber, 1977; Powell and Schwartz, 1979; Roundtree and Able, 1992; Link et al., 2002; Staudinger, 2006). However, the majority of these investigations have documented the diet of summer flounder in coastal waters or in more northern estuarine environments, rather than in the southern estuaries. The latter ecosystems support a high abundance of summer flounder and provide vital summertime habitats for this species (Desfosse, 1995).

The Chesapeake Bay is the largest estuary in the summer flounder range. No known studies have been undertaken to document summer flounder diet in these waters, and thus there has been a gap in our understanding of the feeding habits of this species within an important area of its range. Further, there is growing awareness regionally, nationally, and internationally of the importance of ecosystem-based approaches to fisheries management (EBFM). A necessary element in support of EBFM is nontraditional types of fisheries data, including information on the trophic dynamics of fishes.

In this article, we present the diet composition of summer flounder collected in Chesapeake Bay from 2002 through 2006 to explore ontogenetic, interannual, and intra-annual variability in diet using canonical correspondence analysis (CCA). Collectively, this information provides insight into the role of summer flounder in the Chesapeake Bay foodweb, and contributes to our understanding of the trophic dynamics of this species throughout its range.

Materials and methods

Field collections

The data presented in this article were collected from the Chesapeake Bay Multispecies Monitoring and Assessment Program (ChesMMAP),

which is a bottom trawl survey program designed to sample late-juvenile and adult fishes in the mainstem Chesapeake Bay (i.e., nontributary waters). During 2002–2006, a total of 25 ChesMMAP cruises were conducted (March, May, July, September, and November annually) and approximately 80 to 90 sites were sampled during each cruise. Sampling locations were chosen according to a stratified random design, and strata were defined by water depth (3–9 m, 9–15 m, and >15 m) within five 30-latitudinal minute regions of the bay. The locations sampled in each stratum of each region were randomly selected and the number of locations was in proportion to the surface area of that stratum. At each sampling location, a 13.7-m 4-seam balloon otter trawl (15.2-cm stretch mesh in the wings and body and 7.6-cm stretch mesh in the cod end) was towed for 20 min at approximately 6.5 km/h. The catch from each tow was sorted and individual lengths (total length, TL) were recorded according to species or size-class if distinct classes within a particular species were evident. Stomachs were removed from a subsample of each species or size-class and immersed in preservative for diet composition analysis after each cruise.

Identification of stomach contents

The contents of each stomach were removed for identification to the lowest possible taxon. Prey encountered in the esophagus and buccal cavity were included for identification (and assumed not to be the result of net feeding because of a lack of retention of prey in large mesh gear), whereas prey in the intestines were ignored because of the difficulty associated with identifying digested prey items in advanced stages of decomposition. All prey items were sorted, measured (either fork or total length, as appropriate and when possible), and the wet weight (0.001 g) of each was recorded.

General diet description

To summarize the diet composition of summer flounder in the mainstem of Chesapeake Bay, a measure of percent weight was calculated for each prey type (Hyslop, 1980). Because the ChesMMAP trawl collections yielded a cluster of summer flounder at each sampling location, the aforementioned percentages were calculated by using a cluster sampling estimator (Bogstad et al., 1995; Buckel et al., 1999). Therefore, the contribution of each prey type to the diet by weight ($\%W_k$) was

$$\%W_k = \frac{\sum_{i=1}^{n} M_i q_{ik}}{\sum_{i=1}^{n} M_i} * 100 , \qquad (1)$$

where $q_{ik} = \frac{w_{ik}}{w_i}$,

and where n = the number of trawls containing summer flounder;
M_i = the number of summer flounder collected at sampling site i;
w_i = the total weight of all prey items encountered in the stomachs of summer flounder collected from sampling location i; and
w_{ik} = the total weight of prey type k in these stomachs.

The variance estimate for $\%W_k$ was given by

$$\mathrm{var}(\%W_k) = \frac{1}{n\bar{M}^2} \frac{\sum_{i=1}^{n} M_i^2 (q_{ik} - W_k)^2}{n-1} \times 100^2 , \qquad (2)$$

where $\bar{M} = \frac{\sum_{i=1}^{n} M_i}{n}$ is the average number of summer flounder collected at a sampling location.

Ontogenetic and temporal changes in diet

Canonical correspondence analysis (CCA; ter Braak, 1986), a multivariate direct gradient analysis technique, was used to explore the relationship between summer flounder diet and three factors: fish size (mm), year (2002, 2003, 2004, 2005, 2006), and month (March, May, July, September, November). Spatial variations in summer flounder diet were not explored because the distribution of summer flounder in Chesapeake Bay is restricted primarily to the polyhaline (>18 ppt) region of the bay (Fig. 1).

The summer flounder collected ranged in size from 148 to 712 mm TL (Fig. 2). To examine the effect of fish size on diet using CCA, we grouped summer flounder into size categories such that all members of a given category exhibited a relatively consistent diet composition. Summer flounder were grouped into 25-mm size-classes, and diet was calculated for each with Equation 1. After trimming 10% of the observations (i.e., 25-mm size-classes) on account of low probability density in order to minimize outliers, cluster analysis (Euclidean distance, average linkage method) was used to group size-classes with similar diet compositions into broader categories. A scree plot indicated the presence of four clusters (Fig. 3A) (McGarigal et al., 2000), corresponding to four broad size-categories: <225 mm TL (small), 225–374 mm TL (small–medium), 375–574 mm TL (large–medium), and >574 mm TL (large) (Fig. 3B).

For the CCA, each element of the response matrix was the mean percent weight of a given prey type at a given sampling site in a particular size, month, and year combination. The matrix was log-transformed ($\ln[x+1]$) to account for the log-normal distribution

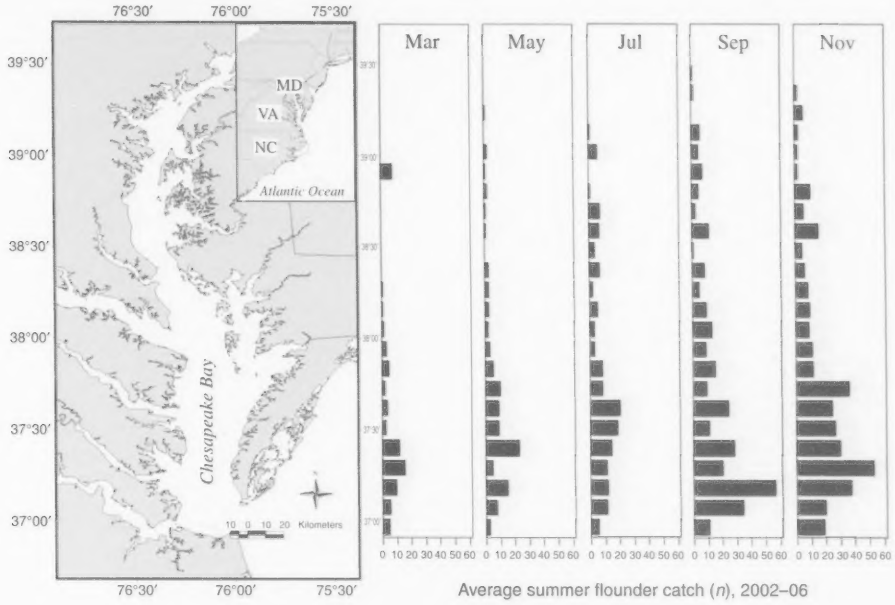

Figure 1

Average catch of summer flounder (*Paralichthys dentatus*) in the mainstem (i.e., nontributary waters) of Chesapeake Bay by sampling month (Mar, May, Jul, Sep, Nov) from 2002 through 2006. Horizontal histograms represent raw catch data by 0.1 latitudinal degrees corresponding to the map scale.

of the data (Garrison and Link, 2000). Size, month, and year were coded by using ordinal variables. Observations (sampling sites) containing fewer than three summer flounder and explanatory variable blocks (size, month, year categories) containing fewer than three observations were excluded to eliminate variance issues related to small sample size.

The CCA was used to determine the amount of variability in the summer flounder diet explained by the canonical axes, which are linear combinations of the three explanatory variables correlated to weighted averages of prey within blocks (ter Braak, 1986; Garrison and Link, 2000). The significance of the ontogenetic and temporal factors was determined by using permutation tests (ter Braak, 1986). A prey species-explanatory factor biplot was constructed to examine the correlations between the factors and the canonical axes and to explore the dietary trends associated with these variables. Detailed diet descriptions were then generated for each of the significant factors identified by the CCA. The CCA was performed with the program CANOCO, vers. 4.5 (Microcomputer Power, Ithaca, NY).

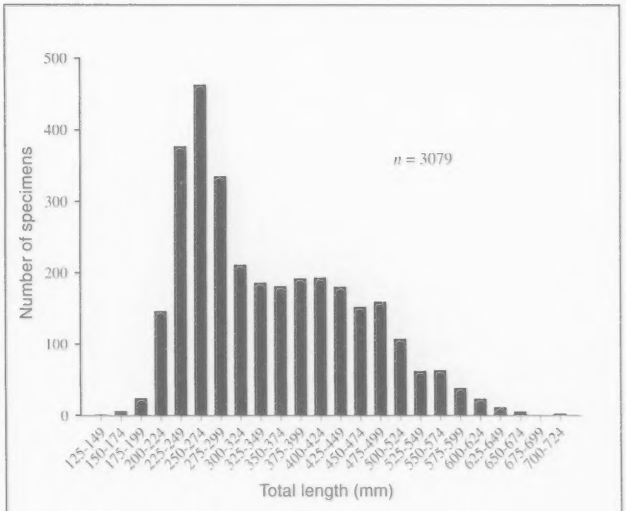

Figure 2

Size frequency of summer flounder (*Paralichthys dentatus*) sampled in the mainstem (i.e., nontributary waters) of Chesapeake Bay from 2002 through 2006.

Results

General diet description

From 2002 through 2006, summer flounder were collected at 877 sampling locations, and at 688 of these locations at least one summer flounder had prey in its stomach. Overall, prey were encountered in 1780 (57.8%) of the 3079 stomachs collected. The total observed diet was composed of 123 prey types, 70 of which were identifiable to the species level (24 fishes and 46 invertebrates). In an effort to present summer flounder diet composition in the most efficient manner, prey types contributing relatively little to the overall diet were combined at higher taxonomic levels.

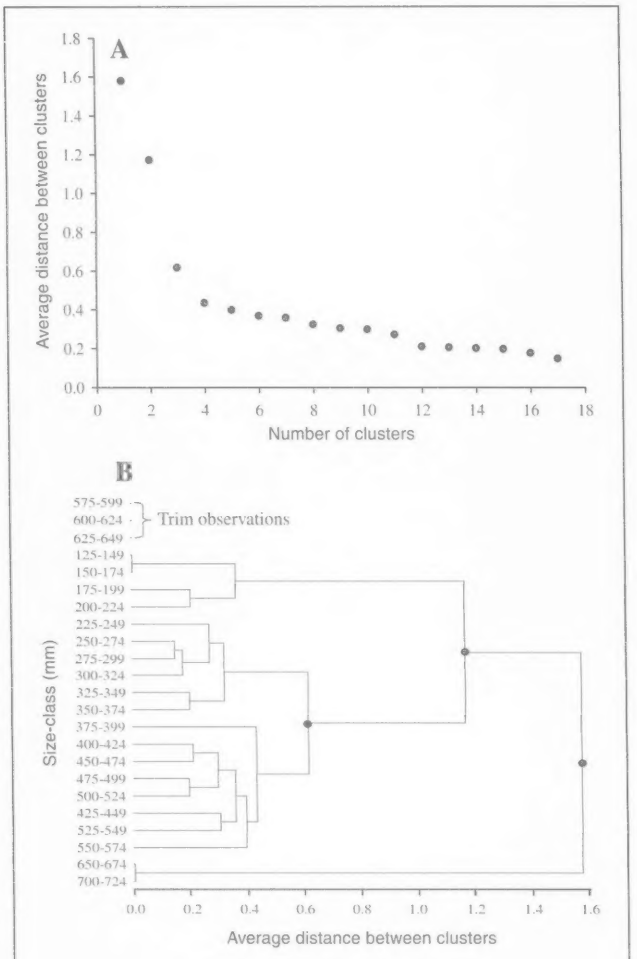

Figure 3

(**A**) Scree plot depicting average distance between clusters versus the number of clusters which was used to identify the number of clusters into which 25-mm size-classes of summer flounder (*Paralichthys dentatus*) should be grouped (four size groups were selected since the curve leveled out at five or more clusters), (**B**) cluster diagram representing the relationships among the diet compositions of 25-mm size-classes of summer flounder. Trim observations represent the 25-mm size-classes omitted from the analysis because of low probability density, and average distance represents the coefficient used as a measure of dissimilarity among size-classes.

Mysid shrimp (*Neomysis* spp.) and bay anchovy (*Anchoa mitchilli*) were the main prey of the summer flounder, accounting for approximately 42% combined (24.1% and 17.9%, respectively, Fig. 4) of the diet by weight, and mantis shrimp (*Squilla empusa*—11.2%) and weakfish (*Cynoscion regalis*—11.1%) were of secondary and nearly equal importance. Of the remaining prey types, spot (*Leiostomus xanthurus*), Atlantic croaker (*Micropogonias undulatus*), and spotted hake (*Urophycis regia*) were the most important fishes, and sand shrimp (*Crangon septemspinosa*) was the main invertebrate prey. Each of these species represented between 2% and 7% of the diet. All other identifiable prey types each contributed <2% to the diet.

Unidentifiable prey items (i.e., unidentifiable fish and unidentifiable material) were prevalent, likely because of the shearing action of the teeth of these predators, and composed 6.0% of the diet by weight. Although many of the unidentifiable items were encountered in stomachs along with identifiable prey and were likely the same species as the latter, they were, however, classified as unidentifiable so as to provide a conservative diet description.

Ontogenetic and temporal changes in diet

The CCA indicated that summer flounder dietary changes by fish size, month, and year were statistically significant. Taken together, the aforementioned factors explained 6.0% (P=0.001) of the variability in diet; the first and second canonical axes accounted for 51.2% and 34.5% of the explainable variation, respectively. Fish size (r=−0.459; P=0.001) more closely corresponded to the first canonical axis than the second and, of the three variables examined, accounted for the greatest portion of the variation that was explicable. Month (r=−0.481; P=0.001) and year (r=−0.094; P=0.001) were more closely correlated to the second axis (Fig. 5).

The amount of fish in the diet of summer flounder increased with increasing size (Fig. 6A). Mysid shrimp, sand shrimp, and mantis shrimp accounted for approximately 79% of the diet of the summer flounder <225 mm TL. Bay anchovy (9.5%) and weakfish (2.3%) were the main fish prey of these individuals. The diet of summer flounder ranging from 225 to 374 mm TL was also dominated by mysid shrimp. The contribution

of sand shrimp to the diet of these fish was approximately the same as in the smallest size-category, whereas that of mantis shrimp increased. Fishes were again of secondary importance and were represented mainly by bay anchovy, weakfish, and Atlantic croaker. Weakfish was the primary prey of the large-medium summer flounder and, although the contribution of bay anchovy declined, anchovy still represented 15.4% of the diet. The contribution of spot to the diet of summer flounder increased from less than 1% in the small-medium fish to 13% in the 375–574 mm TL size-group. Mantis shrimp was the most important invertebrate prey of the large-medium fish. Sciaenids (i.e., spot, weakfish, and Atlantic croaker) were the main prey of of the largest summer flounder and accounted for 67.3% of the diet. Our representation of the diet composition of these fish should be viewed as preliminary because of the small cluster sample size (n_c=23).

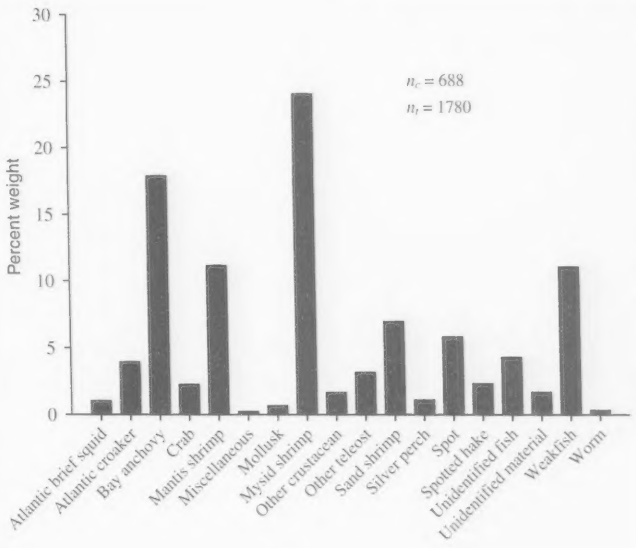

Figure 4

Percent weight of prey types present in the diet of summer flounder (*Paralichthys dentatus*) collected from the mainstem of Chesapeake Bay from 2002 through 2006. The total number of clusters collected is given by n_c, and n_t represents the total number of specimens included in this study. Standard error estimates, represented by error bars, were calculated from cluster sampling variance estimates and all were less than 0.03%.

Seasonal changes in summer flounder diet likely mirrored the temporal variability of prey assemblages in Chesapeake Bay. The contribution of sand shrimp and spotted hake peaked in the spring and early summer (Fig. 6B). Atlantic brief squid (*Lolliguncula brevis*), Atlantic croaker, mantis shrimp, silver perch (*Bairdiella chrysoura*), spot, and weakfish accounted for a greater portion of the diet throughout the summer and autumn. Bay anchovy and mysid shrimp were always two of the top three main prey types in the diet of summer flounder from May to November.

The diet of summer flounder was dominated by mantis shrimp and bay anchovy in 2002, whereas mysid shrimp was the main prey from 2003 through 2006 (Fig. 6C). Atlantic brief squid, crab, mantis shrimp, and spotted hake generally decreased in importance over this time period, whereas the contribution of mysid shrimp and spot generally increased.

Predator-prey size relationships

The available data on sizes of whole prey consumed by summer flounder (the primary prey types excluding mysid shrimp) were examined with respect to summer flounder size. For all prey types, the size of the prey consumed increased significantly with increasing summer flounder size (P<0.05, Fig. 7). With respect to Atlantic croaker and spot, the majority of the individuals consumed were likely young-of-the-year (YOY), and a few of the larger individuals were age-1. However, summer flounder appear to have preyed exclusively on YOY weakfish. At a given size of summer flounder, the sizes of bay anchovy, mantis, and sand shrimp consumed were more variable than the sizes of the sciaenid prey, and this finding may indicate less probability of a size-modulated predator-prey relationship.

Discussion

Summer flounder feed on a diverse array of prey in Chesapeake Bay, as evidenced by over 120 prey types encountered in the diet. However, despite this diversity, approximately half of the diet comprised only two prey types, mysid shrimp and bay anchovy. The other half of the diet consisted of a few fishes (sciaenids-weakfish, spot, and Atlantic croaker) and invertebrates (mantis and sand shrimps). Similar results have been reported for other upper trophic level predators in Chesapeake Bay (i.e., striped bass [*Morone saxatilis*] bluefish [*Pomatomus saltatrix*] and weakfish)—results that further support the notion that although the Chesapeake Bay food web is complex, the number of prey species supporting these predators is relatively few (Hartman and Brandt, 1995).

Mysid shrimp dominate the diets of summer flounder in other estuarine and coastal habitats (Smith and Daiber, 1977; Link et al., 2002). Our study shows that mysid shrimp also play an important role in the trophic dynamics of summer flounder in Chesapeake Bay.

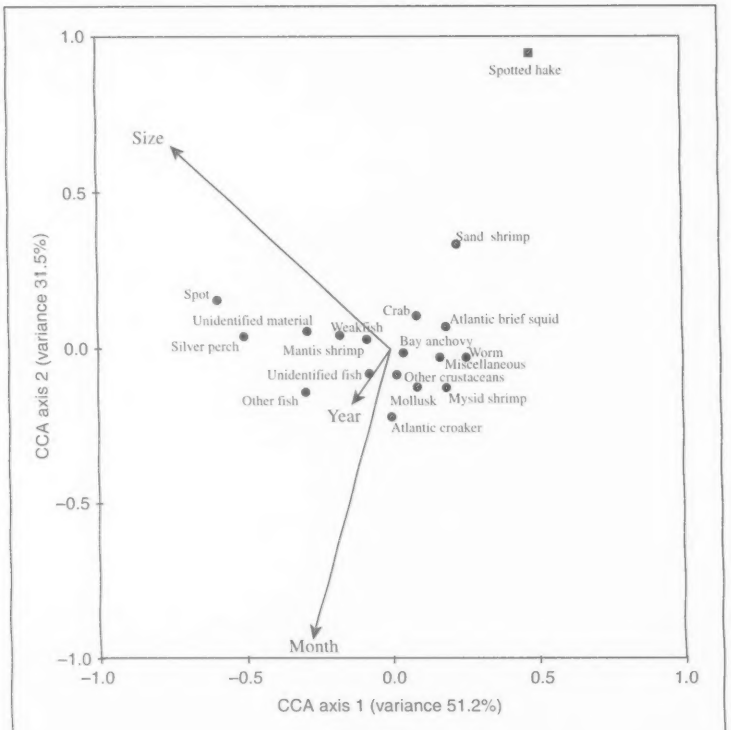

Figure 5

Canonical correspondence analysis (CCA) biplot for summer flounder (*Paralichthys dentatus*) diet in the mainstem of Chesapeake Bay from 2002 through 2006. Arrows represent the significant explanatory factors and dots represent prey types. The canonical axes represent linear combinations of the three explanatory variables (fish size, month, and year).

Moreover, mysid shrimp have dominated the diets of other teleost piscivores in the bay over the past several years, which indicates that this prey represents a crucial linkage between lower and upper trophic level production. Despite the importance of mysid shrimp in the diets of fishes, very little is known about the population dynamics and abundance of this species (when compared to other prey types, e.g., bay anchovy) in Chesapeake Bay. Data on mysid shrimp abundance would be instrumental to better understanding not only trophic interactions of summer flounder, but those of other top teleost predators in this estuary.

Significant ontogenetic changes in the diet were documented; small flounder mainly consumed small invertebrates and bay anchovy. The diversity of the diet in terms of numbers and sizes of prey types increased with increasing summer flounder size. Medium-size flounder continued to consume prey types found in the diet of small flounder, but the diet of medium-size flounder appeared to be an expansion of rather than a shift from the diet of small flounder. Fishes (primarily sciaenids) were found almost exclusively in the diet of the largest summer flounder, and because bay anchovy and the aforementioned invertebrate prey types were absent in the stomachs of these fish, there appeared to be a diet shift at approximately 575 mm TL. Although similar changes in the diet of summer flounder (>500 mm TL) have been documented in offshore waters (Link et al., 2002), cephalopods were the primary prey type as opposed to fishes. This contrast in the diets of the larger summer flounder is likely due to the lack of an abundant and comparable large soft-bodied invertebrate prey in Chesapeake Bay.

Seasonal trends in summer flounder diet composition were not surprising given the well documented spatiotemporal patterns of summer flounder prey. Sand shrimp and spotted hake abundance generally peaks during late winter and early spring in the mainstem of the lower bay; hence, it follows that they composed appreciable fractions of the summer flounder diet during this season (Haefner, 1976; Murdy et al., 1997). Faunal diversity in Chesapeake Bay reaches a maximum during late August and September and corresponds with a highest diversity of prey types in the diet of summer

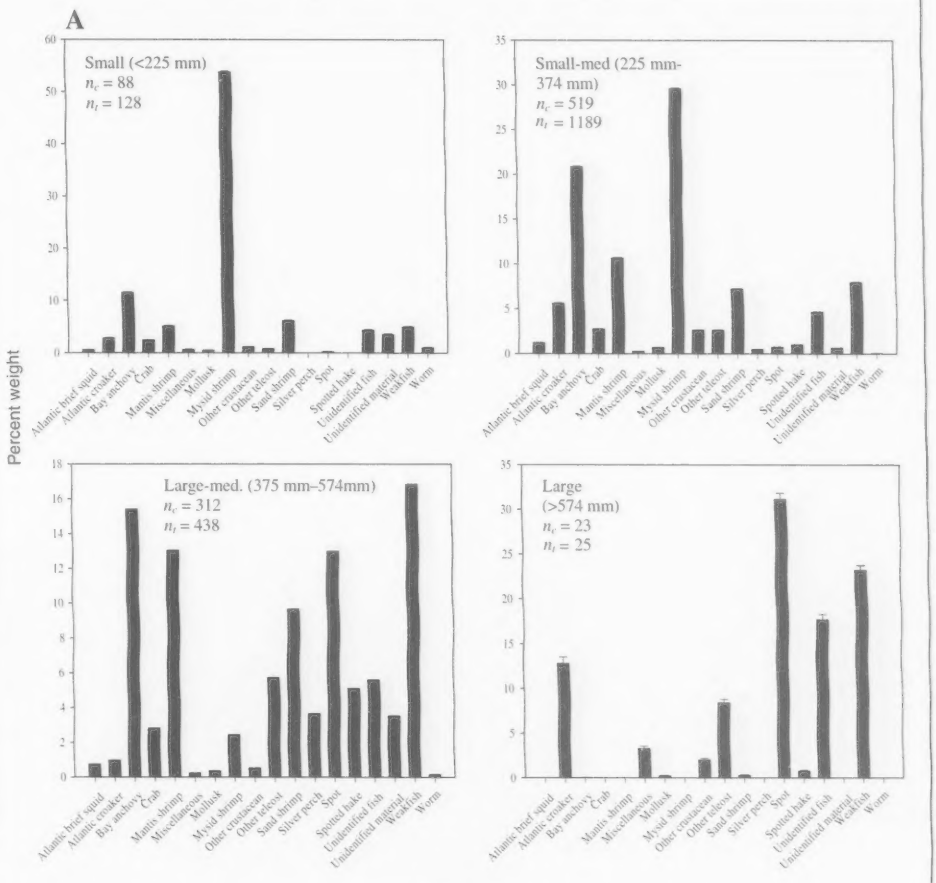

Figure 6

Diet composition (percent weight) of summer flounder (*Paralichthys dentatus*) collected from the mainstem of Chesapeake Bay, presented by (**A**) size-category, (**B**) month, and (**C**) year. The number of clusters collected in each subcategory is given by n_c, and n_t represents the total number of specimens. Error bars represent standard error of the percent weight values of each of the prey types encountered in the summer flounder diet, which were calculated from cluster sampling variance estimates.

flounder. Interannual variations in the diet of summer flounder generally followed fluctuations in the indices of relative abundance for several prey species routinely monitored by the Virginia Institute of Marine Science (VIMS) Juvenile Finfish and Blue Crab Trawl Survey. There was a weak visual correspondence between the trends in relative abundances of bay anchovy and YOY weakfish and their contributions to summer flounder diet throughout the study period. However, the diet of summer flounder more strongly mirrored trends in relative abundance of YOY spot.

In general, it is difficult to compare studies of diet composition of the same species because it is often the case that survey design (including gear types), indices reported (e.g., percent weight, $\%W$ vs. percent number, $\%N$), and the methods used to calculate these indices (e.g., simple random vs. cluster sampling) vary among studies. Although these differences prohibit direct comparisons among investigations, it is still possible to draw some informative qualitative conclusions. For example, Smith and Daiber (1977), using the percent frequency of occurrence (%F) index, reported that the diet of summer flounder in Delaware Bay was dominated by invertebrates; yet their results also indicated that fishes composed an important part of their diet in the estuary. Poole (1964) reported that sand shrimp were the main prey by weight of summer flounder in Great South Bay, NY; however, fishes were also abun-

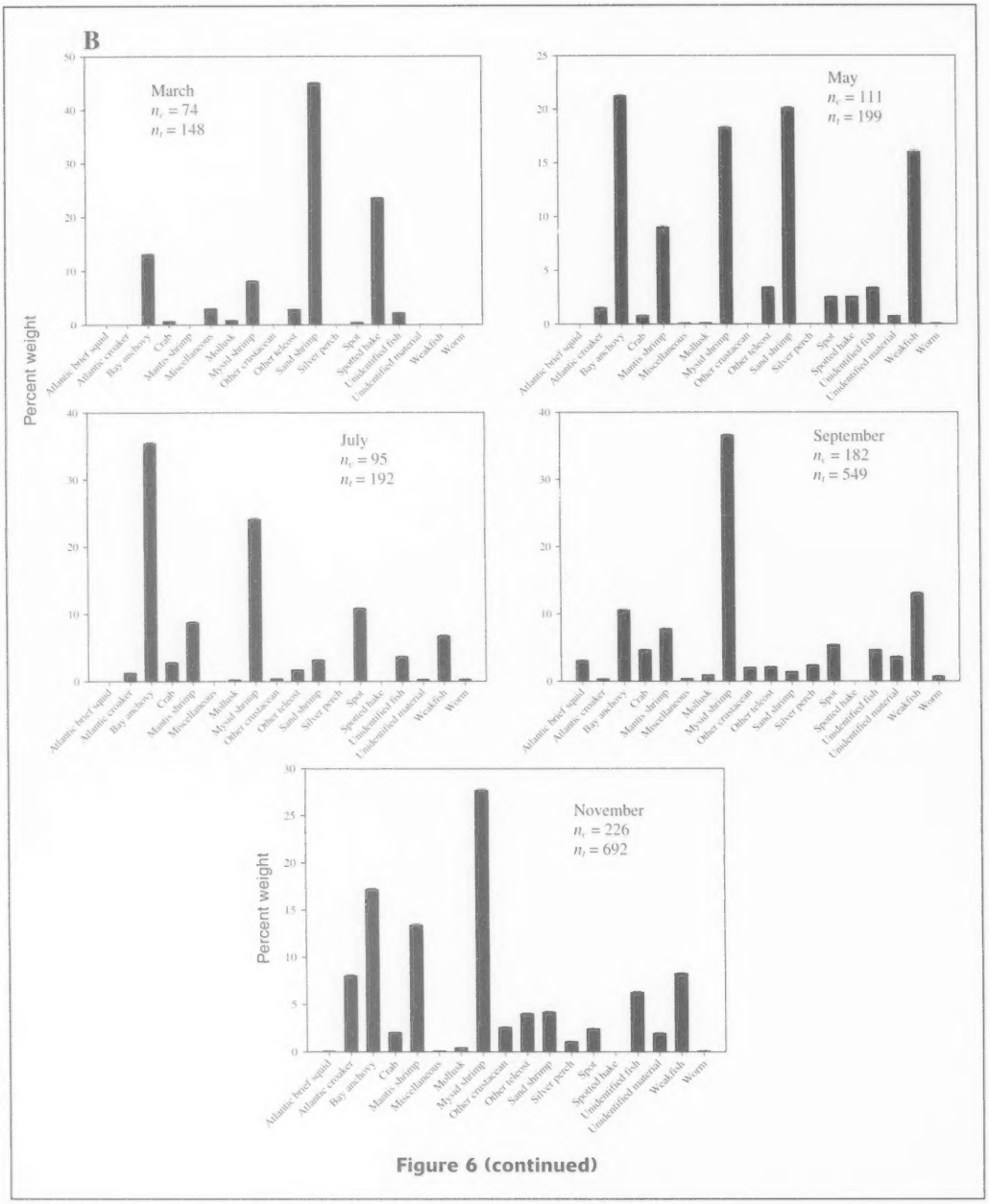

Figure 6 (continued)

dant in the diet. The relative importance of specific fish species in the diet of summer flounder has varied across studies, likely because of spatial variations in prey assemblages and perhaps because of differences in study methods. Nevertheless, these studies in combination with the results of the present study indicate that summer flounder are piscivorous within estuarine environments throughout their range. Additionally, there appears to be appreciable similarity in the invertebrate taxa consumed by summer flounder in estuaries because sand and mysid shrimps have been found in the diet in multiple areas across decades (Poole, 1964; Powell and Schwartz, 1979).

Striped bass, weakfish, and bluefish represent the abundant upper trophic level teleost piscivorous predators in Chesapeake Bay (Dovel, 1968; Boynton et al.,

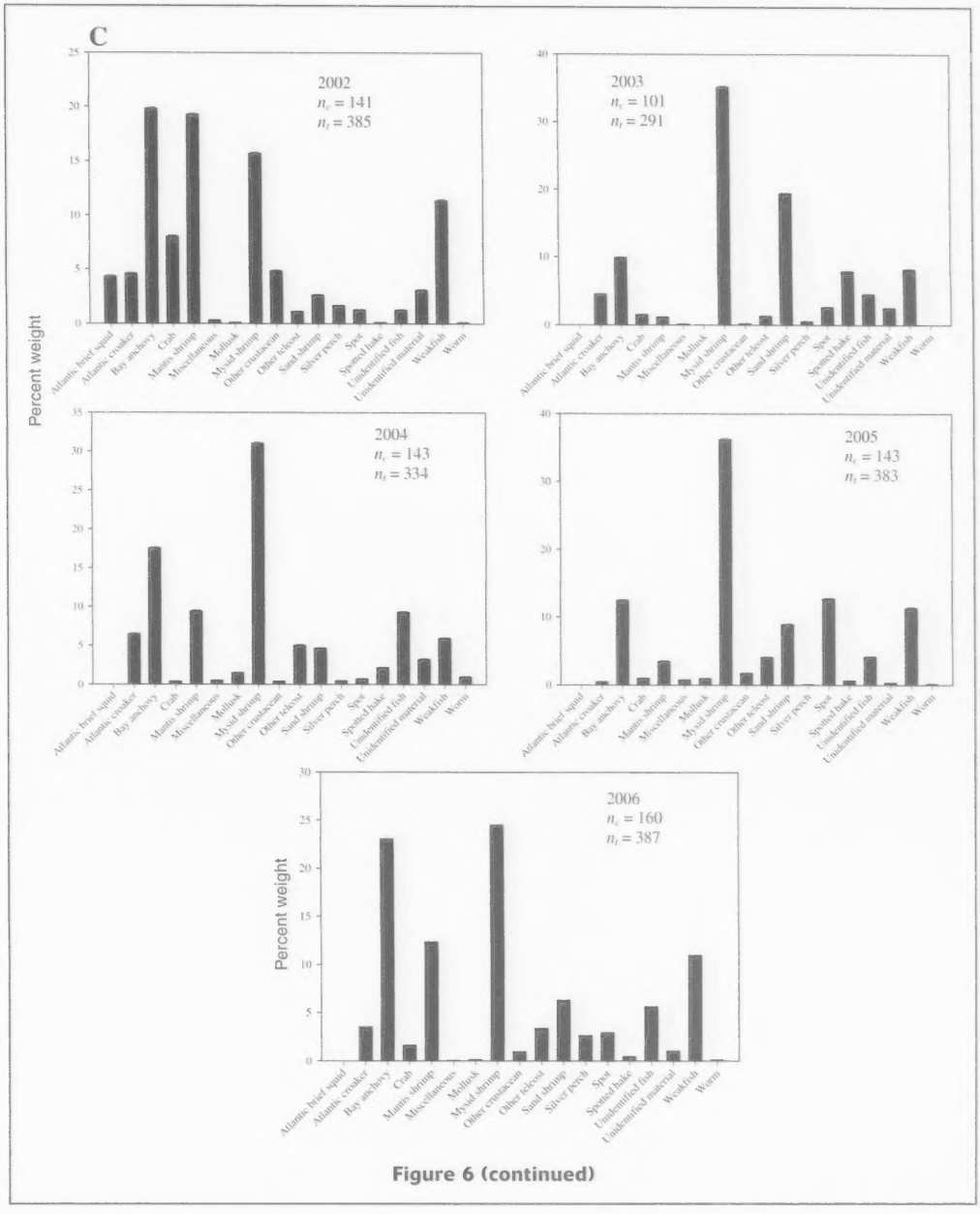

Figure 6 (continued)

1981; Hartman and Brandt, 1995), however, the preponderance of fishes in the diet of summer flounder indicates that this species also fits that characterization (i.e., fishes represent approximately 50% or more of the diet of summer flounder >225 mm TL). In terms of life history and estuarine dependence, appreciable abundances of summer flounder have been consistently present in our samples over the past several years. Hence, the sheer abundance, protracted use of estuarine habitat, and piscivorous diet of summer flounder combine to indicate that the impacts on piscine prey by this species have the potential to match those of the aforementioned three fishes. Piscivory was also documented in several size-classes of summer flounder within offshore habitats along the continental shelf (>10 m depth) from southern New England through the Mid-Atlantic Bight (Link

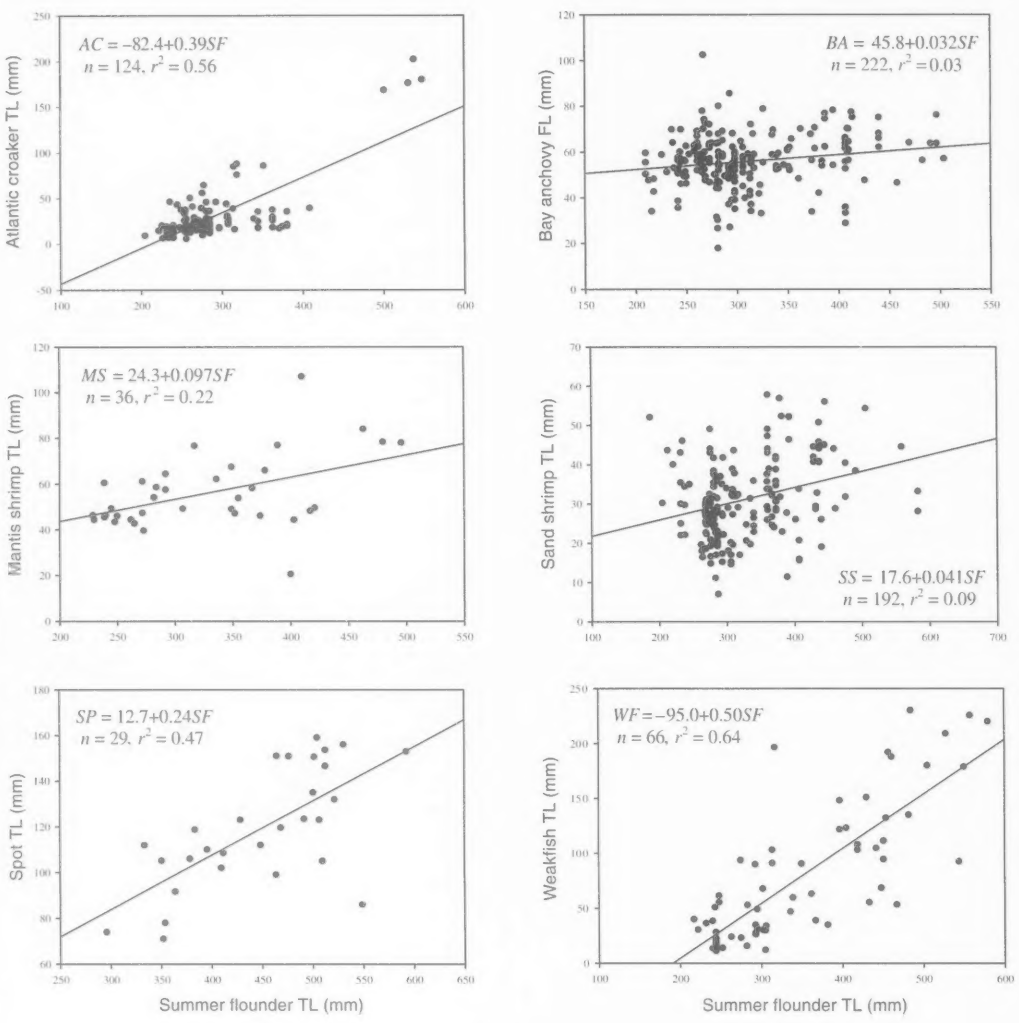
AC = –82.4+0.39SF
n = 124, r² = 0.56
Atlantic croaker TL (mm)
BA = 45.8+0.032SF
n = 222, r² = 0.03
Bay anchovy FL (mm)
MS = 24.3+0.097SF
n = 36, r² = 0.22
Mantis shrimp TL (mm)
SS = 17.6+0.041SF
n = 192, r² = 0.09
Sand shrimp TL (mm)
SP = 12.7+0.24SF
n = 29, r² = 0.47
Spot TL (mm)
WF = –95.0+0.50SF
n = 66, r² = 0.64
Weakfish TL (mm)
Summer flounder TL (mm)
Summer flounder TL (mm)

Figure 7

Relationship of prey size (whole prey items only) consumed by summer flounder (*Paralichthys dentatus*) in the mainstem of Chesapeake Bay from 2002 through 2006 versus summer flounder size (TL, mm). All regressions were significant ($P<0.05$).

et al., 2002; Staudinger, 2006). Hence, fishes represent an important component of summer flounder diet throughout its range implying that this species should be included in analyses designed to quantify pathways of production to piscivorous fishes.

Quantitative analyses of foodweb dynamics provide valuable insights into the structure of ecosystems and ultimately support the development of EBFM plans. However, these analyses require several data types, including information on the ontogenetic and temporal (intra- and interannual) changes in the trophic interactions of species within an ecosystem. This study provides fundamental trophic data for an important fish species in Chesapeake Bay and, taken with previous studies, contributes significantly to our understanding of the role of summer flounder as a predator throughout its range.

Acknowledgments

The authors acknowledge E. A. Brasseur, P. D. Lynch, D. J. Parthree, and M. L. F. Chattin for their efforts

associated with field collections and sample processing. Captain L. Durand Ward and the Virginia Institute of Marine Science (VIMS) vessels staff deserve thanks for their contributions in the field. T. Miller and two anonymous reviewers provided helpful comments on earlier versions of this manuscript. Funding was provided by the Virginia Environmental Endowment, National Oceanic and Atmospheric Administration Chesapeake Bay Office, and the U.S. Fish and Wildlife Service. This article is VIMS contribution no. 2850.

Literature cited

Bogstad, B., M. Pennington, and J. H. Volstad.
1995. Cost-efficient survey designs for estimating food consumption by fish. Fish. Res. 23:36–47.

Boynton, W. R., T. T. Polgar, and H. H. Zion.
1981. Importance of juvenile striped bass food habits in the Potomac estuary. Trans. Am. Fish. Soc. 110:56–63.

Buckel, J. A., D. O. Conover, N. D. Steinberg, and K. A. McKown.
1999. Impact of age-0 bluefish (*Pomatomus saltatrix*) predation on age-0 fishes in the Hudson River estuary: evidence for density-dependent loss of juvenile striped bass (*Morone saxatilis*). Can. J. Fish. Aquat. Sci. 56:275–287.

Desfosse., J. C.
1995. Movements and ecology of summer flounder, *Paralichthys dentatus* tagged in the southern Mid-Atlantic Bight. Ph.D. diss., 187 p. College of William and Mary, Williamsburg, VA.

Dovel, W. L.
1968. Predation by striped bass as a possible influence on population size of the Atlantic croaker. Trans. Am. Fish. Soc. 97:313–319.

Garrison, L. P., and J. S. Link.
2000. Diets of five hake species in the northeast United States continental shelf system. Mar. Ecol. Prog. Ser. 204:243–255.

Ginsberg, I.
1952. Flounders of the genus *Paralicthys* and related genera in American waters. Fish. Bull. 52:267–351.

Gutherz, E. J.
1967. Field guide to the flatfishes of the family Bothidae in the western North Atlantic, 47 p. U.S. Fish and Wildlife Service, Bureau of Commercial Fisheries, Circular 263, Washington, D.C.

Haefner, P. A., Jr.
1976. Seasonal distribution and abundance of sand shrimp *Crangon septemspinosa* in the York River-Chesapeake Bay estuary. Chesapeake Sci. 17:131–134.

Hartman, K. J., and S. B. Brandt.
1995. Trophic resource partitioning, diets, and growth of sympatric estuarine predators. Trans. Am. Fish. Soc. 124:520–537.

Hyslop, E. J.
1980. Stomach contents analysis-a review of methods and the application. J. Fish Biol. 17:411–429.

Leim, A. H., and W. B. Scott.
1966. Fishes of the Atlantic Coast of Canada. Bull. Fish. Res. Board Can. 155:1–485.

Link, J. S., K. Bolles, and C. G. Milliken.
2002. The feeding ecology of flatfish in the Northwest Atlantic. J. North. Atl. Fish. Sci. 30:1–17.

McGarigal, K., S. Cushman, and S. Stafford.
2000. Multivariate statistics for wildlife and ecology research, 283 p. Springer, New York, NY.

Murdy, E. O., R. S. Birdsong, and J. A. Musick.
1997. Fishes of Chesapeake Bay, 324 p. Smithsonian Institution Press, Washington, D.C.

Poole, J. C.
1964. Feeding habits of summer flounder in Great South Bay. NY Fish Game J. 11:28–34.

Powell, A. B., and F. J. Schwartz.
1979. Food of *Paralichthys dentatus* and *P. lethostigma* (Pisces: Bothidae) in North Carolina estuaries. Estuaries 2:276–279.

Roundtree, R. A., and K. W. Able.
1992. Foraging habits, growth, and temporal patterns of salt-marsh creek habitat use by young-of-the-year summer flounder in New Jersey. Trans. Am. Fish. Soc. 121:765–776.

Smith, R. W., and F. C. Daiber.
1977. Biology of the summer flounder, *Paralychthys dentatus*, in Delaware Bay. Fish. Bull. 75:823–830.

Staudinger, M. D.
2006. Seasonal and size-based predation on two species of squid by four fish predators on the Northwest Atlantic continental shelf. Fish. Bull. 104:605–615.

ter Braak, C. J. F.
1986. Canonical correspondence analysis: a new eigenvector technique for multivariate direct gradient analysis. Ecology 67:1167–1179.

Terceiro, M.
2002. The summer flounder chronicles: science, politics, and litigation, 1975–2000. Rev. Fish Biol. Fish. 11:125–168.

Using an inverse-logistic model to describe growth increments of blacklip abalone (*Haliotis rubra*) in Tasmania

Malcolm Haddon (contact author)
Craig Mundy
David Tarbath

Email address for M. Haddon: Malcolm.Haddon@utas.edu.au

Marine Research Laboratory
Tasmanian Aquaculture and Fisheries Institute
University of Tasmania
Nubeena Crescent
Taroona TAS 7051, Tasmania, Australia

Abstract—A new description of growth in blacklip abalone (*Haliotis rubra*) with the use of an inverse-logistic model is introduced. The inverse-logistic model avoids the disadvantageous assumptions of either rapid or slow growth for small and juvenile individuals implied by the von Bertalanffy and Gompertz growth models, respectively, and allows for indeterminate growth where necessary. An inverse-logistic model was used to estimate the expected mean growth increment for different blacklip abalone populations around southern Tasmania, Australia. Estimates of the time needed for abalone to grow from settlement until recruitment (at 138 mm shell length) into the fishery varied from eight to nine years. The variability of the residuals about the predicted mean growth increments was described with either a second inverse-logistic relationship (standard deviation vs. initial length) or by a power relationship (standard deviation vs. predicted growth increment). The inverse-logistic model can describe linear growth of small and juvenile abalone (as observed in Tasmania), as well as a spectrum of growth possibilities, from determinate to indeterminate growth (a spectrum that would lead to a spread of maximum lengths).

Manuscript submitted 9 April 2007.
Manuscript accepted 22 October 2007.
Fish. Bull. 106:58–71 (2008).

The views and opinions expressed or implied in this article are those of the author and do not necessarily reflect the position of the National Marine Fisheries Service, NOAA.

Blacklip abalone (*Haliotis rubra*) constitute the most valuable fishery in Tasmania, Australia, yielding approximately 30% (2500 tonnes) of the resource captured in the wild worldwide, worth more than AU$100 million per year. There are significant difficulties in determining the age of blacklip abalone (McShane and Smith, 1992), making them good candidates for size-structured assessment modeling (Sullivan et al, 1990; Punt and Kennedy, 1997). Although used informally in the Tasmanian fishery, size-structured models are used formally to assess blacklip abalone stocks elsewhere in Australia (Worthington et al., 1998; Gorfine et al., 2005) and to assess Paua (*H. iris*) in New Zealand (Breen et al., 2003). With size-structured models it is important to generate a precise and unbiased mathematical description of growth because the adoption of an inappropriate growth model could have significant effects on the outcome of an assessment.

Day and Fleming (1992) reviewed a range of models previously used to describe abalone growth. In total, 59 growth studies have been undertaken on different abalone species. The von Bertalanffy growth curve (von Bertalanffy, 1938) has been used in 42 (71%) of these studies and the Gompertz model (Gompertz, 1825). has been used in four studies (6.78%). The dominance of the von Bertalanffy growth model reflects its almost universal adoption in abalone fisheries assessments and the relative ease with which it can be fitted to growth data taken from tagging experiments (Fabens, 1965; Francis, 1988; Haddon, 2001). In nine studies (15.25%), linear growth was proposed, but the focus of these nine studies was on juvenile and small abalone and that focus could imply that growth alters its character above a particular size, at least in some species. A flexible growth description has also been given by Francis (1995) who generated a size-based analogue to the age-based growth description by Schnute (1981). Francis's model has been used in New South Wales, Australia (Worthington et al., 1998), and New Zealand assessments of abalone (Breen et al., 2003).

Sainsbury (1982a, 1982b) fitted von Bertalanffy growth curves to abalone tagging data from New Zealand (*H. iris*). Instead of assuming that the familiar parameters (L_∞, the asymptotic maximum size, and K, the growth coefficient in the von Bertalanffy equation) were averages for the population, Sainsbury (1982a) inferred the growth dynamics implied when each individual had its own set of von Bertalanffy parameters. Essentially, the growth characteristics of individuals were assumed to be variable and were described by using probability density functions to represent the model parameters. Similarly, a probability density function form of the Gompertz growth model was used in Victoria, Australia (Troynikov and

Table 1

Data by sites and regional groupings of sites (Fig. 1) in southern Tasmania where blacklip abalone (*Haliotis rubra*) were collected to compare growth rates. Time step relates to whether the analysis was for annual or seasonal growth, count is the number of tags recovered, and Min–Max Init. L (in mm) are the minimum and maximum initial length of blacklip abalone at tagging for each site.

Time step	Longitude (East)	Latitude (South)	Regional grouping	Site name	Count n	Min–Max Init. L
Annual	145.492	–42.969	Southwest	Black Island	116	57–171
Annual	145.667	–43.075	Southwest	Giblin River	84	83–173
Annual	145.781	–43.226	Southwest	Hobbs Island	57	57–181
Annual	146.900	–43.566	Actaeon	Gagens Point	154	50–142
Annual	146.972	–43.549	Actaeon	Middle Ground	353	47–146
Annual	147.381	–43.366	Bruny Island	Fluted Cape	135	83–154
Annual	147.385	–43.111	Bruny Island	One Tree Point	162	52–153
Seasonal	146.996	–43.534	Actaeon	Actaeon Island	390	61–176
Seasonal	146.990	–43.550	Actaeon	Sterile Island	373	48–146

Gorfine, 1998; Troynikov et al., 1998; Bardos, 2005). Like the von Bertalanffy model, the Gompertz equation is deterministic in predicting an asymptotic maximum length. The probabilistic forms of these two models predict a more plausible range of final maximum lengths and some configurations of Francis's (1995) model can also exhibit a spread of final sizes. However, like the von Bertalanffy and Gompertz models, Francis's (1995) model fails to exhibit the linear-like early growth of small abalone that has been observed in Tasmania.

An important characteristic of growth models is an ability to accurately model growth across a broad size range. Nine of the studies cited in Day and Fleming (1992) indicate that early growth in abalone is effectively linear. This linearity contrasts strongly with both the von Bertalanffy curve (which predicts faster early growth) and the Gompertz growth curve (which predicts slower early growth). Neither the von Bertalanffy nor the Gompertz growth models are consistent with observations of effectively linear growth in small blacklip abalone in Tasmania, Australia (Prince et al., 1988; Gurney et al., 2005). Such early linear-like growth would imply constant growth increments in small animals and would require a different structural model to represent such growth dynamics.

Given the wide variation in maximum sizes found in natural abalone populations, an alternative approach to using deterministic models (with a known or even probabilistic asymptotic length) would be to model growth as indeterminate. Indeterminate growth would imply no specific upper limit and animals would be expected to continue growing, even if very slowly, until they die. This indeterminacy would have the disadvantage in that there would be no simple analytical solution for length-at-age, but nevertheless this strategy could provide for intuitively simple empirical descriptions of growth that avoid the complexities of fitting probabilistic models as proposed by Sainsbury (1982a) and Bardos (2005).

Here we present a new empirical description of blacklip abalone growth using an inverse-logistic model for both the mean growth increment and the predicted variation about the mean increment for a given shell length. In contrast to both the von Bertalanffy and Gompertz growth curves, the growth description given here allows for both linear growth of small and juvenile abalone as well as the option of either determinate growth (with a maximum shell length) or indeterminate growth (with a spread of maximum lengths).

Materials and methods

Examination of growth patterns

To provide an initial empirical indication of growth patterns, the size of abalone at tagging were grouped into 10-mm classes and the mean growth increment in each class was then plotted on top of the raw data from the southwest area of Tasmania (a combination of three sites, Fig. 1; Table 1).

Tagging methods and locations

Two sets of data were used in the description of the inverse-logistic model. Firstly, to examine annual growth increments, we used tagging data from seven sites around the south of Tasmania (Fig. 1). Data from those sites were limited to tagged-and-recaptured abalone and the data were collected approximately one year apart (between 0.96 and 1.05 years apart). Abalone from some groups of sites were found to exhibit very similar growth patterns and the data from these sites were combined to generate three larger regions (namely, southwest, Actaeon, and Bruny Island) (Fig. 1; Table 1). Secondly, tagging data from two sites were used to examine seasonal growth (Table 1), and for this analysis,

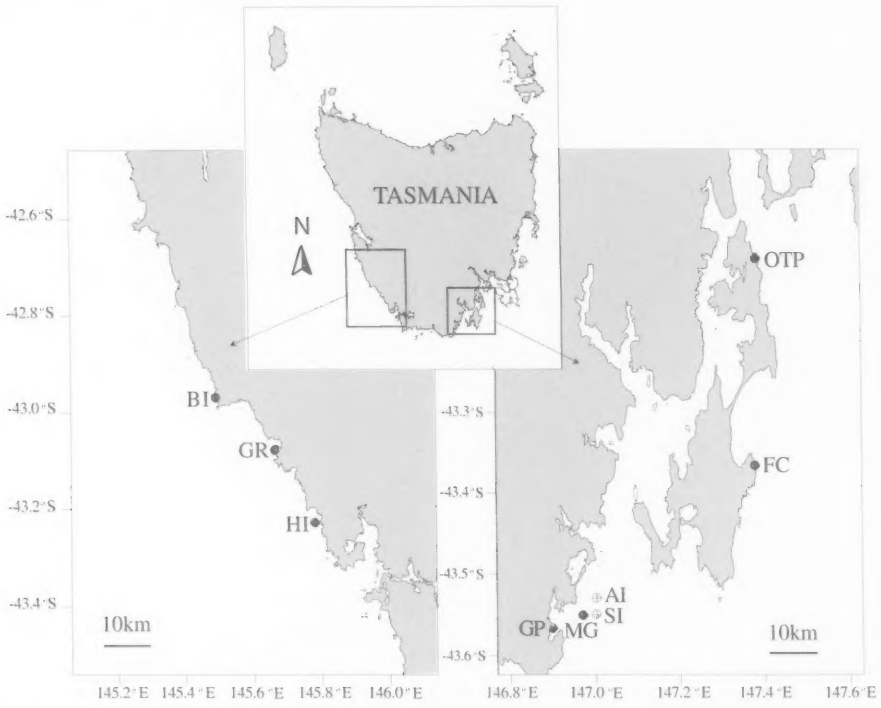

Figure 1

A map of Tasmania indicating the locations (black dots) from which the data on blacklip abalone (*Haliotis rubra*) growth increment patterns were collected. Left panel represents the southwest region comprising three sites: BI=Black Island, GR=Giblin River, and HI=Hobbs Island. Right panel represents the Actaeon region (comprising two sites: the GP=Gagens Point and MG=Middle Ground sites) and the Bruny Island region (comprising two sites: FC=Fluted Cape and OTP=One Tree Point sites). Seasonal data are identified by a combination of a circle and cross for both the Actaeon Island (AI) and Sterile Island (SI) sites (Table 1).

tagging and recaptures were scattered throughout the year and the recapture intervals ranged from 0.06 to 1.99 years.

We tagged blacklip abalone by inserting a plastic rivet into the open exhalent hole furthest from the shell lip. The rate of tag fouling, and the increased risk of the tag not being found, increased dramatically after two years; therefore, only tags at liberty for less than two years were used in the analyses of seasonal growth. Across all sites, tagged abalone ranged in size from 47 mm to 181 mm shell length, but ranges varied at each site (Table 1). Measurements of maximum shell length were taken to the nearest 1.0 mm.

There is some evidence that tagging can negatively affect the growth of tagged animals, producing a tagging shock in affected individuals (Prince et al., 1988). It seems plausible that at least some of the variability in growth observed in abalone tagging experiments derived from different responses to the tagging process. In an attempt to minimize such effects in this study, tagging methods were standardized; animals were kept damp and cool during the tagging process before being returned to their reefs by divers. Blacklip abalone <50 mm shell length were not sampled because they tend to be highly cryptic in Tasmania, initial capture below this size is difficult, and adhesives rather than rivets, must be used to attach tags to young abalone.

Growth model

The units of growth used here are the growth increments (ΔL) produced by animals of known starting lengths (L_t) that have been at liberty for varying lengths of time (Δt). The model structure includes seasonality by default, and the seasonality terms are set to have zero influence to form an annual model. The form of the inverse-logistic curve used is a typical logistic selectivity curve described by Haddon (2001).

Growth of blacklip abalone does not differ between the sexes. An inverse-logistic model was used to describe the expected length increment ΔL for a known initial size L_t:

$$\Delta L = \frac{Max\Delta L \times \left[\begin{array}{l}\Delta t + C\sin\left(2\pi\left(t_R - p\right)\right) - \\ C\sin\left(2\pi\left(t_T - p\right)\right)\end{array}\right]}{1+e^{\frac{Ln(19)\left(L_t - L_{50}^m\right)}{\left(L_{95}^m - L_{50}^m\right)}}} + \varepsilon_{L_t}, \qquad (1)$$

where $Max\Delta L$ = the hypothetical asymptotic maximum growth increment at some initial size of abalone that sets the exponential term to zero;

Δt = the interval between tagging and recapture (as a fraction of a year);

L_t = the size when first tagged;

L_{50}^m = the initial length at which the midway point between the $Max\Delta L$ and lowest growth increment is reached;

L_{95}^m = the initial length at which 95% of the difference between the smallest and maximum increment is reached;

C = the amplitude of the seasonality effect for ΔL;

t_R and t_T = the dates of recapture and tagging, respectively (as fractions of a year, e.g., June 30th = 0.5; $t_R = t_T + \Delta t$); and

p = the date of maximum growth rate (as a fraction of a year).

The error term ε_{L_t} is additive and normal, and is assumed to have a mean of zero and standard deviation σ_{L_t} that can be defined either as a function of initial length, L_t, or as a function of the predicted length increment $\Delta\hat{L}_t$. If the expected length increments ever attain zero, or go negative, then the standard deviation of the residuals σ_{L_t} can be defined in terms of the initial length L_t:

$$\sigma_{L_t} = \frac{Max\sigma_L \times \left[\begin{array}{l}\Delta t + C_\sigma \sin\left(2\pi\left(t_R - p\right)\right) - \\ C_\sigma \sin\left(2\pi\left(t_T - p\right)\right)\end{array}\right]}{1+e^{Ln(19)\frac{L_t - L_{50}^S}{L_{95}^S - L_{50}^S}}}, \qquad (2)$$

where $Max\sigma_L$ = the hypothetical asymptotic maximum standard deviation of the residual values at some initial size of abalone that sets the exponential term to zero;

L_{50}^S and L_{95}^S = the parameters describing the inverse-logistic for how the variability of residuals reduces with increasing L_t; and

C_σ = the amplitude of the seasonality effect for the σ_{L_t} term.

The fact that $Ln(19)$ is used instead of $-Ln(19)$ implies that the logistic is inverse and that the L_{95} parameters relates to the 95% point ($Ln(15)$ would equate to the 75% point). The inverse-logistic description of variation is general; however, if the expected length increments always remain greater than zero then the standard deviation of the residuals σ_{L_t} can be defined as the simpler

$$\sigma_{L_t} = \alpha\left(\Delta\hat{L}_t\right)^\beta, \qquad (3)$$

where α and β are parameters of a power relationship with the expected length increment $\Delta\hat{L}_t$ and the seasonality is achieved from Equation 1.

When seasonality is ignored (when estimating annual growth increments), the C and C_σ parameters are set to zero leaving the simple Δt so that any slight deviations from a Δt of one year are assumed to alter the predicted growth in a linear fashion. Thus, 0.95 of a year permits 95% of the growth increment of that year. With the use of Δt alone, there is the assumption that a simple linear scaling of growth increment with respect to time elapsed will provide sufficient adjustment for small deviations of Δt from one year.

Using a normal distribution to describe the residuals, we found that there was an excellent match of this distribution to available data. However, if some probability density function other than the normal distribution provided a better fit for some other species or population, then the equivalent measure of spread about the expectation would need to be implemented.

Where the tagging interval is greater than one year, the expected growth increment is estimated in two steps. First, the expected growth increment and standard deviation that would be expected during **a** year of growth are estimated, and then the growth increment for the fraction of the year remaining from the date of tagging to the date of recapture (after subtracting one year) is estimated by using the initial size plus the estimated yearly growth increment as the starting length for the second installment of growth. Thus, ΔL is first estimated with Equation 1 with the C and C_σ parameters set to zero, and Δt set to 1.0, and then the fraction of a year remaining from the date of tagging to the date of recapture (after subtracting one year) is used in the full version of Equation 1 and the L_t is set to the original L_t plus the ΔL predicted from one year of growth. The two sequential ΔL estimates are added together to obtain the total predicted growth increment. Using Equation 2 to define the variation about the curve, we applied a similar sequential process to the estimation of the standard deviation of the respective residual errors. In this case, the expectation was that the variability would reduce with increasing size so the C_σ parameter was expected to be negative rather than positive as was expected for the C parameter. The use of Equation 3 requires that it be applied to

the predicted ΔL. Given that the first year of growth is always assumed to equal the average increment, there is an increased chance that the overall variability of the residuals will be underestimated. However, in practice, bias appears to be small as long as the data available from greater than a single year overlap the available data from durations less than a year in terms of the initial shell lengths.

Alternative growth models

To provide a comparison with the inverse-logistic model both the von Bertalanffy (Fabens, 1965) and Gompertz curves (Troynikov et al., 1998) were fitted to the tagging increment data from southwest Tasmania:

$$\Delta L = \left(L_\infty - L_t\right)\left(1 - e^{-K\Delta t}\right), \tag{4}$$

where L_∞ = the asymptotic maximum size; and
K = the von Bertalanffy growth rate coefficient; and

with

$$\Delta L = L_\infty \left(\frac{L_t}{L_\infty}\right)^{\exp(-g\Delta t)} - L_t, \tag{5}$$

where g = the growth rate parameter in the Gompertz equation.

Likelihoods

At each geographical site, normal likelihoods with non-constant variances (Eqs. 2 or 3), were used to fit the inverse-logistic model to the n available data points. The negative log-likelihood was minimized to determine the optimum parameter estimates:

$$-veLL = -\sum_{L_t=1}^{n} Ln\left[\frac{1}{\sqrt{2\pi}\sigma_{L_t}} e^{\frac{-\left(\Delta L - \Delta\hat{L}\right)^2}{2\sigma_{L_t}^2}}\right]. \tag{6}$$

The nonlinear solver in Excel 2003™ (Microsoft, Seattle, WA) was used to fit all models.

Alternative model arrangements

The full seasonal model has nine parameters, but alternative model structures are possible that use fewer parameters. The alternative model structures suggested relate to the description of the variability about the expected curve. With the seasonal growth description, instead of using Equation 2 to describe the expected residual structure with the Tasmanian data, an acceptable alternative was to ignore the denominator and focus only on the seasonal changes in variability, thus reducing the number of parameters to seven:

$$\sigma_{L_t} = Max\sigma_L \times \left[\begin{matrix}\Delta_t + C_\sigma \sin\left(2\pi\left(t_R - p\right)\right) - \\ C_\sigma \sin\left(2\pi\left(t_T - p\right)\right)\end{matrix}\right]. \tag{7}$$

An alternative approach to implementing this structural change would be to set the L_{50}^S and L_{95}^S parameters in the denominator of Equation 2 to values much larger than the maximum observed initial size. This change in the denominator leads to the exponential term becoming insignificant so that the denominator contracts to one, the division thus has no noticeable effect, and Equation 2 becomes equivalent to Equation 7.

When only annual data are available, the seasonality terms could be ignored and thus a six-parameter model could be used. After the six-parameter model was fitted to real data, it became clear that the L_{95}^S value was often close to the maximum size of abalone found in Tasmania; therefore it was possible to generate a five-parameter model by replacing the L_{95}^S parameter with a constant 210 mm (the size of an abalone that was never tagged but sometimes found in nature). In addition, the L_{50}^S value was often close to the L_{95}^m value. By replacing the former with the latter it was possible to generate a four-parameter model:

$$\sigma_{L_t} = \frac{Max\sigma_L \times \Delta t}{1 + e^{\frac{Ln(19)}{210 - L_{95}^m}\left(L_t - L_{95}^m\right)}}. \tag{8}$$

The three alternative annual models (4, 5, and 6-parameter models) were fitted to the available data from the three regional groups of sites from around southern Tasmania. A comparison of the relative fit of each model was made by using Akaike's information criterion, $AIC = -2LL + 2k$, where LL is the log-likelihood and k is the number of parameters. In addition, the Bayesian Information Criterion $BIC = -2LL + k\mathrm{Ln}(n)$ was also used, where n is the total number of observations (Burnham and Anderson, 2002). For each of these statistics, the model with the smallest value is to be preferred (Quinn and Deriso, 1999). The *AIC* only includes the log-likelihood and the number of parameters, whereas the *BIC* also includes the natural log of the sample size. Where the sample size is greater than 7 [Ln(7.389)=2], the *BIC* penalizes the addition of extra parameters more than the *AIC*. Thus, with the sample sizes observed in the tagging data (Table 1) the *BIC* would be expected to recommend more parsimonious models (those with fewer parameters) than would the *AIC*.

In addition to comparing the *AIC* and *BIC* values for the different models, likelihood ratio tests were conducted to compare the alternative model fits by using different numbers of parameters (Quinn and Deriso, 1999; Haddon, 2001). Given the log-likelihood for each model fit, the likelihood ratio test is

$$\chi^2_{df} = -2(LL_R - LL_F), \quad (9)$$

where LL_R = the log-likelihood for the model with fewest parameters; and
LL_F = the log-likelihood of the model with most parameters.

In the chi-squared statistic, χ^2_{df}, df is the difference in number of parameters (in this case comparing 4 with 6 and 5 with 6 means df takes the value of either 2 or 1, respectively).

Defining the growth transition matrix

The data from all sites includes instances of negative increments (Fig. 2) and hence it is not surprising when the predicted increments also feature negative values. This implies that abalone can decrease in size during a time step. However, abalone tend not to exhibit negative growth; instead these negative increments are assumed to be the result of measurement error. The transition probabilities are simply the cumulative normal distribution to the upper size limit of each size class minus the cumulative normal distribution to the lower size limit of each size class in turn:

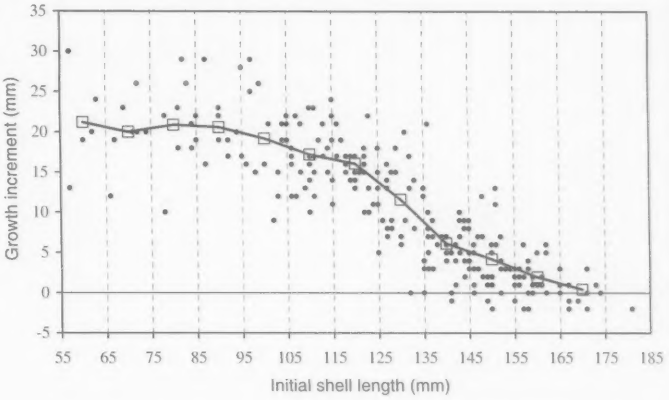

Figure 2

Plot of growth increment (mm) after approximately one year against initial length (mm) for blacklip abalone (*Haliotis rubra*) from the southwest region of Tasmania. The vertical dashed lines represent the boundaries of the 10-mm size classes and the curved line and black squares represent the trend and mean growth increments, respectively, for each class of initial sizes. Mean values are only shown for initial size classes representing more than one observation. Negative increments were included in the mean estimates.

$$G_{i,j} = \int_{-\infty}^{L_i+\frac{LW}{2}} \frac{1}{\sqrt{2\pi}\sigma^j_{L_i}} e^{-\left[\frac{\left(L_i-\bar{L}_{i,j}\right)^2}{2\left(\sigma^j_{L_i}\right)^2}\right]} dL \qquad L_i = L_{Min}$$

$$G_{i,j} = \int_{L_i-\frac{LW}{2}}^{L_i+\frac{LW}{2}} \frac{1}{\sqrt{2\pi}\sigma^j_{L_i}} e^{-\left[\frac{\left(L_i-\bar{L}_{i,j}\right)^2}{2\left(\sigma^j_{L_i}\right)^2}\right]} dL \qquad L_{Min} < L_i < L_{Max}, \quad (10)$$

$$G_{i,j} = \int_{L_i-\frac{LW}{2}}^{+\infty} \frac{1}{\sqrt{2\pi}\sigma^j_{L_i}} e^{-\left[\frac{\left(L_i-\bar{L}_{i,j}\right)^2}{2\left(\sigma^j_{L_i}\right)^2}\right]} dL \qquad L_i = L_{Max}$$

where $G_{i,j}$ = the transition probability of an abalone growing from size class j into size class i;
L_i = the mid-size of size class i;
LW = the size class width; and
$\sigma^j_{L_i}$ = the standard deviation of the normal distribution of growth increments for the initial size class j.
$\bar{L}_{i,j}$ = the expected average final size for initial size class j, which equals $L_j + \Delta\hat{L}_{i,j}$, where $\Delta\hat{L}_{i,j}$ is the average expected growth increment for initial size class j.

Summing the smallest size class to $-\infty$ and the largest size class to $+\infty$ effectively makes both of these size classes plus-groups that ensure that the transition probabilities for all n size classes sum to one.

Length at age

Because of the potentially indeterminate nature of the growth description, there is no analytical version of the growth equation that can provide a length for a given age. Instead, growth needs to be simulated to estimate length at age. That is, an initial length is assumed and then the predicted growth increment in a given time interval (seasonally short or annual) is estimated; this is then added to the initial length and the process is repeated to generate a predicted length at age. The simulated growth increments may include stochasticity (guided by the non-constant variance with initial length) and lead to a scatter of predicted sizes. Alternatively, growth can be simulated by using the growth transition matrix from the model fit. For annual growth only one transition matrix is required, however, to describe seasonal growth there would need to be an array of

growth transition matrices describing the expected growth for different parts of the year.

Comparison of productivity between areas

With the inverse-logistic description of growth the parameter combinations do not provide an intuitively obvious indication of the productivity of different areas. A large $MaxΔL$ does not necessarily mean an area has high productivity if the large growth increments occur only for relatively small animals. An index of relative productivity can be obtained by applying the growth transition matrix derived for an area to a standard initial vector of numbers at size. The areas considered here were compared by generating an annual transition matrix for each area with 31 five-mm size classes from 60 mm up to 210 mm. This transition matrix was multiplied with an initial numbers-at-size vector containing 1000 individuals in the smallest size class. This multiplication was then repeated iteratively for 10 years of growth (i.e., without mortality). The final numbers at size were converted to mass by using the standard $Weight = a Length^b$ where, in southern Tasmania, a = 5.669*E*−05 and b = 3.1792, to provide a comparable index of relative productivity between areas in kilograms.

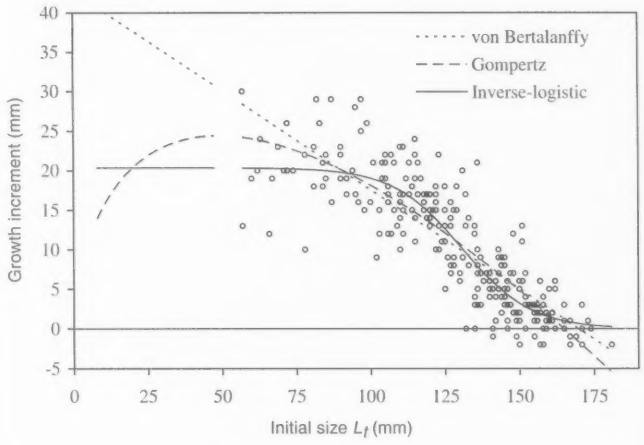

Figure 3

Visual comparison of the von Bertalanffy, Gompertz, and inverse-logistic curves fitted to the annual data from the southwest region of Tasmania. The expected growth increments for smaller blacklip abalone (*Haliotis rubra*) for each curve are also illustrated as extensions of the lines (to the left) and these demonstrate major differences between the curves. The horizontal line at zero represents the point of no growth.

Results

Initial summary of growth patterns

The general growth pattern apparent in the southwest Tasmania (Fig. 2) was also found at other sites around Tasmania, although its full expression was sometimes obscured because the range of available data was limited or truncated by intense size-selective fishing on the larger abalone or because of difficulty in finding cryptic smaller abalone. The growth pattern begins with a relatively constant growth increment (implying linear-like growth) in the smaller-size abalone. This early linear-like growth is followed by a steady decline in growth increment, possibly approaching some minimum annual increment in what would be an asymptotic fashion. Not only do the growth increments follow this decreasing pattern, but a similar pattern is exhibited by the variability of the observed growth increments around the mean trend, although the decrease in variation only occurs at larger sizes (Fig. 2). This pattern of growth differed markedly from the expectation of both the von Bertalanffy and the Gompertz growth models, even when these models were implemented with probability density functions instead of constant parameters (Sainsbury, 1982a; Troynikov et al., 1998; Bardos, 2005).

Instead of these standard curves, the growth pattern observed indicated that some kind of inverse-logistic curve might describe the observations well across the range of available data. If the minimum predicted mean growth increment was greater than zero, it would indicate indeterminate growth in which the dynamics would permit growth to continue (possibly very slowly) until each animal died. An alternative way of looking at indeterminate growth is to note that there may be an upper size limit, at which the growth increment becomes zero, but it is so high that individuals never reach it before death.

Comparison of the inverse-logistic, von Bertalanffy, and Gompertz models

For the southwest region, the three different growth curves all predicted or described the expected growth of blacklip abalone reasonably well . The overlap between the von Bertalanffy and Gompertz curves was especially close over this range (Fig. 3). However, at smaller and larger sizes all three curves diverged significantly. The von Bertalanffy and Gompertz curves both predicted negative growth increments beyond the L_∞ (although using a probabilistic version of these curves could prevent this problem). The major difference between the three curves was therefore found in what was predicted for smaller abalone. The von Bertalanffy curve predicted linearly decreasing growth increments (Fig. 3) as initial size increased. The Gompertz curve predicted initial exponential growth, starting from very small increments

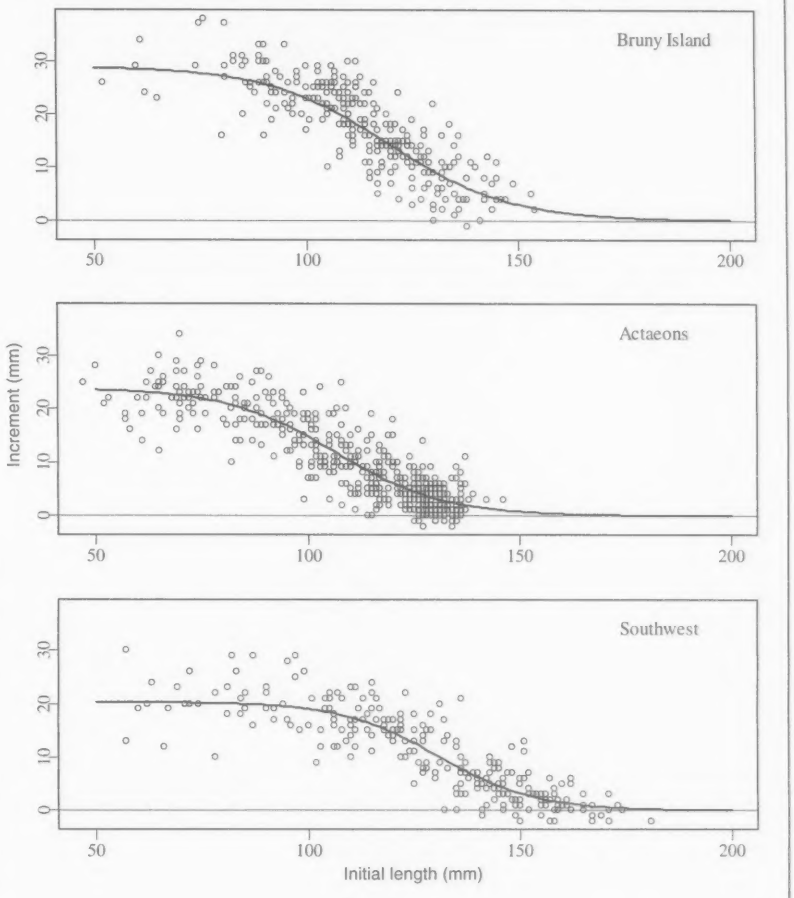

Figure 4

Optimum curves fitted to the three regional groups of sites (southwest, Bruny Island, and Actaeon). Illustrated in each case is the 4-parameter model. Although not illustrated at the given scale, almost no difference would be discernible between the 5- and 6-parameter models. The horizontal lines at zero represent the point of no growth.

for the smallest abalone and reaching a maximum and tailing off as initial length increases. Finally, the inverse-logistic curve predicted constant increments for smaller abalone (initial linear growth) until the growth increments began to decrease with increasing initial length.

The minimum *AIC* and *BIC* were produced by the 4-parameter inverse-logistic curve and not by the 3-parameter von Bertalanffy and Gompertz curves. The log-likelihoods were −726.1 for the von Bertalanffy, −712.2 for the Gompertz, and −681.1 for the inverse-logistic model. With only one more parameter than the other two models, a likelihood ratio test implies that the inverse-logistic curve was a significant improvement over the other two curves.

Annual growth descriptions

Within each of the three regional groups of sites, the predicted mean growth increment for given initial shell lengths for the 4-, 5-, and 6-parameter models was very similar (Fig. 4). In the case of the southwest and Actaeon regions, the predicted lines were visually coincident, whereas for Bruny Island there were only very slight differences in the three curves (Table 2).

For both the southwest and the Actaeon regions, the 4-parameter model was deemed the optimum model configuration by both the AIC and BIC. For the Bruny Island region, the BIC indicated that the 4-parameter model was optimal and the AIC indicated the 6-param-

Table 2

Alternative annual model structures, with their parameters, for the three regional groups of collection sites. The number after each regional name denotes the number of free parameters fitted to the available data. For site locations see Figure 1 and Table 1. $MaxΔL$ is the hypothetical asymptotic maximum growth increment, L^m_{50} is the initial length at which the midway point between the $MaxΔL$ and lowest growth increment is reached, and L^m_{95} denotes the initial length at which 95% of the difference between the smallest and maximum increment is reached. $Max\sigma_L$ is the hypothetical asymptotic maximum standard deviation, L^S_{50} and L^S_{95} are the inverse-logistic parameters describing how the variability of residuals decreases with increasing L_t, and Prod Kg is the relative productivity in kilograms derived from the respective transition matrix. See Equations 1 and 2.

Model	$MaxΔL$	L^m_{50}	L^m_{95}	$Max\sigma_L$	L^S_{50}	L^S_{95}	Prod Kg
Southwest 6	20.393	130.648	164.824	4.461	163.736	214.934	473.5
Southwest 5	20.381	130.669	164.768	4.396	163.735	210	473.1
Southwest 4	20.364	130.688	164.551	4.346	L^m_{95}	210	472.1
Actaeons 6	23.922	106.084	144.431	4.311	138.679	175.809	308.4
Actaeons 5	23.889	106.136	144.243	4.623	142.934	210	308.6
Actaeons 4	23.873	106.165	144.152	4.551	L^m_{95}	210	308.1
Bruny Island 6	28.612	119.736	160.142	4.267	151.438	160.876	459.2
Bruny Island 5	28.386	119.893	159.105	4.297	173.763	210	453.3
Bruny Island 4	28.916	119.421	161.336	4.603	L^m_{95}	210	467.2

Table 3

For each model and parameter combination, the Bayesian information criterion (BIC), Akaike information criterion (AIC), negative log-likelihood (–veLL), and total number of observations n are given. The italicized cells denote the minimum for each criterion and region. The columns labeled "Model 5" and "Model 4" denote the likelihood ratio test values compared to the models in the Model column. The comparisons in Model 5 column had one degree of freedom and for the 5-parameter model to be better than the 4-parameter, it had to be greater than χ^2_1 =3.84, and the comparisons in the Model 4 column had two degrees of freedom and had to be greater than χ^2_2 =5.99 for the models with more parameters to be significantly better than the 4-parameter model.

Model	BIC	AIC	-veLL	n	Model 5	Model 4
Southwest 6	1395.1	1373.9	680.96	252	0.14	0.18
Southwest 5	1389.7	1372.1	681.03	252		0.04
Southwest 4	*1384.2*	*1370.1*	681.05	252		
Actaeons 6	2716.3	2690.9	1339.5	500	3.6	3.8
Actaeons 5	2713.7	2692.7	1341.3	500		0.2
Actaeons 4	*2707.6*	*2690.7*	1341.4	500		
Bruny Island 6	1747.6	*1725.5*	856.7	295	2.4	4.8
Bruny Island 5	1744.2	1725.8	857.9	295		2.4
Bruny Island 4	*1740.9*	1726.2	859.1	295		

eter model was optimal (Table 3). At the same time, the likelihood ratio test indicated in all cases that the 4-parameter model was not significantly worse than any other model (Table 3; Fig. 3).

The key differences that occur between the fitted models relate to how well they describe the trends in variation along the curves. The data for the southwest had the widest size range and the similarity of the fitted L^S_{50} parameter to the L^m_{95} parameter was clear. At the same time, the L^S_{95} parameter was only slightly bigger than 210 mm (Table 2). Thus, the substitutions to create the 4-parameter model had little effect on the outcome if this model was used to predict the likely distribution of growth increments (Fig. 5). The main effect of reducing the number of parameters used was to slightly reduce the variation beyond about 170 mm initial shell length.

The 6-parameter model has sufficient flexibility in that it can accurately describe both the mean growth trend and the pattern of variation around the expected mean growth increments. This was not necessarily an advantage when the high level of fishing mortality applied to legal-size abalone means that the availability of larger size abalone in the tag return data can be

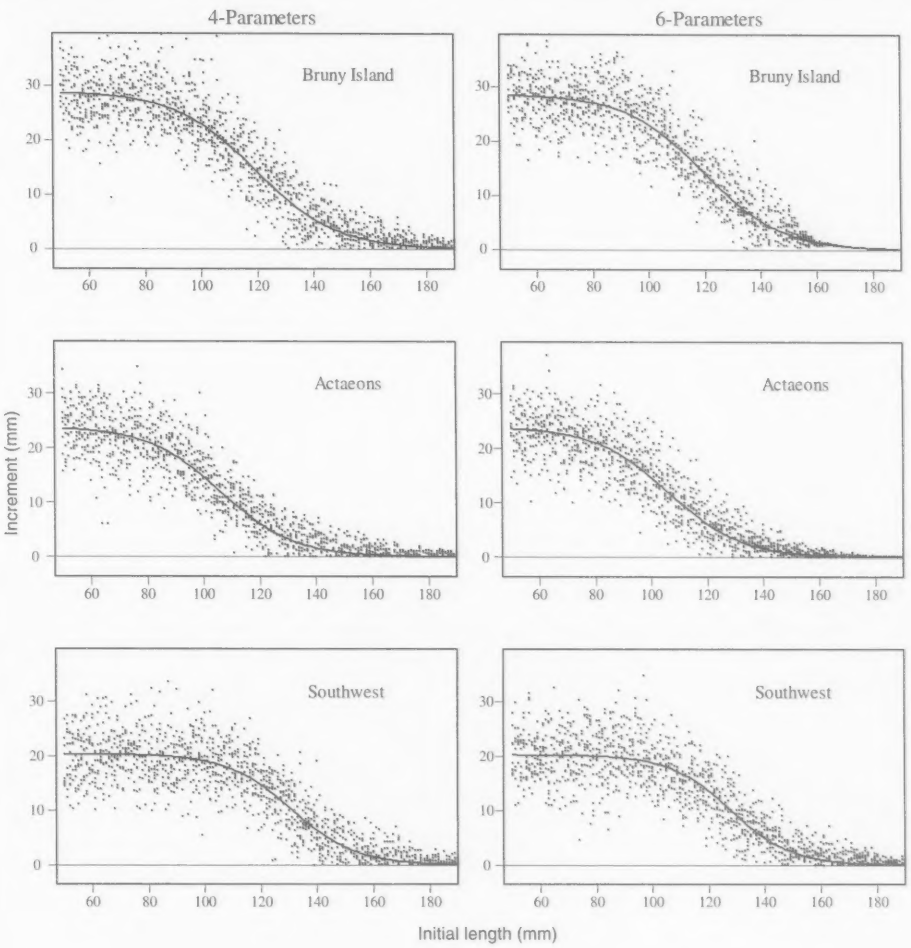

Figure 5

Plots of the mean predicted growth increments (solid black line), and a set of simulated data derived from the optimum model in each case (fine dots). The left hand panel represents the 4-parameter model; the right hand panel represents the 6-parameter models. All predicted negative increments were omitted. For each area the curves were fitted to the same data as those illustrated in Figure 4.

limited and only provided a biased perception of the growth of larger abalone. With the southwest data the difference between the 4- and 6-parameter models was slight; however, larger differences were found when the 4- and 6-parameter models were applied to the other two regions, which were less well represented in the larger initial sizes (Fig. 4). Most obviously, at Bruny Island (Fig. 5), the 6-parameter model so closely described the available data that beyond about 160 mm, the model predicted essentially no variation around the predicted mean growth increments. Although the 6-parameter model accurately described the available data, the 4-parameter model provided a more realistic representation of the spread of predicted growth increments for initial sizes for which there were few or no observed data (Fig. 5).

Of the three regions considered, the southwest and Bruny Island were similar in terms of relative productivity and the Actaeon regional sites were the least productive (Table 2). The parameter combinations for the southwest and Bruny Island regions were rather different, but although the $MaxΔL$ was 8 mm larger at Bruny Island than in the southwest, it was offset in the southwest by the higher value for L^m_{50}. The two sites

constituting the Actaeon region samples were within relatively low productivity areas that may be considered to be atypically low for the Actaeon area (see the seasonal analysis).

Table 4

Seasonal growth-description parameter estimates. All parameter definitions are given with Equation 1 under the heading "Growth model" in the Materials and methods section. In the Actaeon Island estimates L^S_{50} and L^S_{95} reached the limits placed on the parameters. At Sterile Island, the parameter estimates obtained did not change when the L^S_{50} and L^S_{95} estimates were replaced with 209 and 210, respectively. In all cases the logistic reduction in the variance was negligible. The –veLL is the negative log-likelihood. Productivity, in kilograms, is the relative productivity derived from the respective transition matrix.

Parameter	Actaeon Island	Sterile Island
$MaxΔL$	21.8464	20.0111
L^m_{50}	129.9702	121.7953
L^m_{95}	162.1723	161.4016
$Max\sigma_L$	6.7129	6.8766
L^S_{50}	209	186.9362
L^S_{95}	210	192.3000
C	0.1123	0.0907
p	0.1263	0.1561
C_σ	–0.0821	–0.0489
Productivity Kg	484.2	419.4
-veLL	1249.673	944.564

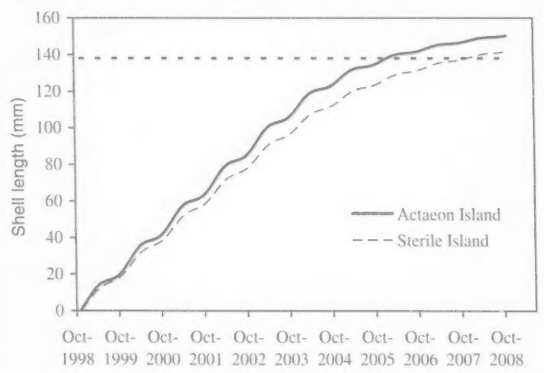

Figure 6

A comparison of the implied seasonal growth curves at the Actaeon and Sterile Islands in southern Tasmania. The fine horizontal dashed line at 138 mm is the current legal minimum length. The curves remain approximately linear until about 100 mm shell length. The slowest growth periods line up approximately with October each year.

Seasonal growth descriptions

Seasonal growth descriptions were fitted to data from two sites in southeast Tasmania: Actaeon Island and Sterile Island (Table 1; Fig. 2). In each case, when the inverse-logistic curve describing the standard deviation of the residual errors was fitted, the estimates of L^S_{50} and L^S_{95} were both much larger than the maximum size observed. In effect, this result implied that the variability was best described with Equation 7 rather than Equation 3. For this reason, the 7-parameter model was preferred to the 9-parameter model, even though the optimum fit in each case lead to the same results in terms of parameter estimates and log-likelihood. The two sites are very close together geographically (~2 km apart) and, in this case, the parameter estimates were similar between the two sites (Table 4).

By assuming a starting size of 0.25 mm on the 25th November (a typical size and date of settlement for a newly settled blacklip abalone) in an arbitrary year, and by calculating the expected size increment in a series of 8-day steps forward in time, adding those increments to the initial size and then repeating the process, it was possible to visualize the seasonal growth of animals (Fig. 6). The main difference in the parameters is in the L^m_{50}, which was 8.0 mm larger at Actaeon Island (Table 4). This difference led to the abalone at Actaeon Island reaching the current minimum legal length of 138 mm in approximately eight years, whereas the difference led to the current minimum legal length in nine years, on average, at Sterile Island (Fig. 6).

The Actaeon Island site was far more productive than Gagens Point and the Middle Ground, both in the Actaeon region and, in fact, was as productive as both the Bruny Island and southwest regions (Tables 2 and 4). The Sterile Island site had a productivity that was only 89% of that of the Actaeon Island site (431 kg vs. 485 kg; Table 4), this was also reflected in a one year difference in time to legal minimum size (Fig. 6).

The pattern of seasonality was very similar between the two sampled sites; linear-like initial growth proceeded at least until 100 mm shell length. The phase parameter, p, value of 0.118 implies that the fastest period of growth occurred on 11th February at the Actaeon Islands, whereas at Sterile Island the estimate of 0.156 indicates the fastest growth occurred two weeks later on 25th February.

Discussion

Comparison of inverse-logistic, von Bertalanffy, and Gompertz models

The major difference between the inverse-logistic growth description, the von Bertalanffy growth curve, and the Gompertz growth curve is seen in the model fit at the extremes of the growth trajectory. Without

a probabilistic interpretation of the parameters, the von Bertalanffy and Gompertz curves predict negative growth increments at initial lengths greater than L_∞, and the inverse-logistic predicts ever decreasing growth increments as the initial length at tagging increases. Thus, a realistic representation of the final size distribution of larger abalone is provided by the inverse-logistic model without the complexity of a probabilistic interpretation of the parameters. In Tasmania, the growth of small abalone, at least above 10 mm, appears to be linear-like and to increase in relatively constant growth increments through time (Prince et al., 1988; Gurney et al., 2005). Although the von Bertalanffy and Gompertz equations can approximate linear-like growth over these small sizes, linear growth limits their capacity to describe accurately the growth of larger animals at the same time. The von Bertalanffy curve predicts a linear relationship between growth increment and initial shell length. The Gompertz equation, on the other hand, predicts that small abalone would have very small growth increments that initially increase with initial length and then decline again. Neither of these alternatives is consistent with observations in Tasmania of linear-like early growth.

Growth pattern

The tagging data on growth increments of blacklip abalone from various sites around the south of Tasmania were able to be grouped according to similarity of growth pattern. All regions exhibited a similar pattern of mean growth increments that were well described by a symmetric inverse-logistic curve.

Negative growth increments observed in the tagging data were not taken to be evidence of negative growth, but were rather taken to be a reflection of measurement or recording errors, a possible chipping of shell edges during collection, or an increased chance of shell erosion in disturbed animals (or a combination of these possibilities). Because of this, when simulating growth, negative increments were not included.

The tagging data were, in some cases, truncated either in the smaller or the larger sizes. The fishing mortality rate on legal-size abalone is high and numbers of animals much larger than the minimum legal length are significantly reduced. In addition, the cryptic nature of undersize abalone means that obtaining representative data across the whole size range can be difficult. It is also possible that the tagging process could influence the subsequent rate of growth. Intuitively, if there were an impact, it would probably be a negative bias on the growth increments that would increase the variation observed (by extending growth into smaller increments).

Despite the limitations of the data, the proposed system of two linked inverse-logistic curves proved capable of fitting and simulating data from three sites in southern Tasmania. The inverse-logistic model was fully capable of producing transition matrices with predicted values across the full range of size classes required (60 mm to 210 mm). The truncation of the available data by high levels of fishing pressure did have effects, however. Surprisingly, the more complex 6-parameter model did not always provide the most workable description of growth because the fit with six parameters could over-emphasize missing data; that is, the absence of data could influence the fitted curve, especially when the flexibility of the 6-parameter curve was used. It can be argued that the simpler 4-parameter model provides a more useful description of growth because it is less likely to be influenced by peculiarities or limitations of the available data. For example, at the legal minimum size limit (136 mm shell length at the time of data collection), abalone from the Bruny Island region were growing an average of 8 mm per annum (with a range from 2 mm to 15 mm). However, fishing mortality rates at Bruny Island were very high and few legal-size animals remained for long at this site with the result that the tagging growth increment data were sparse above 140 mm. The 6-parameter model describes the specific pattern of growth in the data from Bruny Island, truncating any growth beyond the maximum size available, whereas the 4-parameter model extrapolates the growth pattern beyond the maximum size available in the data and, in this case, provides a much more plausible solution. For stock assessment purposes, the 4-parameter model would be more useful in practice. The symmetry of the inverse-logistic curve enables the 4-parameter model to project the growth dynamics into size classes for which there are few or no samples.

Seasonal growth

The independent samples from Actaeon Island and Sterile Island, which are close together geographically, generated very similar estimates of the timing of the seasonal changes in growth rates. These samples were so similar that the mean curves remained close until the abalone reached about 80 mm shell length. The abalone at Actaeon Island, however, continued growing rapidly for longer than the animals at Sterile Island; therefore these curves diverged. An implication of this difference in productivity is that instead of taking about 8 years to reach the legal minimum length, as at Actaeon Island, it takes 9 years at Sterile Island.

The blacklip abalone at the Middle Ground and Gagens Point sites were selected by local abalone divers as having notoriously slow growth. Compared to Actaeon Island, these two sites in the Actaeon Island region did indeed have relatively low productivity compared to the seasonal sample from Actaeon Island (only about 308 kg relative to 484 kg); and this occurred despite the $MaxΔL$ being about 23 mm for the Middle Ground and Gagens Point sites but only 21 mm at Actaeon Island. Productivity was strongly and positively correlated with the L^m_{50} and the L^m_{95} parameter values, which relate to how long the linear-like growth phase continues.

The different sites in the Actaeon region are all relatively close together geographically and yet variation in the parameter estimates and consequent productivity among sites were high. This result is consistent with

the idea that abalone growth is likely to be determined by local site-specific influences in addition to regional scale influences (McShane and Naylor, 1995; Naylor et al., 2006). Thus, although sites within the Actaeon region were variable, similarities were evident between sites located in distant regions (e.g., in the southwest and Bruny Island). This variability in growth has obvious implications for the confidence with which it is possible to conduct stock assessments for abalone over large areas. The description of growth in size-structured models is so influential that the interpretation of any model outputs would need to be made with great attention paid to any potential biases brought about by using an under- or over-productive description of growth.

Estimates of productivity derived from the inverse-logistic description of growth would be expected to lie somewhere between that predicted by the von Bertalanffy curve and the Gompertz curve. The von Bertalanffy curve predicts very rapid early growth and so, all other things being equal, would predict the highest productivity levels, whereas the Gompertz curve predicts very slow early growth and thus would predict the lowest productivity. These differences are why the selection of the most appropriate model of growth is critical for stock assessments. For blacklip abalone in Tasmania the inverse-logistic model provides the most realistic representation of the dynamics of growth.

Acknowledgments

The authors thank the array of divers who contributed to the field work, especially S. Dickson, J. Bridley, T. Karlov, C. Jarvis, and M. Porteus. Some of the diving was undertaken from off the RV *Challenger*, crewed by M. Francis and J. Gibson. We also thank F. Helidoniotis for assistance when preparing the map.

Literature cited

Bardos, D. C.
2005. Probabilistic Gompertz model of irreversible growth. Bull. Math. Biol. 67:529–545.

Breen, P. A., S. W. Kim, and N. L. Andrew.
2003. A length-based Bayesian stock assessment model for the New Zealand abalone *Haliotis iris*. Mar. Freshw. Res. 54:619–634.

Burnham, K. P., and D. R. Anderson.
2002. Model selection and multimodel inference: A practical information-theoretic approach, 2nd ed., 488 p. Springer, New York, NY.

Day, R. W., and A. E. Fleming.
1992. The determinants and measurement of abalone growth. *In* Abalone of the world. Biology, fisheries and culture; proceedings of the 1st international symposium on abalone (S. A. Shepherd, M. J. Tegner, and S. A. Guzman Del Proo, eds.) p. 141–168. Fishing News Books, Carlton, Victoria, Australia.

Fabens, A. J.
1965. Properties and fitting of the von Bertalanffy growth curve. Growth 29:265–289.

Francis, R. I. C. C.
1988. Maximum likelihood estimation of growth and growth variability from tagging data. NZ. J. Mar. Freshw. Res. 22:42–51.

Francis, R. I. C. C.
1995. An alternative mark-recapture analogue of Schnute's growth model. Fish. Res. 23:93–111.

Gompertz, B.
1825. On the nature of the function expressive of the law of human mortality, and on a new model of determining the value of life contingencies. Philos. Trans. R. Soc. Lond. Ser. B.. Biol. Sci 115:513–585.

Gorfine, H., B. Taylor, M. Cleland, M. Haddon, A. Punt, D. Worthington, and I. Montgomery.
2005. Development of a spatially-structured model for stock assessment and TAC decision analysis for Australian abalone fisheries, 42 p. Fisheries Research and Development Corporation. Primary Industries Research Victoria, Queenscliff, Victoria.

Gurney, L. J., C. Mundy, and M. C. Porteus
2005. Determining age and growth of abalone using stable oxygen isotopes: a tool for fisheries management. Fish. Res. 72:353–360.

Haddon, M.
2001. Modelling and quantitative methods in fisheries, 406 p. CRC Press, Chapman and Hall, Boca Raton, FL.

McShane, P. E., and M. G. Smith.
1992. Shell growth checks are unreliable indicators of age of the abalone *Haliotis rubra* (Mollusca, Gastropoda). Aust. J. Mar. Freshw. Res. 43:1215–1219.

McShane, P. E., and J. R. Naylor.
1995. Small-scale spatial variation in growth, size at maturity, and yield- and egg-per-recruit relations in the New Zealand abalone *Haliotis iris*. NZ. J. Mar. Freshw. Res. 29:603–612.

Naylor, J. R., N. L. Andrews, and S. W. Kim.
2006. Demographic variation in the New Zealand abalone *Haliotis iris*. Mar. Freshw. Res. 57:215–224.

Prince J. D., T. L. Sellers, W. B. Ford, and S. R. Talbot.
1988. Recruitment, growth, mortality and population structure in a southern Australian population of *Haliotis rubra* (Mollusca, Gastropoda). Mar. Biol. 100:75–82.

Punt, A. E., and R. B. Kennedy.
1997. Population modelling of Tasmanian rock lobster, *Jasus edwardsii*, resources. Mar. Freshw. Res. 48: 967–980.

Quinn, T. J., and R. B. Deriso.
1999. Quantitative fish dynamics, 542 p. Oxford Univ. Press, Oxford.

Sainsbury, K. J.
1982a. Population dynamics and fishery management of the paua, *Haliotis iris* I. Population structure, growth, reproduction, and mortality. NZ. J. Mar. Freshw. Res. 16:147–161.

Sainsbury, K. J.
1982b. Population dynamics and fishery management of the paua, *Haliotis iris* II. Dynamics and management as examined using a size class population model. NZ. J. Mar. Freshw. Res. 16:163–173.

Schnute, J.
1981. A versatile growth model with statistically stable parameters. Can. J. Fish. Aquat. Sci. 38:1128–1140.

Sullivan, P. J., L. Han-Lin, and V. F. Gallucci.
1990. A catch-at-length analysis that incorporates a

stochastic model of growth. Can. J. Fish. Aquat. Sci. 47:184–198.

Troynikov, V. S., and H. K. Gorfine.
1998. Alternative approach for establishing legal minimum lengths for abalone based on stochastic growth models for length increment data. J. Shell. Res. 17:827–831.

Troynikov, V. S., R. W. Day, and A. M. Leorke.
1998. Estimation of seasonal growth parameters using a stochastic Gompertz model for tagging data. J. Shellfish Res. 17:833–838.

von Bertalanffy, L.
1938. A quantitative theory of organic growth (Inquiries on growth laws. II). Human Biol. 10:181–213.

Worthington, D. C., R. C. Chick, C. Blount, P. A. Brett, and P. T. Gibson.
1998. A final assessment of the NSW abalone fishery in 1997. Fish. Res. Assess. Ser. 5:1–33.

Effects of commercial fishing regulations on stranding rates of bottlenose dolphin (*Tursiops truncatus*)

Barbie L. Byrd (contact author)

Aleta A. Hohn

Email address for B. L. Byrd: Barbie.Byrd@noaa.gov

National Marine Fisheries Service
Southeast Fisheries Science Center
National Oceanic and Atmospheric Administration, Beaufort Laboratory
101 Pivers Island Road
Beaufort, North Carolina 28516

Fentress H. Munden

North Carolina Division of Marine Fisheries
3441 Arendell Street
Morehead City, North Carolina 28557

Gretchen N. Lovewell

Rachel E. Lo Piccolo

National Marine Fisheries Service
Southeast Fisheries Science Center
National Oceanic and Atmospheric Administration, Beaufort Laboratory
101 Pivers Island Road
Beaufort, North Carolina 28516

Abstract—Fisheries management actions taken to protect one species can have unintended, and sometimes positive, consequences on other species. For example, regulatory measures to reduce fishing effort in the winter gillnet fishery for spiny dogfish (*Squalus acanthias*) off North Carolina (NC) also led to decreases in the number of bycaught bottlenose dolphins (*Tursiops truncatus*). This study found that a marked decrease in fishing effort for spiny dogfish in NC also corresponded with a marked decrease in winter stranding rates of bottlenose dolphins with entanglement lesions (P=0.002). Furthermore, from 1997 through 2002, there was a significant positive correlation (r^2=0.79; P=0.0003) between seasonal bycatch estimates of bottlenose dolphins in gill nets and rates of stranded dolphins with entanglement lesions. With this information, stranding thresholds were developed that would enable the detection of those increases in bycatch in near real-time. This approach is valuable because updated bycatch estimates from observer data usually have a time-lag of two or more years. Threshold values could be used to detect increases in stranding rates, triggering managers immediately to direct observer effort to areas of potentially high bycatch or to institute mitigation measures. Thus, observer coverage and stranding investigations can be used in concert for more effective fishery management.

Manuscript submitted 20 April 2007.
Manuscript accepted 30 October 2007.
Fish. Bull. 106:72–81 (2008).

The views and opinions expressed or implied in this article are those of the author and do not necessarily reflect the position of the National Marine Fisheries Service, NOAA.

The occurrence of beach-cast or stranded marine animals has been used to indicate fishery-induced (i.e., bycatch) mortality of marine birds (Salzman, 1989), turtles (Caillouet et al., 1991; Epperly et al., 1996), and mammals (Forney et al., 2001; Friedlaender et al., 2001). Direct documentation of bycatch mortality is obtained by placing trained observers on commercial fishing vessels (Edwards and Perrin, 1993; Epperly et al., 1995), but limited resources allow for observation of only a small proportion of fishing trips and a few types of fisheries. Additionally, updated bycatch estimates can take years to become available, preventing real-time responses to significant changes in bycatch rates. Strandings of marine animals, therefore, can serve as the primary, and sometimes the only, evidence of current bycatch mortality. Gear is rarely present on stranded animals; however, entanglement lesions on the epidermis of cetaceans can help identify animals that have been captured incidentally by fishing gear (Kuiken et al., 1994; Read and Murray, 2000).

Early indications of bottlenose dolphin (*Tursiops truncatus*) bycatch mortality off North Carolina (NC) came from stranding data. From 1993 through 1996, 29% of the 230 stranded bottlenose dolphins recovered in NC exhibited signs of entanglement in fishing gear (Waring et al., 1997). Early observer data (1993–96) were inconsistent with stranding data because only one entanglement was documented in the observer program (Waring et al., 1997). As a result, observer coverage was expanded in 1997 to include more of the various ocean-side gillnet fisheries (Waring et al., 1999).

The annual estimated bycatch mortality in ocean gill nets from November 1995 through October 2000 confirmed high levels of mortality of bottlenose dolphins off NC. All but one observed entanglement was that of the coastal morphotype, which is morphologically and genetically dis-

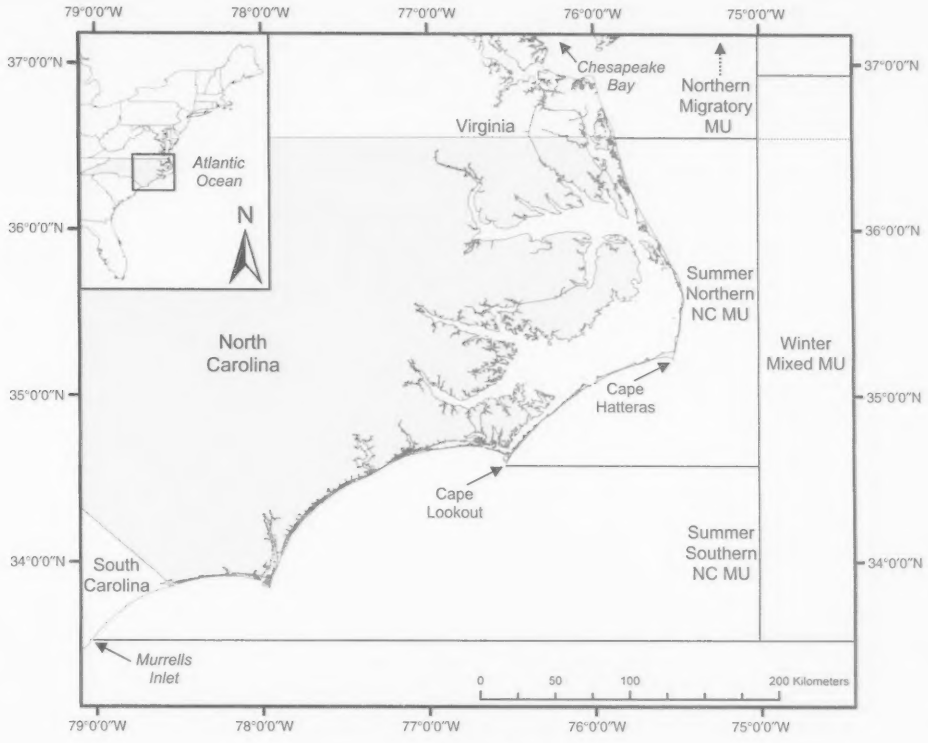

Figure 1

The coastal bottlenose dolphin (*Tursiops truncatus*) is divided into seasonal management units (MUs). During summer (May–October), two of the management units (MUs) occur off North Carolina (NC;) the northern NC MU and the southern NC MU. During winter (November–April), two summer MUs overlap with a third MU, the northern migratory MU, which occurs north of the Virginia-NC border during the summer. These three MUs are referred to collectively as the winter mixed MU (Waring et al., 2006). Solid horizontal lines represent latitudinal boundaries of MUs and does not imply offshore (i.e., longitudinal) distribution. The dashed horizontal line represents the northern boundary of the NC portion of the winter mixed MU.

tinct from the offshore morphotype (Mead and Potter, 1995; Hoelzel et al., 1998; Waring et al., 2002). The bycatch estimates for the coastal morphotype were stratified according to current stock structure of coastal bottlenose dolphins, which consists of seven seasonal management units (MUs) (Waring et al., 2002). Three of the MUs are seasonal off NC: the summer (May–October) northern NC MU, the summer southern NC MU, and the NC portion of the winter (November–April) mixed MU (see Fig. 1 for delineations of the units). Bycatch exceeded the potential biological removal (PBR) level (i.e., the sustainable anthropogenic mortality level) (MMPA 16 U.S.C. 1362 [20]; Barlow et al., 1995) for one of the two summer MUs and for the winter MU (Waring et al., 2002, 2006). During the summer, the annual estimated bycatch for the northern NC MU was 23 animals, exceeding the PBR level (20), and the annual estimated bycatch for the southern NC MU was zero, not exceeding the PBR level (10). For the winter mixed MU (NC and VA submanagement units), the annual estimated bycatch was 180 animals, more than twice the PBR level (68). The majority of this bycatch (146 out of 180 animals) was attributed to the NC submanagement units (Rossman and Palka[1]). The spiny dogfish (FAO common name: picked dogfish) fishery was the primary contributor to the bycatch mortality in the winter mixed MU.

In 2005, new annual bycatch estimates, based on observer data from ocean gill nets from November 2000 through October 2002, became available (Rossman and Palka[1]; Waring et al., 2006). The new bycatch estimate for the summer northern NC MU decreased to eight animals per year and the new estimate for the NC win-

[1] Rossman, M. C., and D. L. Palka. 2005. A review of coastal bottlenose dolphin bycatch mortality estimates in relation to the potential effectiveness of the proposed BDTRP. Bottlenose Dolphin Take Reduction Team Document No. 1-13-05F, 9 p. National Marine Fisheries Service, Northeast Fisheries Science Center, 166 Water Street, Woods Hole, MA 02543.

ter mixed MU decreased to 19 animals per year; both estimates were below their corresponding PBR level. Reductions in bycatch estimates were attributed to a reduction in fishing effort, as measured in landings. In particular, fishing effort was drastically reduced for spiny dogfish, which was listed as overfished by the National Marine Fisheries Service (NMFS) in 1998 (Federal Register, 1998). Fishery Management Plans (FMPs) were implemented by NMFS for federal waters (Federal Register, 2000a, 2000b), and by state agencies for state waters (ASMFC[2]), to reduce fishing effort.

The purpose of this study was to conduct a *post-hoc* analysis of bottlenose dolphin strandings in NC in relation to fisheries bycatch estimates and spiny dogfish landings. First, the frequency of stranded dolphins exhibiting signs of fishery entanglement was examined to determine if this frequency reflected corresponding levels of estimated dolphin bycatch. Second, it was hypothesized that the frequency of those strandings would decrease concomitant with a reduction in spiny dogfish landings, but that the frequency of stranded dolphins without signs of entanglement would not change. Lastly, two methods for establishing stranding threshold levels were evaluated to determine if they could be used in real-time to detect increases in fisheries bycatch before revised bycatch estimates are available or when observer programs do not exist.

Materials and methods

Fishing-effort data

Monthly landings data on spiny dogfish caught in commercial ocean gill nets off NC from November 1997 through April 2005 were obtained through the Trip Ticket Program of the North Carolina Division of Marine Fisheries (NCDMF). These data were used to determine the timing and magnitude of effort reduction in the spiny dogfish fishery for comparison with the frequency of bottlenose dolphin strandings.

Stranding data

Data were derived from ocean-side bottlenose dolphin strandings in NC between November 1997 and April 2005 (n=580) and were stratified by season: winter (November–April) and summer (May–October). These seasons reflect both the seasonal definition for bottlenose dolphin MUs and the two commercial fishing seasons for spiny dogfish as defined by the FMP. November 1997 was chosen as the beginning of the winter season because this month marked the beginning of the first spiny dogfish season in NC (November–April) for which there was consistent coast-wide coverage of the NC shore for strandings. April 2005 was the end of the last season for which landings data were available for this study.

All reported stranded bottlenose dolphins were evaluated for signs of human interaction (HI) and then classified as HI-yes (i.e., with signs of HI), HI-no (i.e., no signs of HI), or HI-CBD (could not be determined) (Kuiken et al., 1994; Read and Murray, 2000). Stranded dolphins categorized as HI-yes were further stratified as fishery interaction (HI-FI) (e.g., entanglement lesions or gear present) or HI-other (e.g., mutilation, propeller wounds evident). All stranded dolphins classified as HI-other in our data set (n=12) were mutilated but too decomposed to determine if entanglement lesions were also present; therefore, they were treated separately. Animals were categorized as HI-CBD when it could not be determined whether or not the animal exhibited signs of HI because of factors such as decomposition, significant damage by scavengers, or lack of experience on the part of the stranding responder.

Several criteria were established for the stranding records used in this study. Animals genetically confirmed as being the offshore morphotype (n=6) were excluded so that comparisons could be made to bycatch data of coastal bottlenose dolphins. Animals <119 cm in total length (n=109), presumed to be neonates (Fernandez and Hohn, 1998), were also excluded to prevent a bias from the high natural mortality rates of neonates during the spring and fall birthing seasons (Hohn, 1980; Thayer et al., 2003). Unless they were classified as adults, stranded dolphins for which no total length was recorded were excluded (n=21). Dolphins removed from gear other than a gill net (e.g., trawlers, crab pots, hook-and-line gear) were also excluded (n=5).

Stranding rates through time were examined in relation to bycatch estimates and changes in fishing effort in the spiny dogfish fishery. Regression analyses (SAS, vers. 9.1, SAS Inst., Inc., Cary, NC) were used to compare the number of HI-FI strandings per season (winter and summer) per year to the corresponding bycatch estimates for ocean gill nets provided in Rossman and Palka.[1] Because stranding rates can never be less than zero, the regression line was forced through the origin. Rank-sum tests for each HI category were used to determine if the mean number of bottlenose dolphin strandings per month was different between the first time period (TP1: November 1997–October 2000), when bycatch estimates were greater than the PBR levels, and the second time period (TP2: November 2000–April 2005), when bycatch estimates were either less than PBR levels or were unknown. For the rank-sum tests, only winter data (November–April) were used after a preliminary investigation of spiny dogfish landings revealed that the fishery operates only off NC during those months.

Stranding thresholds

Two methods were used to calculate stranding thresholds. One calculation emulated a method currently

[2] ASMFC (Atlantic States Marine Fisheries Commission). 2006. Review of the Atlantic States Marine Fisheries Commission's interstate fishery management plan for spiny dogfish (*Squalus acanthias*) May 2004–April 2005 fishing year, 18 p. Prepared by the Spiny Dogfish Plan Review Team, ASMFC, 1444 Eye Street, NW, 6th Floor, Washington, DC 20005.

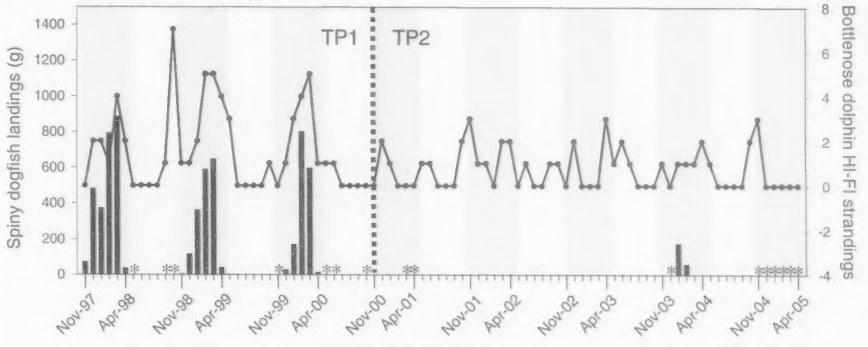

Figure 2

Spiny dogfish (*Squalus acanthias*) landings in metric tons (denoted by bars) and numbers of bottlenose dolphin (*Tursiops truncatus*) strandings (denoted by a line) classified as HI-FI (i.e., having evidence of fishery interaction) in North Carolina from November 1997 through April 2005. Shaded areas represent winter months (November–April). Asterisks (*) represent months when minimal landings occurred. No bars or asterisks represent months with no landings. Monthly strandings in winter decreased between time period (TP) 1 and TP2, delineated by a dashed vertical line.

used to help detect unusual mortality events (UME) for overall strandings by the Marine Mammal Health and Stranding Response Program (Wilkinson, 1996) and was termed the "UME threshold method." It was calculated as the mean number of strandings (in this case HI-FI) per month plus two standard deviations (SD). Stranding thresholds were calculated for each bottlenose dolphin MU in NC. For the NC winter mixed MU, data collected in TP2 were used. The stranding threshold was then compared to monthly HI-FI strandings during TP1 and TP2 to determine whether it serves as an adequate indicator of relative bycatch levels. For the summer northern NC MU, the stranding threshold also was calculated with data collected in TP2. For the summer southern NC MU, the stranding threshold was calculated with data from TP1 and TP2 because estimated bycatch levels never exceeded PBR levels in TP1.

The second method that was investigated to establish stranding threshold levels was based on the regression analysis of seasonal HI-FI strandings and estimated bycatch. This method used the maximum likelihood estimates to calculate the predicted values of bycatch and the 68% confidence intervals (CIs) and 95% CIs. The CI values of predicted bycatch rates were then evaluated to determine if they would be appropriate for identifying periods of elevated bycatch.

Results

From November 1997 through April 2005, NC gillnetters landed 6310 t (metric tons) of spiny dogfish. Landings occurred almost entirely in winter (November–April), and less than 0.1% occurred in other months (Fig. 2). More than 96% of all landings occurred before November 2000 (TP1). During winter, mean landings were 2020 t (SD=561) per fishing season during TP1 and 49 t (SD=104) during TP2. After November 2000, 96% of these landings occurred during the 2003–04 fishing year.

During the same time period (November 1997 through April 2005), 439 bottlenose dolphin strandings met the criteria for inclusion in this study. Overall, more strandings occurred during winter than summer in each HI category (Table 1). For all years, HI-CBD strandings comprised 60% of winter (range: 45–69%) and 52% of summer (range: 25–65%) totals (HI-yes, HI-no, and HI-CBD). HI-FI strandings comprised 22% of winter (range: 11–35%) and 21% of summer (range: 11–33%) totals for all years. However, of strandings for which it was possible to determine whether an interaction occurred (HI-FI, HI-other, and HI-no), HI-FI strandings comprised 56% (range: 27–75%) of winter and 44% (range: 20–57%) of summer totals for all years.

Rates of HI-FI strandings had a similar pattern to that of bycatch estimates and effort in the spiny dogfish fishery. There was a significant positive relationship between the number of HI-FI strandings and the bycatch estimate per season (r^2=0.79, P=0.0003). Additionally, the mean number of winter HI-FI strandings per month was significantly greater during TP1 than TP2 (P=0.001) (Table 2). There was no significant difference in winter HI-no or HI-CBD strandings between TP1 and TP2. HI-FI strandings showed a monthly periodicity similar to that for fishing effort during TP1 (Fig. 2); four to six animals were recovered per month during the height of the fishery, compared to generally two or

Table 1

Numbers of bottlenose dolphin (*Tursiops truncatus*) recovered ocean-side in North Carolina between November 1997 and April 2005. Strandings are listed by winter (W) (November–April), summer (S) (May–October), and all months (T), and categorized according to the human interaction (HI) classification: HI-yes (evidence of human interaction including HI-FI [evidence of fishery interaction], and HI-other [evidence of mutilation, propeller wounds]), HI-no (no signs of HI), and HI-CBD (human interaction could not be determined). For this study, data were not available (n/a) for the 2005 summer season (May–October) and thus totals for 2005 are for a partial year, denoted by an asterisk.

	HI-yes														
	HI-FI			HI-other			HI-no			HI-CBD			Total		
	W	S	T	W	S	T	W	S	T	W	S	T	W	S	T
1998 (Nov 97–Oct 98)	11	8	19	4	0	4	7	6	13	18	14	32	40	28	68
1999 (Nov 98–Oct 99)	18	4	22	0	0	0	6	5	11	27	17	44	51	26	77
2000 (Nov 99–Oct 00)	14	2	16	2	3	5	7	5	12	36	8	44	59	18	77
2001 (Nov 00–Oct 01)	3	4	7	1	0	1	7	3	10	17	7	24	28	14	42
2002 (Nov 01–Oct 02)	9	3	12	0	0	0	6	4	10	32	10	42	47	17	64
2003 (Nov 02–Oct 03)	5	4	9	1	1	2	6	4	10	24	3	27	36	12	48
2004 (Nov 03–Oct 04)	6	3	9	0	0	0	2	4	6	18	9	27	26	16	42
2005 (Nov 04–Apr 05)*	3	n/a	n/a	0	n/a	n/a	6	n/a	n/a	12	n/a	n/a	21	n/a	n/a
Total	69	28	97	8	4	12	47	31	78	184	68	252	308	131	439

less during TP2. One notable exception was in October 1998, when seven strandings occurred but minimal spiny dogfish landings were reported. Monthly HI-no and HI-other strandings showed no seasonal pattern across months and years (Fig. 3). Monthly HI-CBD strandings, however, showed a similar pattern to HI-FI strandings during TP1 and continued to show some periodicity afterwards, with increases primarily during winter months.

With the UME threshold method, the stranding threshold for HI-FI strandings for the NC winter mixed MU was 2.95. This threshold was exceeded 7 out of 18 months of the winter spiny dogfish fishing seasons during TP1, or 39% of the time (Fig. 4). During TP2, the threshold was exceeded as a result of bycatch in other fisheries in three months, or only 10% of the time: November 2001 from strandings south of Cape Lookout; April 2003 from strandings north of Cape Hatteras, and November 2004 from strandings south of Cape Lookout.

During summer, the stranding threshold produced by the UME threshold method for the northern NC MU was 1.77, and the stranding threshold for the southern NC MU was 2.19. The stranding threshold was exceeded three times for the northern NC MU, once during TP1 in May 1999 (6% of the time; 1 out of 18 months) and twice during TP2 in October 2001 and October 2004 (8% of the time; 2 out of 24 months) (Fig. 4). For the southern NC MU, the stranding threshold was exceeded only once, in October 1998 during TP1 (2% of the time; 1 out of 42 months) (Fig. 4).

With the use of the regression equation, the 68% CI and 95% CI values had wide bounds around the predicted bycatch estimates

Table 2

Mean (standard deviation [SD]) of monthly bottlenose dolphin (*Tursiops truncatus*) strandings by human interaction (HI) categories in the winter (November–April) during time period (TP) 1 (November 1997–October 2000) (n=18) and TP2 (November 2000–April 2005) (n=30). The HI categories are as follows: HI-FI (evidence of fishery interaction), and HI-other (evidence of mutilation, propeller wounds), HI-no (no signs of HI), and HI-CBD (human interaction could not be determined). For this study, data were not available (n/a) for the 2005 summer season (May–October) and thus totals for 2005 are for a partial year, denoted by an asterisk.

HI category	Time period	Mean (SD) per month	P-value
HI-FI	TP1	2.39 (1.72)	*0.001
HI-FI	TP2	0.87 (1.04)	
HI-other	TP1	0.33 (0.69)	0.11
HI-other	TP2	0.07 (0.25)	
HI-no	TP1	1.11 (1.02)	0.54
HI-no	TP2	0.90 (0.80)	
HI-CBD	TP1	4.50 (3.31)	0.16
HI-CBD	TP2	3.43 (2.45)	

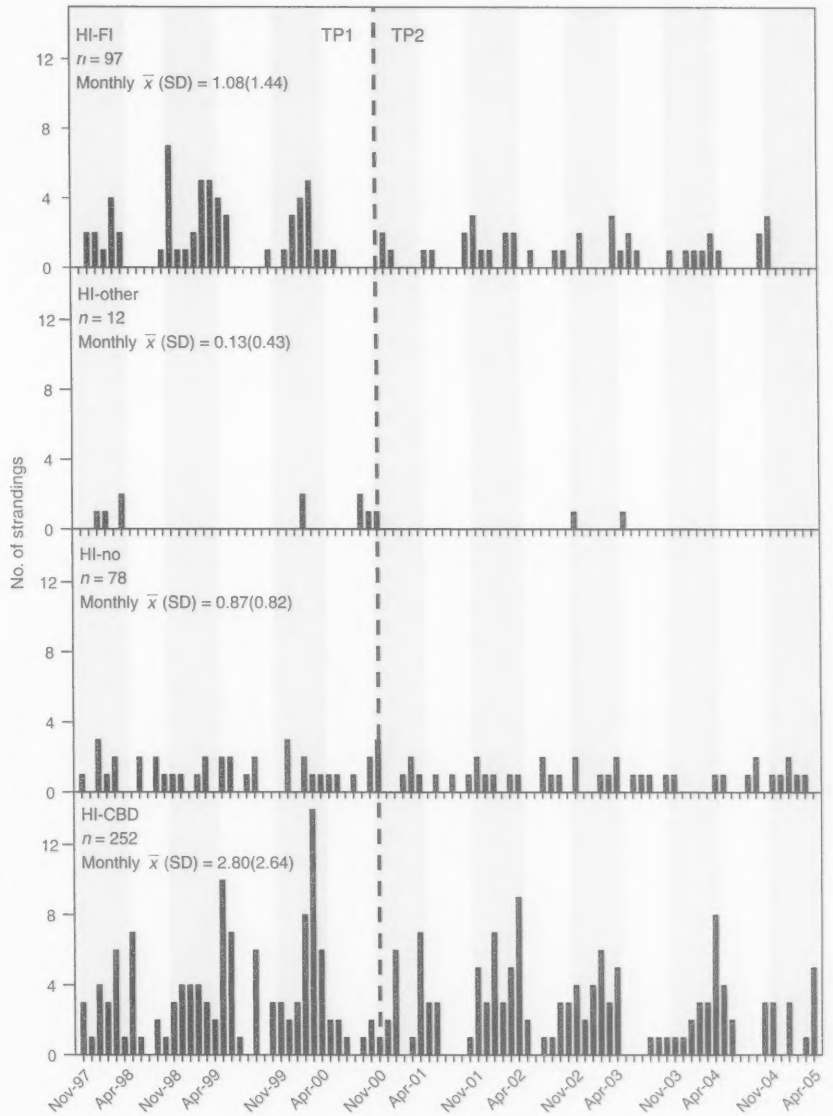

Figure 3

Number (n), mean ($\bar{x}$), and standard deviation (SD) of stranded bottlenose dolphins (*Tursiops truncatus*) recovered per month in North Carolina from November 1997 through April 2005 for each human interaction (HI) category: HI-FI (i.e., evidence of fishery interaction) or HI-other (e.g., evidence of mutilation, propeller wounds), HI-no (i.e., no signs of HI), and HI-CBD (human interaction could not be determined). Shaded areas represent winter months (November–April). The vertical dashed line delineates the two time periods (TPs), TP1 and TP2. Monthly HI-FI strandings increased during winters of TP1, but were more diffuse during TP2. Numbers of stranded dolphins classified as HI-other and HI-no showed little variability among months and years. Numbers of monthly HI-CBD strandings were variable; increased rates were evident generally during winter months.

(Fig. 5). For example, the predicted bycatch for two HI-FI strandings per season was 14 animals, but may have equaled between –23 to 51 animals (68% CI) or –65 to 93 animals (95% CI). The lower CI bounds are negative statistically; however, in reality they cannot be less than the number of HI-FI strandings recovered.

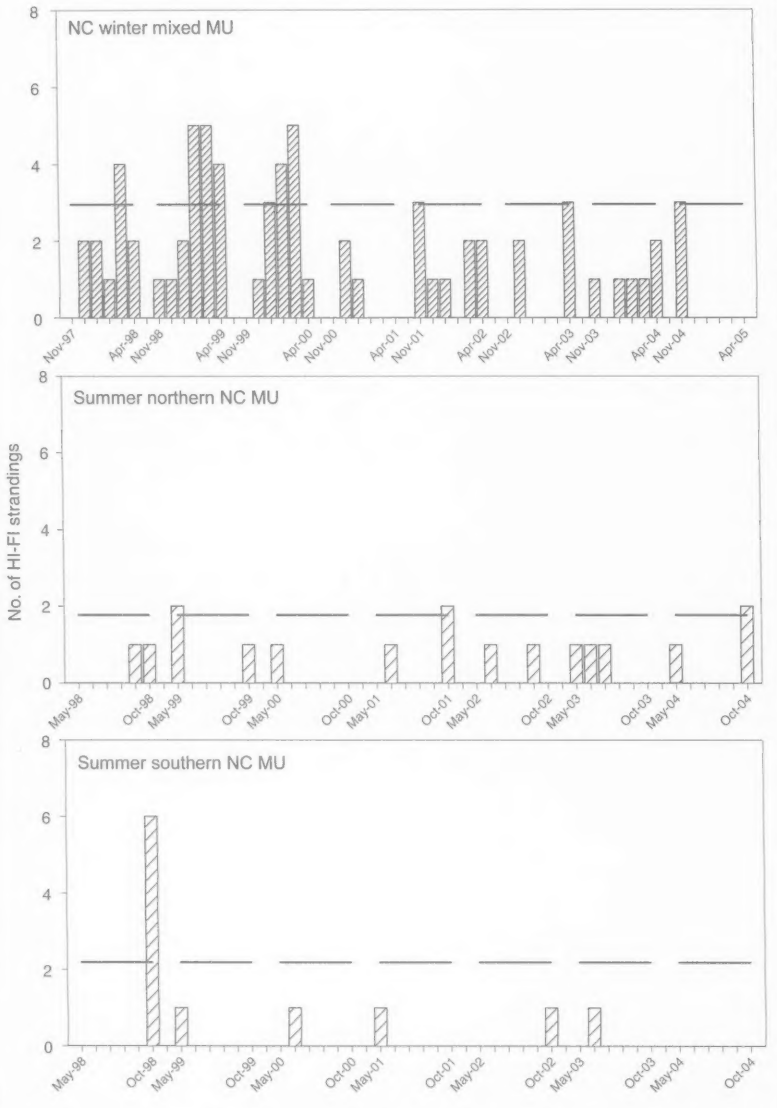

Figure 4

Number of bottlenose dolphin (*Tursiops truncatus*) strandings classified as HI-FI (i.e., having evidence of fishery interaction) per month and the stranding threshold (mean + 2 standard deviations; horizontal dashed lines) by seasonal management unit (MU) in North Carolina (NC). During winter (November–April), the threshold was exceeded seven out of 18 months during time period (TP) 1 and only three out of 30 months during TP2. During summer (May–October), the threshold was exceeded once during TP1 and twice during TP2 for the northern NC MU, and once during TP1 for the southern NC MU. The vertical dashed lines indicate separation between TP1 and TP2.

Discussion

This study provides a unique situation in which three concurrent data sets can be used to test the model of using strandings as an indicator of fishery bycatch. It was demonstrated that fisheries regulations can affect the level of dolphin bycatch mortality and that increases in bycatch mortality can be detected in near real-time by monitoring changes in stranding rates. There was a significant positive correlation between seasonal HI-FI strandings and bycatch estimates of bottlenose dolphins in gill nets. That correlation was mirrored by a marked decrease in winter stranding rates of bottlenose dolphins with entanglement lesions coincident with a marked decrease in the fishing effort for spiny dogfish off NC.

Many factors can influence the rate of deposition of dead dolphins on beaches. For example, the overall increases in the number of strandings during winter compared to summer are likely due, in part, to an increase in local bottlenose dolphin abundance when three MUs overlap off the NC coast (Waring et al., 2006). Within winter, stranding rates of HI-FI strandings were further influenced by changes in fishing effort for spiny dogfish between TP1 and TP2 (Table 2) rather than to changes in environmental factors such as wind direction and currents. This finding was consistent with the reduction in bycatch estimates (Rossman and Palka[1]) and the nonsignificant difference for HI-**no** strandings between the two time periods. There were reductions,

albeit insignificant, in the mean strandings per month for the HI-other and HI-CBD categories between TP1 and TP2. However, stranding rates for these categories could have been influenced by bycatch reductions. All stranded dolphins categorized as HI-other were found either with missing appendages, cuts on the abdomen, or both, but they were too decomposed for a determination of whether or not entanglement lesions were present. Fishermen occasionally cut appendages from a marine mammal to aid in the removal of the animal from their nets, or they slit the abdomen to aid in the sinking of the carcass, or do both (Kuiken et al., 1994; Read and Murray, 2000). It is likely, therefore, that a portion of the HI-other stranded dolphins were indeed entangled in fishing gear because of the mutilations they exhibited. Of the HI-CBD strandings, an unknown proportion was likely caused by fishing interaction, but decomposition obscured evidence of entanglement lesions. Reductions in bycatch would decrease rates of strandings categorized as HI-other and HI-CBD because of the portion of them that were really HI-FI but could not be identified as such.

Because the rate of HI-FI strandings is proportional to the number of bycaught animals, stranding rates may be used as a proxy to detect increases in bycatch mortality and to determine a threshold for triggering a management response. The CI values calculated with the regression analyses were too broad for this method to be useful for setting threshold values even though the *r*-squared (coefficient of determination) value was high (0.79). The UME threshold method proved more useful; the stranding threshold value for the NC winter mixed MU adequately identified elevated stranding levels during months when the spiny dogfish fishery was most active and bycatch levels were highest. Furthermore, with the UME threshold method we were able to identify other periods of elevated strandings during winter and summer.

The stranding thresholds calculated by the UME threshold method, while informative, have some limitations. First, stranding data between October 2002 and April 2005 were included in the calculations, but the corresponding bycatch estimates were not yet available. If new bycatch estimates for that time period exceeded PBR levels, then stranding thresholds would need to be recalculated after eliminating the corresponding stranding data. New thresholds may result in the identification of other months that exceed the revised stranding threshold because the current threshold would be biased upward. Another limitation of a stranding threshold is the level at which increased bycatch is apparent as HI-FI strandings. The bycatch estimate for years with an active spiny dogfish fishery was more than 7.5 times greater than bycatch estimates for years after an active fishery (Rossman and Palka[1]); our method of calculating a threshold may be too conservative in that it may not detect increases in strandings soon enough. Alternative methods to determine thresholds may be more sensitive and could be investigated by using this or a similar data set that has periods of estimated bycatch that are greater and lesser than the PBR level.

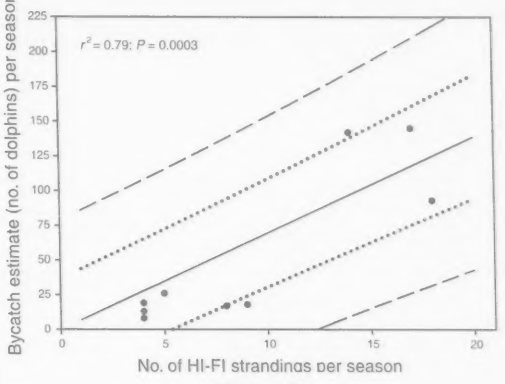

Figure 5

Predicted bycatch (solid line) of bottlenose dolphin (*Tursiops truncatus*) in ocean gill nets, with 95% confidence intervals (CIs; dashed lines) and 68% CIs (dotted lines) by using HI-FI strandings (i.e., having evidence of fishery interaction) per season (winter: November–April, summer: May–October) and their corresponding bycatch estimates from observer data (dots).

Once an appropriate threshold is established and exceeded, a series of response actions can be triggered, as is done for UMEs (Wilkinson, 1996). Most importantly, active fisheries in the area would need to be identified. The possibilities for response actions then would vary from immediately increasing observer coverage in these fisheries to implementing emergency fishing regulations to reduce mortality (MMPA 16 U.S.C. 1387[118]) such as gear modifications, time and area closures, or limited soak durations. The advantage of an increase in observer coverage is to not only increase the precision of the bycatch estimate but to also document fishing practices and determine if practices have changed in a way that may be affecting the level of bycatch.

Stranding data provide valuable information about fisheries bycatch if there is consistent, thorough determination of human interaction and comprehensive coverage of shorelines to establish baseline data and to detect changes. For example, stranding data have served as indicators of bycatch in fisheries that do not have federal observer coverage, such as crab-pot, stop-net, pound-net, and inshore gillnet fisheries (Steve et al., 2001; Waring et al., 2002).

Additionally, stranding data provide additional information about bycatch in gillnet fisheries that have low observer coverage. Although observers have not documented a bottlenose dolphin entanglement in the gillnet fishery for spot (FAO name: spot croaker; *Leiostomus xanthurus*), stranding data indicated that bycatch had occurred. In 1997 and 1998, more than 50% of

stranded bottlenose dolphins that were found spatially and temporally concurrent with the spot fishery exhibited entanglement lesions (Friedlaender et al., 2001). In the current study, stranding thresholds were exceeded twice coincident in time (October and November) and place (south of Cape Lookout) with the typical gillnet season for spot (Steve et al., 2001), spanning both MU seasons. The disparity between bycatch and stranding data likely is due, in part, to low observer effort in nearshore waters of southern NC where the spot fishery is most active (Rossman and Palka[1]). In 2006, NMFS implemented an Alternative Platform Observer Program in NC whereby observers use an independent vessel to find and observe gill nets fished from small boats, which are commonly used in nearshore waters (Kolkmeyer et al., 2007) but difficult for traditional observers to get onboard. There is no observer program, however, for recreational gill nets, which are not regulated by the MMPA (MMPA 16 U.S.C. 1362[20]) but are commonly used in NC to target spot (NCMFC, 2003); thus, it is not known if or at what level bycatch occurs in the recreational fishery. Given the rate of HI-FI strandings, it is reasonable to assume that the PBR level was approached or exceeded because of mortality in the spot fishery during some years. However, one importance of a threshold value is to represent periods when fishery-related mortality does not exceed levels the population can sustain (i.e., PBR levels). In the case of the spot fishery, it is likely that the threshold values used in the present study are too high. Establishing threshold values is an iterative process, whereby values are adjusted according to changes in either PBR or bycatch estimates.

Management actions for the spiny dogfish fishery had unintentional but beneficial consequences on the bycatch of bottlenose dolphins. State and federal regulations severely decreased fishing effort off the NC coast (Federal Register, 2000b; ASMFC[2]), essentially closing the NC fishery in November 2000. For the 2003–04 season, NC was allowed a 227-t quota of spiny dogfish from state waters, about 7% of the average annual landings in NC before November 2000. Fishing effort occurred almost exclusively in January and February of 2004. Only two HI-FI stranded dolphins occurred in these months, one of which was wrapped in a large-mesh gill net (20.3-cm stretch mesh) more indicative of the striped bass (*Morone saxatilis*) fishery than spiny dogfish fishery (Steve et al., 2001). No bycatch was reported by federal observers on fishing vessels during the 2003–04 spiny dogfish fishery off NC (Rossman and Palka[1]). The soak times were shorter in the 2003–04 season than during previous years (Rossman and Palka[1]) due to trip limits imposed by the NCDMF and these likely contributed to a lower bycatch rate. Quota shares were not allocated on a state-by-state basis for the next fishing year (May 2004–April 2005) (ASMFC[2]) and, as a result, landings of spiny dogfish in NC were almost nonexistent.

Independently, managers enacted fisheries regulations for spiny dogfish that inadvertently decreased bottlenose dolphin bycatch. The opposite situation conceivably could occur; that is, fisheries regulations could alter fishing practices or effort in a manner that could increase dolphin bycatch. Gillnetters in NC are dynamic, altering their fishing practices in response to a variety of factors including changes in fishery regulations (Steve et al., 2001). Thus, researchers and managers need to be proactive, working towards managing species as an interrelated community and considering how regulations for one species may affect others.

These analyses indicate that, at least in some situations, strandings can serve as a near real-time indicator of fishery bycatch. Absolute estimates of bycatch mortality must be obtained using observer data, but the multi-year time lag associated with obtaining those estimates prevents real-time mitigation of that mortality. Near real-time detection of increased bycatch can also be used to direct observer effort to areas of potentially high bycatch. Thus, observer coverage and stranding investigations can be used in concert for more effective management.

Acknowledgments

We are grateful for the dedicated participants in the North Carolina Marine Mammal Stranding Network. We also thank the North Carolina Division of Marine Fisheries, Statistics Division, for providing NC fisheries data and P. Rosel (National Marine Fisheries Service [NMFS], Southeast Fisheries Science Center [SEFSC], Layfayette, LA) for providing results for the stranding database on the six strandings genetically confirmed as the offshore morphotype. L. Hansen, M. Prager, and D. Vaughan (NMFS/SEFSC, Beaufort, NC), M. Rossman (NMFS/Northeast Fisheries Science Center, Woods Hole, MA), M. Scott (Inter-American Tropical Tuna Commission, La Jolla, CA), and three anonymous reviewers provided thoughtful comments on the manuscript. E. Griffith (contract employee with NMFS/SEFSC) assisted with statistical analyses.

Literature cited

Barlow, J., S. L. Swartz, T. C. Eagle, and P. R. Wade.
1995. U.S. Marine Mammal Stock Assessments: Guidelines for Preparation, Background, and a Summary of the 1995 Assessments. NOAA Tech. Memo. NMFS-OPR-95-6, 73 p.

Caillouet, C. W., Jr., M. J. Duronslet, A. M. Landry Jr., D. B. Revera, D. J. Shaver, K. M. Stanley, R. W. Heinly, and E. K. Stabenau.
1991. Sea turtle strandings and shrimp fishing effort in the northwestern Gulf of Mexico, 1986–89. Fish. Bull. 89:712–718.

Edwards, E. F., and C. Perrin.
1993. Effects of dolphin group type, percent coverage, and fleet size on estimates of annual dolphin mortality derived from 1987 U.S. tuna-vessel observer data. Fish. Bull. 91:628–640.

Epperly, S. P., J. Braun, A. J. Chester, F. A. Cross, J. V. Merriner, and P. A. Tester.
1995. Winter distribution of sea turtles in the vicinity of Cape Hatteras and their interactions with the summer flounder trawl fishery. Bull. Mar. Sci. 56:547–567.

Epperly, S. P., J. Braun, A. J. Chester, F. A. Cross, J. V. Merriner, P. A. Tester, and J. H. Churchill.
1996. Beach strandings as an indicator of at-sea mortality of sea turtles. Bull. Mar. Sci. 59:289–297.

Federal Register.
1998. Magnuson-Stevens Act provisions; overfished fishery for spiny dogfish. Notification of an overfished fishery. Federal Register 63(69):17820–17821. Office of the Federal Register, National Archives and Records Administration (NARA), College Park, MD.
2000a. Fisheries of the northeastern United States; spiny dogfish fishery management plan. Final rule. Federal Register 65(7):1557–1571. Office of the Federal Register, NARA, College Park, MD.
2000b. Fisheries of the northeastern United States; spiny dogfish fishery. 2000 specifications. Interim final rule. Federal Register 65(87):25887–25891. Office of the Federal Register, NARA, College Park, MD.

Fernandez, S., and A. A. Hohn.
1998. Age, growth, and calving season of bottlenose dolphins, *Tursiops truncatus*, off coastal Texas. Fish. Bull. 96:357–365.

Forney, K. A., S. R. Benson, and G. A. Cameron.
2001. Central California gillnet effort and bycatch of sensitive species, 1990–1998. *In* Seabird bycatch: trends, roadblocks, and solutions (E. F. Melvin, and J. K. Parrish, eds.), p. 141–160. Univ. Alaska Sea Grant College Program, Fairbanks, AK.

Friedlaender, A. S., W. A. McLellan, and D. A. Pabst.
2001. Characterising an interaction between coastal bottlenose dolphins (*Tursiops truncatus*) and the spot gillnet fishery in southeastern North Carolina, USA. J. Cetacean Res. Manag. 3:293–303.

Hoelzel, A. R., C. W. Potter, and P. B. Best.
1998. Genetic differentiation between parapatric 'nearshore' and 'offshore' populations of the bottlenose dolphin. Proc. R. Soc. Lond. 265:1177–1183.

Hohn, A. A.
1980. Age determination and age related factors in the teeth of western north Atlantic bottlenose dolphins. Sci. Rep. Whales Res. Inst. 32:39–66.

Kolkmeyer, T., B. Guthrie, B. L. Byrd, and A. A. Hohn.
2007. Report on the alternative platform observer program in North Carolina: March 2006 to March 2007. NOAA Tech. Memo. NMFS-SEFSC-558, 20 p.

Kuiken, T., V. R. Simpson, C. R. Allchin, P. M. Bennett, G. A. Codd, E. A. Harris, G. H. Howes, S. Kennedy, J. K. Kirkwood, R. J. Law, N. R. Merrett, and S. Phillips.
1994. Mass mortality of common dolphins (*Delphinus delphis*) in south west England due to incidental capture in fishing gear. Vet. Rec. 134:81–89.

Mead, J. G., and C. W. Potter.
1995. Recognizing two populations of the bottlenose dolphin (*Tursiops truncatus*) off the Atlantic coast of North America: Morphological and ecological considerations. Int. Mar. Biolog. Res. Inst. Rep. 5:31–44. National Museum of Natural History, Smithsonian Institution, Washington, DC.

NCMFC (North Carolina Marine Fisheries Commission).
2003. North Carolina fisheries rules for coastal waters, 297 p. North Carolina Department of Environment and Natural Resources, North Carolina Division of Marine Fisheries, Morehead City, NC.

Read, A. J., and K. T. Murray.
2000. Gross evidence of human-induced mortality in small cetaceans. NOAA Tech. Memo. NMFS-OPR-15, 21 p.

Salzman, J. E.
1989. Scientists as advocates: the Point Reyes Bird Observatory and gill netting in central California. Conserv. Biol. 3:170–180.

Steve, C., J. Gearhart, D. Borggaard, L. Sabo, and A. A. Hohn.
2001. Characterization of North Carolina commercial fisheries with occasional interactions with marine mammals. NOAA Tech. Memo. NMFS-SEFSC-458, 57 p.

Thayer, V. G., A. J. Read, A. S. Friedlaender, D. R. Colby, A. A. Hohn, W. A. McLellan, D. A. Pabst, J. L. Dearolf, N. I. Bowles, J. R. Russell, and K. A. Rittmaster.
2003. Reproductive seasonality of western Atlantic bottlenose dolphins off North Carolina, USA. Mar. Mamm. Sci. 19:617–629.

Waring, G. T., E. Josephson, C. P. Fairfield, and K. Maze-Foley (eds.).
2006. Bottlenose dolphin (*Tursiops truncatus*): western North Atlantic coastal stock. *In* U.S. Atlantic and Gulf of Mexico marine mammal stock assessments—2005. NOAA Tech. Memo. NMFS-NE-194, p. 89–99.

Waring, G. T., D. L. Palka, P. J. Clapham, S. Swartz, M. C. Rossman, T. V. N. Cole, L. J. Hansen, K. D. Bisack, K. D. Mullin, R. S. Wells, D. K. Odell, and N. B. Barros.
1999. Bottlenose dolphin (*Tursiops truncatus*): western North Atlantic coastal stock. *In* U.S. Atlantic and Gulf of Mexico marine mammal stock assessments—1999, p. 128–135. NOAA Tech. Memo. NMFS-NE-153, 187 p.

Waring, G. T., D. L. Palka, K. D. Mullin, J. H. W. Hain, L. J. Hansen, and K. D. Bisack.
1997. Bottlenose dolphin (*Tursiops truncatus*): western North Atlantic coastal stock. *In* U.S. Atlantic and Gulf of Mexico marine mammal stock assessments—1996. NOAA Tech. Memo. NMFS-NE–114, p. 128–133.

Waring, G. T., J. M. Quintal, and C. P. Fairfield (eds.).
2002. Bottlenose dolphin (*Tursiops truncatus*): western North Atlantic coastal stock. *In* U.S. Atlantic and Gulf of Mexico marine mammal stock assessments—2002. NOAA Tech. Memo. NMFS-NE-169, p. 169–180.

Wilkinson, D. M.
1996. National contingency plan for response to unusual marine mammal mortality events. NOAA Tech. Memo. NMFS-OPR-9, 188 p.

Age, growth, and reproduction of dolphinfish (*Coryphaena hippurus*) caught off the coast of North Carolina

Kara L. Schwenke (contact author)
Jeffrey A. Buckel

Email address for K. L. Schwenke: Kara.Schwenke@noaa.gov

Department of Zoology
Center for Marine Sciences and Technology
North Carolina State University
303 College Circle
Morehead City, North Carolina 28557

Present address (for K. L. Schwenke): National Ocean Service (NOS)
National Oceanic and Atmospheric Administration (NOAA)
1305 East West Highway
Silver Spring, Maryland 20910

Abstract—Age, growth, and reproductive data were obtained from dolphinfish (*Coryphaena hippurus*, size range: 89 to 1451 mm fork length [FL]) collected between May 2002 and May 2004 off North Carolina. Annual increments from scales (n=541) and daily increments from sagittal otoliths (n=107) were examined; estimated von Bertalanffy parameters were L_∞ (asymptotic length)=1299 mm FL and k (growth coefficient)=1.08/yr. Daily growth increments reduced much of the residual error in length-at-age estimates for age-0 dolphinfish; the estimated average growth rate was 3.78 mm/day during the first six months. Size at 50% maturity was slightly smaller for female (460 mm FL) than male (475 mm FL) dolphinfish. Based on monthly length-adjusted gonad weights, peak spawning occurs from April through July off North Carolina; back-calculated hatching dates from age-0 dolphinfish and prior reproductive studies on the east coast of Florida indicate that dolphinfish spawning occurs year round off the U.S. east coast and highest levels range from January through June. No major changes in length-at-age or size-at-maturity have occurred since the early 1960s, even after substantial increases in fishery landings.

Manuscript submitted 21 February 2007.
Manuscript accepted 6 November 2007.
Fish. Bull. 106:82–92 (2008).

The views and opinions expressed or implied in this article are those of the author and do not necessarily reflect the position of the National Marine Fisheries Service, NOAA.

The dolphinfish (*Coryphaena hippurus*) is a highly migratory oceanic pelagic fish found worldwide in tropical and subtropical waters. The distribution range for dolphinfish in the western Atlantic Ocean is from Nova Scotia (Vladykov and McKenzie, 1935; Tibbo, 1962) to Brazil (Shcherbachev, 1973). However, this species is most common from North Carolina, throughout the Gulf of Mexico and Caribbean, to the northeastern coast of Brazil where it is seasonally abundant (Oxenford, 1999). Dolphinfish support economically important recreational and commercial fisheries in the United States, Caribbean, and Brazil, and is thus a shared resource among multiple countries. Previous reviews of the scientific literature on dolphinfish biology in the western Atlantic were completed by Palko et al. (1982) and Oxenford (1999).

Landings of dolphinfish from the Atlantic, Caribbean, and Gulf of Mexico have increased. According to the National Marine Fisheries Service landings statistics, recreational landings in the Atlantic Ocean have increased gradually, whereas commercial landings in the Atlantic have increased dramatically from approximately 20 metric tons (t) in the 1980s to over 620 t in the 1990s. Although dolphinfish are fast growing and mature early, concern has been raised about this trend in landings and the potential for localized depletion of stocks. Intense harvesting may select for traits such as slow growth (Conover and Munch, 2002) or early maturity (Trippel, 1995); it is important to update growth and reproductive data to test for changes in these data and to provide current information for stock assessments. Unfortunately, the most recent estimates of these parameters for dolphinfish in the southeast United States were based on data from the 1960s (Beardsley, 1967; Rose and Hassler, 1968).

Here, we update the age and growth relationship and collect reproductive data on dolphinfish captured in North Carolina from recreational and commercial sources and fishery-independent collections. Our specific objectives were 1) to determine daily ages of age-0 dolphinfish and determine age-0 dolphinfish growth rates, 2) to identify the best method of aging >age-0 dolphinfish (either by otolith or scale annual marks) and, with the method determined to be the best, to determine the annual ages of >age-0 dolphinfish, 3) to validate annual marks, and 4) to estimate time of spawning and size-at-maturity.

Materials and methods

Collections

Dolphinfish from recreational fishery sources were obtained every month between May 2002 and May 2004 (except December 2002 and 2003, January 2003, and February 2004) from fishing ports in North Carolina. Recreational anglers typically fished for dolphinfish in waters associated with the western wall of the Gulf Stream. In the summers of 2002–03, samples of large fish were provided through various sportfishing tournaments held in these same areas. To supplement length-at-maturity data once peak spawning was identified, maturity staging was conducted on male and female dolphinfish from April 2005 through July 2005.

Sampling of commercial dolphinfish catches was done in addition to recreational dolphinfish sampling and was primarily conducted in the winter months to increase the sample sizes available for this time period. Small dolphinfish were not readily available through recreational and commercial sampling; therefore sample sizes were augmented by two different methods. First, a total of four fishery-independent trips were made in August 2003 and July 2004. During these trips, the distance traveled offshore averaged 20 km, and small lures were trolled, as opposed to large dead bait or large lures as is done in the recreational and commercial fishery. Second, small and intact dolphinfish were obtained from stomachs of larger dolphinfish and yellowfin tuna (*Thunnus albacares*) caught by anglers from recreational charter boats.

Dolphinfish were measured to the nearest mm for fork length (FL) and total length (TL), sex was determined (through macroscopic examination of the gonads), and the fish were weighed (to the nearest 0.1 kg) and tagged. Date and location of port sampled were recorded for each dolphinfish. Scale samples were collected before the fish were filleted according to methods established by Beardsley (1967). In some instances, filleted dolphinfish carcasses were only available; therefore scale samples were not obtained on all sampled fish. All tagged carcasses were brought to the laboratory for extraction of otoliths and gonads.

Age and growth

To determine if daily rings were present on sagittal otoliths of age-0 dolphinfish, the otoliths were removed, cleaned, and stored dry until mounted in epoxy resin. To avoid interotolith variability, only the left otolith was used for reading. Otoliths were prepared for reading following methods described for transverse sections in Secor et al. (1992). Reading was done with a light microscope equipped with a digital camera. The image from the camera was transmitted to a computer and examined by using Image-Pro Plus software (Image-Pro, vers. 4.5, Media Cybernetics, Silver Spring, MD). Growth increments were counted from the core, beginning at the first clearly defined mark that encircled the primordium (Massutí et al., 1999), towards either the dorsal or ventral edge, depending on ease of counting. To determine the precision of the readings of juvenile dolphinfish ages, blind readings of daily growth increments were conducted twice by the same investigator. Error greater than 10% in reading precision for an individual otolith caused that otolith to be rejected. If error in reading precision was less than or equal to 10%, then the average between the first and second readings was taken as the final age.

The deposition of increments in dolphinfish otoliths begins on the hatching date, and rings are laid down daily (Uchiyama et al., 1986; Massutí et al., 1999). Thus, no adjustment was required to estimate age from incremental counts of sagittae, and it was assumed that rings were formed daily. Previous studies on the microstructure of sagittal otoliths of dolphinfish from the western Mediterranean Sea had found that the daily ages from larger dolphinfish (>650 mm FL) appeared to be underestimated (Massutí et al., 1999). Furthermore, daily ages of dolphinfish have been validated to a size of 554 mm FL (Uchiyama et al., 1986). Therefore, our analysis was restricted to dolphinfish less than or equal to 650 mm FL. To determine individual dolphinfish growth rates, the fork length at capture was divided by the daily age.

The annual age of dolphinfish was estimated with scales. Eight to ten scales were mounted, sculptured side down, on sheets of cellulose acetate 0.5 mm thick, and then placed on a scale press to make impressions. Scale impressions were examined with a microfiche reader at 32× magnification to permit detection of circuli, annual marks, and other features of the scale. Age groups were classified according to the number of annual marks present (see Beardsley, 1967, for a figure of an annual mark on a dolphinfish scale).

To determine the precision of dolphinfish age estimates, blind readings of annual marks on scales were conducted twice by the same investigator. If agreement between the first and second reading was not 100%, then a scale was reread a third time and was only used in the analyses if the third reading agreed with either the first or second reading. Additionally, blind readings of a subsample (n=50) of dolphinfish scales were conducted by an independent reader who was trained to identify annual marks on dolphinfish scales.

To validate annual marks in dolphinfish scales, an indirect validation based on marginal increment analysis was used. Marginal increment widths were determined by measuring the distance from the outer edge of the scale to the closest annual mark. Marginal increment width was measured only on dolphinfish with one annual mark in order to standardize the method, and because the majority of dolphinfish aged with annual marks were age-1. Measurements (mm) were taken from the magnified (32×) scale image on a microfiche reader along a straight line from the lateral edge of the scale to the outermost annual mark by using a digital caliper. Marginal increment widths were analyzed by analysis of variance (ANOVA) to test for an effect of month.

Marginal increment widths were only analyzed for the months of March through November because of the low sample sizes of dolphinfish scales from the winter months (December through February). To differentiate between changes in the marginal increment width attributed to potentially sampling different cohorts of age-1 dolphinfish, we calculated the monthly mean fork length of all age-1 dolphinfish whose scales were measured for a marginal increment width.

A subsample (n=50) of dolphinfish that was determined to be >age-0 by using scales was further examined for the presence of annual marks by using otoliths. We prepared transverse cross sections of sagittal otoliths using methods described above. These sections were viewed under the light microscope (first at 100×, then 400×) to determine if annual marks could be detected in these structures.

The von Bertalanffy growth curve was fitted to two dolphinfish age-length data sets: 1) daily ages from age-0 dolphinfish with a fork length less than 650 mm and annual marks on scales from >age-0 dolphinfish by using absolute ages, and 2) daily ages from age-0 dolphinfish with a fork length less than 650 mm and relative scale ages. Relative scale ages were assigned by adding the number of days after the fixed birth date of 15 April (middle of estimated southeastern U.S. spawning season) when the dolphinfish was caught to the absolute annual age determined from scales. The 15 April birth date was chosen according to the trends in gonadosomatic indices in Florida and North Carolina and back-calculated hatching dates (Beardsley, 1967; this study).

The von Bertalanffy growth parameters were estimated separately by nonlinear regression for male and female dolphinfish and were compared by using the likelihood-ratio test (Kimura, 1980; Cerrato, 1990; Haddon, 2001). To detect if any significant changes in growth had occurred since the last dolphinfish aging study in North Carolina, the mean size-at-age values from Rose and Hassler (1968) were plotted with the von Bertalanffy growth curve fit (relative age data set) and compared qualitatively. Additionally, von Bertalanffy growth functions estimated from past studies within different regions were plotted together for comparison.

Reproduction

Gonadosomatic indices and back-calculated hatching dates were used to determine timing of spawning, and maturity staging was used to determine length-at-maturity. When available, intact gonads were removed, weighed to the nearest 0.1 g, and assigned a maturity stage determined by gross examination of the gonads. Maturity stages for both male and female dolphinfish have been described (Beardsley, 1967; Oxenford, 1985). Female dolphinfish were considered mature or immature on the basis of the criteria developed by Beardsley (1967). Male dolphinfish were classified as mature on the basis of the presence or absence of milt in their gonads.

A gonadosomatic index (GSI) was calculated as *gonad weight*/(*body weight* – *gonad weight*) separately for male and female dolphinfish pooled for 2002–04. Because dolphinfish body weight and length are correlated with GSI values (Chatterji and Ansari, 1982) and dolphinfish size differed significantly by month (see below), ANCOVA was used to compare *ln* (*gonad weight*) by month with *ln* (*fork length*) as the covariate for males and females separately. Log transformations were used to meet assumptions of ANCOVA. To determine which months had significantly different gonad weights, the length-adjusted mean *ln* (*gonad weight*) value was compared among months for both male and female dolphinfish by using ANCOVA univariate test of significance for planned comparisons. Significance levels were adjusted by the standard Bonferroni technique to account for multiple comparisons.

Hatching dates were determined by subtracting age in days (determined from age-0 otoliths) from the catch date. Because the daily deposition of increments in dolphinfish sagittal otoliths begins on the hatching date (Uchiyama et al., 1986; Massutí et al., 1999), and because ripe eggs hatch within 50–60 hours after fertilization (Palko et al., 1982), back-calculated hatching dates provide an estimate of spawning dates for surviving offspring.

The length at which 50% of the fish had become mature was determined for both sexes by using a logistic model. The model was fitted by using nonlinear regression analysis based on the following equation:

$$\%\ Maturity = 1/(1 + e^{(-Q \times (L - L_{50}))}),$$

where Q = model parameter;
L = fork length (mm); and
L_{50} = fork length (mm) at 50% maturity.

Results

Collections

Dolphinfish were collected mostly from the recreational charter fishery (n=611, 76%), but also from the commercial fishery (n=45, 6%), sportfishing tournaments (n=130, 16%), and from four fishery-independent trips (n=16, 3%). There was a seasonal trend in the total amount (number) of dolphinfish collected by month, with nearly half (n=364, 45%) of all dolphinfish collected in the months of June, July, and August. Only 17 fish (2%) were obtained in the months of November, December, and January (Table 1). The majority of the dolphinfish were sampled from catches in Morehead City, NC (n=676, 84%).

The size range for the pooled sample of dolphinfish was 89 to 1451 mm FL (mean=736 mm FL, standard error (SE)=9.3). Males (n=257) ranged in length from 310 to 1451 mm FL (mean length and weight of all males sampled was 855 mm FL [SE=16.0] and 6.44 kg [SE=0.4]) and females (n=422) ranged in length

Table 1

Monthly mean (±SE) fork length (FL; mm), FL range, and sample size (n) for male and female dolphinfish (*Coryphaena hippurus*) collected from May 2002 through May 2004. Sex was unable to be determined for six dolphinfish and their size information is not shown here. No dolphinfish were caught in December. SE=standard error.

	Male			Female		
	Mean FL (SE)	FL range	n	Mean FL (SE)	FL range	n
January	682 (81.1)	559–835	3	708 (70.3)	575–966	5
February	—	—	0	699 (62.4)	545–850	4
March	709 (61.3)	453–915	6	730 (17.9)	560–889	20
April	820 (26.1)	550–1130	24	773 (12.1)	608–1020	50
May	935 (17.4)	582–1315	92	765 (14.2)	485–1275	101
June	1123 (25.4)	552–1395	72	688 (31.8)	295–1145	43
July	705 (50.9)	395–1451	31	607 (25.5)	205–980	48
August	805 (41.5)	310–1333	46	650 (24.1)	295–1205	101
September	689 (51.0)	462–1280	16	510 (19.8)	278–800	40
October	594 (25.6)	432–798	17	556 (26.1)	410–1435	41
November	570 (50.0)	520–620	2	628 (60.7)	460–905	7

from 205 to 1435 mm (mean length and weight of all females sampled was 655 mm FL [SE=9.0] and 3.13 kg [SE=0.2]; Table 1). There were significant differences in male dolphinfish mean weight (Kruskal-Wallis ANOVA: χ^2=80.6, df=9, P<0.001) and fork length (χ^2=98.9, df=9, P<0.001) by month (pooled over 2002–04). There were also significant differences in the mean weight of female dolphinfish (Kruskal-Wallis ANOVA: χ^2=85.1, df=9, P<0.001) and fork length (χ^2=140.0, df=10, P<0.001) by month (pooled over 2002–04).

Age and growth

Because of the small size and complex structure of dolphinfish sagittae, counts were typically made on the dorsal side of the otolith as that region was the easiest to follow a clear increment sequence (Massutí et al., 1999). Alternating light and dark bands, assumed to be daily increments (see Methods section), varied in width; tightly packed increments were located more toward the core and outer edge of the sagittae, and wider increments were located more in the center of the dorsal wing (see Massutí et al., 1999, for a picture of growth increments).

A total of 181 dolphinfish otoliths were examined (n=131 age-0 otoliths, n=50 >age-0 otoliths). Annual marks could not be detected in transverse cross-sections of sagittal otoliths of >age-0 dolphinfish. Daily increment counts were possible for a total of 107 (82%) otoliths from age-0 dolphinfish (designated age-0 because of a lack of annual marks on scales [see below]). Of these, 62 were from female dolphinfish (mean FL=509; range: 278–650 mm) and 39 were from males (mean FL=538; range: 310–650 mm). Sex could not be determined for five of the smallest dolphinfish whose sagittae were examined (mean FL=152; range: 89–285 mm) and was not recorded for one of the larger dolphinfish aged from daily growth increments (FL=575 mm); however, these dolphinfish were still used in the von Bertalanffy analyses. Four of the 131 otoliths from age-0 dolphinfish were rejected because percent agreement between the first and second count exceeded 10%, and 20 age-0 otoliths were unreadable because of problems with cross-sectioning or polishing. Minimum and maximum age estimates ranged from 31 to 204 days. Average growth rates based on daily ring counts were 3.78 mm FL/day for all age-0 fish less than 650 mm FL.

Scales were collected from 560 fish; 14 of the resulting scale impressions were unreadable and five more were discarded because of uncertainty in the determination of age (i.e., the three counts did not agree with each other). A total of 234 scales were classified as age-1 or older (84 females, 150 males) and the remaining scales (n=307) were estimated to be age-0. The >age-0 dolphinfish were classified as follows: 175 age-1 dolphinfish ranging from 575 to 1435 mm FL (mean=938 mm, SE=9.8), 46 age-2 dolphinfish ranging from 925 to 1451 mm FL (mean=1197 mm, SE=17.3), and 13 age-3 dolphinfish ranging from 1095 to 1334 mm FL (mean=1249 mm, SE=17.9). Final agreement between readings by the same investigator was 99%; an independent reader who was trained to identify annual marks on dolphinfish scales examined a subsample of 50 >age-0 dolphinfish scales, and agreement between the independent reader's reading and the first reader's final age was 69% (Schwenke, 2004).

Marginal increment widths from age-1 dolphinfish (n=182) were greatest in May, June, and July, dropped slightly in August, then dropped considerably during

Table 2

Von Bertalanffy growth parameters calculated for male, female, and combined sexes (including individuals whose sex could not be determined) of dolphinfish (*Coryphaena hippurus*) from nonlinear regression model fits. Data are presented for (**A**) daily ages of otoliths (from dolphinfish <650 mm) along with annual ages of >age-0 dolphinfish presented as absolute ages, and (**B**) daily aged otoliths (from dolphinfish <650 mm) along with annual ages of >age-0 dolphinfish presented as relative ages, assuming a 15 April hatching date. The standard errors of each parameter are shown in parentheses. n=sample size, L_∞=asymptotic length, k=growth coefficient, and t_0=theoretical age at zero length.

Method	n	$L_{\infty\,(\mathrm{mm})}$	k (1/yr)	$t_{0\,(\mathrm{yr})}$
A Otoliths (<650 mm) aged daily and scales aged yearly (absolute ages)				
Males	189	1286 (29.10)	1.33 (0.12)	−0.016 (0.04)
Females	146	1250 (109.60)	1.24 (0.28)	−0.059 (0.05)
Combined sexes	341	1289 (25.95)	1.27 (0.08)	−0.026 (0.02)
B Otoliths (<650 mm) aged daily and scales aged yearly (in relation to a 15 April hatching date)				
Males	188	1299 (30.80)	1.12 (0.11)	−0.089 (0.05)
Females	145	1237 (92.14)	1.10 (0.23)	−0.116 (0.06)
Combined sexes	339	1299 (26.31)	1.08 (0.07)	−0.086 (0.03)

the fall, and stayed low during winter months (Fig. 1). There was a significant difference in marginal increment width per month (ANOVA: P=<0.001) for the period of March through November. Mean marginal increment width in May was significantly higher than in April (Tukey HSD: P=0.03) and October (P=0.03), whereas in June, it was significantly higher than in April (P<0.001), September (P=0.04), and October (P<0.001). All other comparisons were nonsignificant.

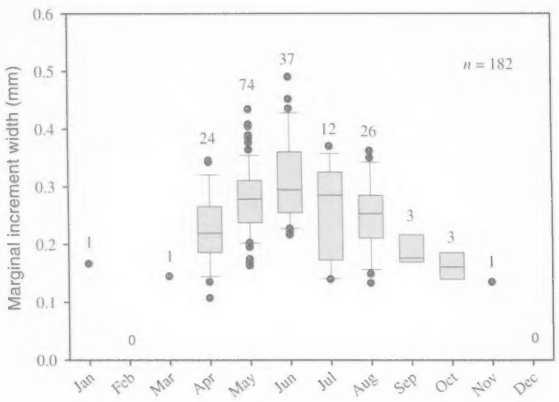

Figure 1

Box plot of the marginal increment width (mm) for age-1 dolphinfish (*Coryphaena hippurus*) (sampled from May 2002 through May 2004) pooled by month (January–December). The 25th percentile of the marginal increment width data is represented by the boundary of the box closest to zero, relative to the y-axis, and the 75th percentile is represented by the boundary of the box farthest from zero. The line within each box is the median value. Whiskers (error bars) above and below the boxes indicate the 90th and 10th percentiles, respectively. Outlying values for both upper and lower ranges are represented by closed circles. Sample sizes are given above the box for each month.

Growth rates of dolphinfish are extremely fast during their first year and their maximum longevity is only three years (Fig. 2A). Female dolphinfish appeared to have a slower growth and shorter longevity than male dolphinfish; only three female dolphinfish reached age 2. However, there was no significant difference between the male and female von Bertalanffy growth models (likelihood ratio tests: χ^2=6.52, df=3, P=0.08).

The growth model fitted the relative age data well (under the assumption of a biological hatching date of 15 April) for >age-0 dolphinfish. However, the sizes of age-0 dolphinfish (where age was estimated by using annual marks on scales) at their relative age (Fig. 2B) did not show good agreement with size-at-age based on daily ages determined from otoliths. Thus, a combination of otolith-based daily ages for age-0 dolphinfish and scale-based relative ages for >age-0 dolphinfish were used when fitting a second von Bertalanffy growth model. The second von Bertalanffy growth function showed that males grow faster and reach a larger maximum size than females (likelihood ratio test: χ^2=10.14, df=3, P=0.02) (Fig. 2C; Table 2). By using a biological hatching date, the combined sexes model fit was improved from an r^2 of 0.67 to an r^2 of 0.73. The mean length-at-age values for dolphinfish collected in June, July, and August

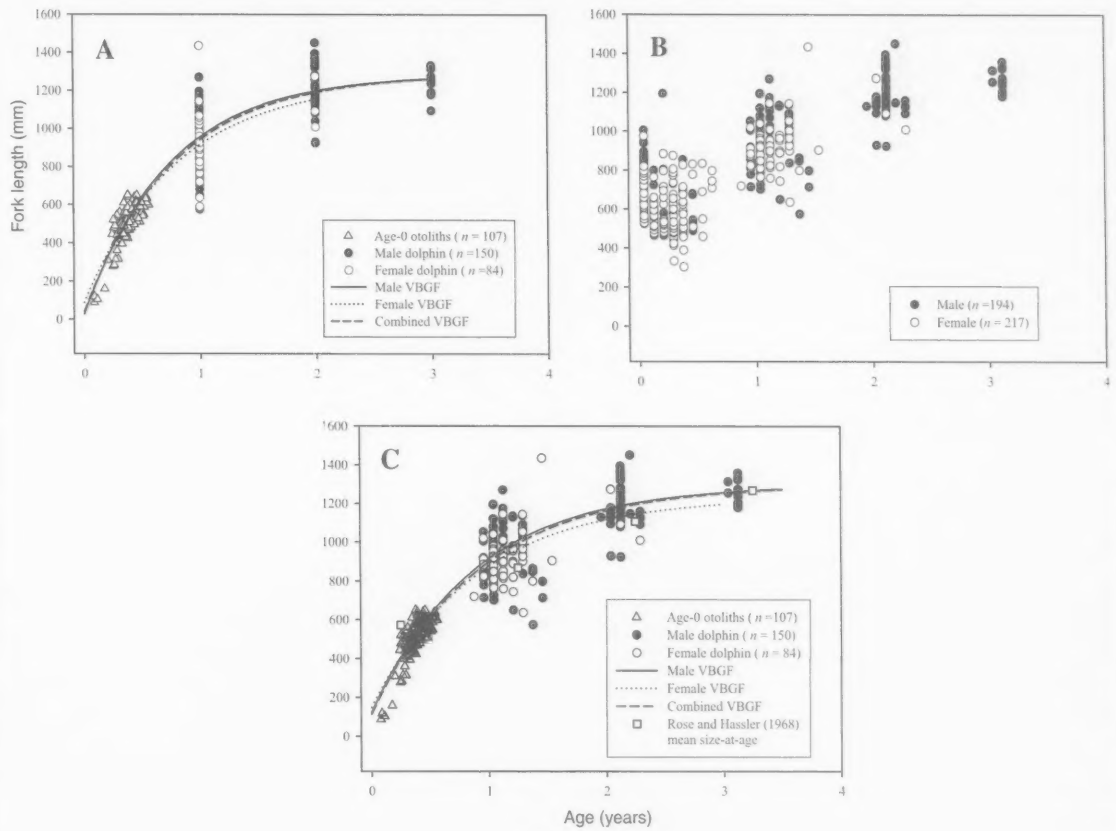

Figure 2

Length-at-age data for male (filled circles) and female (open circles) dolphinfish (*Coryphaena hippurus*) from (**A**) annual marks on scales from >age-0 dolphinfish, (**B**) annual marks on scales from age-0 and >age-0 dolphinfish (with the assumption of a 15 April hatching date, and (**C**) annual marks on scales from >age-0 dolphinfish (with the assumption of a 15 April hatching date). Length-at-age data (A and C) from daily otolith increments for age-0 dolphinfish with fork length <650 mm (male, female, and sex undetermined; open triangles) are presented. Functions A and C are presented for von Bertalanffy model fits to male (solid line), female (gray dashed line), and combined sexes (dark dashed line) length-at-age data (otolith and scale data combined for model fitting). Mean size-at-age data for dolphinfish from Rose and Hassler (1968) are plotted (C; open squares) for comparison with 2002–04 length-at-age values; values from Rose and Hassler (1968) were not used in fitting the von Bertalanffy growth function. VBGF=von Bertalanffy growth function.

1961–62 are shown in Figure 2C (where a mean capture date of 15 July was assumed for all plots; Rose and Hassler, 1968), and are similar to length-at-age values from the present study.

Length-at-age data for dolphinfish from past studies from different regions show an apparent trend in regional groupings (Fig. 3). The von Bertalanffy growth functions calculated for the Gulf of Mexico and Caribbean all display faster growth rates than those for Florida, North Carolina, and the Mediterranean, and an average longevity of less than one year. Dolphinfish collected from Florida, North Carolina, and the Mediterranean Sea all displayed similar first-year growth rates and a maximum age of 3 or 4 years (Fig. 3). However, Mediterranean dolphinfish have a slightly smaller size at age 2 and 3 compared to size for these ages of Florida and North Carolina dolphinfish.

Reproduction

Males reached 50% maturity at 476 mm FL and 100% maturity was reached at 645 mm FL (Table 3). Females reached 50% maturity at a slightly smaller size than males, although confidence limits for this parameter overlapped with those of males. At 458 mm FL, 50% of female dolphinfish were mature, and 100% were mature at about 560 mm FL.

Table 3

Length at 50% maturity for male and female dolphinfish (*Coryphaena hippurus*). Lengths were estimated by fitting a logistic model (see text) with nonlinear regression analysis. The standard errors (SE) of each parameter are shown in parentheses. n = sample size, Q = model parameter, L_{50} = fork length (mm) at 50% maturity, and CI = 95% confidence interval for L_{50}.

Sex	n	Q (SE)	L_{50} (SE)	CI
Males	74	0.05 (0.02)	476.13 (6.24)	460.9–494.7
Females	154	0.08 (0.02)	457.58 (2.54)	453.1–462.5

The highest median GSI values occurred in May for both male (Fig. 4A) and female (Fig. 4B) dolphinfish; however, these values were not corrected for differences in body size. Length-adjusted mean gonad weights were significantly different by month (ANCOVA: $P<0.001$) for both male and female dolphinfish (Fig. 4C). Length-adjusted mean gonad weights were highest in the late spring and summer and then decreased from midsummer into the fall. Gonad weights from November to February were not included because of the low sample size ($n=9$). September gonad weights were significantly lower than May and June gonad weights in males (Fig. 4C); all other male comparisons were nonsignificant. There were significant differences in the length-adjusted gonad weights of females between almost every month, but most differences were found for October, when gonad weights were significantly lower than in May, June, July, and August ($P<0.001$ for all) (Fig. 4C).

For both 2002 and 2003, hatching dates of dolphinfish occurred for all months, but the bulk occurred from January to June (Fig. 5). In 2002, the majority of age-0 dolphinfish sampled (83%) had back-calculated hatching dates in the months of January through June. Similarly, in 2003, 76% of age-0 dolphinfish had back-calculated hatching dates for this same period.

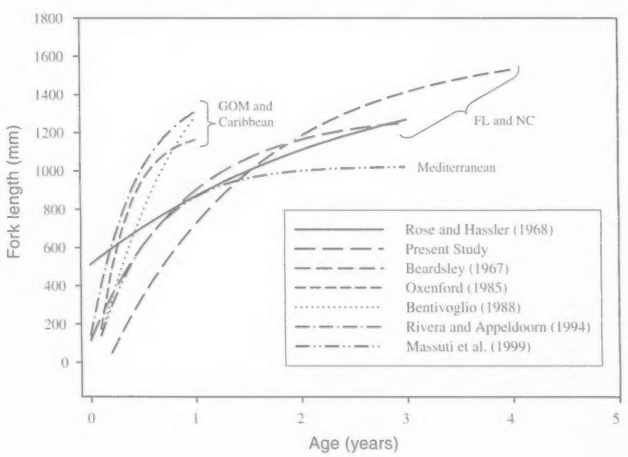

Figure 3

Calculated von Bertalanffy growth functions (VBGFs) for dolphinfish (*Coryphaena hippurus*) from various locations in the North Atlantic. GOM = Gulf of Mexico, FL = Florida, NC = North Carolina.

Discussion

Age and growth

This study is the first to use transverse cross-sections of sagittal otoliths to determine daily ages of dolphinfish; whole otoliths (Oxenford and Hunte, 1983; Uchiyama et al., 1986; Rivera and Appledoorn, 2000) or exposed sagittal planes (Massutí et al., 1999; Morales-Nin et al., 1999) were used in prior studies. Our estimated birth dates are in good agreement with known spawning dates (Beardsley, 1967; this study); a similar independent comparison indirectly validated daily age data for dolphinfish in the Mediterranean Sea (Massutí et al., 1999; Morales-Nin et al., 1999). Future work is needed to compare the multiple techniques that have been used to prepare age-0 dolphinfish otoliths in order to determine which technique is most efficient.

The daily growth rates for dolphinfish are faster than those of many species, but are a common characteristic of pelagic piscivores (Brothers et al., 1983; La Mesa et al., 2005). Our estimate of daily growth rate (3.78 mm FL/day) is similar to that of 550–1325 mm FL dolphinfish from Puerto Rico (3.59 mm/day; Rivera and Appledoorn, 2000) and 200–600 mm FL dolphinfish from the western Mediterranean Sea (~3.50 mm/day; Massutí et al., 1999). In Barbados, the average growth rate of dolphinfish of 174–1100 mm SL is estimated at 4.71 mm standard length per day (Oxenford and Hunte, 1983). Based on daily growth increments in sagittal otoliths of dolphinfish from the Gulf of Mexico, average first-year growth rate is 4.15 mm FL/day for fish in the size range of 250–1200 mm SL (Bentivoglio, 1988).

Annual marks are not detectable on sagittal otoliths of >age-0 dolphinfish with

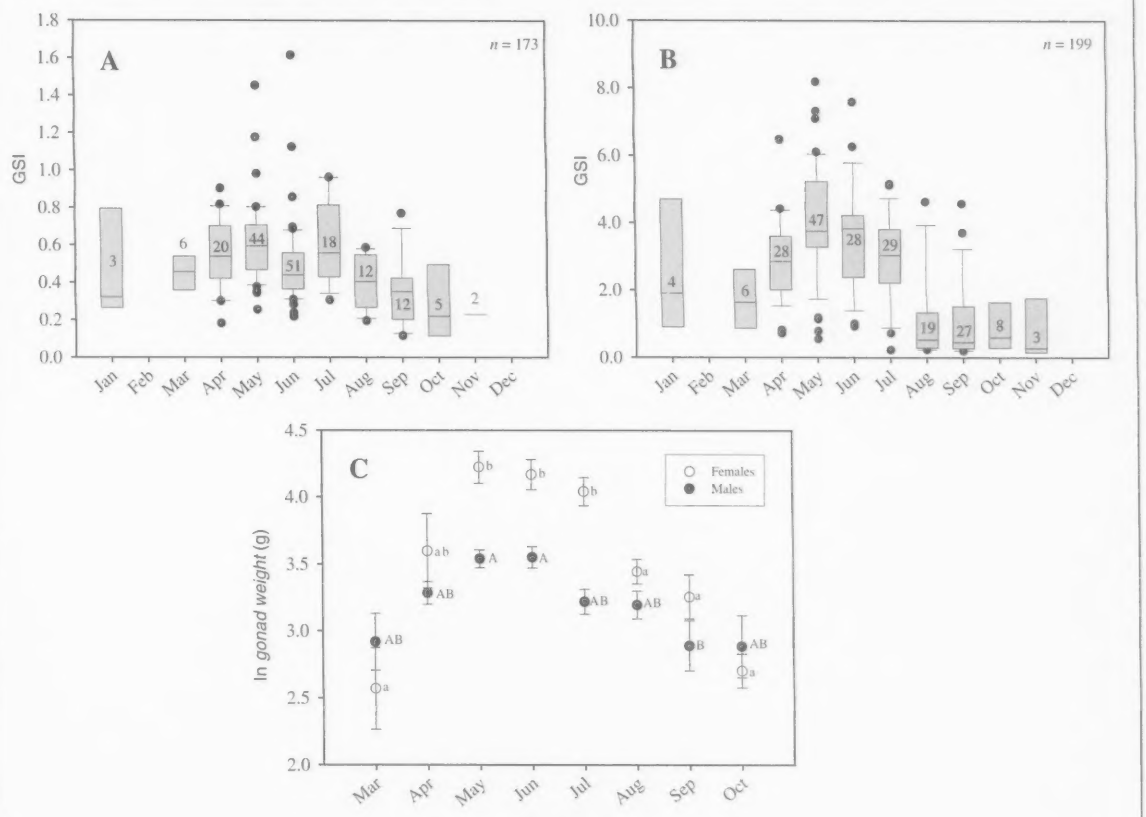

Figure 4

Box plots of gonadosomatic indices (GSI) for (**A**) males and (**B**) female dolphinfish (*Coryphaena hippurus*) collected from January 2002 through December 2004, and (**C**) mean (±SE) ln (*gonad weight*) of male (closed circles) and female (open circle) dolphinfish adjusted to a common length for March through October of 2002–04. Like letters for each sex in C indicate no significant difference between months as determined with ANCOVA. The 25th percentile of the GSI data is represented by the boundary of the box closest to zero, in relation to the *y*-axis, and the 75th percentile is represented by the boundary of the box farthest from zero. The line within the box is the median value. Whiskers (error bars) above and below the box indicate the 90th and 10th percentiles, respectively. Outlying values for both upper and lower ranges are represented by closed circles (in A and B). SE=standard error. Sample sizes are given inside the boxes (in A and B).

methods used to date. Massutí et al. (1999) using sagittal plane sections did not observe annual marks on dolphinfish otoliths from the Mediterranean Sea, although the authors speculated that detection of annual marks on the outer edges of adult otoliths may have been hindered by otolith preparation. A transverse cross-section approach was used in our study in an attempt to obtain a view of the outer edges, but the technique used in otolith preparation or the complex structure of >age-0 dolphinfish otoliths may have prevented detection of any annual marks. Alternatively, annual marks may not exist on sagittal otoliths of dolphinfish.

Validation of scale annuli has been attempted in only a few studies of dolphinfish. Although the annual marks on scales of >age-0 dolphinfish were relatively easy to interpret and within-laboratory agreement of age assignments was good in our study, these features do not establish that the ages are correct. In general, the monthly pattern in marginal increment widths in our study was similar to prior work in Florida (Beardsley, 1967). After measuring the distance between the last annulus and the margin of the scale for all dolphinfish with one or more year marks, Beardsley (1967) considered November to be the period of annulus formation because of an abrupt decrease in width of the increments from October to November. The smallest mean marginal increment in our study occurred during winter; this finding supports the hypothesis that dolphinfish lay a new annulus in winter as a result of decreased water temperature. The temperature of the

Gulf Stream and associated waters off the North Carolina coast is variable enough to cause a decrease in growth rates during the winter (Rose, 1966); the same conclusion was reached for Florida dolphinfish (Beardsley, 1967). It is unknown what proportion of the dolphinfish population inhabits these regions during winter and whether some dolphinfish are not exposed to environmental conditions that lead to annulus formation.

It is surprising that the mean marginal increment width dropped during late summer and fall in our study. The age-1 dolphinfish sampled in the late summer and early fall were smaller than those collected in the spring and early summer months of the same year, and for that reason perhaps a different cohort was sampled (Schwenke, 2004). Sampling from different cohorts is likely given the highly migratory nature of dolphinfish. Marginal increment width is correlated with dolphinfish body size (Schwenke, 2004); therefore, monthly differences in the mean fork length can affect the monthly marginal increment width. Wide variation in marginal growth in any given month was also noted by Beardsley (1967).

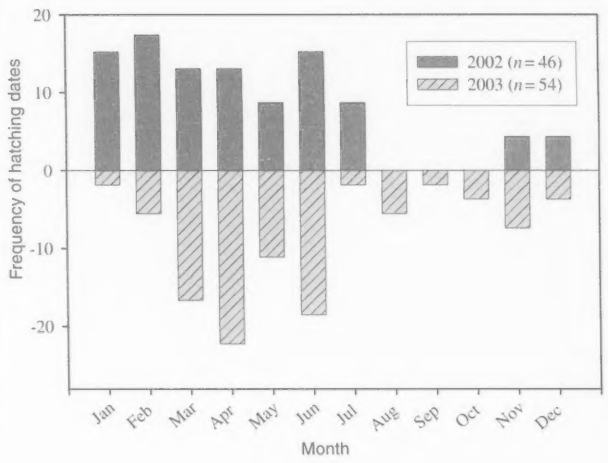

Figure 5

Frequency distribution of back-calculated hatching dates estimated from daily otolith increments for age-0 dolphinfish (*Coryphaena hippurus*) collected off North Carolina. The hatching dates were pooled by month for both 2002 (solid bars) and 2003 (hatched bars).

The assumption of a winter-formed annulus was supported by evidence of deposition of a winter-formed annulus in scales from a dolphinfish that had previously been tagged. The dolphinfish was tagged 18 October 2003 off Hudson Canyon (Mid-Atlantic Bight) at a fork length of 660 mm through the Dolphin Tagging Program run by Cooperative Science Services, Charleston, SC. The dolphinfish was recaptured on 16 May 2004 off Morehead City, NC, at a fork length of 864 mm and was estimated to be a one year old with a clearly defined annulus. This finding supports the assumption that dolphinfish lay down a new annulus in the winter. The likelihood that this dolphinfish had already laid down an annulus when tagged is not great, because 98% of the fish that were age-1 in our study had a fork length greater than 660 mm.

To date, scales seem to be the most appropriate hard part to use to determine annual ages of dolphinfish because findings are comparable between studies where this structure was used. With scales used for age determination, the maximum age of dolphinfish from Straits of Florida is four years (n=511; Beardsley, 1967), three years off North Carolina (n=738, Rose and Hassler, 1968; n=339, this study), and three years in the Mediterranean Sea (n=150, Massutí et al., 1999). Longevity and first-year growth for dolphinfish in Florida (Beardsley, 1967) and North Carolina (Rose and Hassler, 1968; this study) have greater similarity to longevity and first-year growth of western Mediterranean Sea dolphinfish (Massutí et al., 1999) than to longevity and first-year growth of dolphinfish in other regions (Fig. 3). First-year growth of dolphinfish in the Gulf of Mexico (Bentivoglio, 1988) and the Caribbean (Oxenford, 1985; Rivera and Appeldoorn, 2000) is faster and maximum age is younger than corresponding measures for other regions (Fig. 3). Differences in estimated growth between regions can be due to different laboratory methods, genetics, or environmental conditions (i.e., water temperature, food availability, exploitation levels). For example, the aging of dolphinfish solely with otoliths is found to underestimate the age of older, larger fish (Massutí et al., 1999). Alternatively, regional differences may represent different genetic stocks (reviewed by Oxenford, 1999). One of the first ways to make progress in identifying the factors responsible for this inter-region variability in growth would be to standardize age and growth methods.

Lengths of age-0 dolphinfish are highly variable and age-0 dolphinfish comprised the majority of the sampled population in this study. The large age-0 dolphinfish that were caught near the time of the theoretical hatching date may have represented fall-spawned dolphinfish whose annual marks would not be discernible on scales. Previous age and growth studies on the U.S. east coast have relied solely on annual marks on scales for their age estimates, and for these studies all samples were obtained through fishery-dependent sources. Because dolphinfish do not become fully recruited to the fishery until ~400 mm FL, past length-at-age-0 curves may be biased because smaller dolphinfish were not represented. In our study, small dolphinfish obtained through fishery-independent sampling allowed for daily aging of dolphinfish, and thus reduced the variability associated with length-at-age of age-0 dolphinfish and provided an estimate of first-year growth rates.

Reproduction

Peak spawning in dolphinfish off the southeastern United States extends from January through July (Beardsley, 1967; this study). Previous reviews of the reproductive characteristics of dolphinfish revealed that young dolphinfish are throughout the year in the Florida current and their presence may indicate year round spawning there (Oxenford, 1999). However, there are regional peaks in spawning activity off the southeastern U.S. coast. Peaks occur from January to March in Florida (Beardsley, 1967) and from May and June (Schuck, 1951) or June and July (Rose, 1966) in North Carolina. Unfortunately, sampling in North Carolina was limited to May and June in the former study (Schuck, 1951) and June, July, and August in the latter study (Rose, 1966). Based on our nearly year round collections of gonad weights, peak spawning in dolphinfish occurs from May to July off the coast of North Carolina; interestingly, peak spawning (determined from GSI values) occurs from May to June in Barbados (Oxenford, 1985).

Back-calculated hatching dates of age-0 fish collected in North Carolina confirm a spawning period from January through July off the southeastern United States; hatching dates do occur in other months, but at lower levels. Similarly, there is good correspondence between dolphinfish spawning and back-calculated hatching dates for the Mediterranean Sea (Morales-Nin et al., 1999). There is interannual variation in the hatching-date distribution of dolphinfish (Massutí et al., 1999; this study); this may be due to changes in the spawning peak or to differential mortality (Massutí et al., 1999). Given the lack of information on dolphinfish mortality, corrections for mortality in hatching-date distributions were not made.

The assignment of a 15 April biological hatching date to all >age-0 dolphinfish in this study reduces much of the variability associated with length-at-age seen in the von Bertalanffy growth curve where a biological hatching date is not used. Some variability in length-at-age still exists, however, and may be a result of other environmental factors experienced by an individual dolphinfish (i.e., water temperature, differences in prey consumption and prey quality). However, the protracted spawning season is likely the most important factor responsible for variability in length-at-age.

Overall, there has been little evidence of changes in size-at-maturity in dolphinfish off the U.S. east coast from the 1960s to the time of our study. Males first begin to mature at a fork length of about 435 mm, which is in agreement with Beardsley's (1967) observation of first maturity in males at a fork length of 427 mm. A previous estimate of the length at 50% maturity for female dolphinfish caught off Florida in the 1960s (Beardsley, 1967) is nearly identical to our estimate (450 [Beardsley, 1967] vs. 457 mm FL [our study]); however, Beardsley (1967) found earlier first maturity in females (~350 mm FL) compared to our study (~430 mm FL).

Summary and implications

Age, growth, and reproduction data for dolphinfish caught off the coast of North Carolina are provided. Using scale annual marks and daily growth increments from otoliths, we determined an updated age-length function. Furthermore, comprehensive seasonal estimates of gonad weights and marginal increment widths, as well as back-calculated hatching dates and daily growth-rate estimates, are the first for dolphinfish in North Carolina waters. Because this species is highly migratory, a much broader study encompassing the U.S. east coast or western North Atlantic may be needed in order to truly characterize dolphinfish reproduction and marginal increment widths. Direct validation through mark and recapture studies could also confirm annual marks on scales and provide good estimates of growth rates for tagged dolphinfish that remain at large through suspected periods of annulus deposition.

Intense positive size-selective mortality can lead to changes in life history parameters (Pitcher and Hart, 1982; Conover and Munch, 2002). However, there have been no changes in size-at-age or size-at-maturity of dolphinfish; therefore, the increased harvests in the 1980s and 1990s have not influenced these life history parameters to date. Because of their fast growth rates and small size-at-maturity, dolphinfish appear an ideal fishery resource species capable of withstanding high rates of fishing mortality.

Acknowledgments

We thank Captain J. Gay of the FV *Old Smokey* for his field assistance, R. Gregory and L. Daniel from North Carolina Division of Marine Fisheries for discussions and use of equipment, and J. Arnott and J. Edwards from Center for Marine Science and Technology (CMAST), North Carolina State University, for extensive help with dolphinfish sampling. We thank P. Rudershausen for his assistance with scale readings. P. Rudershausen, J. Hightower, and L. Stefanski reviewed an earlier draft of the manuscript. We also thank B. Morales-Nin, E. Massutí, and J. Moranta from the Mediterranean Institute for Advanced Studies (IMEDEA) in Mallorca, Spain, D. Ahrenholz from the Center for Coastal Fisheries and Habitat Research, National Oceanic and Atmospheric Administration, in Beaufort, North Carolina, and S. Searcy from CMAST for their assistance with our otolith preparation technique. This project was funded by a North Carolina Fishery Resource Grant no. 02-EP-01.

Literature cited

Beardsley, G. L., Jr.
1967. Age, growth, and reproduction of the dolphin, *Coryphaena hippurus*, in the Straits of Florida. Copeia 1967:441–451.

Bentivoglio, A. A.
1988. Investigations into the growth, maturity, mortality rates and occurrence of the dolphin (*Coryphaena hippurus*, Linnaeus) in the Gulf of Mexico. M.S. thesis, 37 p. Univ. College of North Wales, Bangor, UK.

Brothers, E. B., E. D. Prince, and D. W. Lee.
1983. Age and growth of young-of-the-year bluefin tuna, *Thunnus thynnus*, from otolith microstructure. *In* Proceedings of the international workshop on age determination of oceanic pelagic fishes: tunas, billfish, and sharks (E. D. Prince, and L. M. Pulos, eds.), p. 49–59. NOAA Tech. Rept. NMFS 8.

Cerrato, R. M.
1990. Interpretable statistical tests for growth comparisons using parameters in the von Bertalanffy equation. Can. J. Fish. Aquat. Sci. 47:1416–1426.

Chatterji, A., and Z. A. Ansari.
1982. Fecundity of dolphinfish, *Coryphaena hippurus* L. Mahasagar 15(2):129–133.

Conover, D. O., and S. B. Munch.
2002. Sustaining fisheries yields over evolutionary time scales. Science 297:94–96.

Haddon, M.
2001. Modelling and quantitative methods in fisheries, 424 p. Chapman and Hall, CRC, Boca Raton, FL.

Kimura, D. K.
1980. Likelihood methods for the von Bertalanffy growth curve. Fish. Bull. 77:765–776.

La Mesa, M., M. Sinopoli, and F.Andaloro.
2005. Age and growth rate of juvenile bluefin tuna *Thunnus thynnus* from the Mediterranean Sea (Sicily, Italy). Sci. Mar. 69 (2):241–249.

Massutí, E., B. Morales-Nin, and J. Moranta.
1999. Otolith microstructure, age, and growth patterns of dolphin, *Coryphaena hippurus*, in the western Mediterranean. Fish. Bull. 97:891–899.

Morales-Nin, B., M. Di Stefano, A. Potoschi, E. Massutí, P. Rizzo, and S. Gancitano.
1999. Differences between the sagitta, lapillus and vertebra in estimating age and growth in juvenile Mediterranean dolphinfish (*Coryphaena hippurus*). Sci. Mar. 63(3–4):327–336.

Oxenford, H. A., and W. Hunte.
1983. Age and growth of dolphin, *Coryphaena hippurus*, as determined by growth rings in otoliths. Fish. Bull. 81:906–909.

Oxenford, H. A.
1985. Biology of the dolphin *Coryphaena hippurus* and its implications for the Barbadian fishery. Ph.D. diss., 366 p. Univ. West Indies, Cave Hill, Barbados.

Oxenford, H. A.
1999. Biology of the dolphinfish (*Coryphaena hippurus*) in the western central Atlantic: a review. Sci. Mar. 63 (3–4):277–301.

Palko, B. J., G. L. Beardsley, and W. J. Richards.
1982. Synopsis of the biological data on dolphin fishes, *Coryphaena hippurus* Linnaeus and *Coryphaena equiselis* Linnaeus. U.S. Dept. Commer., NOAA Tech. Rept. NMFS Circ. 443, 28 p.

Pitcher, T. J., and P. J. B. Hart.
1982. Fisheries ecology, 414 p. Croom Helm, London.

Rivera, G. A., and R. S. Appeldoorn.
2000. Age and growth of dolphinfish, *Coryphaena hippurus*, off Puerto Rico. Fish. Bull. 98:345–352.

Rose, C. D.
1966. The biology and catch distribution of the dolphin, *Coryphaena hippurus* (Linnaeus), in North Carolina waters. Ph.D. diss., 153 p. North Carolina State Univ., Raleigh, NC.

Rose, C. D., and W. W. Hassler.
1968. Age and growth of the dolphin, *Coryphaena hippurus* (Linnaeus) in North Carolina waters. Trans. Am. Fish. Soc. 97:271–276.

Schuck, H. A.
1951. Notes on the dolphin (*Coryphaena hippurus*) in North Carolina waters. Copeia 1951:35–39.

Schwenke, K. L.
2004. Age, growth and reproduction of dolphin (*Coryphaena hippurus*) caught off the coast of North Carolina. M.S. thesis, 62 p. North Carolina State Univ., Raleigh. NC.

Secor, D. H., J. M., Dean, and E. H. Laban.
1992. Otolith removal and preparation for microstructural examination. *In* Otolith microstructure examination and analysis (D. Stephenson, and S. Campana, eds.), p. 17–59. Special Publication, Can. J. Fish. Aquat. Sci. 117.

Shcherbachev, Y. N.
1973. The biology and distribution of the dolphins (Pisces, Coryphaenidae). J. Ichthyol. 13:182–191.

Tibbo, S. N.
1962. New records for occurrence of the white-tip shark, *Pterolamiops longimanus* (Poey), and the dolphinfish, *Coryphaena hippurus* L., in the northwest Atlantic. J. Fish. Res. Board Can. 9:517–518.

Trippel, E. A.
1995. Age at maturity as a stress indicator in fisheries. Bioscience 45:759–771.

Uchiyama, J. H., R. K., Burch, and S. A. Kraul Jr.
1986. Growth of dolphins, *Coryphaena hippurus* and *C. Equiselis*, in Hawaiian waters as determined by daily increments on Otoliths. Fish. Bull. 84:186–191.

Vladykov, V. D., and R. A. McKenzie.
1935. The marine fishes of Nova Scotia. Proc. Nova Scotian Inst. Sci. 19:17–113

Importance of shoreface sand ridges as habitat for fishes off the northeast coast of the United States

James M. Vasslides (contact author)

Email address: vasslide@marine.rutgers.edu

Marine Field Station
Institute of Marine and Coastal Sciences
Rutgers University
800 c/o 132 Great Bay Blvd.
Tuckerton, New Jersey 08087-2004

Kenneth W. Able

Marine Field Station, Institute of Marine and Coastal Sciences
Rutgers University
800 c/o 132 Great Bay Blvd.,
Tuckerton, New Jersey 08087-2004

Abstract—To determine if shoreface sand ridges provide unique habitats for fish on the inner continental shelf, two cross-shelf trawl surveys (23 km in length) were conducted in southern New Jersey (July and September 1991–95 with a beam trawl and July and September 1997–06 with an otter trawl) to assess whether species abundance, richness, and assemblages differed on and away from the ridge. The dominant species collected with both gears were from the families Paralichthyidae, Triglidae, Gobiidae, Serranidae, Engraulidae, Stromateidae, and Sciaenidae. Overall abundance (n=41,451 individuals) and species richness (n=61 species) were distributed bimodally across the nearshore to offshore transect, and the highest values were found on either side of the sand ridge regardless of gear type. Canonical correspondence analysis revealed three species assemblages: inshore (<5 meters depth), near-ridge (9–14 meters depth), and offshore (>14 meters depth), and variation in species composition between gear types. Environmental factors that corresponded with the assemblage changes included depth, temperature, distance from the top of the ridge, and habitat complexity. The most abundant near-ridge assemblages were distinct and included economically important species. Sand ridges of the inner continental shelf appear to be important habitat for a number of fish species and therefore may not be a suitable area for sand and gravel mining.

Manuscript submitted 20 July 2007.
Manuscript accepted 19 November 2007.
Fish. Bull. 106:93–107 (2008).

The views and opinions expressed or implied in this article are those of the author and do not necessarily reflect the position of the National Marine Fisheries Service, NOAA.

Shoreface sand ridges are common features within the inner continental shelf of the northeast Atlantic coast, although the importance of these sand ridges as fish habitat has received little attention. These topographic features consist of unconsolidated fine- to medium-grain sand, typically have vertical relief up to 10 meters, and are generally oriented obliquely to the adjacent shoreline (Stahl et al., 1974; McBride and Moslow, 1991). Over 200 shoreface sand ridges have been identified from Montauk Point, New York, to Miami Beach, Florida, and over 71 are found along the coast of New Jersey (McBride and Moslow, 1991).

These sand ridges may be important bathymetric features for commercial and recreational fishing areas if they provide important fish habitat; however, there is little evidence to refute or support that possibility. Adults, settled juveniles, and larvae of a number of fish species have been documented on sand ridges and in the immediate vicinity of sand ridges, indicating that these features are used by multiple fish at various life history stages (Able et al., 2006). Although sand ridges may provide habitat for important fish species, sand ridges from Massachusetts to North Carolina, including ridges off New Jersey (Byrnes et al., 2004), have gained attention as potential locations from which to extract sand and gravel for ongoing beach nourishment projects and to provide construction materials (Drucker et al., 2004). Extraction of sand and gravel reduces the complexity of a ridge, rendering it similar to the surrounding bottom.

Recent research on the effects of sand mining at ridges has focused on physical oceanographic processes (Nairn et al., 2004), and others with a focus on benthic invertebrates and their role in providing trophic support to fishes have provided limited evaluation of the biological response to sand mining (Diaz et al., 2004; Nairn et al., 2004). Although seasonal and spatial patterns of aquatic organisms near sand ridges have been examined for the presence of decapod crustaceans (Viscido et al., 1997) on and near sand ridges off New Jersey and for juvenile fish off Delaware and Maryland (Diaz et al., 2003), there have been no evaluations of correspondingly varying spatial patterns in the fish community or of their causal relationships with sand ridges.

If sand ridges provide unique habitat within inner continental shelf

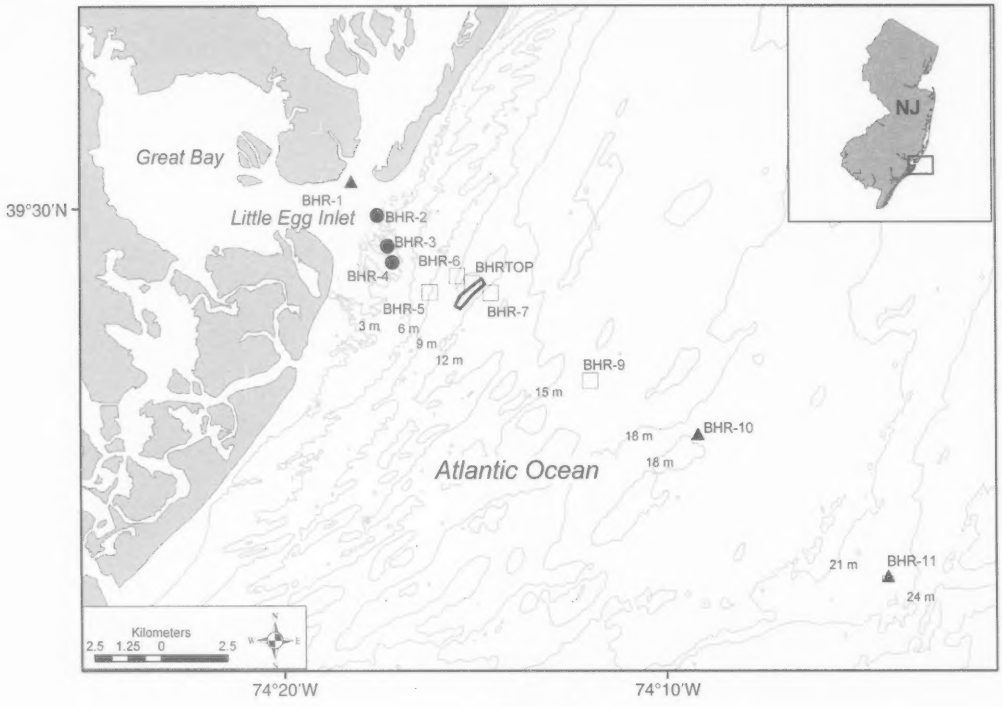

Figure 1

Station locations for the 1991–95 beam trawl surveys and 2001–06 otter trawl surveys off Little Egg Inlet off southern New Jersey. Locations sampled only by beam trawl are denoted by (●), those sampled only by otter trawl, by (▲), and those sampled with both gears, by (□). The thick black line delineates the top contour of Beach Haven Ridge.

ecosystems, then changes to fish assemblages associated with changes in the structure of sand ridges could be excellent indicators of the effects of sand and gravel mining or other habitat alterations. Additionally, sand ridges may not be the optimal choice for sand and gravel mining if it is shown that sand ridges act as strategic ecological features (whether in their influence on increased fish abundance or species richness) or provide essential fish habitat (EFH) for economically important species. The purpose of this study was to determine how use of habitat by fish varies between shoreface sand ridges and the surrounding inner continental shelf through an analysis of abundance and species assemblage patterns. The specific objectives were 1) to ascertain if there is a difference in fish abundance and species richness between the sand ridge and adjacent areas; 2) to determine if there are spatial or temporal patterns in species assemblages that are different between the sand ridge and adjacent areas; and 3) to describe any relationships between the species assemblages and environmental factors. Collectively, this information can provide resource managers a better understanding of the potential impacts of the mining of sand ridges on fishes.

Materials and methods

Study area

The study area encompassed the inner continental shelf waters off southern New Jersey between Barnegat Inlet and Brigantine Inlet (Fig. 1). Sampling was conducted along a 23-km transect across a shoreface sand ridge, Beach Haven Ridge (BHR). Beach Haven Ridge extends northeastward from the ebb tidal delta of Little Egg Inlet; it has a maximum relief of 8 m between the ridge crest and the trough on the seaward side, and the relief on the shoreward side is 4–5 m (Stahl et al., 1974). The substrate on top of the ridge is composed primarily of coarse sand (Craghan, 1995). The seaward side of the ridge has two major substrate types: 1) coarse sand with shells of the surf clam (*Spisula solidissima*) and 2) areas with a mixture of semilithified clay and sand. The landward side of the ridge is characterized as having two major substrate types: 1) areas of sand and clay mixture and 2) patches of semilithified clay and sand mixture. Mounds composed of tubes of the polychaete worm *Asabellides occulata* can also be found landward of the ridge, but are temporally variable. Bedforms (ripples) are

Table 1

Physical attributes of individual sampling stations along the Beach Haven Ridge (BHR) transect. Distance to ridge top is the distance (m) from that station to the station located on top of the ridge, plus signs indicate distances seaward of the ridge top, negative signs indicate distances landward of the ridge top. Habitat complexity index is an index of complexity from 1 to 3 and is based on the amount and type of substrate and macroalgae or other structural components present. See Figure 1 for station locations.

Sampling Station	Distance to ridge top (m)	Distance from shore (m)	Water depth (m)	Trawl type	Number of samples	Type of habitat	Habitat complexity index
BHR-1	−6000	0	2.8	Otter	67	Bare sand	1
BHR-2	−4600	300	3.1	Beam	4	Bare sand	1
BHR-3	−3700	750	5.1	Beam	8	Bare sand	1
BHR-4	−3200	1250	4.7	Beam	8	Bare sand	1
BHR-5	−1400	3050	9.4	Beam	10	Sand with patches of macroalgae and *Diopatra* tubes; clay+silt	3
				Otter	66		
BHR-6	−500	3950	11.5	Beam	22	Clay and sand with *Diopatra* tubes; clay+silt	3
				Otter	64		
BHRTOP	0	4450	10.3	Beam	16	Bare sand	1
				Otter	18		
BHR-7	1100	5550	13.6	Beam	27	Sand with shell hash and *Diopatra* tubes; clay/sand	3
				Otter	61		
BHR-9	5300	9750	16.3	Beam	2	Shell hash	2
				Otter	62		
BHR-10	10000	14450	18.0	Otter	29	Shell hash	2
BHR-11	19000	23450	19.9	Otter	22	Shell hash	2

consistently largest on the crest and flanks of the ridge. The crests are often bare, but the troughs are filled with varying amounts of shell valves and shell hash, which are frequently buried and uncovered. Although patches of *Diopatra cuprea* (plumed worm) tubes were found along the flanks and base of the ridge, they were never identified on the crest of the ridge.

Field sampling

Data from two independent sampling surveys, one with a beam trawl (1991–95), and the other with an otter trawl (1997–2006), were analyzed. Although the data sets were not collected concurrently, they did overlap both temporally (sampling months) and spatially (four sampling stations). This overlap between gear types provided the opportunity to observe temporal and spatial variation in species abundance and richness both within and between gears.

Beam-trawl sampling Sampling for fishes was conducted at eight stations along a transect from Little Egg Inlet across Beach Haven Ridge with a 2 meter (3-mm bar mesh) beam trawl (Fig. 1; Table 1). Both midsummer (July or the first few days in August) and late summer (September) samples were collected. The number of tows conducted at each station varied from 2 to 22 (Table 1). Tow speed was approximately 2.8–3.7 km/h and each tow was one minute in duration in an attempt to sample from discrete habitat types. All fish captured were identified to species where possible and measured to the nearest millimeter. Surface and bottom water samples were obtained with a Nansen bottle. Temperature and salinity were obtained from the water samples by using a stem thermometer and hand-held refractometer, whereas oxygen concentrations were determined by using Winkler titration for samples collected from 1991 through 1995.

Otter trawl sampling Eight stations on and within the vicinity of Beach Haven Ridge were sampled in midsummer (July or the first few days in August) and late summer (September) (Fig. 1; Table 1). Samples were collected with an otter trawl (4.9-m head rope, 19-mm mesh wings, 6-mm-mesh codend) in four replicate tows at the inlet station (BHR-1) with various small boats (4–7 meters) and in three replicate tows at each of the deeper stations with RV *Arabella* (15 meters). Sampling at BHR-10 and BHR-11 did not commence until September 2001. Tow speed varied depending on the

prevailing ocean conditions, but duration of tows never exceeded two minutes in an attempt to ensure that fish were collected from discrete habitat types. For each tow, a random selection of up to 20 individuals of each species were measured to the nearest millimeter fork length (FL) or total length (TL), and the remainder were counted. Beginning in 2001, bottom and surface salinity, temperature, dissolved oxygen, and pH were measured with a YSI model 85 handheld dissolved oxygen and conductivity instrument (Yellow Springs Instruments, Yellow Springs, OH) and recorded after the first tow. Depth and bottom topography were determined with a Furuno model 256 video depth recorder (Furuno, Hyogo, Japan). Water transparency was measured with a Secchi disk at each station.

Habitat characteristics

To assess the importance of habitat complexity to the structure of fish assemblages, the substrate was characterized qualitatively. Because Beach Haven Ridge and its vicinity have been intensively studied in the past, it was possible to identify habitat characteristics for each station from previous research where SCUBA, submersible, and remotely operated vehicle, or sidescan sonar were used, or where structural samples of the habitat were collected during trawl sampling. Additionally, any benthic material (clay and silt clods, sea stars, sand dollars, algae, shell hash, *Diopatra* tubes, *Asabellides* mounds) retained by the 2006 otter trawl sampling was categorized and quantified to evaluate if any changes in substrate had occurred over time. Stations were assigned an index of complexity of 1, 2, or 3 based upon the type and amount of substrate and macroalgae or other structural components present, with 1 being the least complex (bare sand) and 3 being the most complex (one or more substrate types present with multiple biogenic components). Habitat complexity was lowest inshore, peaked on the sides of the ridge, and was of an intermediate value offshore (Table 1). Stations BHR-5, BHR-6, and BHR-7 had multiple substrate types and structural components and were given an index value of 3. Station BHRTOP and the inlet stations were all dominated by bare sand substrates and had no structures and were assigned a value of 1. The offshore stations varied in their substrates but had some complexity owing to biogenic features and were assigned a value of 2. In addition, the distance from a sampling location to the station located at the top of the ridge (BHRTOP), as well as the distance from a sampling location to the shore, were determined by using ArcGIS (Environmental Systems Research Institute, Inc., Redlands, CA).

Data analyses

A number of univariate and multivariate techniques were used to calculate population measures and assemblage structure. Catch per unit of effort (CPUE), or the number of fish captured per tow, was determined for each species at each station. Significant differences in patterns of CPUE among stations were tested by using ANOVA procedures. CPUE data were log transformed before analysis to correct for heterogeneity of variance (Underwood, 1997). Mean species richness per unit of effort (RPUE), or the number of different species caught in a tow, was also calculated for each sampling station. ANOVA and Tukey multiple comparison tests were used to assess the differences in mean species richness (RPUE) between stations. Frequency of occurrence was calculated for each species across tows at each sampling station. All univariate statistics were performed with SAS (vers. 9.1, SAS Inst., Inc., Cary, NC).

To determine the structure of the assemblages in the different habitats, two related ordination techniques were employed. Canonical correspondence analysis (CCA) is a constrained ordination technique in which the sample scores are constrained to be linear combinations of the explanatory variables (Van den Brink and Ter Braak, 1999). This technique is one of the most widely used gradient analysis tools in ecology because of its capacity to handle highly skewed species distributions, high noise levels, complex sampling designs, and the fact that it does not create an artificial arch effect (Palmer, 1993). Canonical correspondence analysis was performed on a subset of the overall data matrix for which environmental information was available for all stations. For the beam trawl data this "subset" was the entire data set, whereas for the otter trawl samples, the subset was limited to Beach Haven Ridge from 2001 to 2006. The data were arranged in a species-by-sample matrix, where the samples were the combination of all tows for a given location and date, and the CPUE represented the value fields. The data were log ($CPUE+1$) transformed to reduce the influence of abundant species. Any species whose abundance did not exceed five percent from at least one station was removed from the matrix.

Because CCA orders species only along gradients of the measured environmental variables, it may not, depending on the environmental variables available, be representative of the assemblages encountered. Therefore, the CCA was checked for bias by using correspondence analysis (CA), an unconstrained ordination method (McGarigal et al., 2000). The species-by-sample matrices were treated in the same manner as in the CCA.

Results

Environmental gradients

Summer temperature tended to decrease with increasing distance from the shoreline, and depth, salinity, and water transparency generally increased with increasing distance (Fig. 2). Average station depth increased with increasing distance from the shoreline (range: 2.8–19.9 m), with the exception of the station located on the top of the ridge (BHRTOP) (Table 1). Within the Beach Haven Ridge transect there was a change in depth from BHR-4

to BHR-5 of 4.7 m, indicating the transition from the Little Egg Inlet to nearshore coastal waters.

Although a number of previous studies incorporating a variety of techniques were used to determine habitat homogeneity, the similarity in descriptions when the same station was sampled by multiple sources provided confidence in the accuracy of the habitat descriptions, as well as the stability of the habitat over time.

Species abundance and richness

The specific patterns in species abundance and richness varied with sampling gear and habitat. The locations near the ridge typically had the largest number of species and individuals and the inshore, top of ridge, and locations offshore of the ridge had the least, regardless of sampling gear (Fig. 3). Fish abundance was higher in late summer than mid-summer for both gears, but the spatial patterns in species abundance were similar between seasons. There was no difference in species richness between seasons for either gear. Beam trawl catches were dominated by demersal fish families including Triglidae, Gobiidae, and Serranidae, whereas the dominant families found in the otter trawl consisted of Engraulidae, Stromateidae, Sciaenidae, Triglidae, and Bothidae (Tables 2–4).

In beam-trawl tows during 1991–95 (n=97), 2049 individuals were collected (primarily demersal but also some pelagic fishes) belonging to 34 species. Fish abundance (CPUE) was lowest inshore, increased slightly towards BHR-5, increased significantly (df=94, P<0.0001) at the stations on either side of the ridge (BHR-6<BHR-7), and was highest at the offshore station (BHR-9) (Fig. 3). The station on top of the ridge (BHRTOP) had significantly lower fish abundance than the stations on either side of the ridge and offshore (df=89, P<0.0001), but higher abundance than at the inshore stations. In otter-trawl tows during 1997–2006 (n=389), 39,402 benthic and pelagic fishes from 52 species were captured. Fish abundance (CPUE) was highest near the ridge (BHR-5> BHR-7>BHR-6) and significantly lower (df=381, P<0.0001) at all other stations (Fig. 3). Fish abundance at the top of the ridge was not significantly different from that at the inshore station or the offshore stations. The beam trawl typically captured smaller individuals (mean=38.8 mm, standard error [SE]=1.2) than did the otter trawl (mean=104.1 mm, [SE=1.1] Tables 2–4; Fig. 4).

Species richness was highest at the near-ridge stations and decreased offshore across both gear types (Fig. 3). The mean species richness per tow (RPUE) for the beam trawl was significantly higher (df=89, P<0.0001) at the sides of the ridge and offshore than at the other beam-trawl stations. The RPUE for the otter trawl was significantly higher (df=312, P<0.0001) at the near-ridge stations than at all other remaining stations.

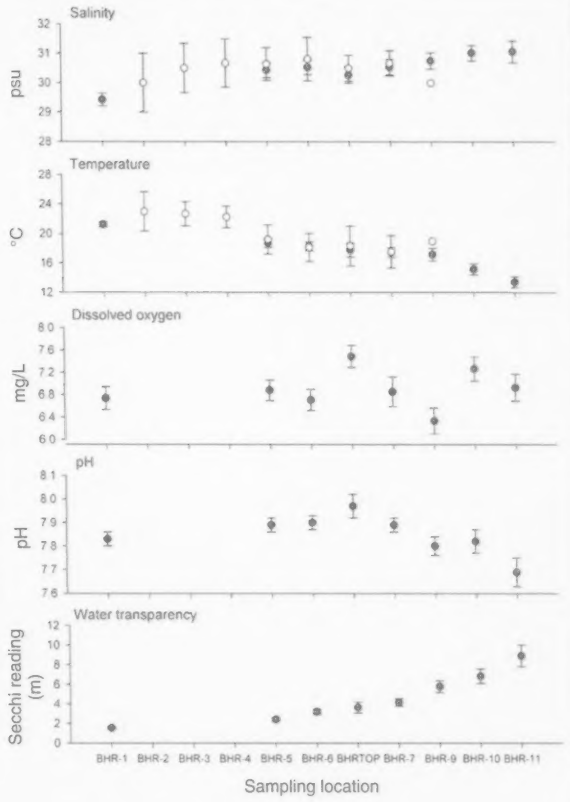

Figure 2

Environmental data (mean bottom values) for the 1991–95 beam trawl samples (○) and 2001–06 otter trawl samples (●). Vertical lines represent standard error. Sampling with a beam trawl at BHR-2 was conducted in midsummer 1995 only and at BHR-9 in midsummer 1993 only. Otter-trawl data at BHRTOP was collected in 2005 and 2006 only. Dissolved oxygen, pH, and a Secchi reading were not recorded at BHR-2, BHR-3, or BHR-4 during sampling with a beam trawl. See Figure 1 for station locations.

Fish-assemblage structure based on beam-trawl samples

Canonical correspondence analysis revealed no discernible pattern in fish-assemblage structure at the stations in midsummer (Fig. 5A), which is in contrast to late summer when there were two distinct, discrete assemblages: the inshore locations (BHR-2, BHR-3, BHR-4, BHR-5) and the near-ridge+offshore stations (BHR-6, BHRTOP, BHR-7, BHR-9) (Fig. 5B). However, within the midsummer samples there was variability in the species associated with each station between years (Fig. 5C). In late summer the near-ridge+offshore

stations shared a number of dominant species, whereas the assemblage of inshore stations varied along both axes. The species composition at each inshore station was not only different from the near-ridge+offshore stations but also from each other (Table 2, Fig. 5D). Within the inshore group, BHR-3 was characterized by American sand lance (*Ammodytes americanus*) and gobies (*Gobiosoma* spp.), and BHR-5 was differentiated as the only station with weakfish (*Cynoscion regalis*). The remaining inshore stations were differentiated from other stations, and to some degree each other, by the abundance of Atlantic croaker (*Micropogonias undulatus*) and kingfish (*Menticirrhus* spp.). Less than half (39%) of the species identified were captured in both assemblages (Table 2), and no species were shared among the top five species loading scores for each assemblage.

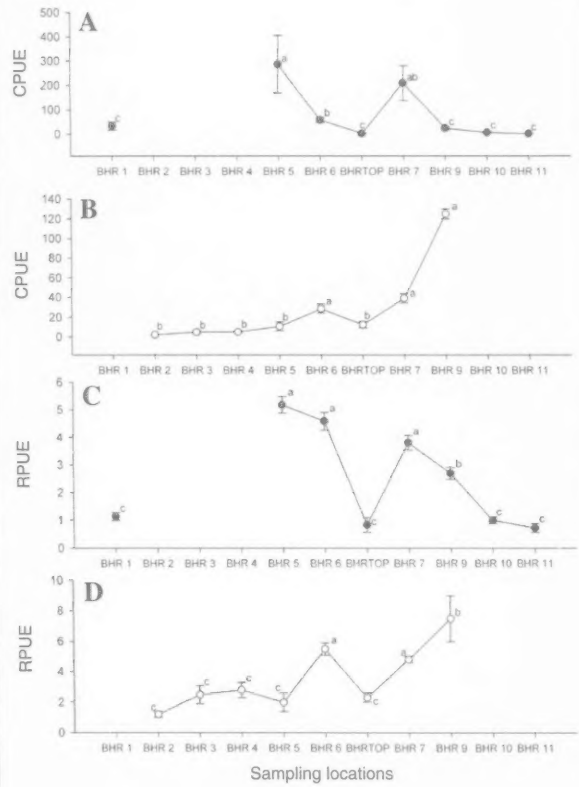

Figure 3

Mean abundance per tow (CPUE) and mean number of species per tow (RPUE) by sampling location for the otter trawl surveys (**A** and **C**) in 2001–06 and beam-trawl surveys (**B** and **D**) in 1991–95. Vertical lines represent standard error. Sampling locations with different superscripts are significantly different from each other at the alpha=0.05 level. See Figure 1 for station locations.

Over 60% of the variance in the species-environment interaction was reflected in both the mid- and late summer ordinations (Table 5). Temperature and habitat complexity were the dominant environmental variables shaping the late summer ordination (Table 6). The arrangement of the species assemblages in relation to the station assemblages was similar to that produced with correspondence analysis (CA), providing confidence that constrained ordination gave a satisfactory picture of realized distribution.

Fish-assemblage structure based on otter-trawl samples

Three assemblages were apparent in the otter-trawl data regardless of season: inshore (BHR-1), near-ridge (BHR-5, BHR-6, BHRTOP, and BHR-7), and offshore (BHR-9, BHR-10, and BHR-11) (Fig. 6). Seasonally, the near-ridge and offshore assemblages overlapped little in midsummer (Fig. 6A) and were discrete in late summer (Fig. 6B). In midsummer, the near-ridge assemblage was spread along both axes, indicating differences between samples, and the offshore assemblage was more compact, indicating a greater similarity in samples (Fig. 6A). In late summer the assemblage configurations were reversed (Fig. 6B). All three assemblages shared a majority of species, although there were some differences in the abundance of each species (Tables 3 and 4; Fig. 6, C and D).

The seasonal difference in assemblages resulted from a change in both the number and identity of species present in the study area (Tables 3 and 4; Fig. 6, C and D). In midsummer the inshore assemblage was composed predominately of northern pipefish (*Syngnathus fuscus*) and other species were present in lesser numbers (Table 3; Fig. 6C). The near-ridge assemblage was dominated by butterfish (*Peprilus triacanthus*) and bay anchovy (*Anchoa mitchilli*), and only striped anchovy (*Anchoa hepsetus*) and spotted hake (*Urophycis regia*) were present with a mean catch per tow greater than one (Table 3). Although butterfish was also the dominant species in the offshore assemblage, its abundance was one third of what was found in near-ridge trawls (Table 3). Of particular interest in the midsummer analysis was a group of species (weakfish, bluefish [*Pomatomus saltatrix*], northern puffer [*Sphoeroides maculatus*], bay anchovy, and striped anchovy) separated along the primary axis from the rest of the species centroids in the near-ridge assemblage. These species were associated with samples from near-ridge stations taken in 2001 and 2005 (Fig. 6A). During late summer, the abundance of bay anchovy increased substantially within the inshore assemblage, as did the abundance of northern pipefish (Table 4, Fig. 6C). At that time, bay anchovy was the most abundant species in the near-ridge assemblage by nearly two orders of magnitude, and Atlantic

Table 2

Catch per unit of effort (CPUE, with standard error in parentheses) and mean size (mm, with standard error in parentheses) for species captured during late summer beam trawl sampling from 1991 through 1995. Station assemblages were determined by using canonical correspondence analysis as shown in Figure 5B. Taxa were measured to total length (†), fork length (*), or body width (‡). A dash indicates that no data were available.

	Station assemblage			
	Inshore		Near-ridge+offshore	
Species	CPUE	Size	CPUE	Size
Syngnathus fuscus †	0.61 (0.27)	108 (13)	0.37 (0.11)	128 (11)
Prionotus carolinus †	0.17 (0.09)	55 (9)	4.16 (0.95)	24 (2)
Scophthalmus aquosos †	0.28 (0.18)	114 (14)	0.23 (0.09)	233 (7)
Sphoeroides maculatus †	0.11 (0.08)	105 (5)	0.40 (0.12)	47 (9)
Etropus microstomus †	0.5 (0.25)	45 (10)	17.79 (3.39)	27 (1)
Micropogonias undulatus †	1.06 (0.61)	15 (2)	0.81 (0.54)	25 (1)
Prionotus evolans †	0.17 (0.12)	48 (14)	0.53 (0.24)	74 (18)
Hippocampus erectus †	0.11 (0.08)	68 (17)	0.05 (0.03)	59 (4)
Centropristis striatus †	0.11 (0.11)	52 (8)	4.09 (1.58)	38 (1)
Cynoscion regalis †	0.22 (0.17)	75 (4)	—	—
Ammodytes americanus *	0.06 (0.06)	76 (–)	—	—
Ammodytes spp. *	0.06 (0.06)	81 (–)	—	—
Menticirrhus sp. †	2.83 (1.2)	39 (3)	—	—
Gobiosoma sp. †	0.39 (0.33)	34 (2)	—	—
Urophycis regia †	—	—	0.35 (0.09)	201 (15)
Urophycis chuss †	—	—	1.3 (0.40)	30 (1)
Gobiosoma ginsburgi †	—	—	5.28 (1.71)	30 (1)
Ophidion marginatum †	—	—	0.16 (0.09)	189 (12)
Paralichthys dentatus †	—	—	0.16 (0.09)	165 (51)
Raja erinacea ‡	—	—	0.09 (0.04)	251 (25)
Bothus sp. †	—	—	0.02 (0.02)	22 (–)
Raja eglanteria ‡	—	—	0.02 (0.02)	420 (–)
Tautogolabrus adspersus †	—	—	0.02 (0.02)	29 (–)

croaker, weakfish, and silver perch (*Bairdiella chrysoura*) were all present at relatively high abundances (Table 4). Bay anchovy and butterfish were the dominant species in the offshore assemblage (Table 4). The preponderance of species found near the ridge compared to offshore was reflected in the ordination by the number of species centroids associated with the near-ridge assemblage. However, some species were found at similar abundances in more than one assemblage (i.e., scup [*Stenotomus chrysops*]), and their centroids may have been located closer to, but not within, any one assemblage (Fig. 6D).

The percentage of variance of the species-environment interaction reflected in the midsummer (54%) and late summer (67%) ordinations was substantial across both time periods (Table 5). Temperature, depth, and dissolved oxygen were significant environmental variables that explained the species assemblages in midsummer; whereas distance from the ridge and depth were the primary factors in late summer (Table 6).

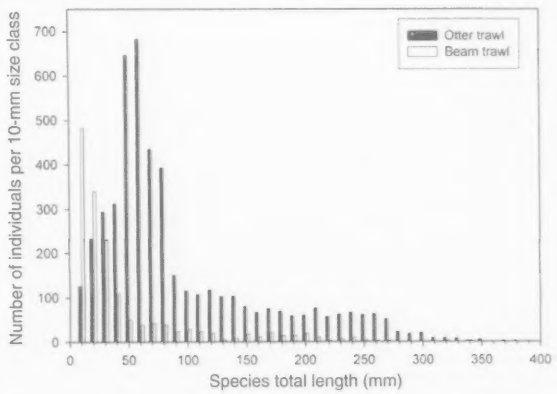

Figure 4

Length frequency (total length in millimeters, in 10-mm bins) of fishes captured by the beam and otter trawls. Seven individuals larger than 400 mm (all *Mustelus canis* [smooth dogfish]) captured in the otter trawl are not shown.

Table 3

Catch per unit of effort (CPUE, with standard error in parentheses) and mean size (mm, with standard error in parentheses) for species captured during mid-summer otter trawl sampling for 2001–06. Station assemblages were determined with canonical correspondence analysis as shown in Figure 6A. Taxa were measured to total length (†) or fork length (*). A dash indicates that no data were available.

	Assemblage					
	Inshore		Near-ridge		Offshore	
Species	CPUE	Size	CPUE	Size	CPUE	Size
Syngnathus fuscus †	0.64 (0.20)	116 (9)	0.03 (0.03)	127 (6)	—	—
Prionotus carolinus †	0.18 (0.18)	47 (2)	0.38 (0.13)	189 (13)	0.75 (0.26)	224 (8)
Scophthalmus aquosos †	0.18 (0.12)	62 (19)	0.25 (0.07)	129 (12)	0.08 (0.04)	270 (7)
Sphoeroides maculatus †	0.18 (0.18)	38 (23)	0.61 (0.28)	71 (3)	—	—
Anchoa mitchilli *	0.09 (0.09)	30 (–)	16.11 (9.15)	68 (1)	—	—
Etropus microstomus †	0.09 (0.09)	95 (–)	0.88 (0.24)	93 (3)	0.38 (0.10)	94 (10)
Menidia menidia *	0.09 (0.09)	55 (–)	—	—	—	—
Anchoa hepsetus *	—	—	1.92 (0.98)	65 (2)	—	—
Pomatomus saltatrix *	—	—	0.03 (0.02)	123 (7)	—	—
Peprilus triacanthus *	—	—	26.55 (15.8)	40 (1)	9.8 (3.2)	37 (1)
Urophycis regia †	—	—	1.2 (0.35)	173 (4)	0.08 (0.04)	157 (32)
Stenotomus chrysops *	—	—	0.47 (0.14)	111 (5)	0.05 (0.05)	106 (3)
Cynoscion regalis †	—	—	0.12 (0.14)	131 (11)	—	—
Prionotus evolans †	—	—	0.28 (0.12)	179 (13)	0.6 (0.41)	215 (6)
Menticirrhus saxatilis †	—	—	0.03 (0.02)	279 (25)	—	—
Centropristis striatus †	—	—	0.02 (0.02)	114 (–)	0.03 (0.03)	265 (–)
Paralichthys oblongus †	—	—	0.05 (0.03)	29 (2)	0.03 (0.03)	181 (–)
Urophycis chuss †	—	—	0.02 (0.02)	70 (–)	0.03 (0.03)	92 (–)
Hippocampus erectus †	—	—	—	—	0.03 (0.03)	53 (–)
Merluccius bilinearis †	—	—	—	—	0.05 (0.03)	175 (±21)
Citharichthys arctifrons †	—	—	—	—	0.03 (0.03)	68 (–)

Discussion

Species abundance and richness

The dominant fish families (Engraulidae, Paralichthyidae, Gadidae, Triglidae, Serranidae, Sciaenidae, and Stromateidae) and to some degree species (butterfish, spotted hake, northern searobin [*Prionotus carolinus*], black sea bass [*Centropristis striatus*], weakfish) captured by the two gears in the study area were similar to those previously found in inner continental shelf waters off of the northeast United States (Colvocoresses and Musick, 1984; Mahon et al., 1998) and southeast United States (Walsh et al., 2006). Previous comparisons between beam and otter trawls similar in size to those used in our study have shown that otter trawls collect more species and more individuals and that beam trawls catch smaller fish (Vasslides, 2007). This difference is reflected in the length-frequency histogram for all species (Fig. 4), as well as for the dominant species collected in both gears.

Overall species abundance (CPUE) and richness (RPUE) displayed a bimodal distribution across the inlet to the offshore transects, and the highest values occurred on either side of the ridge regardless of gear type (Fig. 3). This bimodal pattern has been previously suggested for fish (Martino and Able, 2003) and decapod crustaceans (Viscido et al., 1997) at Beach Haven Ridge but is in contrast to the findings from a number of studies of larger scale cross-shelf transects, where abundance has been shown to decrease linearly with depth in the Mid-Atlantic Bight (Colvocoresses and Musick, 1984), Chukchi Sea (Barber et al., 1997), and Mediterranean Sea (Colloca et al., 2003), but not in the Bering Sea (Mueter and Norcross, 1999).

The species composition and richness, and thus assemblage structure, varied between sampling gears. This was expected because beam trawls sample fishes on the bottom better than otter trawls (Wennhage et al., 1997) and thus capture more demersal species, including small, recently settled fish and small juveniles. This selectivity may explain the differences at certain sampling stations in regard to both abundance and species richness between the two trawl types. In the beam trawl, both abundance per tow and richness per tow at

Table 4

Catch per unit of effort (CPUE, with standard error in parentheses) and mean size (mm, with standard error in parentheses) for species captured during late summer otter trawl sampling during 2001–06. Station assemblages were determined using canonical correspondence analysis as shown in Figure 6B. Taxa were measured to total length (†) or fork length (*). A dash indicates that no data were available.

	Assemblage					
	Inshore		Near-ridge		Offshore	
Species	CPUE	Size	CPUE	Size	CPUE	Size
Syngnathus fuscus †	1.55 (0.62)	133 (3)	0.16 (0.07)	132 (7)	—	—
Prionotus carolinus †	0.07 (0.07)	47 (2)	0.23 (0.08)	230 (9)	0.12 (0.06)	131 (45)
Scophthalmus aquosos †	0.07 (0.04)	62 (19)	0.05 (0.03)	247 (33)	—	—
Sphoeroides maculatus †	0.21 (0.10)	89 (25)	0.08 (0.03)	98 (12)	0.03 (0.03)	90 (–)
Anchoa mitchilli *	4.69 (2.9)	51 (2)	372.15 (134.37)	58(1)	11.76 (9.49)	65 (1)
Etropus microstomus †	0.03 (0.03)	95 (–)	0.05 (0.03)	71 (4)	—	—
Menidia menidia *	0.41 (0.24)	71 (3)	—	—	—	—
Anchoa hepsetus *	0.24 (0.18)	76 (3)	2.02 (1.04)	86 (1)	—	—
Pomatomus saltatrix *	0.21 (0.13)	141 (17)	0.14 (0.06)	98 (2)	0.03 (0.03)	100 (–)
Peprilus triacanthus *	—	—	0.68 (0.17)	70 (5)	2.52 (0.80)	55 (3)
Urophycis regia †	—	—	0.08 (0.04)	217 (19)	0.06 (0.04)	187 (68)
Stenotomus chrysops *	—	—	0.52 (0.14)	152 (6)	0.35 (0.13)	126 (23)
Cynoscion regalis †	—	—	4.26 (0.66)	190 (4)	—	—
Prionotus evolans †	—	—	0.06 (0.03)	110 (13)	—	—
Menticirrhus saxatilis†	—	—	0.05 (0.03)	182 (54)	—	—
Centropristis striatus †	—	—	0.03 (0.02)	58 (24)	0.03 (0.03)	35 (–)
Micropogonias undulatus †	—	—	5.58 (2.29)	209 (4)	0.35 (0.21)	309 (9)
Bairdiella chrysoura †	—	—	1.09 (0.62)	131 (2)	—	—
Hippocampus erectus †	—	—	0.02 (0.02)	63 (–)	—	—
Merluccius bilinearis †	—	—	0.02 (0.02)	79 (–)	—	—

stations BHRTOP and BHR-9 were of intermediate and high values, respectively, whereas in the otter trawl these stations accounted for the lowest and intermediate values, respectively. Over 70% of the individuals captured at stations BHRTOP and BHR-9 during the beam trawl were young of the year (YOY) smallmouth flounder (*Etropus microstomus*), and the majority of these averaged 27 mm and 35 mm TL, respectively. During previous direct comparisons between beam and otter trawls it was found that CPUE and frequency of occurrence for smallmouth flounder were greater in beam trawls and that mean length was substantially less. Because this single species accounted for such a large proportion of the abundance at BHRTOP and BHR-9 as compared to the abundance at other stations, it appears that the selectivity of beam trawls plays a large role in estimating fish abundance and thus the fish assemblages in general.

The seeming discrepancies in RPUE between gear types at particular locations can be partially explained by the limited numbers of tows. At station BHR-9, data were collected from only two beam-trawl tows. Although ten species were collected, five species were represented by one individual and two species were represented by two individuals. Given this apparent patchiness, there is a possibility that additional sampling at this station would yield a RPUE that would more closely reflect the pattern observed in the otter-trawl tows. Even though a limited number of samples were taken with an otter trawl at BHRTOP (n=6), our previous opportunistic surveys with the same gear at other locations on the top of Beach Haven Ridge yielded low numbers of species per tow. However, twice the number of species were caught during midsummer sampling in 2006 at this station, but abundance of each new species was five individuals or less.

Fish-assemblage structure and environmental relationships

The number of assemblages and their constituent members varied by both gear and season. Two general groups were identified in the beam trawl (inshore and near-ridge+offshore) and three in the otter trawl (inshore,

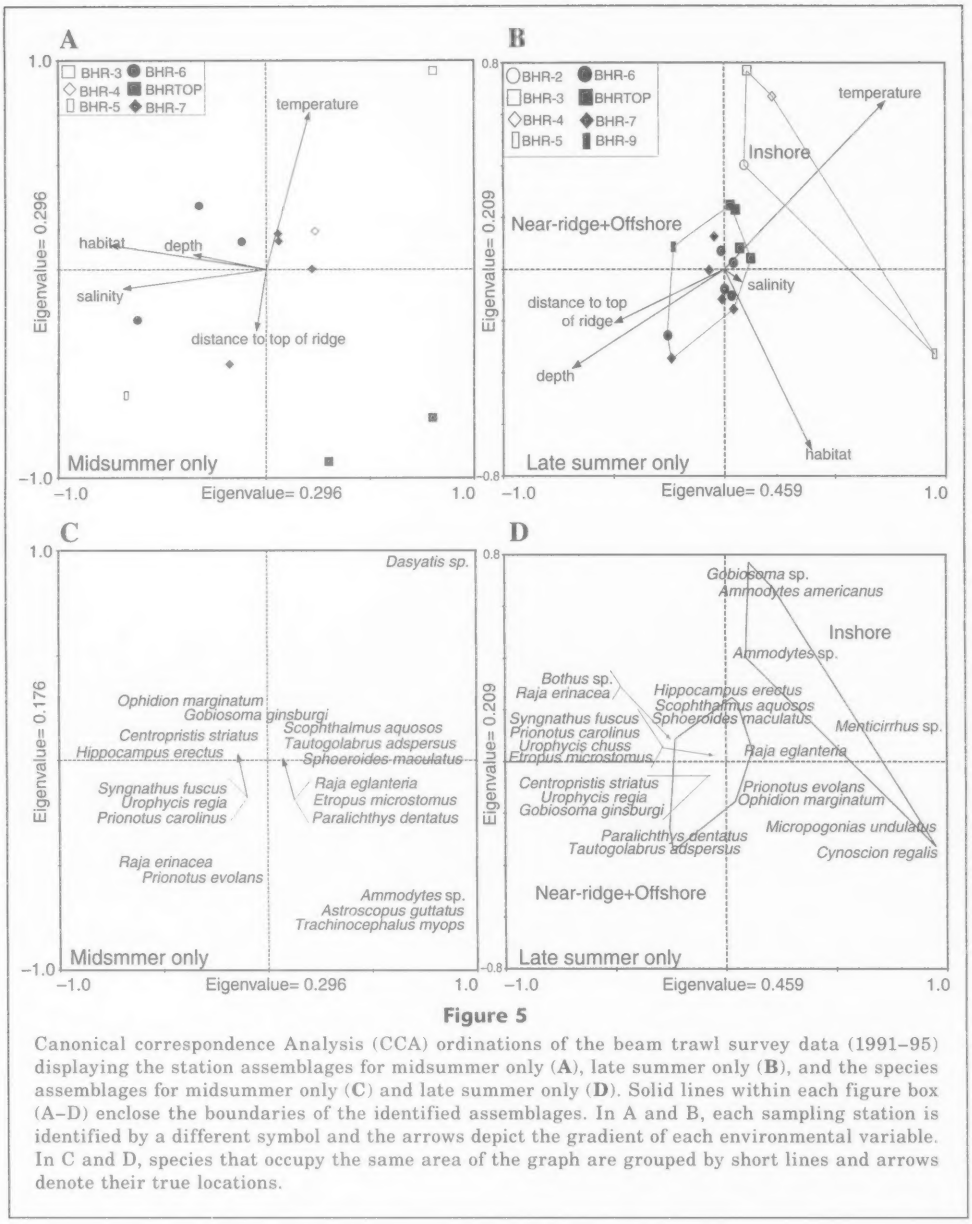

Figure 5

Canonical correspondence Analysis (CCA) ordinations of the beam trawl survey data (1991–95) displaying the station assemblages for midsummer only (**A**), late summer only (**B**), and the species assemblages for midsummer only (**C**) and late summer only (**D**). Solid lines within each figure box (A–D) enclose the boundaries of the identified assemblages. In A and B, each sampling station is identified by a different symbol and the arrows depict the gradient of each environmental variable. In C and D, species that occupy the same area of the graph are grouped by short lines and arrows denote their true locations.

near-ridge, and offshore). Within the Beach Haven Ridge beam trawl samples, 55% of the fish used in the analysis were found in both species assemblages, leaving nearly half of the species captured to be found in only one assemblage or the other. This is in stark contrast to the 2001–06 Beach Haven Ridge otter-trawl data subset, where 82% of the species were found in at least two of the three assemblages and only 18% of the species (silver perch, Atlantic silverside [*Menidia menidia*], northern kingfish [*Menticirrhus saxatilis*], and Gulf stream flounder [*Citharichthys arctifrons*]) were present in only one assemblage. Thus it appears that there is a definite gradient along the transect, represented by changes in species present in the beam trawl and by the relative abundances of shared species in the otter trawl.

Although cross-shelf gradients in demersal fish assemblages have been identified along the northeast United States (Sullivan et al., 2000), northwest United States (Mueter and Norcross, 1999), southwest United States (Johnson et al., 2001), and worldwide (Gray and

Table 5

Eigenvalues and cumulative percentage variance for each axis analyzed by season for the 1991–95 beam trawl data and 2001–06 otter trawl data by using canonical correspondence Analysis (CCA). The eigenvalues are a relative measure of the importance of each axis.

		CCA axis			
		1	2	3	4
1991–95 beam trawl data					
Midsummer	Eigenvalue	0.296	0.176	0.145	0.117
	Cumulative percentage variance				
	of species data	21.3	34.0	44.4	52.8
	of species environment	39.1	62.3	81.4	96.8
Late summer	Eigenvalue	0.459	0.209	0.153	0.132
	Cumulative percentage variance				
	of species data	17.2	25.0	30.8	35.7
	of species environment	46.8	68.1	83.8	97.2
2001–06 otter trawl data					
Midsummer	Eigenvalue	0.572	0.356	0.277	0.176
	Cumulative percentage variance				
	of species data	10.5	17.0	22.0	25.3
	of species environment	33.0	53.6	69.6	79.8
Late summer	Eigenvalue	0.343	0.236	0.128	0.067
	Cumulative percentage variance				
	of species data	10.7	18.1	22.1	24.3
	of species environment	39.8	67.2	82.0	89.9

Table 6

The *P* values from Monte Carlo permutation tests on the significance of the environmental variables in each data set. Significant *P* values ($P<0.05$) are shown in bold. A dash indicates that the variable was not measured.

	1991–95 beam trawl		2001–06 otter trawl	
Variable	Midsummer	Late summer	Midsummer	Late summer
Salinity	**0.036**	0.874	0.200	0.996
Temperature	0.212	**0.002**	**0.002**	0.360
Depth	0.120	0.266	**0.004**	**0.090**
Distance from ridge	0.062	0.094	0.406	**0.002**
Habitat complexity	0.796	**0.028**	0.132	0.112
Dissolved oxygen	—	—	**0.022**	0.654
Water clarity	—	—	0.218	0.824
pH	—	—	0.212	0.172

Otway, 1994), these gradients were all at substantially larger spatial scales. Few studies of either juveniles or adults have been conducted at a resolution similar to that of our study in inner continental shelf waters. Juvenile fish assemblages of the nearshore (<40 km) coast of Georgia exhibited a cross-shelf pattern in winter and spring, and a shallow group (8 m in depth) was separated from the other stations (12–18 m in depth) (Walsh et al., 2006). Fish assemblages in northern Argentina in the spring were identified as either those of the inner, central, or middle regions of the coastal shelf (Jaureguizar et al., 2006).

Analyses of fish assemblages across continental shelves often point to depth as the primary environmental variable correlated with the changes in fish-assemblage structure (Mahon et al., 1998; Walsh et al., 2006), whereas studies focused on shorter distances indicate a combination of environmental and physi-

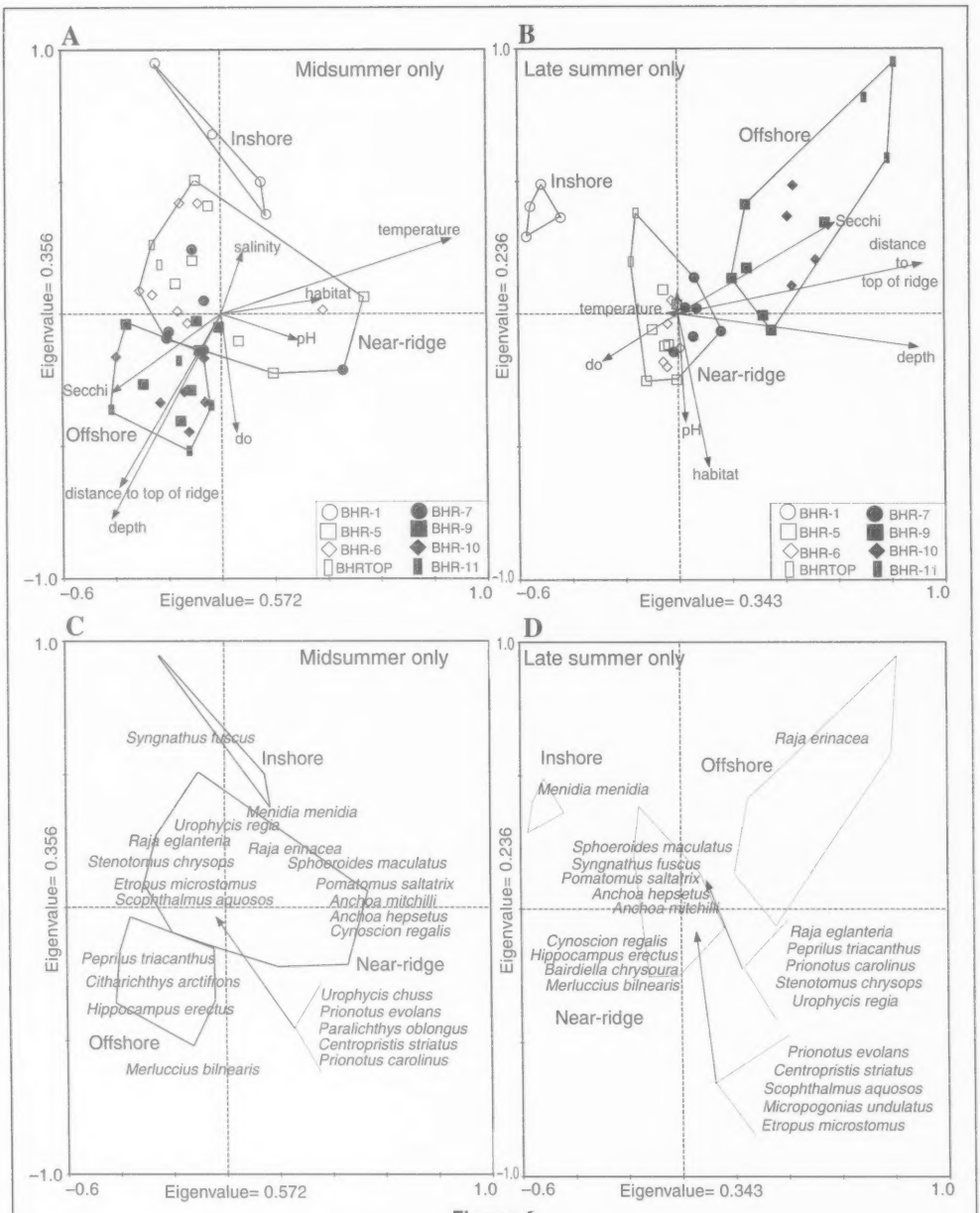

Figure 6

Canonical correspondence analysis (CCA) ordinations of the otter trawl survey data (2001–06) displaying the station assemblages for midsummer only (**A**), late summer only (**B**), and the species assemblages for midsummer only (**C**) and late summer only (**D**). Solid lines within each figure box (A–D) enclose the boundaries of the identified assemblages. In A and B, each sampling station is identified by a different symbol and the arrows depict the gradient of each environmental variable. In C and D, species that occupy the same area of the graph are grouped by short lines and arrows denote their true locations.

cal variables (Martino and Able, 2003; Jaureguizar et al., 2006). The results of our study point to the latter case. Temperature and distance from the top of the ridge were often as important explanatory factors as depth, and habitat complexity and dissolved oxygen were also correlated with the distribution of fish along

the transect. Temperature has played an important role in regulating fish distribution in temperate waters (e.g., Colvocoresses and Musick, 1984; Able et al., 2006), and it may explain the variation in the species assemblages between mid- and late summer for both the beam and otter trawl. Furthermore, the temperature differences along a transect can also shape the species assemblages within a season, as seen in the significance levels for temperature between seasons in the otter trawl CCA (Table 6). In midsummer, when the CCA identified temperature as a statistically important environmental variable, there was a large temperature gradient from BHR-1 to BHR-5 and a slightly smaller change from BHR-7 to BHR-9. These temperature gradients are coincident with the three assemblages identified for the otter trawl midsummer samples in the CCA (Fig. 6A). In contrast, the late summer temperatures were fairly constant across the transect, and this constancy was reflected in the nonsignificant *P*-value for temperature in the CCA.

Although we examined seasonal and annual temporal scales, episodic events can also have a dramatic effect on species assemblages. The study area is well known as a region of upwelling during the summer months; it often has up to five upwelling events each year, typically lasting a week or more (Glenn et al., 2004). These upwelling events bring cooler water generally found at the offshore sampling locations onto the near-ridge stations. When sampling occurred during an upwelling event, similar species were captured at all stations along the transect (excluding BHR-1). However, in years where the bottom temperatures during sampling were higher than the average study temperature (1997, 1998, 2001, and 2005), the near-ridge species assemblage included weakfish and northern puffer, species more commonly associated with late summer when temperatures are warmer (Fig. 6C). It is interesting to note that upwelling events of 2001 were some of the most intense recorded during a 9-year study (Glenn et al., 2004). However, when the samples of 2001 were collected, the water temperatures had returned to the seasonal norm, thus illustrating the rapidity with which upwelling events break down and fish assemblages can change.

Although dissolved oxygen appears to be a significant factor in the arrangement of species assemblages along the sampling transect, its importance may be confounded by its relationship with temperature and depth. As expected, the highest mean dissolved oxygen levels were found at the stations with the coldest mean temperatures, which were also the deepest stations. However, the lowest mean dissolved oxygen value was found at a station in the same assemblage that had the highest value; thus the importance of dissolved oxygen remains unclear.

The trend toward less well-defined species assemblages when the environmental gradients were less pronounced lends some support to the idea that cross shelf patterns in species distributions are attributable to environmental gradients (Jaureguizar et al., 2006; Walsh et al., 2006). However, the importance of habitat complexity in the analyses of assemblages from both gear types (Table 6) indicates selection of specific habitats by some species within a large-scale environmental gradient (see Stoner and Abookire, 2002). This has been shown in many laboratory and field experiments for flatfishes (Neuman and Able, 1998; Stoner and Abookire, 2002) and other demersal fishes (Sullivan et al., 2000; Diaz et al., 2003). As suggested by Mueter and Norcross (1999), this difference may be due to differences in how juvenile or small fishes use benthic habitat compared to larger adult fishes.

The selection of habitat within the study area changed with ontogenetic stage; this is particularly true for the sandy substrate found on the top of the ridge. The beam trawl samples, which contained smaller, presumably younger juveniles, had greater species richness and abundance values on the ridge top than did the otter trawl, which captured larger juveniles and adults. The sandy substrate on the top of the ridge provided important habitat for species that bury themselves, such as northern stargazer (*Astroscopus guttatus*) (Able and Fahay, 1998) and snakefish (*Trachinocephalus myops*) (Sulak, 1990). These species were found only on the top of Beach Haven Ridge, although admittedly in small numbers. Sand lances, another group that buries itself in sand, was also found predominantly in the sandy substrates. In a paired video sled and beam trawl survey (where a video camera sled was towed along the bottom and then a beam trawl was dragged along the same area) on sand ridges off the coast of Maryland and Delaware, a substantially larger number of sand lances were captured in the video sled than in the beam trawl (Diaz et al., 2003), indicating that sand lance may be more important to the assemblage at Beach Haven Ridge than expected from the trawl results.

Time of day also affects the abundance, species richness, and identity of species captured in various habitats. A study of sand ridges offshore of Maryland and Delaware found that when complex habitats were located in proximity to simple habitats, fish abundance was twice as great in the complex habitats during the day, and the pattern was reversed at night (Diaz et al., 2003). This pattern is most likely due to 1) changes in foraging behavior over a diel period and to 2) smaller demersal fish selecting refuge from predators in complex habitats. The fact that all of the trawls in this study were conducted during daytime may explain why the stations located on either side of the top of the ridge, which had more complex habitats, had the highest values for abundance and richness.

There are a number of other possible explanations for the patterns in species abundance and assemblages identified herein that were not explored as part of this study. Investigations into the abundance and distribution of planktonic larvae around Beach Haven Ridge have revealed physical processes as important mechanisms in concentrating mollusk larvae on either side of the sand ridge (Ma et al., 2006). These same processes may be causing the increased abundance of pelagic fish species seen on the flanks of the sand ridges. The

availability of preferred prey items, such as pelagic fishes like bay anchovy and butterfish, may also be affecting the abundance and distribution of fish species (Vasslides, 2007).

In summary, shoreface sand ridges may have a distinct influence on fish abundance and assemblages. The near-ridge habitats have higher species abundances and richness compared to the surrounding inner continental shelf and also possess a distinct species assemblage, including both recreationally and commercially important species. Additionally, the fish found at the top of the ridge were typical prey species (sand lances, anchovies, smallmouth flounder) favored by both resident and transient piscivores in the Mid-Atlantic Bight (Chao and Musick, 1977; Chase, 2002; Walter et al., 2003; Gartland et al., 2006) and thus sand ridges may influence the distribution of these economically important piscivores. As such, sand ridges appear to be important features of the inner continental shelf and may not be suitable areas for resource extraction activities.

Acknowledgments

This study owes a great deal to the post-doctoral students, graduate students, and technicians of the Rutgers University Marine Field Station who collected over 15 years worth of data used in this research. S. Hagan and T. Grothues provided assistance with the data analysis and C. Van Pelt provided editorial support. This research was supported by a National Oceanic and Atmospheric Administration Cooperative Marine Education and Research Grant and the Rutgers University Marine Field Station. This is contribution number 2007-12 of The Institute of Marine and Coastal Sciences, Rutgers University.

Literature cited

Able, K. W., and M. P. Fahay.
1998. The first year in the life of estuarine fishes in the Middle Atlantic Bight, 342 p. Rutgers Univ. Press, New Brunswick, NJ.

Able, K. W., M. P. Fahay, D. A. Witting, R. S. McBride, and S. M. Hagan.
2006. Fish settlement in the ocean vs. estuary: Comparison of pelagic larval and settled juvenile composition and abundance from southern New Jersey, U.S.A. Estuar. Coast. Shelf Sci. 66:280–290.

Barber, W. E., R. L. Smith, M. Vallarino, and R. M. Meyer.
1997. Demersal fish assemblages of the northeastern Chukchi Sea, Alaska. Fish. Bull. 95:195–208.

Byrnes, M. R., R. H. Hammer, T. D. Thibaut, and D. B. Snyder.
2004. Effects of sand mining on physical processes and biological communities offshore New Jersey, U.S.A. J. Coastal Res. 20(1):25–43.

Chao, L .N., and J. A., Musick,
1977. Life history, feeding habits, and functional morphology of juvenile sciaenid fishes in the York River estuary, Virginia. Fish. Bull. 75:657–702.

Chase, B. C.
2002. Differences in diet of Atlantic bluefin tuna (*Thunnus thynnus*) at five seasonal feeding grounds on the New England continental shelf. Fish. Bull. 100:168–180.

Colloca, F., M. Cardinale, A. Belluscio, and G. Ardizzone.
2003. Pattern of distribution and diversity of demersal assemblages in the central Mediterranean Sea. Estuar. Coast. Shelf Sci. 56:469–480.

Colvocoresses, J. A., and J. A. Musick.
1984. Species associations and community composition of Middle Atlantic Bight continental shelf demersal fishes. Fish. Bull. 82:295–313.

Craghan, M.
1995. Topographic changes and sediment characteristics at a shoreface sand ridge-Beach Haven Ridge, New Jersey. M.S. thesis, 112 p. Rutgers Univ., New Brunswick, NJ.

Diaz, R. J., G. R. Cutter Jr., and K. W. Able.
2003. The importance of physical and biogenic structure to juvenile fishes on the shallow inner continental shelf. Estuaries 26(1):12–20.

Diaz, R. J., G. R. Cutter Jr., and C. H. Hobbs III.
2004. Potential impacts of sand mining offshore of Maryland and Delaware: Part 2—biological considerations. J. Coastal Res. 20(1):61–69.

Drucker, B. S., W. Waskes, and M. R. Byrnes.
2004. The U.S. Minerals Management Service outer continental shelf sand and gravel program: Environmental studies to assess the potential effects of offshore dredging operations in federal waters. J. Coastal Res. 20(1):1–5.

Gartland, J., R. J. Latour, A. D. Halvorson, and H. M. Austin.
2006. Diet composition of young-of-the-year bluefish in the lower Chesapeake Bay and coastal ocean of Virginia. Trans. Am. Fish. Soc. 135:371–378.

Glenn, S., R. Arnone, T. Bergmann, W. P. Bissett, M. Crowley, J. Cullen, J. Gryzmski, D. Haidvogel, J. Kohut, M. Molline, M. Oliver, C. Orrico, R. Sherrell, T. Song, A. Weidemann, R. Chant, and O. Schofield.
2004. Biogeochemical impacts of summertime coastal upwelling on the New Jersey Shelf. J. Geophys. Res. 109, C12S02, doi:10.1029/2003JC002265, 15 p.

Gray, C. A., and N. M. Otway.
1994. Spatial and temporal differences in assemblages of demersal fishes on the inner continental shelf off Sydney, south-eastern Australia. Aust. J. Mar. Freshw. Res. 45:665–676.

Jaureguizar, A. J., R. Menni, C. Lasta, and R. Guerrero.
2006. Fish assemblages of the northern Argentine coastal system: spatial patterns and their temporal variations. Fish. Oceanogr. 15(4):326–344.

Johnson, K. A., M. M. Yoklavich, and G. M. Cailliet.
2001. Recruitment of three species of juvenile rockfish (*Sebastes* spp.) on soft benthic habitat in Monterey Bay, California. Calif. Coop. Oceanic Fish. Invest. Rep. 42:53–166.

Ma, H., J. P. Grassle, and R. J. Chant.
2006. Vertical distribution of bivalve larvae along a cross-shelf transect during summer upwelling and downwelling. Mar. Biol. 149:1123–1138.

Mahon, R, S. K. Brown, K. C. T. Zwanenburg, D. B. Atkinson, K. R. Buja, L. Claflin, G. D. Howell, M. E. Monaco, R. N. O'Boyle, and M. Sinclair.
1998. Assemblages and biogeography of demersal fishes of the east coast of North America. Can. J. Fish. Aquat. Sci. 55:1704–1738.

Martino, E., and K. W. Able.
2003. Fish assemblages across the marine to low salinity transition zone of a temperate estuary. Estuar. Coast. Shelf Sci. 56(5–6):969–987.

McBride, R. A., and T. F. Moslow.
1991. Origin, evolution, and distribution of shoreface sand ridges, Atlantic inner shelf, USA. Mar. Geol. 97:57–85.

McGarigal, K., S. Cushman, and S. Stafford.
2000. Multivariate statistics for wildlife and ecology research, p. 20–73. Springer-Verlag Inc., New York, NY.

Mueter, F. J., and B. L. Norcross.
1999. Linking community structure of small demersal fishes around Kodiak Island, Alaska, to environmental variables. Mar. Ecol. Prog. Ser. 190:37–51.

Nairn, R., J. A. Johnson, D. Hardin, and J. Michel.
2004. A biological and physical monitoring program to evaluate long-term impacts from sand dredging operations in the United States outer continental shelf. J. Coastal Res. 20(1):126–137.

Neuman, M. J., and K. W. Able.
1998. Experimental evidence of sediment preference by early life history stages of windowpane flounder (*Scophthalmus aquosos*). J. Sea Res. 40:33–41.

Palmer, M. W.
1993. Putting things in even better order: the advantages of Canonical Correspondence Analysis. Ecology 74(8):2215–2230.

Stahl, L., J. Koczan, and D. Swift.
1974. Anatomy of a shoreface-connected sand ridge on the New Jersey shelf: implications for the genesis of the shelf surficial sand sheet. Geology 2:117–120.

Stoner, A. W., and A. A. Abookire.
2002. Sediment preferences and size-specific distribution of young-of-the-year Pacific halibut in an Alaska nursery. J. Fish Biol. 61:540–559.

Sulak, K. J.
1990. Synodontidae. *In* Check-list of the fishes of the eastern tropical Atlantic (CLOFETA) (J. C. Quero, J. C. Hureau, C. Karrer, A. Post, and L. Saldanha, eds.), vol. 1, p. 365–370. Junta Nacional de Investigação Científica e Tecnológica, Lisbon; European Ichthyological Union, Paris; and UNESCO, Paris.

Sullivan, M. C., R. K. Cowen, K. W. Able, and M. P. Fahay.
2000. Spatial scaling of recruitment in four continental shelf fishes. Mar. Ecol. Prog. Ser. 207:141–154.

Underwood, A. J.
1997. Experiments in ecology: their logical design and interpretation using analysis of variance, 504 p. Cambridge Univ. Press, Cambridge, England.

Van den Brink, P. J., and C. J. F. Ter Braak.
1999. Principal response curves: analysis of time-dependent multivariate responses of biological community to stress. Environ. Toxicol. Chem. 18(2):138–148.

Vasslides, J. M.
2007. Fish assemblages and habitat use across a shoreface sand ridge in southern New Jersey. M.S. thesis, 106 p. Rutgers Univ., New Brunswick, NJ.

Viscido, S. V., D. E. Stearns, and K. W. Able.
1997. Seasonal and spatial patterns of an epibenthic decapod crustacean assemblage in north-west Atlantic continental shelf waters. Estuar. Coast. Shelf Sci. 45:377–392.

Walsh, H. J., K. E. Marancik, and J. A. Hare.
2006. Juvenile fish assemblages collected on unconsolidated sediments of the southeast United States continental shelf. Fish. Bull. 104:256–277.

Walter, J. F. III, A. S. Overton, K. H. Ferry, and M. E. Mather.
2003. Atlantic coast feeding habits of striped bass: a synthesis supporting a coast-wide understanding of trophic biology. Fish. Manag. Ecol. 10:349–360.

Wennhage, H., R. N. Gibson, and L. Robb.
1997. The use of drop traps to estimate the efficiency of two beam trawls commonly used for sampling juvenile flatfishes. J. Fish Biol. 51:441–445.

Fishery Bulletin

Guidelines for authors

Content of manuscripts

Contributions published in *Fishery Bulletin* describe original research in marine fishery science, fishery engineering and economics, as well as the areas of marine environmental and ecological sciences (including modeling). Preference will be given to manuscripts that examine processes and underlying patterns. Descriptive reports, surveys, and observational papers may occasionally be published but should appeal to an audience outside the locale in which the study was conducted. Although all contributions are subject to peer review, responsibility for the contents of papers rests upon the authors and not on the editor or publisher. *Submission of an article implies that the article is original and is not being considered for publication elsewhere.* **Articles** may range from relatively short contributions (10–15 typed, double-spaced pages, tables and figures not included) to extensive contributions (20–30 typed pages). **Notes** are reports of 5 to 10 pages without an abstract and describe methods or results not supported by a large body of data. Manuscripts must be written in English; authors whose native language is not English are strongly advised to have their manuscripts checked by English-speaking colleagues before submission.

Manuscript Preparation

Title page should include authors' full names and mailing addresses and the senior author's telephone, fax number, and e-mail address, and a list of key words to describe the contents of the manuscript. **Abstract** should be limited to 200 words (one-half typed page), state the main scope of the research, and emphasize the author's conclusions and relevant findings. Do not review the methods of the study or list the contents of the paper. Because abstracts are circulated by abstracting agencies, it is important that they represent the research clearly and concisely. **Text** must be typed in 12 point Times New Roman font throughout. A brief introduction should convey the broad significance of the paper; the remainder of the paper should be divided into the following sections: **Materials and methods, Results, Discussion** (or **Conclusions**), and **Acknowledgments**. Headings within each section must be short, reflect a logical sequence, and follow the rules of multiple subdivision (i.e., there can be no subdivision without at least two items). The entire text should be intelligible to interdisciplinary readers; therefore, all acronyms, abbreviations, and technical terms should be written out in full the first time they are mentioned. Include FAO common names for species in the list of keywords and in the introduction. Regional common names may be used throughout the rest of the text if they are different from FAO common names which can be found at http://www.fishbase.org/search.html. Follow the U.S. Government Printing Office Style Manual (1984 ed.) and the CBE Style Manual (6th ed.) for editorial style; for fish nomenclature follow the most current issue of the American Fisheries Society's Common and Scientific Names of Fishes from the United States and Canada. Dates should be written as follows: 11 November 2000. Measurements should be expressed in metric units, e.g., 58 metric tons (t); if other units of measurement are used, please make this fact explicit to the reader. Write out the numbers zero through nine unless they form part of measurement units (e.g., nine fish but 9 mm). Refrain from using the shorthand slash (/), an ambiguous symbol, in the general text

Literature cited comprises published works and those accepted for publication in peer-reviewed literature (in press). Follow the name and year system for citation format in the "Literature cited" section (that is say, citations should be listed alphabetically by the authors' last names, and then by year if there is more than one citation with the same authorship). If there is a sequence of citations in the text, list chronologically: (Smith, 1932; Green, 1947; Smith and Jones, 1985). Abbreviations of serials should conform to abbreviations given in the Serial Sources for the BIOSIS Previews Database. Authors are responsible for the accuracy and completeness of all citations. Literature citation format: Author (last name, followed by first-name initials). Year. Title of report or manuscript. Abbreviated title of the series to which it belongs. Always include number of pages. Cite all software and special equipment or chemical solutions used in the study, not in a footnote but within parentheses in the text (e.g., SAS, vers. 6.03, SAS Inst., Inc., Cary, NC).

Tables and figures—general format

- Zeros should precede all decimal points for values less than one.
- Sample size, n, should be italicized.
- Capitalize the first letter of the first word in all labels within figures.
- Do not use overly large font sizes in maps and for units of measurements along axes in figures.
- Do not use bold fonts or bold lines in figures.
- Do not place outline rules around graphs.
- Do not use horizontal lines through graphs to indicate measurement units.
- Use a comma in numbers of five digits or more (e.g. 13,000 but 3000).
- Maps require a North arrow and degrees latitude-longitude (e.g., 170°E).

Tables are often overused in scientific papers; it is seldom necessary or even desirable to present all the data associated with a study. Tables should not be excessive in size and must be cited in numerical order in the text. Headings should be short but ample enough to allow the table to be intelligible on its own. All unusual symbols must be explained in the table legend. Other incidental comments may be footnoted with italic numeral footnote markers. Use asterisks to indicate probability in statistical data. Do not type table legends on a separate page; place them above the table data. *Do not submit tables in photo mode.*

Figures include line illustrations, photographs (or slides), and computer-generated graphs and must be cited in numerical order in the text. Graphics should aid in the comprehension of the text, but they should be limited to presenting patterns rather than raw data. Figures should not exceed one figure for every four pages of text. Figures must be labeled with author's name and number of the figure. Avoid placing labels vertically (except of y axis). Figure legends should explain all symbols and abbreviations and should be double-spaced on a separate page at the end of the manuscript. Please note that we do not print graphs in color.

Failure to follow these guidelines and failure to correspond with editors in a timely manner will delay publication of a manuscript.

Copyright law does not apply to *Fishery Bulletin*, which falls within the public domain. However, if an author reproduces any part of an article from *Fishery Bulletin* in his or her work, reference to source is considered correct form (e.g., Source: Fish. Bull 97:105).

Submission

The Scientific Editorial Office encourages authors to submit their manuscripts as a *single* PDF (preferred) or Word (zipped) document by e-mail to Fishery.Bulletin@noaa.gov. Please use the subject heading, "Fishery Bulletin manuscript submission". *Do not* send encrypted files. For further details on electronic submission, please contact the Scientific Editorial Office directly (see address below). Or you may send your manuscript on a compact disc in one of the above formats along with four printed copies (one original plus three copies [stapled]) to the Scientific Editor, at the address shown below.

Dr. Adam Moles
Scientific Editor, *Fishery Bulletin*
NOAA/NMFS/AFSC
17109 Point Lena Loop Road
Juneau, AK 99801-8626

Once the manuscript has been accepted for publication, you will be asked to submit a final electronic copy of your manuscript. When requested, the text and tables should be submitted in Word or Word Rich Text Format. Figures should be sent as PDF files, Windows metafiles, tiff files, or EPS files. Send a copy of figures in the original software if conversion to any of these formats yields a degraded version.

Questions? If you have questions regarding these guidelines, please contact the Managing Editor, Sharyn Matriotti, at

Sharyn.Matriotti@noaa.gov

Questions regarding manuscripts under review should be addressed to Adam Moles, Scientific Editor, at Adam.Moles@noaa.gov

Fishery Bulletin

Subscription form

Superintendent of Documents **Publications** Order Form

*5178

☐ YES, please send me the following publications:

____ Subscriptions to *Fishery Bulletin*
for $36.00 per year ($50.40 foreign)

The total cost of my order is $ _____ . Prices include regular domestic postage and handling and are subject to change.

_____
(Company or Personal Name) (Please type or print)

_____
(Additional address/attention line)

_____
(Street address)

_____
(City, State, ZIP Code)

_____
(Daytime phone including area code)

_____
(Purchase Order No.)

Charge your order.
IT'S EASY!

VISA

MasterCard

Please Choose Method of Payment:

☐ Check Payable to the Superintendent of Documents
☐ GPO Deposit Account ☐☐☐☐☐☐–☐
☐ VISA or MasterCard Account
☐☐☐☐☐☐☐☐☐☐☐☐☐☐☐☐
☐☐☐☐ (Credit card expiration date)

To fax your orders (202) 512-2250

_____
(Authorizing Signature)

Thank you for your order!

Mail To: Superintendent of Documents
P.O. Box 371954, Pittsburgh, PA 15250-7954
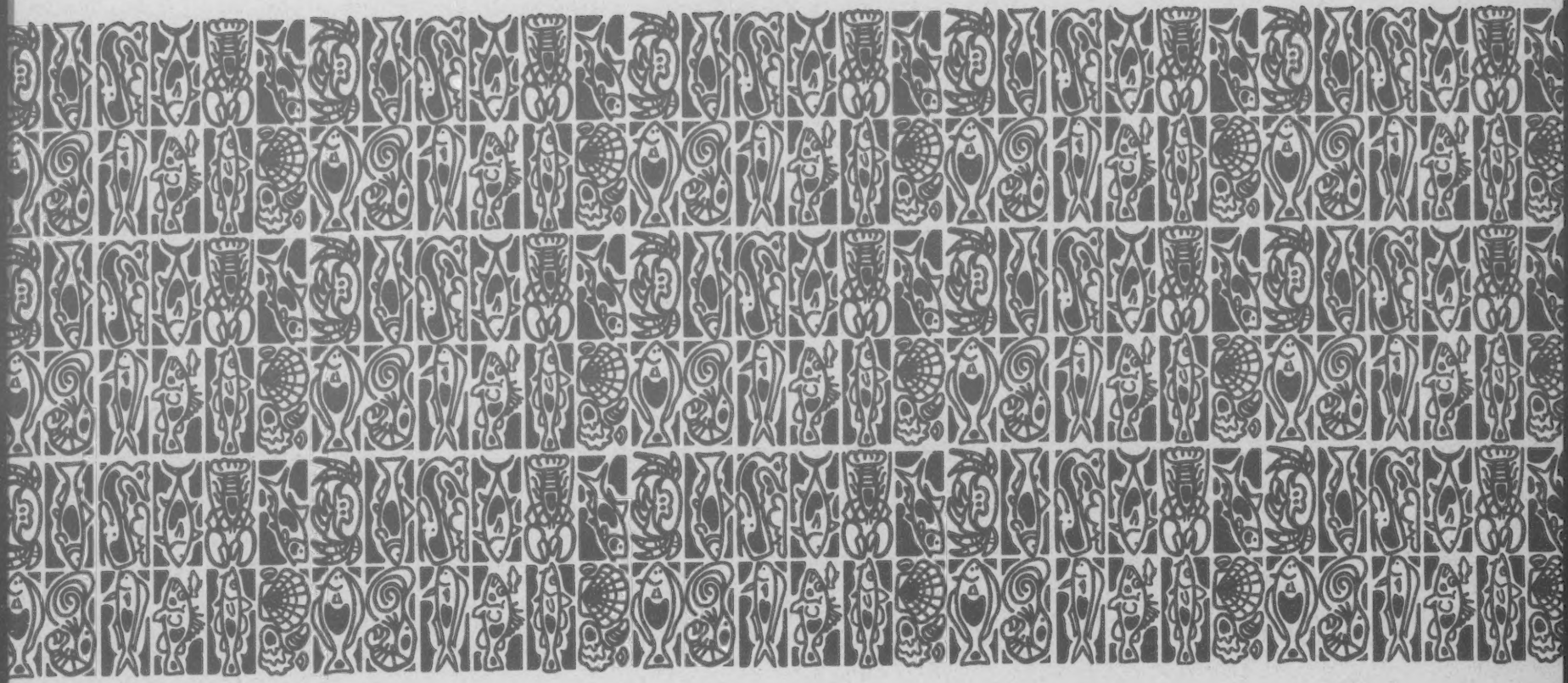
Also available online at http://bookstore.gpo.gov/collections/fishery-bulletin